DOCTOR OF PHILOSOPHY

Evaluation of physical properties of ionic liquids

Zhao, Nan

Award date:
2017

Awarding institution:
Queen's University Belfast

QUEEN'S UNIVERSITY BELFAST

DOCTORAL THESIS

EVALUATION OF PHYSICAL PROPERTIES OF IONIC LIQUIDS

Nan Zhao, BEng

This thesis is submitted for the fulfilment of requirements for the degree of

Doctor of Philosophy

in the

SCHOOL OF CHEMISTRY AND CHEMICAL ENGINEERING

May 29th, 2017

ACKNOWLEDGEMENTS

I would like to express my gratitude to all staff, students and friends whom helped me during my PhD at Queen's University Belfast. My deepest gratitude goes first and foremost to my principal supervisor Dr. Jacquemin, for his constant encouragement and patient guidance in both academic studies and English improvements. During the preparation of my thesis, he have spent a significant amount of time reading through each draft and provided me with detailed suggestions.

I would like to thank my co-supervisors, Dr. Degirmenci and Dr. Bendová. Their patient guidance and academic experience have been invaluable to me. I would also like to thank Zdeněk Wagner, who helped me with the mathematical gnostic analysis. I would like to acknowledge gratefully EPSRC for supporting my work financially (EPSRC First Grant Scheme, Grant No EP/M021785/1). Special thanks for Jingjing Zhou, Weiye Hao, Ryan Oozeerally, Yu Wang, and Tee Yong Goh, they helped with my modeling work. I appreciated their patience and kindness for giving me a hand in my project.

Last thanks would go to my beloved family and friends for their never-ending help, support and encouragement during my study in Queen's.

ABSTRACT

Firstly, experimental data for ionic liquids properties; density, viscosity of pure ionic liquids, viscosity of binary ionic liquid mixtures, and solubility in molecular solvents were collected from the literature and thus four databases were compiled. Then mathematical gnostics was used to analyse the uncertainty and discrepancy of experimental data reported from different resources and to recommend reliable data sets.

The volumetric properties of ionic liquids were evaluated by using a group contribution method. The volumetric parameters of 55 ions were calculated by correlating 5,399 training data points using the Tait-type equations. 2,522 test data points were used to validate the accuracy of this method. This method also allows the calculation of mechanical coefficients with a good agreement.

The viscosity of pure and binary mixtures of ionic liquids was estimated using a new method based on the UNIFAC-VISCO model. The dataset containing 819 experimental viscosity data points for 70 pure ionic liquids was correlated using the modified UNIFAC-VISCO method, thus the interaction parameters and ion VFT parameters were estimated, which were used for the evaluation of 11 types of binary mixtures. A good agreement with the evaluation of binary mixtures in turn proved that the parameters estimated were accurate enough to estimate the viscosity of pure and mixtures ionic liquids.

The liquid-liquid-equilibrium data for binary mixtures; ionic liquid and a molecular

solvent, were modelled using the UNIQUAC and UNIFAC methods. A user-friendly web based interface was established and all the mutual solubility data between the ionic liquid and molecular solvents were uploaded to the online database, which allows end user to get reference data in academy and industry.

ABBREVIATIONS

Cations

$[amim]^+$ 1-allyl-3-methylimidazolium

$[C_1mim]^+$ 1,3-dimethylimidazolium

$[C_2mim]^+$ 1-ethyl-3-methylimidazolium

$[C_2eim]^+$ 1,3-diethylimidazolium

$[C_3mim]^+$ 1-propyl-3-methylimidazolium

$[C_4mim]^+$ 1-butyl-3-methylimidazolium

$[C_5mim]^+$ 1-pentyl-3-methylimidazolium

$[C_6mim]^+$ 1-hexyl-3-methylimidazolium

$[C_7mim]^+$ 1-heptyl-3-methylimidazolium

$[C_8mim]^+$ 1-octyl-3-methylimidazolium

$[C_{10}mim]^+$ 1-decyl-3-methylimidazolium

$[C_{12}mim]^+$ 1-dodecyl-3-methylimidazolium

$[C_{14}mim]^+$ 1-tetradecyl-3-methylimidazolium

$[benmim]^+$ 1-benzyl-3-methylimidazolium

$[C_2mmim]^+$ 1-ethyl-2,3-dimethylimidazolium

$[C_3mmim]^+$ 1-propyl-2,3-dimethylimidazolium

$[C_4mmim]^+$ 1-butyl-2,3-dimethylimidazolium

$[C_6mmim]^+$ 1-hexyl-2,3-dimethylimidazolium

$[C_2py]^+$ 1-ethylpyridinium

$[C_3py]^+$ 1-propylpyridinium

$[C_4py]^+$ 1-butylpyridinium

$[C_6py]^+$ 1-hexylpyridinium

$[C_8py]^+$ 1-octylpyridinium

$[C_3mpip]^+$ 1-propyl-1-methylpiperidinium

$[CNpy]^+$ 1-cyanomethylpyridinium

$[C_2m_{(3)}py]^+$ 1-ethyl-3-methylpyridinium

$[C_3m_{(1)}py]^+$ 1-methyl-3-propylpyridinium

$[C_3m_{(3)}py]^+$ 1-propyl-3-methylpyridinium

$[C_4m_{(2)}py]^+$ 1-butyl-2-methylpyridinium

$[C_4m_{(3)}py]^+$ 1-butyl-3-methylpyridinium

$[C_4m_{(4)}py]^+$ 1-butyl-4-methylpyridinium

$[C_6m_{(3)}py]^+$ 1-hexyl-3-methylpyridinium

$[C_6m_{(4)}py]^+$ 1-hexyl-4-methylpyridinium

$[C_8m_{(3)}py]^+$ 1-octyl-3-methylpyridinium

$[C_8m_{(4)}py]^+$ 1-octyl-4-methylpyridinium

$[C_4m_{(3)}m_{(4)}py]^+$ 1-butyl-3,4-dimethylpyridinium

$[C_4m_{(3)}m_{(5)}py]^+$ 1-butyl-3,5-dimethylpyridinium

$[C_6m_{(3)}m_{(5)}py]^+$ 1-hexyl-3,5-dimethylpyridinium

$[C_6m_{(2)}m_{(4)}py]^+$ 1-hexyl-2,4-dimethylpyridinium

$[C_4C_2py]^+$ 1-ethyl-2-butylpyridinium

$[C_6C_2mmpy]^+$ 1-hexyl-2-ethyl-3,5-dimethylpyridinium

$[C_6DMApy]^+$ 1-hexyl-4-(dimethylamino)pyridinium

$[C_6mDMApy]^+$ 1-hexyl-3-methyl-4-(dimethylamino)pyridinium

$[C_1OC_2mpyrro]^+$ 1-(2-methoxyethyl)-1-methylpyrrolidinium

$[CNmPyrro]^+$ 1-cyanomethyl-1-methylpyrrolidinium

$[C_1mpyrro]^+$ 1,1-dimethylpyrrolidinium

$[C_3mpyrro]^+$ 1-propyl-1-methylpyrrolidinium

$[C_4mpyrro]^+$ 1-butyl-1-methylpyrrolidinium

$[C_6mpyrro]^+$ 1-hexyl-1-methylpyrrolidinium

$[C_8mpyrro]^+$ 1-octyl-1-methylpyrrolidinium

$[C_4C_2pyrro]^+$ 1-butyl-1-ethylpyrrolidinium

$[COC_2mpyrro]^+$ 1-(2-methoxyethyl)-1-methylpyrrolidinium

$[COC_2mmor]^+$ 4-(2-methoxyethyl)-4-methylmorpholinium

$[COC_2mpip]^+$ 1-(2-methoxyethyl)-1-methylpiperidinium

$[C_2OHC_1NH_2]^+$ n-methyl-2-hydroxyethylammonium

$[C_2OHmim]^+$ 1-(2-hydroxyethyl)-3-methylimidazolium

$[N_{1112OH}]^+$ 2-hydroxy-n,n,n-trimethylethanammonium

$[N_{1114}]^+$ butyl-trimethyl-ammonium

$[N_{8881}]^+$ methyl-trioctyl-ammonium

$[choline]^+$ 2-hydroxy-n,n,n-trimethylethanaminium

$[P_{i(444)1}]^+$ tri(isobutyl)methylphosphonium

$[P_{66614}]^+$ trihexyl(tetradecyl)phosphonium

Anions

$[B(CN)_4]^-$ tetracyanoborate

$[BF_4]^-$ tetrafluoroborate

Br^- bromide

Cl^- chloride

$[I_3]^-$ triiodide

$[C(CN)_3]^-$ tricyanomethanide

$[C_2COO]^-$ propionate

$[C_3COO]^-$ butyrate

$[C_4COO]^-$ pentanoate

$[C_1SO_3]^-$ methanesulfonate

$[HSO_4]^-$ bisulfate

$[C_1SO_4]^-$ methylsulfate

$[C_2SO_4]^-$ ethylsulfate

$[C_4SO_4]^-$ octylsulfate

$[C_6SO_4]^-$ hexylsulfate

$[C_8SO_4]^-$ octylsulfate

$[Meesu]^-$ 2-(2-methoxyethoxy) ethylsulfate

$[DCA]^-$ dicyanamide

$[DEP]^-$ diethylphosphate

$[FAP]^-$ tris(pentafluoroethyl)trifluorophosphate

$[Lactate]^-$ 2-hydroxypropanoic acid

$[DMP]^-$ dimethyl phosphate

$[MP]^-$ methylphosphate

$[NTf_2]^-$ bis(trifluoromethylsulfonyl)amide

$[Tf_3C]^-$ tris(trifluoromethylsulfonyl)methide

$[OAc]^-$ acetate

$[OTf]^-$ triflate

$[PF_6]^-$ hexafluorophosphate

$[SCN]^-$ thiocyanate

$[Tos]^-$ tosylate

Roman Letters

a_i Tait parameter

A VFT equation parameter

B VFT equation parameter

B_i Tait parameter

b_i Tait parameter

C Tait parameter

N_C total number of components in UNIFAC-VISCO method

D_i volumetric parameter

g_c^E combinatorial contribution term in UNIFAC-VISCO method

g_r^E residual contribution term in UNIFAC-VISCO method

H_i volumetric parameter

G volumetric parameter

$n_{i,k}$ total number of k^{th} group present in component i

M number of data points

N total number of groups

p pressure (MPa)

p_{ref} reference pressure (0.1 MPa)

q_i van der Waals' surface area of component i

Q_k group surface area parameter

r_i van der Waals' volume of component i

R_k group volume parameter.

$\mathcal{R}$ gas constant (J/mol·K)

s constant in eq. 2-12

K_1 constant in eq. 2-12

K equilibria constant

OF objective function

S concentration-based objective function

S_c scale parameter

T temperature (K)

T_0 VFT equation parameter

V_i pure-component molar volume (m^3/kmol)

V_m mixture molar volume (m^3/kmol)

$V_{m_{IL}}$ molar volume of the ionic liquid

V_{ion}^* effective molar volume of the ion

V_{cation}^* effective molar volume of the cation

V_{anion}^* effective molar volume of the anion

V_i^{COSMO} COSMO volume

x_i mole fraction of the component i

x_{IL} mole fraction of the ionic liquid

x_{exp} experimental value of property

x_{cal} calculated value of property

z coordinate value in UNIFAC based method

Z_O location of the maximum distribution

Z_L lower bound of the typical data

Z_U upper bound of the typical data

Z_{OL} lower bound of the tolerance interval

Z_{OU} upper bound of the tolerance interval

LB lower bound of the data support

UB upper bound of the data support

$mol\%$ mole fraction

w_i gnostic parameter

w_{IL} weight fraction of ionic liquid

w_w water content

w_{Cl} chloride content

Greek Letters

α_{mn} group interaction potential energy parameter between groups m and n

γ activity coefficient

$ln\gamma^C$ combinatorial contribution in UNIQUAC method

$ln\gamma^R$ residual contribution in UNIQUAC method

$ln\gamma_m$ residual activity coefficient

$ln\Gamma_k$ residual activity coefficient

θ_i molecular surface area fraction of component i

Θ_i area fraction for group i

ρ density ($g \cdot cm^{-3}$)

ρ_{IL} ionic liquid density

η viscosity (mPa·s)

μ viscosity of mixture (mPa·s)

μ_i viscosity of component i

μ_{exp} viscosity experimentally measured

μ_{cal} viscosity calculated by our method

μ_o viscosity value with the maximum distribution density

μ_{ion} effective viscosity of ion

κ_T isothermal compressibility

α_p isobaric thermal expansion coefficient

ϕ_i molecular volume fraction of component i

$\Psi_{m,i}$ group interaction parameter

Ψ distribution factor

ω gnostic weight

$\delta(x)$ root mean square deviation

TABLE OF CONTENTS

Chapter 1
Introduction

1.1 Ionic Liquids

Ionic Liquids (ILs) are a diverse group of salts that are found to be in the liquid state at temperatures near or around ambient conditions. Fig. 1-1 shows examples of most common cations and anions that form ionic liquids. Cations in ILs are typically organic structures, often containing nitrogen or phosphorus atoms with linear alkyl chains; such as, ammonium, phosphonium, imidazolium, pyridinium or pyrrolidinium cations. Anions contained within ILs can be either organic or inorganic-based compounds. Most commonly used anions in ILs are $[PF_6]^-$, $[BF_4]^-$, $[NTf_2]^-$, $[SCN]^-$, $[DCA]^-$, $[FAP]^-$, $[OTf]^-$, and $[C_1SO_4]^-$.

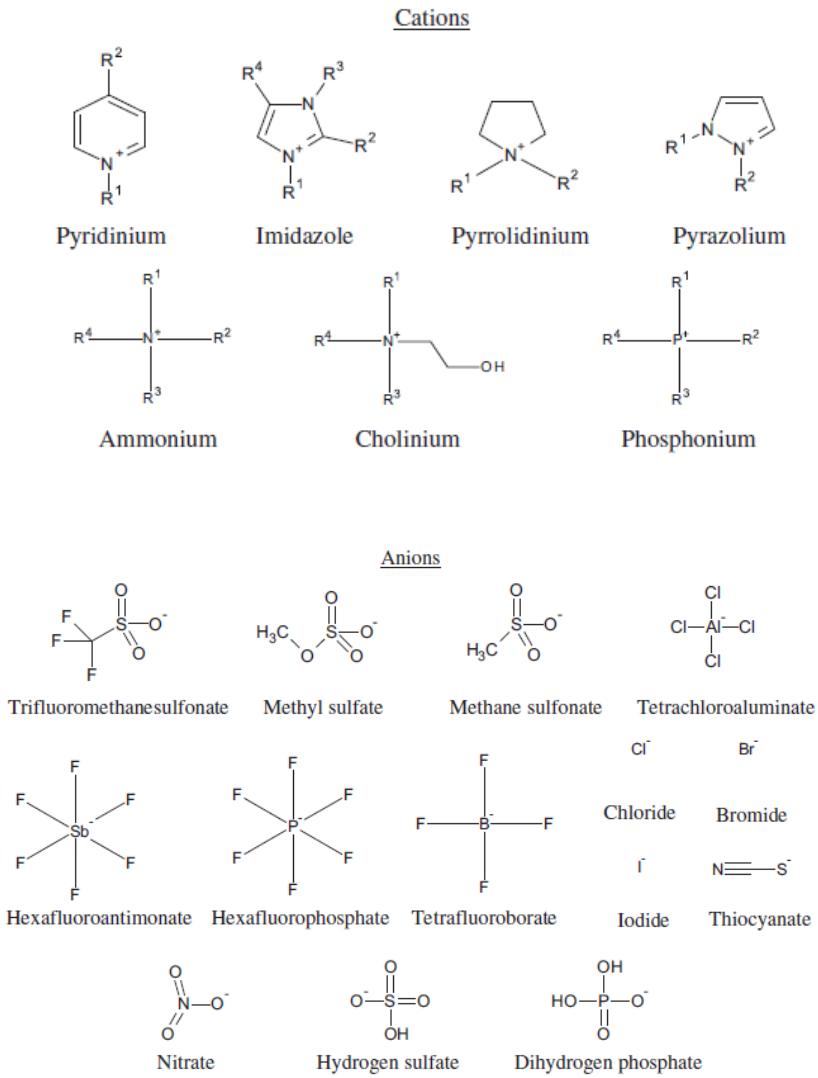

Figure 1-1. Common ionic liquid cations and anions

1.2 Physical Properties of Ionic Liquids

In recent years, ionic liquids have attracted an explosion of interest from research groups and industry for a range of potential applications. Seddon *et al.*[1] have predicted and illustrated the future usages of ionic liquids, as shown in figure 1-2. Many of these require a thorough knowledge of the physicochemical properties of ionic liquids. Some properties of ionic liquids are listed in table 1-1.

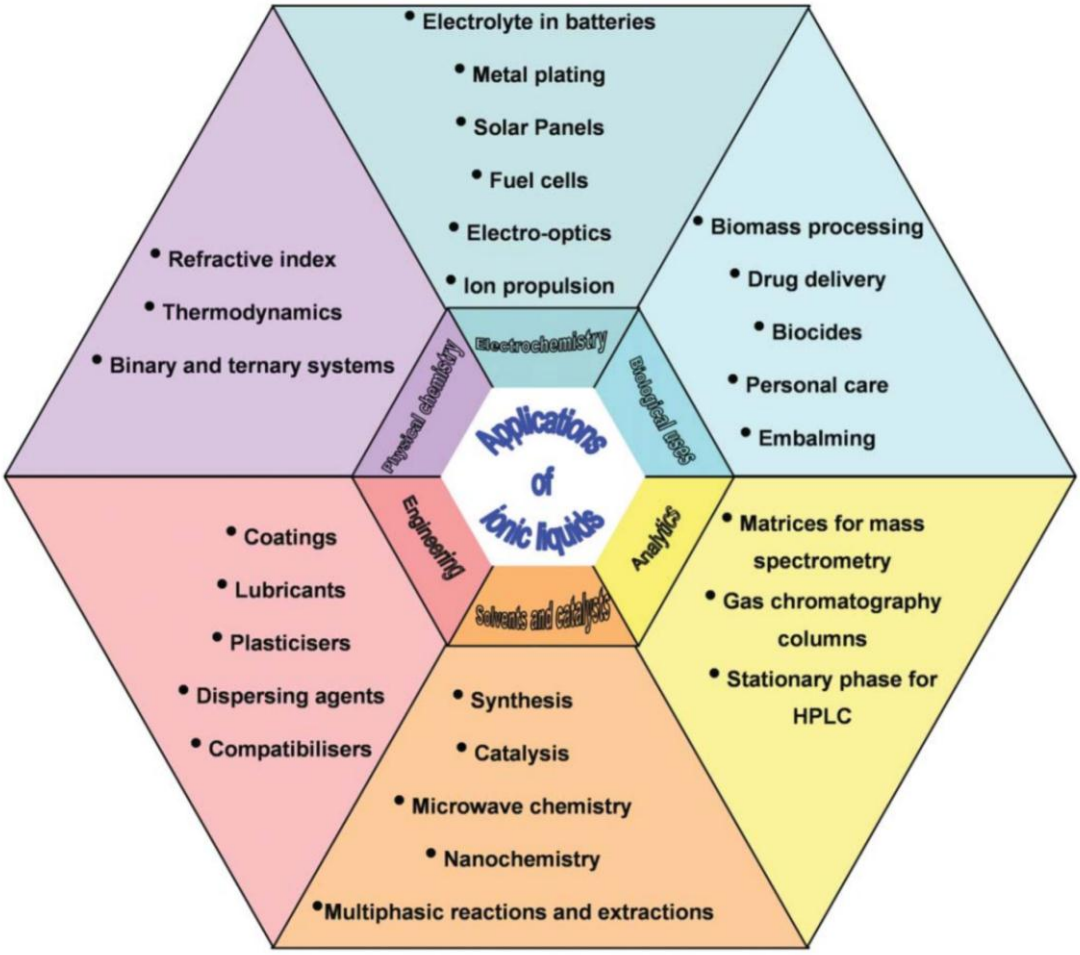

Figure 1-2. Predicted future applications of ionic liquids[1]

Table 1-1. Common properties of ILs.

Physical Property	Value
Freezing point	Preferably below 100˚C
Liquid range	Often > 200˚C
Thermal stability	Usually high
Viscosity	Normally < 100 cP
Polarity	Moderate
Specific conductivity	Usually < 10 $mS \cdot cm^{-1}$
Solvent and/or catalyst	Excellent for many organic reactions
Vapor pressure	Usually negligible

1.2.1 Melting Point

The melting points of ILs are different from typical salts such as sodium chloride that has a very high melting point of 801˚C.[2] Cations and anions in NaCl are small, spherical and of similar size and they pack well next to each other, which contributes to extremely strong coulomb forces. In general, but not exclusively cations in ionic liquids are large and asymmetric compared to the most commonly used anions, resulting in low lattice energies, thus in turn resulting in low melting points.

1.2.2 Conductivity

Specific conductivities of different liquids from 10^{-8} to 4 $S \cdot cm^{-1}$ are shown in Table 1-2. ILs have moderate specific conductivities, usually one order of magnitude lower than those of aqueous electrolytes and five orders of magnitude higher than water, therefore ILs are potential alternatives to common electrolytes.

Table 1-2. Specific conductivities of liquids (25˚C)[3]

Liquids	**Specific Conductivity ($S \cdot cm^{-1}$)**
NaCl	3.88 (900˚C)
$[C_4py][BF_4]$	0.0019
$[C_2mim][NTf_2]$	0.0057
H_2O	4×10^{-8}
KCl (0.1 M aq.)	0.013
H_2SO_4	0.0104

The ionic conductivity is affected by the diffusion rate of charged ions within the liquid itself. If the rate of diffusion within an IL is high, then the ions are able to move

faster, hence allowing charges to be transported through the liquid faster than if the rate of diffusion is low.

1.2.3 Viscosity

The rate of diffusion is inversely proportional to the viscosity of an IL. In less viscous ILs, ions are able to move more freely in comparison to ILs with high viscosity. As such, viscous ILs will exhibit lower ionic conductivity than less viscous ILs. In general, a low viscosity is desired for solvent applications in order to increase mass transfer rates, while higher viscosities may be favourable for other applications such as lubrication or for use in supported membrane separation processes.

In general, the viscosity of ILs is orders of magnitude greater than that of water and most common molecular solvents. For various types of cations and anions, the viscosities of ILs vary widely. Figure 1-3 shows the viscosities of common ILs. The IL whose cation has the longest alkyl chain has the highest viscosity. The viscosities of ILs comprising the same cation and different anions generally follows this order: $[CH_3COO]^-$ > $[PF_6]^-$ > $[C_1SO_4]^-$ > $[C_2SO_4]^-$ > $[BF_4]^-$ > $[OTf]^-$ > $[NTf_2]^-$ (shown in figure 1-3). This viscosity change may be due to the effect of the anions' ability to form weak hydrogen bonds with the cation.[4] The $[NTf_2]^-$ based ILs combine better charge delocalization with greater chain flexibility, which increases the chain mobility so that the viscosity is lower than that of other anion based ILs.[5] In general, ILs having highly symmetric or almost spherical anions are more viscous.

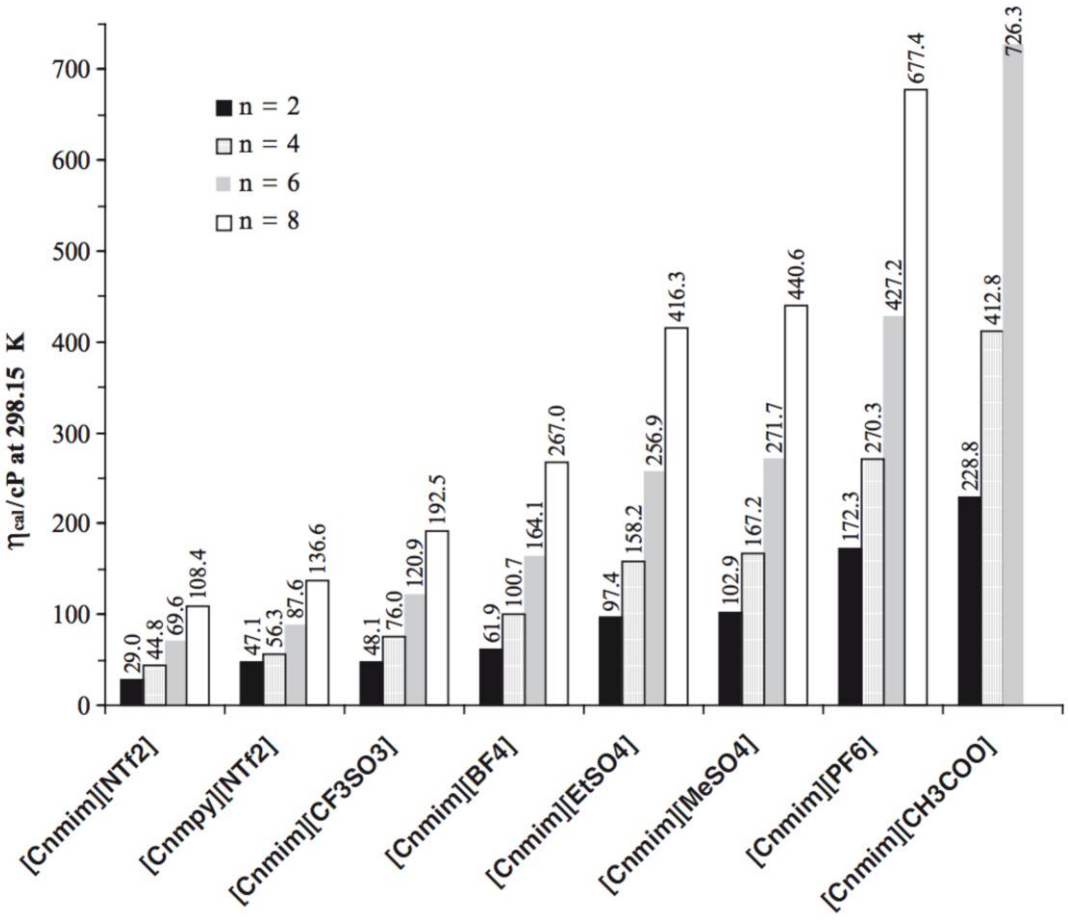

Figure 1-3. Viscosity at 298 K of common ILs as a function of chain length, *n*.[6]

The viscosity of pyridinium-based ionic liquids is greater than that of imidazolium-based ionic liquids, and lower than that of pyrrolidinium-based ionic liquids, for the ionic liquids having a common anion and a similar alkyl chain length on the cation.[7] This is in agreement with the result reported by Crosthwaite *et al.*[8] showing that pyridinium salts are generally more viscous that the equivalent imidazolium salts, as shown in figure 1-4.

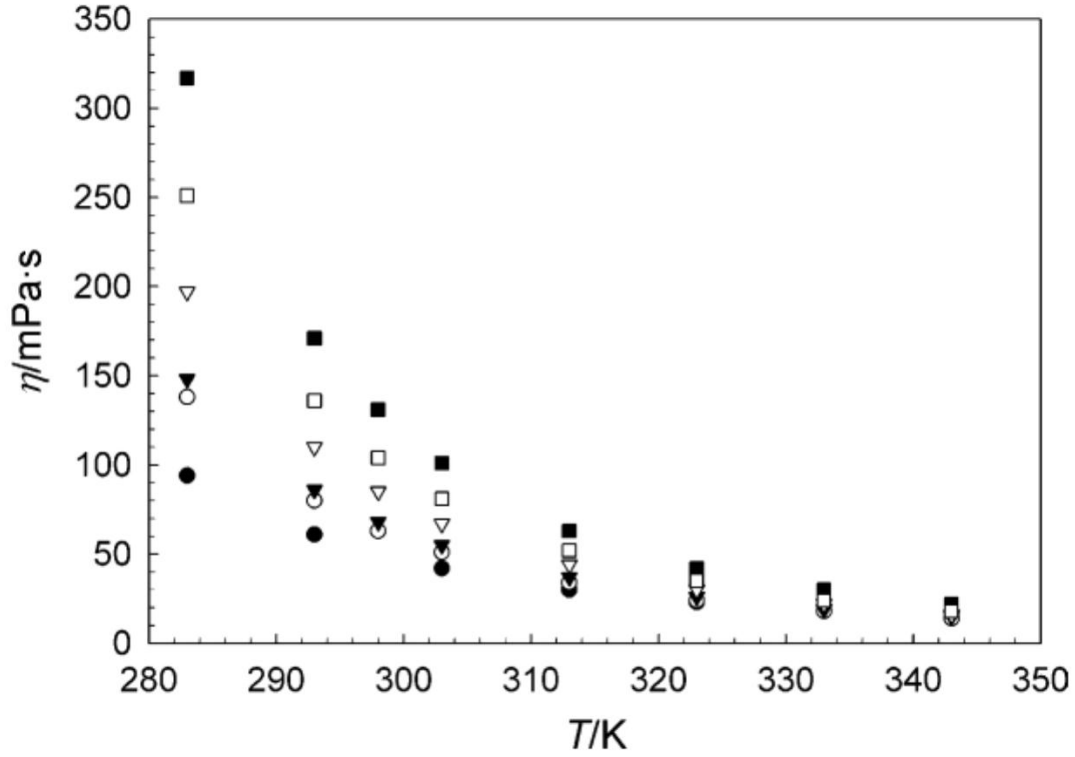

Figure 1-4. Comparison of the viscosity (η) of pyridinium- and imidazolium-based ionic liquids as a function of temperature: ●, $[C_4mim][NTf_2]$; ○, $[C_4m_{(3)}py][NTf_2]$; ▼, $[C_6mim][NTf_2]$; ▽, $[C_6m_{(3)}py][NTf_2]$; ■, $[C_6mmim][NTf_2]$; □, $[C_6mmpy][NTf_2]$.[8]

1.2.4 Density

Generally, the density decreases with temperature going up and increases with pressure increasing. In terms of density of ILs, an increase in the anion mass results in a density increase, and the density decreases with enlarging alkyl chain length in cation. The density of ionic liquids, composed of the same cation, follows the order: $[BF_4]^- < [OTf]^- < [PF_6]^- < [NTf_2]^-$. Figures 1-5 and 1-6 show experimental densities of ionic liquids based on $[C_4mim]^+$ and based on $[NTf_2]^-$, respectively.

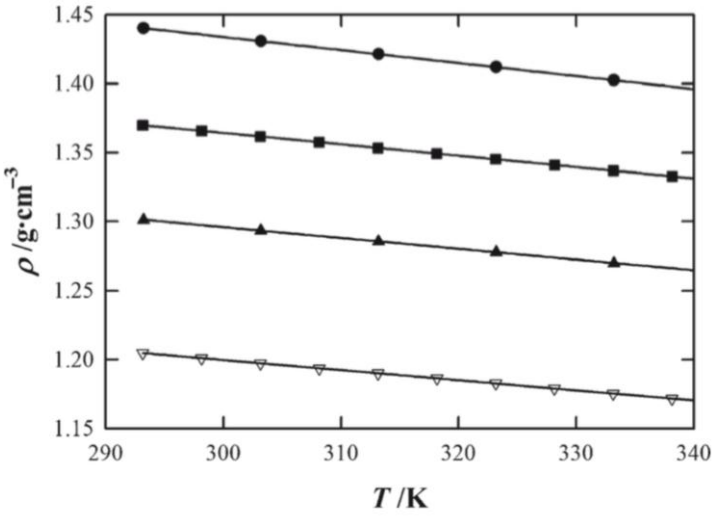

Figure 1-5. Comparison of the density of $[C_4mim]^+$ based ionic liquids as a function of temperature: ●, $[C_4mim][NTf_2]$; ■, $[C_4mim][PF_6]$; ▲, $[C_4mim][OTf]$; ▽, $[C_4mim][BF_4]$.[9]

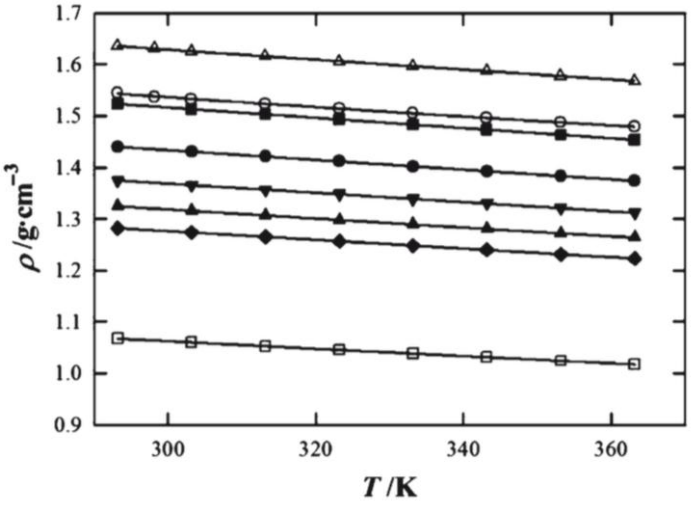

Figure 1-6. Comparison of the density of $[NTf_2]^-$ based ionic liquids as a function of temperature: ■, $[C_2mim][NTf_2]$; ●, $[C_4mim][NTf_2]$; ▼, $[C_6mim][NTf_2]$; ▲, $[C_8mim][NTf_2]$; ◆, $[C_{10}mim][NTf_2]$; ○, $[CNmpyrro][NTf_2]$; △, $[CNpy][NTf_2]$; □, $[P_{66614}][NTf_2]$.[9]

1.2.5 Mutual Solubility of Ionic Liquids and Molecular Solvents

Physical properties of ionic liquids include pure component properties and mixture properties. Density, viscosity, and melting point, described above, are pure component properties. The most important one among the various mixture properties is the phase behaviour of ionic liquids with other compounds. The use of ionic liquids into reactions, separations and materials processing requires a prior knowledge of the phase behaviour of ionic liquids in the mixture. During my PhD work, the mutual solubility of only binary systems (pure ionic liquid + molecular solvent) were studied and discussed herein.

The cation, the substituents on the cation, the anion, and the solvents have an effect on the mutual solubility of ionic liquids with other compounds. Crosthwaite *et al.*[10] reported the influence of the anion on the phase behaviour of imidazolium-based ionic liquids with alcohol. As shown in figure 1-7, the mutual solubility of $[C_4mim][NTf_2]$ with 1-butanol is greater than the solubility of the equivalent ionic liquid based $[BF_4]^-$ in 1-butanol, which is higher than that of $[C_4mim][PF_6]$. $[C_4mim][OTf]$ is miscible with alcohols (1-$C_nH_{2n+1}OH$, n = 2, 4, 6, and 8) at room temperature, and occurs a phase split with 1-dodecanol. While, $[C_4mim][DCA]$ is completely miscible with all the investigated alcohols. Therefore, the mutual solubility of imidazolium-based ionic liquids with alcohol follows the order: $[DCA]^- > [OTf]^- > [NTf_2]^- > [BF_4]^- > [PF_6]^-$. This fact results from the hydrogen bonding between the anion and the alcohol.

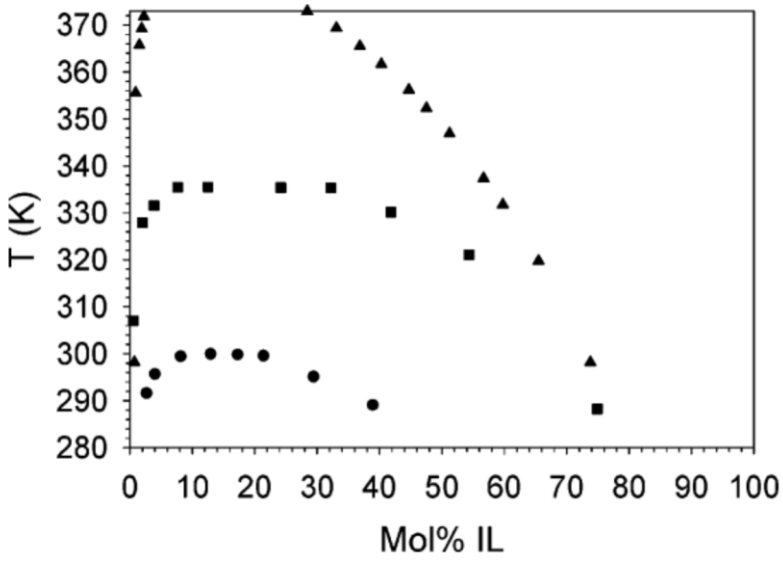

Figure 1-7. *T-x* diagram for $[C_4mim][NTf_2]$ (●), $[C_4mim][BF_4]$ (■), and $[C_4mim][PF_6]$ (▲) with 1-butanol.[10]

Increasing the alkyl chain length of the alcohols, the mutual solubility of the IL and alcohol decrease. For example, Heintz *et al.*[11] tested three systems, $[C_2mim][NTf_2]$ with 1-propanol, 1-butanol, and 1-pentanol, respectively (figure 1-8). This result corresponds to the increased hydrophobicity of alcohols with increasing alkyl chain length. Crosthwaite *et al.*[10] measured the mutual solubility of $[C_4mim][BF_4]$ with 1-butanol, 2-butanol, isobutanol, and tert-butyl alcohol (figure 1-9). The increase in alkyl branching resulted in higher dissolution of the ionic liquid compared with the corresponding linear alcohol. This was thought due to the reduced infinite dilution activity coefficient of the branched alcohols.[12,13]

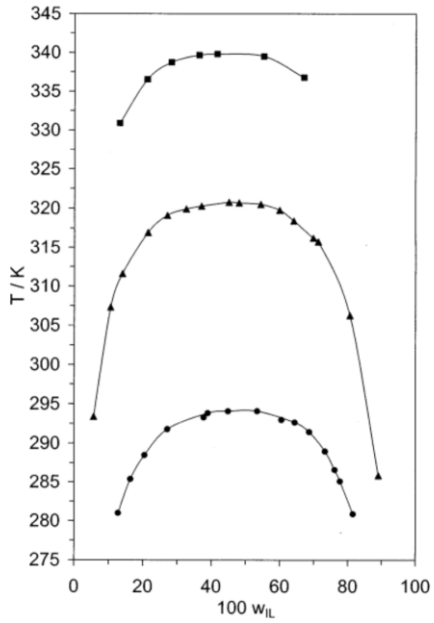

Figure 1-8. *T-w* diagram for $[C_2mim][NTf_2]$ with 1-propanol (●), 1-butanol (▲), and 1-pentanol (■).[11]

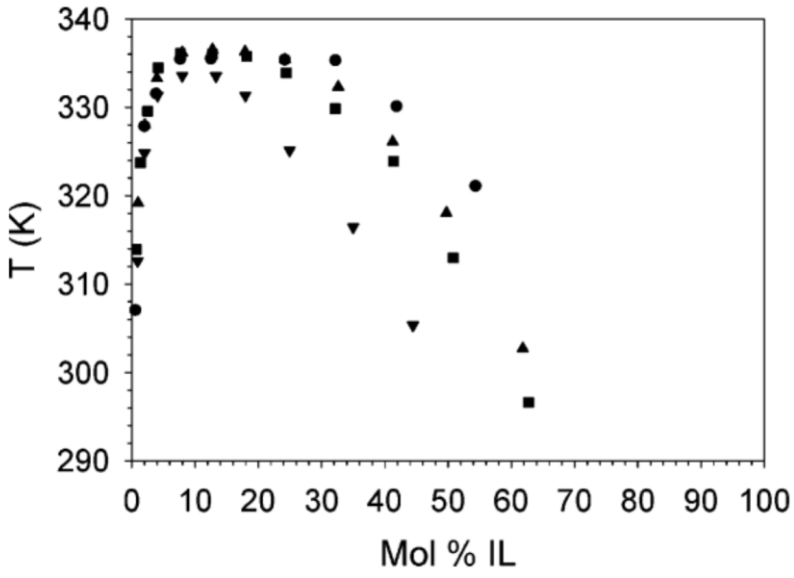

Figure 1-9. *T-x* diagram for $[C_4mim][BF_4]$ with 1-butanol (●), 2-butanol (■), isobutanol (▲), and tert-butyl alcohol (▼).[10]

With increase of the chain length on the cation, the van der Waals interactions increase between the alkyl chain on the cation and the alkyl chain on the alcohol,[14] which is

responsible for the enhancement of the mutual solubility of IL with alcohols. Figure 1-10 shows the comparison between the $[C_4m_{(3)}py][NTf_2]$ and $[C_6m_{(3)}py][NTf_2]$ with 1-hexanol.

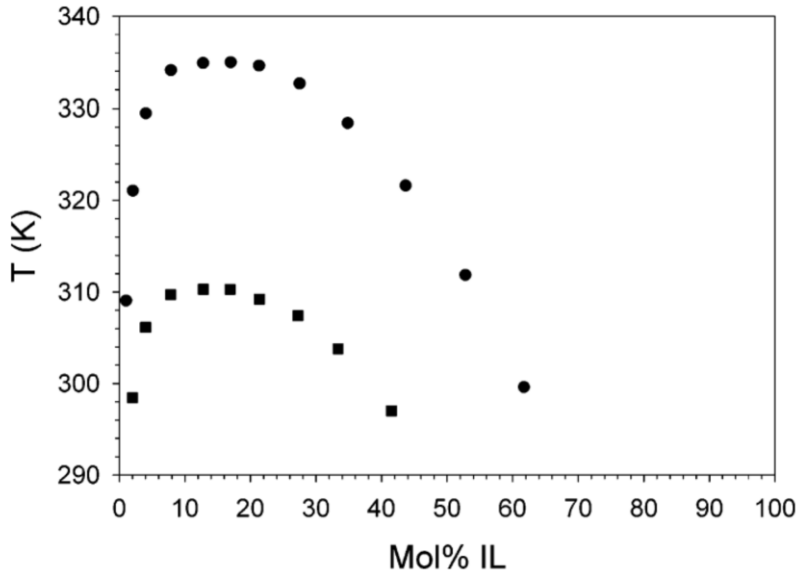

Figure 1-10. *T-x* diagram for $[C_4m_{(3)}py][NTf_2]$ (●) and $[C_6m_{(3)}py][NTf_2]$ (■) with 1-hexanol.[15]

Generally, polar hydrocarbons are quite soluble in ILs *a contrario* of most of non-polar hydrocarbons, which are less soluble in ILs. This can be explained by the 'like dissolves like' principle, as ILs are extremely polar molecules. Figure 1-11 shows the comparison of the mutual solubility of a polar and associative liquid (*i.e.* ethanol) or a non-polar liquid (*i.e.* toluene) with an IL (*i.e.* $[C_4m_{(2)}py][BF_4]$). This clearly shows that the mutual solubility between ethanol and $[C_4m_{(2)}py][BF_4]$ is greater than that between toluene and $[C_4m_{(2)}py][BF_4]$, mainly due to the stronger polarity of ethanol. However, as the aliphatic character of ILs increases (i.e. increase of van der Waals forces), an enhancement of the solubility of the non-polar hydrocarbon is generally

observed as exemplified in Figure 1-12.

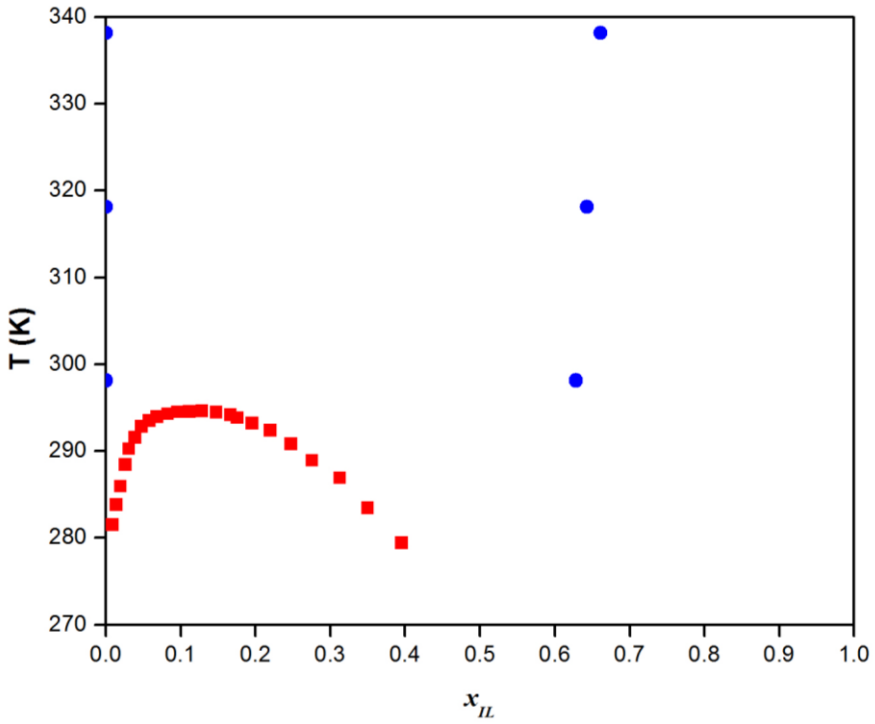

Figure 1-11. *T-x* diagram for $[C_4m_{(2)}py][BF_4]$ with ethanol (■) and toluene (●).

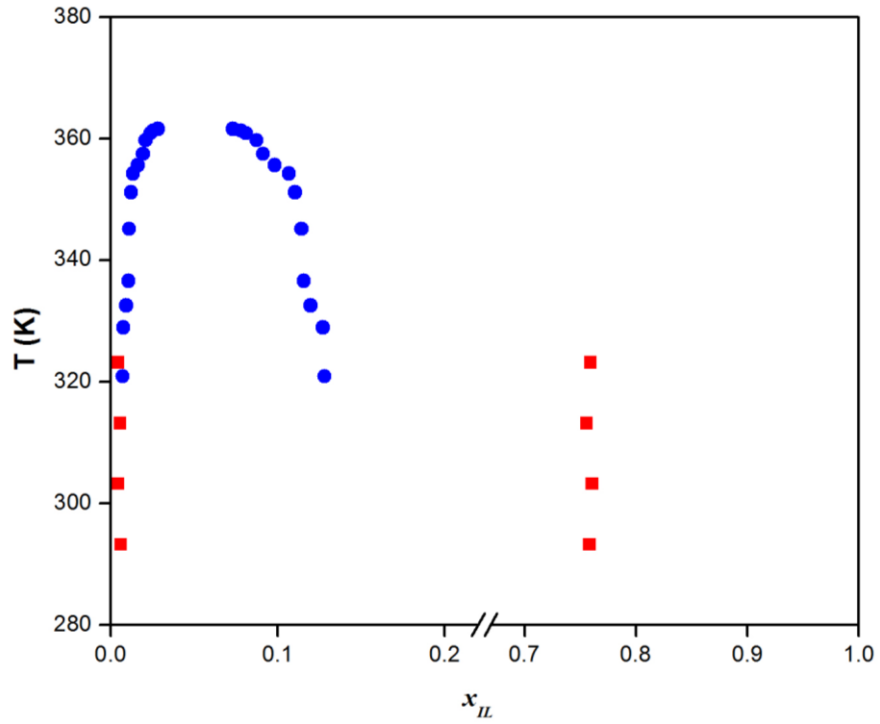

Figure 1-12. *T-x* diagram for $[C_2mim][SO_4]$ (■) and $[P_{i(444)1}][Tos]$ (●) with toluene.

Furthermore, it is very well reported that the mutual solubility of water and $[C_nmim]^+$ based ILs decreases with an increase of the alkyl chain length on this cation.[16] This behaviour can also be referred to a net change on the cohesive energy of this ILs series driven by an increase of the van der Waals forces with the alkyl chain length. Figure 1-13 shows an example of the mutual solubility between water and $[C_nmim][PF_6]$ (*n* = 4, 6, and 8) reported in the literature,[16] which clearly indicates the order of the solubility of ILs in water: $[C_4mim][PF_6] > [C_6mim][PF_6] > [C_8mim][PF_6]$.

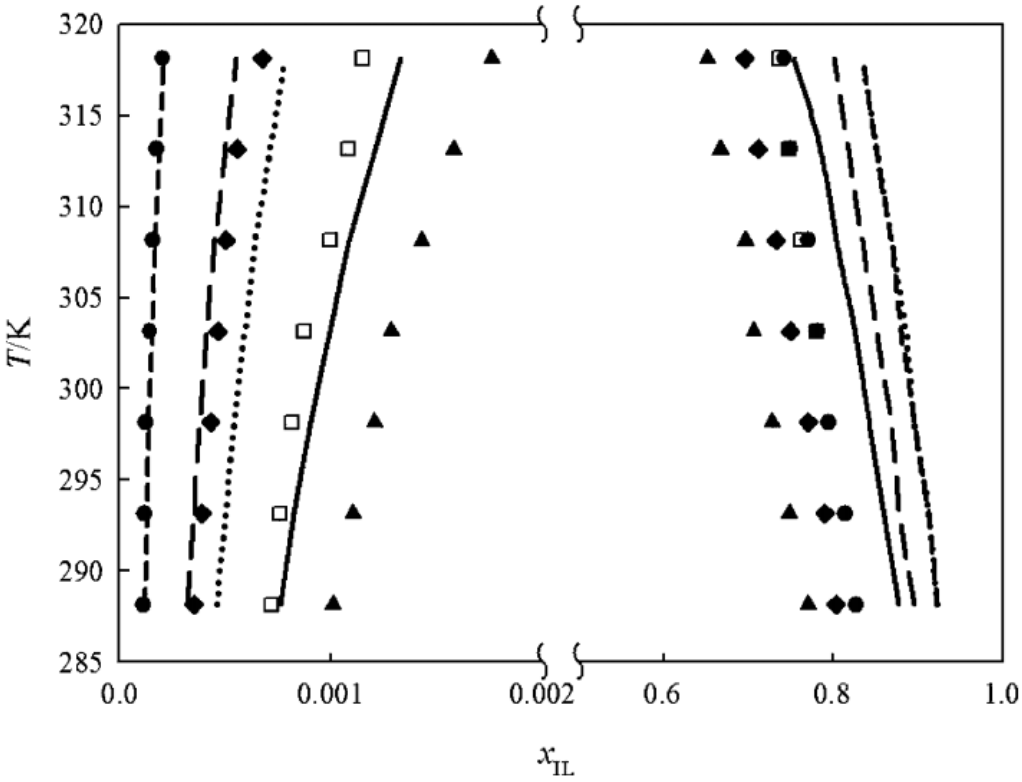

Figure 1-13. Liquid-liquid phase diagram for water and ILs: (▲) (-), $[C_4mim][PF_6]$; (◆) (--), $[C_6mim][PF_6]$; (●) (---), $[C_8mim][PF_6]$; (□) (●●●●), $[C_4C_1mim][PF_6]$. The single symbols and the solid lines represent, respectively, the experimental data and COSMO-RS predictions.[16]

1.3 Effects of Impurities

The requirement for the purity of an IL depends on its application. This is because the impurities within the IL may have a dramatic effect on the specific properties[17–22].

Of all the possible impurities within an IL, water and halides are the most common ones. Impurities can originate from the starting materials used to synthesize an IL, the synthesis procedure, or through the take up of water from air. Therefore, in order to minimize impurities, and maximize the purity of an IL, it's better to remove impurities from the starting materials, select a method of synthesis that brings in few side reactions and accommodates the easy separation of impurities from samples.

The impact of chloride on the density and viscosity of ILs have been studied by Seddon *et al*.[17] In this study, with an increase of chloride concentration, exponential growth of viscosity occurred to the IL, [C_4mim][BF_4], and a nonlinear decrease in density was caused to the same IL, as shown in figure 1-14.

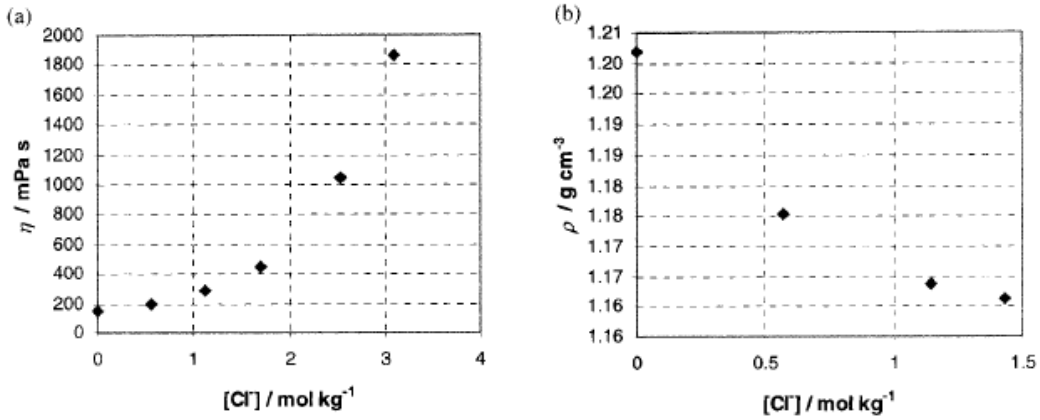

Figure 1-14. Viscosity (a) at 20˚C and density (b) at 30˚C of [C_4mim][BF_4] as a function of chloride concentration.[17]

With regards to the effect of water on the density and viscosity of ILs, Jacquemin *et al.*[23] measured and compared dry and water saturated samples at various temperatures. As can be seen in the figure 1-15, water decreases the density of ionic liquids by 1% - 2%. The difference is almost negligible compared with the difference of viscosities resulted from water. The presence of water dramatically affects the viscosities of ILs, shown in figure 1-16. For example, the viscosity of dry $[C_4mim][PF_6]$ at 293.59K is 375.9 mPa · s and that of saturated one at almost the same temperature is 84.8 mPa · s. The presence of water causes the viscosity of $[C_4mim][PF_6]$ to decrease by a magnitude greater than four. As the temperature increases, the difference in viscosity between the dry and saturated samples is less than that observed at lower temperatures. The effect of water on the viscosity is greatest at low temperatures, which also can be seen in figure 1-16.

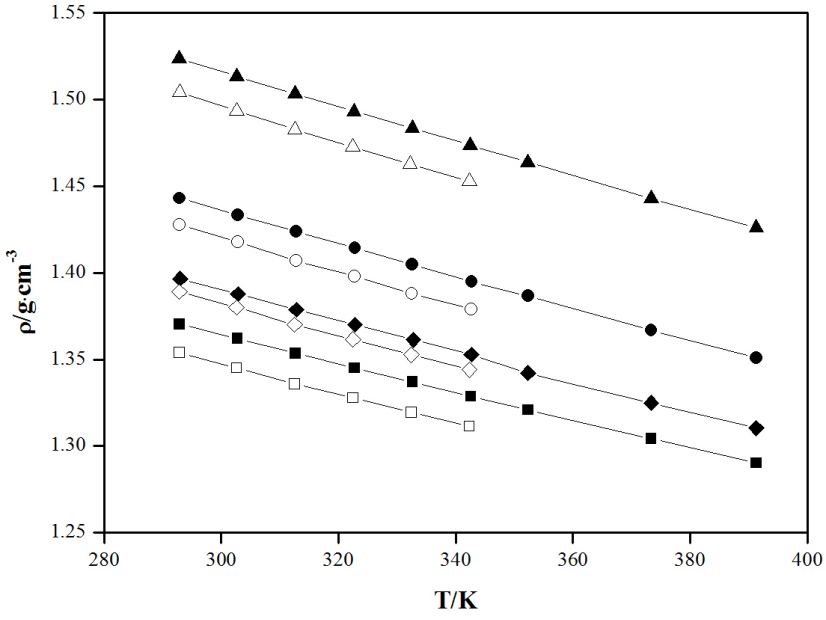

Figure 1-15. Experimental densities of dried (filled symbol) and water saturated (empty symbol) ILs as a function of temperature at atmospheric pressure: (a)

[C_4mim][PF_6], (□■); (b) [C_4mim][NTf_2], (○●); (c) [N_{1114}][NTf_2], (◇◆); (d) [C_2mim][NTf_2], (△▲).[23]

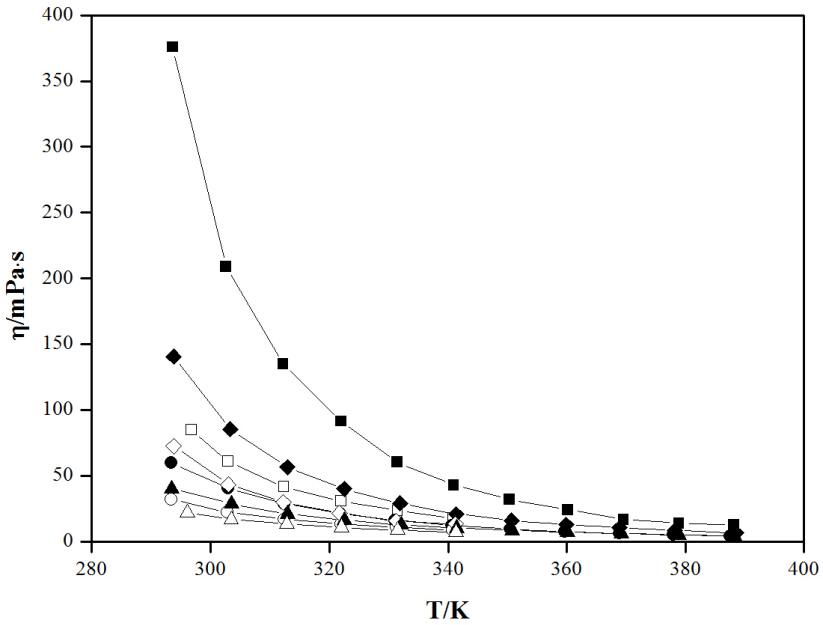

Figure 1-16. Experimental viscosities of dried (filled symbol) and water saturated (empty symbol) ILs as a function of temperature at atmospheric pressure: (a) [C_4mim][PF_6], (□■); (b) [C_4mim][NTf_2], (○●); (c) [N_{1114}][NTf_2], (◇◆); (d) [C_2mim][NTf_2], (△▲).[23]

1.4 The Advantage of Evaluation/Correlation

The properties of ionic liquids can be fine-tuned by varying the combination of anions and cations contained within, in order to suit a particular application. For instance, by modifying the structure of the cation with different substituent groups, the cation-anion interactions in solution are affected leading to different solvation properties of the IL in mixture with other fluids.[24,25] However, due to approximately 10^{18} cation-anion combinations existing,[26] there are a seemingly endless number of

theoretically possible ILs. Therefore, it would be impractical, time consuming, and highly costly to search for an IL that is suitable for a specific application through trial-and-error. In addition, the necessary experimental data for many properties is scarce and often inconsistent in literature.

However, evaluation and correlation is a faster, more efficient, and a cheaper alternative to find particular ILs with key desired attributes. Various estimation methods have been developed. There exists a great variety of analytical expressions that allow correlation and evaluation the properties of liquids. Such expressions are usually based on the use of adjustable parameters for each fluid (correlations), on the corresponding state principle (semi-empirical and predictive), and on group contribution methods (semi-empirical and predictive). However, these types of generalized correlations and models were not developed for ILs from the beginning and have not been thoroughly adapted and tested for their appropriateness and accuracy for ILs.

To develop evaluation methods to estimate properties of ionic liquids, methods already known for molecular liquids can be extended and applied into the properties of ILs.

1.5 State of the Art

1.5.1 Volumetric Properties Prediction of Ionic Liquids in the Literature

Different methods have already been reported in the literature to estimate the density and molar volume of ionic liquids over a broad range of temperature and pressure. These methods are mainly based on i) the group contribution model (GCM), ii) the

equation of state (EoS), iii) the quantitative structure-property relationship (QSPR) model, iv) the artificial neural network (ANN), and vi) simple correlations between density and other physical properties.

Ye and Shreeve[27] proposed the use of group contribution method for the density correlation of ionic liquids. The volume parameters of groups and fragments in ionic liquids were estimated at ambient temperature and reference pressure. These estimated volume parameters were used to evaluate the density of 59 ionic liquids, with a mean absolute deviation of 0.007 g·cm^{-3}. Then Gardas and Coutinho[28] made an extension of the method reported by Ye and Shreeve,[27] allowing the estimation of ionic liquid density over a wide range of temperature (273.15-393.15 K) and pressure (0.1-100 MPa) with a good agreement.

Rebelo and co-workers[29] defined the molar volume (V_m) of an IL as the sum of the effective molar volumes of the constituent cation and anion (V^*_{cation} and V^*_{anion}). This concept was also reported by Slattery *et al.*[30] to calculate the molar volume of unknown ILs and thus correlate with other physical properties. Rebelo and co-workers[29] proposed an "ideal" volumetric behaviour for a series of 1-C_n-3-methylimidazolium-based ionic liquids, that the molar volume (V_m) is linearly dependent on the number of CH_2 groups in the alkyl chain. Based on the assumption of the "ideal" volumetric behaviour, Jacquemin *et al.*[9,31] developed a group contribution model by correlating the effective molar volumes of ions using a Tait-type equation. This model established by Jacquemin *et al.*[9,31] evaluated the ionic liquid densities of over 5080 data points over a wide temperature range (273 to 423 K) and a broad

pressure range (0.1 to 207 MPa) within 0.36%.

The functional group contributions were taken into account in some group contribution methods.[32–34] However, differences existed in the definition of functional groups. For example, Lazzús *et al*.[34] divided each IL into three parts: cation core, substituents attached to the cation core, and the whole anion. Qiao *et al*.[33] defined each IL as a combination of cation center, substituents attached to the cation center, and functional groups making up of the anion. Paduszyński *et al*.[32] reported that each IL was composed of three basic elements: cation core, anion core, and substituents attached to the cores.

Qiao *et al*.[33] selected 51 groups to establish the GCM. The density of each IL as a function of temperature and pressure was a sum of the contributions of all included groups dependent on the temperature and pressure. The temperature and pressure dependences of contributions for each group were estimated respectively by correlation of 7,381 data points for 123 ILs. However, only 188 data points of three ILs were used to test the quality of this model. It still needs further investigation to prove its applicability.

Lazzús *et al*.[34] expressed the molar volume of IL (298.15 K and 0.1 MPa) as a summation of the contributions of all involved groups. Thus, the density was calculated as the molecular weight divided by the molar volume. Lazzús *et al*.[34] described the temperature and pressure dependence of density using a linear equation. The developed linear model estimated 3,530 data points for 310 ILs within 0.73%.

Paduszyński *et al.*[32] estimated the contributions of 177 functional groups at reference temperature (298.15 K) and reference pressure (0.1 MPa). The molar volume of IL (298.15 K and 0.1 MPa) was the sum of contributions of all functional groups occurring in the IL, and thus the density (298.15 K and 0.1 MPa) was calculated. Then the density as a function of temperature at 0.1 MPa was represented using a linear equation, and the density at high pressure was correlated using a Tait-type equation. This work estimated 16,830 densities for 1028 ILs with an observed RAAD% of 0.51%.

Besides the group contribution methods, another approach is the correlation between the density and other physical properties of ionic liquids. Bandrés *et al.*[35] calculated the molar volume of each ionic liquid from its refractive index by means of the Lorentz-Lorenz relation and estimated the density based on its surface tension using the parachor parameter model.

Recently, various equations of state (EoS) have been developed by some researchers to predict the density of ionic liquid. Ji and Adidharma[36] described the density of imidazolium-based ionic liquids, over a temperature range (293.15 to 415) K and a pressure range up to 650 bar using heterosegmented statistical associating fluid theory (hetero-SAFT) with the deviation better than 0.9%. Only imidazolium-based ionic liquids were examined using this theory, thus limiting the applicability of this theory to other cation-based ionic liquids. Alavianmehr *et al.*[37] reconstructed an ion contribution equation of state (EoS) based on the electrolyte perturbation theory to model the volumetric properties of ILs with an average deviation of about 0.64%. Each ionic

liquid was divided into two charged hard-spheres representing the cation and anion. Some density data were required for the optimization of the hard-sphere diameter and the non-bonded interaction energy. Shen *et al*.[38] made an extension of the Valderrama and Robles group contribution model for the critical properties to predict the density of ionic liquids using the Patel-Teja (PT) equation of state (EoS). Therein, 918 data points at ambient temperature and atmospheric pressure were correlated with a global relative average absolute deviation (RAAD) of 4.4%. This method may lead to large errors for the density prediction up to high pressures.

Lazzús *et al*.[39] proposed a method combining a simple group contribution model and an artificial neural network (ANN). Therein, 2,410 density data of 250 ILs were used to train the ANN method and 773 experimental data points for 72 other ILs were compared with the predicted ones with an RAAD lower than 0.5%. The same author[40] also reported a quantitative structure-property relationship (QSPR) method containing 11 descriptors to correlate 2,465 experimental data and predict 555 data points with accuracy of 2%.

Ten QSPRs was applied by Trohalaki *et al.*[41] to predict the density of bromide based ionic liquids. Each QSPR used by Trohalaki *et al.*[41] only had a single descriptor, providing accurate density prediction for 13 bromide salts.

Palomar *et al*.[42] performed for the first time COSMO-RS calculations to predict the density and molar volume of ionic liquids at 298 K and atmosphere pressure. COSMOtherm software was used to achieve this simulation. As the prediction only

carried on a single temperature and pressure, this approach has not been inferred yet.

1.5.2 Viscosity Prediction of Ionic Liquids

A variety of methods have been reported for the prediction/correlation of the ILs viscosities.[43–63] Some methods, based on the different equations, provide the correlation of viscosity, which describes the exponential behaviour and the temperature dependency, such as the Vogel-Fulcher-Tamman (VFT) equation,[44–46] the Litovitz equation,[46,47] the Arrhenius equation,[46,48] the fluidity equation,[46] the power law equation[49] and the Daubert and Danner correlation.[48]

The VFT equation provide information near the ideal glass transition temperature, which can be used to analyse the dynamical divergence in the temperature dependence on the viscosity, for example.[64] The Arrhenius equation principle is related to the activation energy theory, which gives an estimation of the energy needed by the ions to move freely in the solution. Both equations also contain information of the property at infinite temperature, which can be used to probe the effect of ions structures on the transport properties of the ILs, for example.[45] It was also proposed to consider the fluidity instead of the viscosity, which seems to vary rather smoothly with the temperature.[49] The power law equation provides also information of the crossover temperature in which a transition (from fragile to strong) takes place for the liquid.[49] According to the comparisons of the fitting results by different equations in literature,[46,48,49] the best fit for ILs is by using the VFT equation (due to mathematical and physical meanings). Therefore, the VFT correlation equation was selected to

represent the temperature dependence on the viscosity of ILs during this work.

Evaluation methods for the viscosity can be categorized as either a group contribution method (GCM)[43,50–53] or as a quantitative structure-property relationship (QSPR).[54–61] Gardas *et al.*[43] and Daniel *et al.*[51] developed a group contribution method based on the Orrick-Erbar model[65] to evaluation the ILs viscosity. The Orrick-Erbar model requires density data for the evaluation of the viscosity. To overcome this limitation and to attempt the development of an improved viscosity model with lower deviations in estimated viscosities, Gardas *et al.*[53] proposed a new group contribution method based on the Vogel-Fulcher-Tammann (VFT) equation. Gharagheizi *et al.*[52] employed a total of 46 sub-structures in addition to the temperature to evaluate the ILs viscosity. Lazzús and Pulgar-Villarroel[50] estimated the viscosity of ILs using an improved Andrade-type approach that is a linear combination of the contribution of groups in the cation and the anion.

Other approaches reported in the literature to describe the ILs viscosity are based on the Statistical Association Fluid Theory (SAFT) equation of state (EoS)[62,63]. Polishuk[62] modelled the viscosity of ILs using SAFT-Cubic equation of state coupled with two models, free volume theory (FVT) and modified Yarranton-Satyro (MYS) correlation. In spite of the unsatisfactory results of free volume theory, the modified Yarranton-Satyro correlation predicted the viscosity of two families of ILs ($[C_n mim][PF_6]$ and $[C_n mim][BF_4]$) with an appropriate accuracy. Furthermore, Abolala *et al.*[63] modelled the viscosity of pure imidazolium ILs ($[C_n mim][PF_6]$, $[C_n mim][BF_4]$, and $[C_n mim][NTf_2]$) using SAFT-VR-Mie equation of state coupled

with three models, namely frictional theory (FT), free-volume theory (FVT) and modified Yarranton-Satyro (MYS) correlation. The result showed that the MYS model calculated the viscosity more precisely than the FVT and FT models. Additionally, a comparative result from the SAFT-Cubic EoS proposed by Polishuk[62] showed that the performance of SAFT-VR-Mie EoS was better than the SAFT-Cubic EoS.

1.5.3 Liquid-liquid Equilibrium Prediction of Ionic Liquids

In recent years, the liquid-liquid equilibrium in systems including ionic liquids has been modelled by many groups. In general, those methods are based on: 1) the excess Gibbs energy; or the 2) equation of state.

Those based on the excess Gibbs energy include: *UNI*versal *QU*asi chemical *A*ctivity *C*oefficient (UNIQUAC), *UNI*versial *F*unctional *A*ctivity *C*oefficient (UNIFAC), *N*on-*R*andom *T*wo *L*iquids (NRTL), and electrolyte *N*on-*R*andom *T*wo *L*iquids (e-NRTL). E-NRTL is a modification of the NRTL model, which includes a Debye–Hückel term, to consider the long range forces. Therefore, e-NRTL is more appropriate for systems containing electrolytes.[66]

Arce[67] fitted the LLE data of a ternary system ([C_4mim][OTf], ethanol and TAEE) at 298.15 K within 0.32%. Aznar[68] correlated the LLE data (184 tie-lines) for 24 ternary systems by the NRTL model (Renon and Prausnitz,[69] 1968) with a global deviation of 1.4%. Hu *et al.*[70] correlated two ternary systems ([C_2OHmim][BF_4] or [C_2OHdmim][BF_4], water and 1-Butanol), leading to 0.01 root-mean-square deviation.

Meindersma *et al.*[71] correlated four ternary mixtures of toluene, n-heptane with the ILs ([C_2mim][C_2SO_4], [C_4mim][C_1SO_4], [$C_4m_{(4)}$py][BF_4], or [C_1mim][C_1SO_4]). The same values of the binary interaction parameters between toluene and n-heptane in these four systems were used. The deviations of the correlations are generally below 0.015. 12 tie lines for the system ([C_2mim][C_2SO_4], TAEE and ethanol) were correlated by means of the NRTL model with satisfactory results of 0.429%.[72] Domańska and Marciniak[73] modeled binodal curves of 8 binary systems containing the same ionic liquid ([C_4mim][$MDEGSO_4$]), with the deviation of all cases lower than 0.001.

Banerjee *et al.*[74] made a comparison between the fitting results by UNIQUAC and NRTL for 7 ternary systems involving ILs, showing that the room mean square deviation obtained with UNQUAC decreased by 40% compared to the NRTL model. Simoni *et al.*[75] simulated LLE data in ternary systems that contain ILs, using NRTL, e-NRTL, and UNIQUAC methods. The binary interaction parameters used to predict ternary LLE were estimated solely from binary LLE measurement data. The authors concluded that both UNIQUAC and e-NRTL provided potentially better results than NRTL. However, Maia *et al.*[66] evaluated the NRTL and e-NRTL equations by comparing the correlations of two binary systems (water and [C_6mim][BF_4] or [C_8mim][BF_4]). The dependence of the binary interaction parameters with temperature was quadratic. In that work, the calculated values using both models showed a good agreement at low temperature, but NRTL model provided a better prediction result near the upper critical solution temperature (UCST). Haghtalab and Paraj[76] correlated 36 ternary systems with 12 ionic liquids using the NRTL and UNIQUAC model with

1.85% and 2.15% of root mean square deviation (RMSD) respectively. Santiago *et al*.[77,78] correlated 91 liquid-liquid equilibrium of ternary system including 687 tie-lines with 1.75% of average deviation based on the UNIQUAC model.

The same authors[79,80] also correlated 39 liquid-liquid equilibrium of ternary ionic liquid based systems including 324 tie-lines with 1.6% of RMSD based on the UNIFAC model.

Those methods based on the equation of state, such as Peng-Robinson EoS, Non-Random Hydrogen-Bonding (NRHB) EoS, Statistical Associating Fluid Theory (SAFT-type) EoS, and Cubic Plus Association (CPA) EoS, are commonly reported in recently years.

The Non-Random Hydrogen-Bonding (NRHB) model was reported to describe the phase behaviour of binary systems with $[C_n\text{mim}][NTf_2]$.[81] This model is a non-electrolyte equation-of-state model. The main novelty of NRHB model is that all electrostatic interactions (ionic, polar, hydrogen bonding, and Lewis acid-base interactions) were treated as strong specific interactions. This method was able to correlate LLE data with a good agreement but overpredicted the critical point.

The liquid-liquid phase equilibrium of binary systems ($[C_3\text{mpip}][NTf_2]$ and $C_nH_{2n+1}OH$, n = 5, 6, ⋯, 11) was modelled with non-random hydrogen bonding (NRHB) and perturbed-chain polar statistical associating fluid theory (PCP-SAFT), respectively.[82] Neither model provides accurate correlation in the alcohol-rich phase. The PCP-SAFT model generally yields a better correlation result than NRHB,

according to the mean deviation of 0.057 for NRHB and 0.039 for PCP-SAFT. However, NRHB does more accurate description for the USCT.

Moreover, the same author, Paduszyński, noticed that the influence of the Gross-Vrabec term in the SAFT model on pure properties of ILs could be negligible. Thus, Paduszyński and Domańska[83] reported a modified method, PC-SAFT, to describe the phase behaviour of 10 binary systems composed of $[C_3mpip][NTf_2]$ or $[C_4mpip][NTf_2]$ and aliphatic hydrocarbons, resulting in a relative average absolute deviation of 4.1%. These ten binary systems were modelled using NRHB as well, within 3.5% deviation.

The correlation of LLE for binary systems (ester and protic IL) was performed using the Peng-Robinson EoS, coupled with the Wong-Sandler mixing rule.[84] The activity coefficient involved in the Wong-Sandler mixing rule was calculated using the COSMO-SAC activity coefficient model. However, the deviation of 132.5% for modelling the low concentration of IL in the organic phase was not satisfactory.

Maia *et al.*[85] for the first time applied the Cubic Plus Association (CPA) EoS method into the systems containing ionic liquids. However, the result, for the description of LLE of ionic liquids with water, showed deviations ranging from 4 to 100%. Therefore, more work is required to investigate the capability of this method for LLE with ionic liquids.

Another approach, having been reported is COSMO-RS. Ferreira *et al.*[86] proposed an overview for the LLE of ternary systems modelling including ionic liquid and

aromatic and aliphatic hydrocarbons by using the COSMO-RS method. It presented root-mean-square-deviation values around 5−6% and a priori screening ability of ILs to be used in separations of aliphatic−aromatic hydrocarbons mixtures. The COSMO-RS method, based on computational quantum mechanics and the dielectric continuum model, is a priori predictive method. In the COSMO-RS method, molecules are divided into segments, which were calculated from quantum mechanics simulation and represented the molecules and the charge density distribution around them (σ-profile). From these sigma profiles, the COSMO-RS based method quantifies the interactions between the surfaces and takes into account the possibility of forming hydrogen bonds.[87,88]

In comparison, the UNIFAC method takes into account the interactions between functional groups and it requires experimental data to regress interaction parameters between the groups, while the COSMO-RS based method calculates the activity coefficient by considering interactions between the charge of each segment on the molecule. This allows the COSMO-RS based method to calculate the real mixture behaviour based on the sigma profiles of the components only, leading to the fact that it does not require any experimental data to predict the activity coefficients. However, it does not always give satisfactory results, because the COSMO-RS method is so universal that it has to rely on the assumption that the complex behaviour of liquid mixtures can be calculated from only a few simple and universal equations and empirical constants. Thus, the UNIFAC method normally gives more satisfactory results than the COSMO-RS method.

1.6 Outline of the Thesis

The aim of my PhD thesis is to develop semi-empirical models to evaluate the physical properties of ionic liquids, such as their volumetric properties as a function of temperature and pressure; their viscosity as a function of temperature as well as their equilibrium when mixed with another liquid (LLE).

A database for the density of ionic liquids was established by collecting more than 16,092 experimental data points of 81 different ionic liquids over a broad temperature range (217 to 473) K and a wide pressure range (0.1 to 207) MPa from the literature. Experimental data of ILs were measured by several different research groups. Discrepancies in the experimental data affect the quality of the correlation and thus the development of the proposed model. Mathematical gnostics was used to analyse data to recommend a dataset for each ionic liquid. These recommended datasets were used to establish a group contribution model for the estimation of the volumetric properties of ILs. Among these recommended data, 5,399 data points of 54 ILs were correlated to obtain the volumetric parameters of 31 cations and 24 anions. Additionally, 2,522 data points of another 27 ILs were used to compare with the evaluated values. The RAAD of correlation is lower than 0.005% and the RAAD of pure evaluation is close to 0.96%. This model is able to estimate the volumetric properties with an excellent agreement with RAAD being 0.31%. Furthermore, the mechanical coefficients were calculated by using the thermodynamic formalism.

A database for the viscosity of ILs were established by collecting 2,765 data points for

70 ILs from the literature. A new method based on the UNIFAC-VISCO model was developed for the estimation of viscosity of pure ILs, and then binary mixtures of ILs.[89] Then 25 different ILs with high purity were selected to prove the feasibility of this novel method. The binary interaction parameters α_{mn} and VFT parameters of ions were estimated. The calculated viscosities showed a good agreement with the experimental data with RAAD lower than 1.7% for all the 25 ILs. The estimated binary interaction parameters were used for the evaluation of binary mixtures of ILs following the same methodology. Experimental data of four binary systems were selected. One dataset for each binary system was correlated to obtain the binary interaction parameters ($\alpha_{cation/cation}$ or $\alpha_{anion/anion}$) and the other data were used for comparison with the pure evaluated values. The estimation result for these four binary mixtures was highlighted by the RAAD value of being 5%.

Then an extension of the proposed model for viscosity have been developed. Mathematic gnostics was used first to analyse data and recommend dataset for each IL. Originally, 154 experimental data of the selected 25 ILs were used.[89] These datasets were substituted by the recommended ones to estimate the corresponding binary interaction parameters and the VFT parameters. Then based on these parameters, binary interaction parameters and ions VFT parameters for another 45 ILs were optimized using their recommended dataset. Totally 819 data points describing the viscosity as a function of temperature for 70 ILs were correlated by using the modified UNIFAC-VSICO model to obtain an extended set of binary interaction parameters and ions VFT parameters, with a good accuracy close to 1.4%. Furthermore, a database for

the viscosity of binary mixtures of ILs was established by collecting 966 data points of eleven binary systems, as a function of the mole fraction of components (x_i = 0.0495 to 0.9552). The estimated binary interaction parameters were used for the evaluation of binary mixtures of ILs following the same methodology, showing a good agreement with RAAD lower than 3.8%.

In addition, a LLE database for 142 ionic liquids in 128 solvents was compiled by collecting 6948 data points from 131 articles. The LLE data was uploaded into a user-friendly web based interface, including 718 tie-line (*x*-*x*-*T*) data points and 5,512 *x*-*T* data points. The tie-line data have been modelled using UNIFAC and UNIQUAC methods. Data analysis has been done based on the mathematical gnostics.

Chapter 2
Methodology

2.1 Tait Equation

The Tait equation is an equation of state, used to fit liquid density data over a wide pressure range.[90] The Tait equation was used to fit the IL density as a function of temperature and pressure

$$\rho_{IL}(T,p,C,B) = \frac{\rho_{IL}(T,p_{ref})}{1-C\cdot\ln(\frac{B(T)+p}{B(T)+p_{ref}})} \quad (2\text{-}1)$$

where $\rho_{IL}(T,p_{ref})$ is the density at reference pressure, p_{ref}= 0.1 MPa.

$\rho_{IL}(T,p_{ref})$ is expressed as a quadratic equation,

$$\rho_{IL}(T,p_{ref}) = \sum_{i=0}^{2}(a_i\cdot(T)_{p_{ref}}^{i}) \quad (2\text{-}2)$$

and $B(T)$ is a second-order polynomial:

$$B(T) = \sum_{i=0}^{2}(B_i\cdot T^i) \quad (2\text{-}3)$$

The Tait parameters for each investigated IL are listed in Table 8-1.

2.2 The Group Contribution Model (GCM)

An extension of the group contribution model previously developed by Jacquemin *et al.*[9,31] has been developed to evaluate the molar volume of ILs as a function of temperature and pressure. This model is based on the 'ideal-volume' model assuming that the molar volume of the ionic liquid is a sum of the effective molar volume of cation and that of anion proposed by Rebelo *et al.*[29,91,92] as follows

$$V_{m_{IL}} = V_{cation}^{*} + V_{anion}^{*} \quad (2\text{-}4)$$

where $V_{m_{IL}}$ is the molar volume of the ionic liquid constituted by the cation with

effective molar volume V^*_{cation} and the anion with effective molar volume V^*_{anion}.

Second-degree polynomials (eq. 2-5) were identified as satisfactorily fit the variation of the ions effective molar volume with temperature.

$$V^*_{ion}(\delta T, p_{ref}) = \sum_{i=0}^{2}(D_i \cdot \delta T^i) \quad (2\text{-}5)$$

where $\delta T = (T - 298.15\ K)$ and D_i are the coefficients obtained by fitting the data at 0.1 MPa.

The ions effective molar volumes as a function of pressure were correlated using the equation:

$$V^*_{ion}(\delta T, p, G, H) = \frac{V^*_{ion}(\delta T, p_{ref})}{1 - G \cdot \ln\left(\frac{H(\delta T)+p}{H(\delta T)+p_{ref}}\right)} \quad (2\text{-}6)$$

where $V^*_{ion}(\delta T, p_{ref})$ is the reference effective molar volume calculated using eq. 2-5; and $p_{ref} = 0.1$ MPa. G is an adjustable parameter, and $H(\delta T)$ is a second-order polynomial;

$$H(\delta T) = \sum_{i=0}^{2}(H_i \cdot \delta T^i) \quad (2\text{-}7)$$

2.3 Mechanical Coefficients

The mechanical coefficients; the isothermal compressibility (κ_T) and the isobaric thermal expansion coefficient (α_p), were calculated by using the thermodynamic formalism. The calculation of these mechanical coefficients provides a valuable knowledge of the temperature and pressure dependence of the volumetric properties.

The isothermal compressibility, κ_T, is related to the variation of the density with

pressure

$$\kappa_T = \frac{1}{\rho}\left(\frac{\partial \rho}{\partial p}\right)_T \tag{2-8}$$

The isothermal compressibility can be calculated[93,94] using the Tait equation and eq. 2-8

$$\kappa_T = \left(\frac{C}{B+P}\right)\left(\frac{\rho}{\rho(T,p_{ref})}\right) \tag{2-9}$$

The isobaric thermal expansion coefficient, α_p, is related to the variation of the density with temperature and is defined as;

$$\alpha_p = -\frac{1}{\rho}\left(\frac{\partial \rho}{\partial T}\right)_p \tag{2-10}$$

and the following expression[93,94] is derived from the Tait equation, eq. 2-1.

$$\alpha_p = -\left\{\frac{\left[\frac{d\rho(T,p_{ref})}{dT}\right]}{\rho(T,p_{ref})}\right\} + C\left\{\frac{\frac{dB}{dT}(P-0.1)}{\left[1-C\cdot\ln\left(\frac{B+P}{B+0.1}\right)\right](B+0.1)(B+P)}\right\} \tag{2-11}$$

2.4 Van der Waals Volumes (R) and Surface Area (Q) of Ions

The van der Waals volume is the volume occupied by an individual atom or molecule. For a spherical single atom, the van der Waals volume is the volume of the sphere, which can be calculated using its van der Waals radius. For a molecule, the van der Waals volume is determined by the volume enclosed by the van der Waals surface.[95] The molar van der Waals volume is different from the molar volume of the substance. The molar van der Waals volume only counts the volume occupied by the molecules, while the molar volume of the substance also accounts for the intermolecular empty

spaces between each molecules in the solution. Furthermore, the molar volume of the substance is temperature and pressure dependent. The UNIFAC-VISCO, UNIFAC, and UNIQUAC models require a priori knowledge of the van der Waals volumes (*R*) and surface area (*Q*) of functional groups. Volume and surface area for functional groups in traditional solvents were taken from Magnussen *et al*.[96] The cation and anion, constituting the ionic liquid, are regarded as individual groups in the UNIFAC method. Due to lack of the volumes and surface areas of ions, TURBOMOLE and COSMO*therm*X were used to simulate these parameters. It is necessary to optimize the molecular geometry through energy minimization before the determination of the volume and surface area of ions.

The optimised structure and conformers of each investigated ion were determined through quantum mechanical calculation using the TURBOMOLE (TmoleX version 4.1.1) program. The 3D coordinates of each atom constituting a given molecule or ion were firstly drawn in TURBOMOLE. Then its 3D geometry was optimized through energy minimization by using the basic set DFT-B3LYP-TZVP,[97] which led us to further obtain then the '.cosmo' (COSMO*therm*X)[98] file for each species which has been used during this thesis.

The COSMO files were then implemented into COSMO*therm*X (version C30_1301, release 01.13, COSMOlogic) to obtain the COSMO volumes and surface areas. The van der Waals volumes and surface areas were then approximated by the following eqs. 2-12 and 2-13

$$R = s \times V_i^{COSMO}/K_1 \quad (2\text{-}12)$$

$$l_i{}' = \frac{z}{2} \times (R - Q) - (R - 1)\ (\mathrm{z} = 10) \quad (2\text{-}13)$$

where $s = 0.9226$, $K_1 = 29.9802$, and $l_i' = 0$.

Volume and surface area for cations and anions are provided in Table 8-2.[99]

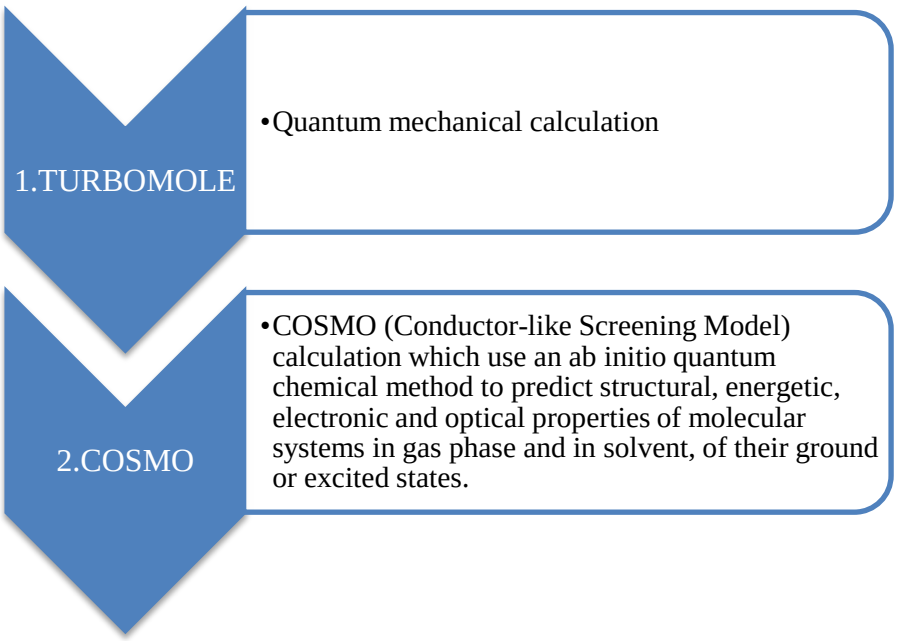

Figure 2-1. Procedure to generate the COSMO file

2.5 UNIQUAC model

The UNIQUAC model (short for *UNIversal QUAsi-Chemical*) is an activity coefficient model used in the description of phase equilibrium.[100,101] The UNIQUAC model also served as the basis for the development of the group contribution method UNIFAC. The liquid-liquid-equilibrium (LLE) of binary mixture (ionic liquid + solvent) has also been modeled using the UNIQUAC method, in my work.

The UNIQUAC model comprises two parts: a combinatorial contribution, which

accounts the molecules size and shape effects, and a residual contribution, that accounts for the energy interaction effects,[77,78] expressed as eq. 2-14.

$$ln\gamma_i = ln\gamma_i^C + ln\gamma_i^R \quad (2\text{-}14)$$

The combinatorial component of the activity is shown as below:

$$ln\gamma_i^C = ln\frac{\phi_i}{x_i} + \frac{z}{2}q_i ln\frac{\theta_i}{\phi_i} + l_i - \frac{\phi_i}{x_i}\sum_{j=1}^{n} x_j l_j \quad (2\text{-}15)$$

where θ_i and ϕ_i are the area fraction and segment fraction for the *i* molecule in the total system, respectively and are defined in eq. 2-16 and eq. 2-17. l_i is the pure component's parameters, as function of *r*, *q* and *z* values of component *i*, as shown in equation 2-18.

$$\theta_i = \frac{q_i x_i}{\sum_{j=1}^{n} q_j x_j} \quad (2\text{-}16)$$

$$\phi_i = \frac{r_i x_i}{\sum_{j=1}^{n} r_j x_j} \quad (2\text{-}17)$$

$$l_i = \frac{z}{2}(r_i - q_i) - (r_i - 1) \;\; (z = 10) \quad (2\text{-}18)$$

where *x*, r_i and q_i are the pure component's molecular van der Waals volumes and surface areas, respectively. *z* is the coordination number of the system as a constant having the value of 10. The parameters r_i and q_i are calculated based on the summation of functional group's volume and surface area parameters, R_k and Q_k for each molecule given by the following equations:

$$q_i = \sum_{k=1}^{N} n_{i,k} Q_k \quad (2\text{-}19)$$

$$r_i = \sum_{k=1}^{N} n_{i,k} R_k \quad (2\text{-}20)$$

where subscript k denotes the groups; $n_{i,k}$ is the total number of k^{th} group present in

component i; N is the total number of groups present; Q_k is the group surface area parameter; and R_k is the group volume parameter.

The residual term are defined as follows:

$$ln\gamma_i^R = -q_i' \ln\left(\sum_{j=1}^{n} \theta_j' \Psi_{ji}\right) + q_i' - q_i' \sum_{j=1}^{n} \frac{\theta_j' \Psi_{ij}}{\sum_{k=1}^{n} \theta_k' \Psi_{kj}} \quad (2\text{-}21)$$

$$\theta_i' = \frac{q_i' x_i}{\sum_{j=1}^{n} q_i' x_j} \quad (2\text{-}22)$$

For most of the substances, $q = q'$, except for water and some small alcohols, such as methanol and ethanol.

For each binary mixture, there are two adjustable parameters, Ψ_{mn} and Ψ_{nm}, which are given by

$$\Psi_{mn} = \exp(-\frac{\alpha_{mn}}{298.15}) \quad (2\text{-}23)$$

2.8 UNIFAC model

The *UNIversal Functional Activity Coefficient* (UNIFAC) model is a group contribution model proposed by Fredenslund *et al.*[102] This model provides valuable information on the liquid equilibrium and allows the calculation of the activity coefficients. The UNIFAC model was used to correlate the liquid-liquid-equilibrium (LLE) of the binary mixture (ionic liquid + solvent).

In a multi-component mixture, the UNIFAC equation for the activity coefficient of (molecular) component *i* is shown in Eq. 2-14.

$$ln\gamma_i = ln\gamma_i^C + ln\gamma_i^R \quad (2\text{-}14)$$

The combinatorial component of the activity is shown as below:

$$ln\gamma_i^C = ln\frac{\phi_i}{x_i} + \frac{z}{2}q_i ln\frac{\theta_i}{\phi_i} + l_i - \frac{\phi_i}{x_i}\sum_{j=1}^{n} x_j l_j \quad (2\text{-}15)$$

where θ_i and ϕ_i are the area fraction and segment fraction for the *i* molecule in the total system, respectively and are defined in eq. 2-16 and eq. 2-17. l_i is the pure component's parameters, as function of *r*, *q* and *z* values of component *i*, as shown in equation 2-18.

$$\theta_i = \frac{q_i x_i}{\sum_{j=1}^{n} q_j x_j} \quad (2\text{-}16)$$

$$\phi_i = \frac{r_i x_i}{\sum_{j=1}^{n} r_j x_j} \quad (2\text{-}17)$$

$$l_i = \frac{z}{2}(r_i - q_i) - (r_i - 1) \;\; (z = 10) \quad (2\text{-}18)$$

where *x*, r_i and q_i are the pure component's molecular van der Waals volumes and surface areas, respectively. *z* is the coordination number of the system as a constant having the value of 10. The parameters r_i and q_i are calculated based on the summation of functional group's volume and surface area parameters, R_k and Q_k for each molecule given by the following equations:

$$q_i = \sum_{k=1}^{N} n_{i,k} Q_k \quad (2\text{-}19)$$

$$r_i = \sum_{k=1}^{N} n_{i,k} R_k \quad (2\text{-}20)$$

where subscript k denotes the groups; $n_{i,k}$ is the total number of k^{th} group present in component i; N is the total number of groups present; Q_k is the group surface area parameter; and R_k is the group volume parameter.

The residual part of the activity coefficient term γ_i^R can be written for each i component of the system containing n number of functional groups to be shown as

follows:

$$ln\gamma_i^R = \sum_{k=1}^{n} v_k^{(i)}(ln\Gamma_k - ln\Gamma_k^{(i)}) \quad (2\text{-}24)$$

where, Γ_k is the group residual activity coefficient, and $\Gamma_k^{(i)}$ is the residual activity coefficient of an isolated group *k* in a reference solution comprising only of molecules of type *i*. Both Γ_k and $\Gamma_k^{(i)}$ can be derived from the following equation:

$$ln\Gamma_k = Q_k[1 - ln\left(\sum_m \Theta_m \Psi_{mk}\right) - \sum_m\left(\frac{\Theta_m \Psi_{km}}{\sum_n \Theta_n \Psi_{nm}}\right)] \quad (2\text{-}25)$$

where, Θ_m is the segment fraction of group m over all different groups. Θ_m is calculated similar in form but not the same as θ_i. The equation is shown as below.

$$\Theta_m = \frac{x_m Q_m}{\sum_{i=1}^{N} X_i Q_i}, m = 1,2,3 \ldots N \quad (2\text{-}26)$$

where the subscripts represent the groups.

The group interaction, Ψ_{mn}, from eq. 2-25 is a measure of the interaction energy between groups. The calculation equation is given by:

$$\Psi_{mn} = \exp(-\frac{\alpha_{mn}}{298.15}) \quad (2\text{-}23)$$

2.5 Vogel-Fulcher-Tamman (VFT) Equation

The most popular viscosity model is the Vogel-Fulcher-Tamman (VFT) equation, which originally was used to describe the temperature dependence on the transport properties of glass-forming liquids.[103–105] To date, the VFT equation is also widely used for the ILs. According to the literature,[46,48,49] the VFT equation provides the best temperature dependence correlation for ILs, this has been concluded through a comparison of its fitting performance with those obtained using different equations:

such as Litovitz,[46,47] Arrhenius,[46,48] and the Daubert and Danner equations,[48] for example. In our study, the VFT equation is used to describe the dependence of viscosity on the temperature for ionic liquids or ions:

$$\mu_\alpha = A \cdot \exp[\frac{B}{T-T_0}] \quad (2\text{-}27)$$

where α stands for an ionic liquid or ion; A, B, and T_0 are the fitting parameters.

2.6 UNIFAC-VISCO model

The UNIFAC-VISCO model is based on the theory of Eyring and the UNIFAC group contribution model proposed by Fredenslund *et al.*[102] and developed by Chevalier *et al.*[106,107] This model is used to predict the viscosity of liquid mixtures originally.

The core equation of the UNIFAC-VISCO model is defined as:[106–108]

$$\ln(\mu) = \sum_{i=1}^{N_C} x_i \ln\left(\mu_i \cdot \frac{V_i}{V_m}\right) + \frac{g_c^E}{\mathcal{R}T} - \frac{g_r^E}{\mathcal{R}T} \quad (2\text{-}28)$$

where μ is the mixtures viscosity (mPa·s); subscript i represents the component; N_C is the total number of components; x_i is the mole fraction of the component i. V_i is the molar volume ($m^3 \cdot kmol^{-1}$) of the pure component i while V_m is molar volume ($m^3 \cdot kmol^{-1}$) of the mixture. $\mathcal{R}$ is the gas constant ($J \cdot mol^{-1} \cdot K^{-1}$), T is temperature (K). g_c^E and g_r^E are the combinatorial and the residual contribution terms of the UNIFAC-VISCO method, respectively.

The combinatorial contribution term is described as follows:

$$\frac{g_c^E}{RT} = \sum_i x_i ln \frac{\phi_i}{x_i} + \frac{z}{2} \sum_i x_i q_i ln \frac{\theta_i}{\phi_i} \quad (2\text{-}29)$$

where z is a coordinate value equal to 10. x_i is the mole fraction of the component i.

ϕ_i is the molecular volume fraction of component i; q_i represents the van der Waals' surface area of component i; and θ_i is the molecular surface area fraction of component i.

θ_i and ϕ_i can be obtained by the following the equations 2-16 and 2-17:

$$\theta_i = \frac{x_i q_i}{\sum_j x_j q_j} \tag{2-16}$$

$$\phi_i = \frac{x_i r_i}{\sum_j x_j r_j} \tag{2-17}$$

where subscript i and j represent the components. q_i and q_j represent the van der Waals' surface area of components i and j, respectively. r_i and r_j represent the van der Waals' volume of components i and j, respectively.

The surface area (q) and the volume (r) can be determined by following the equations 2-19 and 2-20:

$$q_i = \sum_{k=1}^{N} n_{i,k} Q_k \tag{2-19}$$

$$r_i = \sum_{k=1}^{N} n_{i,k} R_k \tag{2-20}$$

where subscript k denotes the groups; $n_{i,k}$ is the total number of k^{th} group present in component i; N is the total number of groups present; Q_k is the group surface area parameter; and R_k is the group volume parameter.

The residual contribution term is described as follows:

$$\frac{g_r^E}{RT} = \sum_{i=1}^{N_C} x_i \left[\sum_{m=1}^{N} n_{m,i} (\ln \gamma_m - \ln \gamma_{m,i})\right] \tag{2-30}$$

where N_C is the total number of components; x_i is the fraction of component i in the mixture; N is the total number of groups; n_m and γ_m refer to the group values in mixture and $n_{m,i}$ and $\gamma_{m,i}$ refer to the group values in pure-component.

$\ln \gamma_m$ represents the residual activity coefficient and is defined as:

$$\ln \gamma_m = Q_m \left[1 - \ln\left(\sum_{i=1}^{N} \Theta_i \Psi_{i,m}\right) - \sum_{i=1}^{N} \frac{\Theta_i \Psi_{m,i}}{\sum_{j=1}^{N} \Theta_j \Psi_{j,i}}\right] \tag{2-31}$$

where N is the total number of groups present; Θ_i represents the area fraction for group i; and $\Psi_{m,i}$ represents the group interaction parameters.

The Θ values for each group both in mixture and in pure component can be calculated using the eq. 2-26:

$$\Theta_m = \frac{x_m Q_m}{\sum_{i=1}^{N} X_i Q_i}, m = 1,2,3 \dots N \quad (2\text{-}26)$$

where the subscripts represent the groups.

The group interaction parameters (Ψ) are then calculated as follows:

$$\Psi_{mn} = \exp(-\frac{\alpha_{mn}}{298.15}) \quad (2\text{-}23)$$

where α_{mn} are group interaction potential energy parameters between the groups m and n. It is important to note that the values for the group interaction parameters α_{mn} and α_{nm} are not the same, giving rise to non-reflexive parameters.

2.7 Marquardt Optimization

The binary interaction parameters and VFT parameters in the UNIFAC-VISCO model were optimized by minimizing the objective function using the Marquardt optimization technique.[109]

$$OF = \frac{1}{M}\sum_{i=1}^{M}(\frac{\mu_{exp}-\mu_{cal}}{\mu_{exp}})^2 \rightarrow min \quad (2\text{-}32)$$

where M is the number of data points; μ_{exp} and μ_{cal} are the experimental and calculated viscosity data, respectively.

Chapter 3
Volumetric Properties

3.1 Data Treatment

3.1.1 Data Collection

The experimental density data of ionic liquids over a temperature range from 217 to 473 K and a pressure range from 0.1 to 207 MPa were collected from the literature data. NIST standard reference database[110] is the primary source for the collection of thermophysical data of ILs. However, references checking is still required to make sure our database was without errors. the A database was created containing over 16,092 experimental densities for 81 ILs. Table 8-3 in the appendix presents an overview of all the experimental data, summarizing the references where data for each IL were collected, the number of data points, temperature and pressure range.

3.1.2 Data Analysis

The experimental data of ILs were measured by several groups. Discrepancies in the experimental results affect the quality of the correlation and thus the development of the proposed model. Mathematical gnostics was utilized to analyse data and recommendation dataset for each IL. For ILs of which its experimental densities were reported by only one reference, recommended dataset could thus not be obtained by mathematical gnostics and the given set was then considered as the recommendation dataset.

Mathematical gnostics is a novel paradigm of uncertainty.[111] This axiomatic theory is built upon the theory of measurement and based on principle laws of nature such as the special theory of relativity and thermodynamics. The properties of each individual

measurement are analysed, and properties of a data sample are obtained by their aggregation. The results are thus valid even for small data samples because, unlike in statistics, the extrapolation from an infinite to a finite data sample is not required. Besides, the data are let to speak for themselves; there is no prior assumption on the distribution function of errors, but it is estimated during data analysis. It is possible to describe both unimodal and multimodal distribution using the same approach. The global distribution function was evaluated for each density data sample. The probable value located on the maximum distribution density and the marginal intervals were analysed to clarify the precise data, less accurate data and outliers in the data sample.

Herein, we give an example of data analysis of $[C_8mim][BF_4]$. Table 3-1 shows the references, the number of data points, temperature range, and pressure range for density data of $[C_8mim][BF_4]$.

Table 3-1. The References, Number of Data Points, and Temperature Range at 0.1 MPa and > 0.1 MPa, Respectively, and Pressure Range for Experimental Density Data of $[C_8mim][BF_4]$.

N_{data} (0.1 MPa)	$\Delta T_{0.1\ MPa}$	N_{data} (> 0.1 MPa)	$\Delta T_{>0.1\ MPa}$	ΔP	Ref.
9	283.15-323.15	108	283.15-323.15	0.1-60	[112]
6	298.2-343.2	13	298.2-323.2	0.1-206.94	[113]
11	293.15-393.15	66	293.15-393.15	0.1-10	[114]
4	293.15-353.15	16	293.15-353.15	0.1-20	[115]

*N_{data}, No. of data points. ΔT, temperature range (K). ΔP, pressure range (MPa).

The Tait equations (eqs. 2-1 and 2-2) were used to fit the density data from each reference, respectively. The Tait parameters of $[C_8mim][BF_4]$ are presented in Table

3-2 together with the relative average absolute deviations (RAAD) of the fits.

The relative average absolute deviation (RAAD) is defined as:

$$RAAD = \frac{1}{M}\sum_{i=0}^{M}\left|\frac{x_{exp}-x_{cal}}{x_{exp}}\right| \quad (3\text{-}1)$$

where M is the number of data points, x_{exp} and x_{cal} are the experimental and calculated values of properties, respectively.

Table 3-2. Tait Parameters a_0, a_1, a_2, B_0, B_1, B_2, and C from Equations 2-1 and 2-2 Used to Fit the Experimental Densities of $[C_8mim][BF_4]$ Reported by Each Reference and the Relative Average Absolute Deviations (RAAD) of the Fit.

Ref.	a_0 g·cm^{-3}	a_1 g·cm^{-3}·K^{-1}	a_2 g·cm^{-3}·K^{-2}	RAAD %	B_0 MPa	B_1 MPa·K^{-1}	B_2 MPa·K^{-2}	C	RAAD %
[112]	1.3330	-8.53E-04	2.88E-07	0.001	99.48	4.9956	0.0811	3.7832	0.102
[113]	1.2341	-3.16E-04	-5.42E-07	0.028	100.00	4.9914	0.1030	3.7836	0.599
[114]	1.4660	-1.62E-03	1.38E-06	0.007	99.53	4.9936	0.0509	3.7816	0.056
[115]	1.3433	-9.15E-04	3.75E-07	0.007	98.91	4.996	0.0594	3.7805	0.101

The calculation process is completed using the least square method in MATLAB software. The Tait parameters for all the other ILs are given in the table 8-1 of the appendix.

As any thermodynamic property, the density depends on the pressure and temperature, the analysis of the density data by mathematical gnostics should be done under identical conditions. Herein, we calculated the density values at temperatures of (273.15, 303.15, 333.15, and 363.15 K) and pressures of (0.1, 20, 40, and 60 MPa) based on the Tait correlations using the experimental data from different references.

Then mathematical gnostics was used to analyse data samples at each identical condition. The calculated densities values of $[C_8mim][BF_4]$ at these temperatures and pressures are shown in table 3-3. For each data sample, the location of the maximum distribution (Z_O) was estimated. The lower bound and the upper bound of the data support (LB and UB), the typical data (Z_L and Z_U), and the tolerance interval (Z_{OL} and Z_{OU}) were also analysed (presented in table 3-4). Z_O locating at the maximum of the global distribution function is the most probable value. A value within the tolerance interval (Z_{OL} and Z_{OU}) is said to be "in tolerance". A value within the range of typical data (Z_L and Z_U) and outside the tolerance interval is deemed to be "typical". A value within the data support (LB and UB) and outside the interval of typical data is said to be "possible" and is less precise measurement. A value outside the bounds of the data support is improbable.

Traditionally the domain of the distribution function is infinite, from minus infinity to plus infinity in the additive model, or from zero to plus infinity in the multiplicative model. However, physical quantities cannot have infinite values, and they are always bounded although the bounds are not known in advance. We assume that the density is only between the lower and upper bounds (LB and UB). Such definition agrees with the definition of the distribution function in statistics. A weighted empirical distribution function is then built from the experimental data and the gnostic distribution function is fitted to it. Three parameters are optimized, namely a scale parameter S_c and both bounds LB and UB.

Statistics offers several parameters that can be used for representation of a data set, a

mean value, a mode (the most probable value), and a median (a quantile at probability equal to 0.5). If a distribution function is symmetric, which is a frequent case in classical (non-robust) statistical analysis, all these parameters coincide. The mean value is then used because it has important statistical properties. On the contrary, gnostic distribution functions are generally asymmetric. Thus, the most probable value (the mode) is the representation having the natural meaning because it is unbiased. Z_O is the location of the model. During data analysis, we first verify homogeneity of the data sample. If the data sample is not homogeneous, the outliers are discarded in order to obtain a homogeneous subsample. The distribution function then has a single maximum. Finding a unique maximum of a continuous, continuously differentiable function is then a simple task of functional analysis.

Z_O is an estimate of an ideal value which corresponds to the true value in statistics. Parameters Z_L, Z_{OL}, Z_{OU}, and Z_U are quantitative measures of uncertainty. They express sensitivity of Z_O to a value of a single additional value. If we extend the sample with a single datum Z', the new location of the model will be Z_O'. For $Z_O < Z' < Z_U$, the location of the model will satisfy $Z_O < Z_O' < Z_{OU}$. Owing to natural robustness of the gnostic estimator, this inequality will hold also for $Z' > Z_U$. The situation is analogical for $Z' < Z_O$. The location of the model is thus always bounded by inequality $Z_{OL} <= Z_O' <= Z_{OU}$. For this reason, $[Z_{OL}, Z_{OU}]$ is called "tolerance interval" because the most probable value always lies in this interval. The dependence of Z_O' on Z' behaves "typically" in the interval of $[Z_L, Z_U]$, which is called the "interval of typical data". The tolerance interval thus gives the repeatability of the

estimated most probable value, while the interval of typical data delimits the range where a single measured value should be expected. It is not necessary to repeat this trial-and-error search, an analytical equation can be derived. The derivation is shown in the book of Kovanic and Humber "The Economics of Information-Mathematical Gnostics for Data Analysis",[111] in section 16.4 "Interval analysis" starting at page 288, and the equations are given in corollary 17.1 at page 294. It implies from the derivation and its proof that the following inequality always holds: $LB < Z_L < Z_{OL} < Z_O < Z_{OU} < Z_U < UB$.

Table 3-3. The calculated densities of $[C_8mim][BF_4]$ based on the Tait correlations using the experimental data from different references

T/K	P/MPa	Calculated densities/g·cm^{-3}			
		Sanmamed *et al.*[112]	Gu *et al.*[113]	Gardas *et al.*[114]	Tomida *et al.*[115]
273.15	0.1	1.1215	1.1074	1.1255	1.1212
303.15	0.1	1.1009	1.0885	1.1007	1.1002
333.15	0.1	1.0808	1.0687	1.0783	1.0799
363.15	0.1	1.0612	1.0479	1.0584	1.0603
273.15	20	1.1328	1.1165	1.1418	1.1357
303.15	20	1.1101	1.0959	1.1140	1.1120
333.15	20	1.0884	1.0748	1.0893	1.0897
363.15	20	1.0676	1.0530	1.0677	1.0685
273.15	40	1.1444	1.1259	1.1586	1.1505
303.15	40	1.1195	1.1035	1.1276	1.1241
333.15	40	1.0961	1.0810	1.1006	1.0997
363.15	40	1.0740	1.0582	1.0772	1.0769
273.15	60	1.1562	1.1354	1.1758	1.1657
303.15	60	1.1290	1.1112	1.1415	1.1365
333.15	60	1.1039	1.0873	1.1121	1.1099
363.15	60	1.0806	1.0634	1.0868	1.0854

Table 3-4. Interval analysis of the data samples at each condition

T/K	P/MPa	LB	Z_L	Z_{OL}	Z_O	Z_{OU}	Z_U	UB
					$g \cdot cm^{-3}$			
273.15	0.1	0.9978	1.1099	1.1191	1.1213	1.1230	1.1253	1.1261
303.15	0.1	1.0125	1.0919	1.0998	1.1005	1.1007	1.1009	1.1009
333.15	0.1	0.9943	1.0710	1.0779	1.0793	1.0801	1.0807	1.0809
363.15	0.1	0.9664	1.0504	1.0580	1.0596	1.0604	1.0611	1.0613
273.15	20	0.9674	1.1196	1.1310	1.1343	1.1370	1.1413	1.1436
303.15	20	0.9873	1.0990	1.1091	1.1112	1.1125	1.1139	1.1142
333.15	20	1.0809	1.0883	1.0890	1.0893	1.0895	1.0897	1.0898
363.15	20	0.9586	1.0566	1.0665	1.0676	1.0682	1.0685	1.0685
273.15	40	0.9372	1.1296	1.1432	1.1477	1.1514	1.1577	1.1622
303.15	40	0.9609	1.1070	1.1188	1.1221	1.1245	1.1273	1.1284
333.15	40	0.9634	1.0851	1.0961	1.0985	1.0997	1.1006	1.1007
363.15	40	1.0444	1.0626	1.0742	1.0762	1.0769	1.0772	1.0772
273.15	60	0.9074	1.1398	1.1556	1.1613	1.1662	1.1744	1.1817
303.15	60	0.9349	1.1152	1.1287	1.1332	1.1366	1.1410	1.1433
333.15	60	0.9409	1.0915	1.1040	1.1076	1.1099	1.1119	1.1126
363.15	60	0.9247	1.0679	1.0806	1.0837	1.0854	1.0867	1.0870

For example, at 303.15 K and 40 MPa, the calculated value from the Tait correlation using the experimental data reported by Tomida *et al.*[115] is very close to Z_O and is the most precise. The values based on Sanmamed *et al.*[112] also show a good accuracy. The values based on Gu *et al.*[113] and Gardas *et al.*[114] are less precise measurements.

The residual between the density and the maximum location is a characterization of the measurement accuracy. The global deviation of residuals for one dataset is determined as eq. 3-2.

$$deviation = \sqrt{\frac{\sum_{i=0}^{N}(M-x_i)^2}{N}} \quad (3\text{-}2)$$

where N is the number of equally likely values, and M is the maximum location.

The data set with the smallest global deviation is recommended. The residual is not the difference between the maximum location and the experimental data, but the difference between the maximum location and the correlated densities. The calculated densities based on the Tait correlation using the data from each reference can represent the trend of the experimental data from this reference, due to excellently fitted parameters. Figure 3-1 indicates the deviation of the dataset for [C_8mim][BF_4] from each reference. It can be observed that the dataset measured by Harris *et al.*[116] perform better.

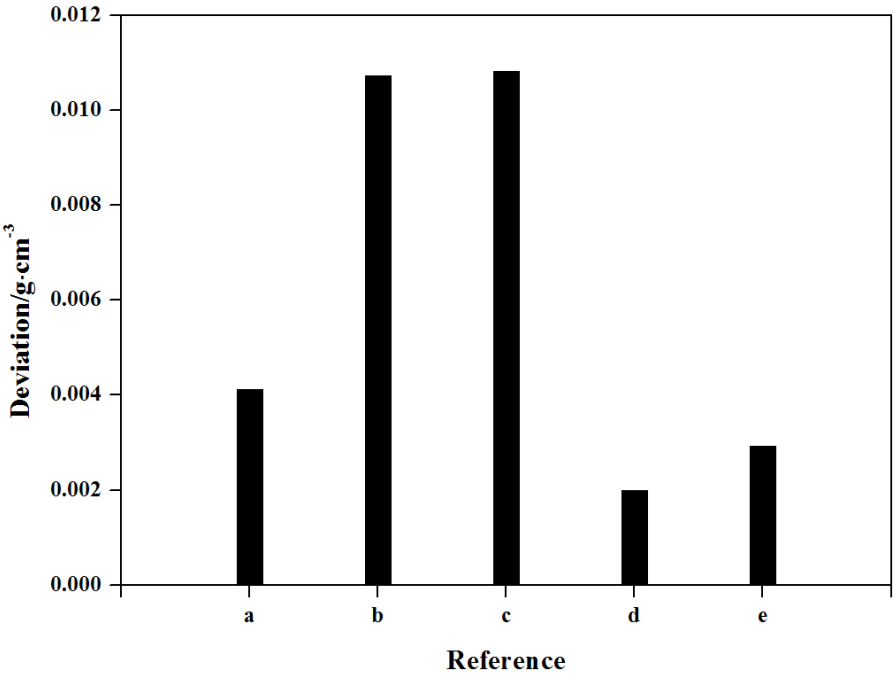

Figure 3-1. Global deviation of the dataset for [C_8mim][BF_4] from each reference: a) Sanmamed *et al.*[112] b) Gu *et al.*[113] c) Gardas *et al.*[114] and d) Tomida *et al.*[115]

The experimental density data of some ILs have been reported by only two references, which mean only two data points at each identical condition need to be analysed and compared. In this case, mathematical gnostics is not applicable, and the statistical analysis is adopted. Firstly, the experimental data collected from each reference were correlated to obtain the Tait parameters. Second, experimental data from both references were correlated altogether to obtain another set of Tait parameters. Then the calculated densities from the Tait correlations using the density data of each reference were compared with the calculated densities from the Tait correlation using both two sets of experimental data to recommend one set of them.

For example, Gołdon *et al.*[117] and Aparicio *et al.*[118] reported 34 and 168 experimental data points of $[C_1mim][C_1SO_4]$ as a function of pressure (0.1 – 25 MPa) and (0.1 – 60 MPa), respectively. The Tait parameters used to correlate each dataset and two sets altogether are listed in Table 3-5. Then the density values at temperatures of (273.15, 303.15, 333.15, and 363.15 K) and pressures of (0.1, 20, 40, and 60 MPa) were calculated using the three sets of Tait parameters separately and compared, shown in Figure 3-2. In figure 3-2, these estimated densities based on the correlation of experimental data from Aparicio *et al.*[118] show a better agreement than those based on the correlation of the data from Gołdon *et al.*[117] Therefore, the dataset reported by Aparicio *et al.*[118] is recommended.

Table 3-5. Tait parameters used to correlate the datasets for $[C_1mim][C_1SO_4]$.

Ref.	a_0	a_1	a_2	RAAD	B_0	B_1	B_2	C	RAAD
	$g \cdot cm^{-3}$	$g \cdot cm^{-3} \cdot K^{-1}$	$g \cdot cm^{-3} \cdot K^{-2}$	%	MPa	$MPa \cdot K^{-1}$	$MPa \cdot K^{-2}$		%
[117]	2.6207	-7.34E-03	1.02E-05	0.006	100.00	4.9918	0.1065	3.7829	0.052
[118]	1.5611	-9.00E-04	3.86E-07	0.019	99.46	4.9985	0.0981	3.7822	0.176
Both	1.6516	-1.36E-03	9.71E-07	0.091	99.50	4.9960	0.1033	3.7804	0.217

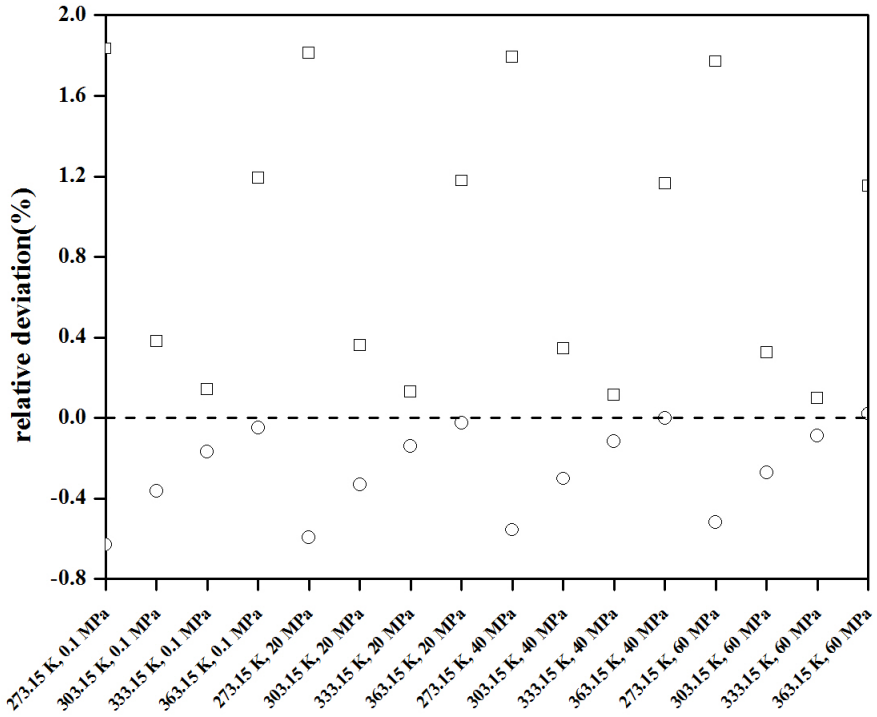

Figure 3-2. Comparison between the global fits and the local fits for $[C_1mim][C_1SO_4]$: □, Gołdon *et al.*[117] and ○, Aparicio *et al.*[118]

Following the described methodology, the dataset for each IL was recommended, totally including 7,921 data points for 81 ionic liquids over a wide temperature range (256 to 473 K) and pressure up to 200 MPa. A summary of the recommended dataset for each IL is shown in table 3-6.

Table 3-6. Overview of the Recommended Density Data Used to Establish the Group Contribution Model for Molar Volume (Density) of ILs as a Function of the Temperature and Pressure.

Code	IL	Molecular weight	Temperature Range	Pressure Range	Number of	Ref.
		$g \cdot mol^{-1}$	(K)	(MPa)	Data points	
1	$[C_2mim][SCN]$	169.25	298.15 to 338.15	0.1 to 10	65	[119]
2	$[C_2mim][OAc]$	170.21	293.14 to 353.20	0.1 to 25	63	[120]
3	$[C_4mim]Cl$	174.67	348.15 to 452.00	0.1 to 200	127	[121]
4	$[C_2mim][DCA]$	177.21	256.82 to 346.23	0.1 to 60.1	85	[122]
5	$[N_{1112OH}][Lactate]$	193.24	293.15 to 392.40	0.1 to 200	114	[121]
6	$[C_4mim][SCN]$	197.30	298.15 to 338.15	0.1 to 10	65	[119]
7	$[C_2mim][BF_4]$	197.97	283.15 to 323.15	0.1 to 60	117	[112]
8	$[C_4mim][OAc]$	198.26	273.15 to 413.16	0.1 to 140	170	[123]
9	$[C_2mim][Lactate]$	200.23	293.15 to 432.20	0.1 to 200	153	[121]
10	$[C_4mim][DCA]$	205.26	283.13 to 393.17	0.1 to 99.92	104	[124]
11	$[C_1mim][C_1SO_4]$	208.24	318.15 to 428.15	0.1 to 60	168	[118]
12	$[C_4m_{(4)}py][SCN]$	208.32	298.15 to 338.15	0.1 to 10	65	[119]
13	$[C_2mim][C_1SO_4]$	222.26	293.15 to 393.15	0.1 to 35	80	[93]
14	$[C_4Py][BF_4]$	223.02	283.15 to 333.15	0.1 to 65	154	[125]
15	$[C_4mim][BF_4]$	226.02	298.34 to 332.73	0.1 to 59.92	67	[126]
16	$[C_4mim][C(CN)_3]$	229.28	293.15 to 393.15	0.1 to 30	96	[127]
17	$[C_2mim][C_2SO_4]$	236.29	283.15 to 343.15	0.1 to 35	117	[128]

18	$[C_4m_{(2)}py][BF_4]$	237.05	293.15 to 333.15	0.1 to 65	120	[129]
19	$[C_4m_{(3)}py][BF_4]$	237.05	283.12 to 393.17	0.1 to100	105	[130]
20	$[C_4m_{(4)}py][BF_4]$	237.05	278.16 to 393.18	0.1 to 100	103	[131]
21	$[C_4mim][C_1SO_4]$	250.32	283.15 to 353.15	0.1 to 35	261	[132]
22	$[C_6py][BF_4]$	251.07	293.15 to 353.15	0.1 to 20	35	[133]
23	$[C_6mim][BF_4]$	254.08	283.15 to 323.15	0.1 to 60	117	[112]
24	$[C_2mim][PF_6]$	256.13	312.80 to 472.40	0.1 to 200	183	[134]
25	$[C_2mim][OTf]$	260.23	293.15 to 393.15	0.1 to 35	91	[94]
26	$[C_8py][BF_4]$	279.13	293.15 to 353.15	0.1 to 20	35	[133]
27	$[C_8mim][BF_4]$	282.13	293.15 to 353.15	0.1 to 20	20	[115]
28	$[C_2mim][Tos]$	282.36	318.15 to 428.15	0.1 to 60	168	[118]
29	$[C_4mim][PF_6]$	284.18	294.9 to 335.1	0.1 to 20	9	[135]
30	$[C_4mim][OTf]$	288.29	293.15 to 393.15	0.1 to 10	77	[114]
31	$[C_4mmim][PF_6]$	298.21	313.15 to 393.15	0.1 to 10	72	[114]
32	$[C_6mim][PF_6]$	312.24	294.1 to 335.2	0.1 to 20	9	[135]
33	$[C_8mim][PF_6]$	340.29	295.1 to 335.2	0.1 to 20	9	[135]
34	$[C_4mim][C_8SO_4]$	348.50	312.9 to 472.6	0.1 to 200	178	[136]
35	$[C_2mim][NTf_2]$	391.31	293.49 to 414.93	0.1 to 40	46	[137]
36	$[N_{1114}][NTf_2]$	396.37	293.48 to 414.94	0.1 to 40	46	[31]
37	$[C_3mim][NTf_2]$	405.34	298.15 to 333.15	0.1 to 60	165	[138]
38	$[C_3mpyrro][NTf_2]$	408.39	293.15 to 393.15	0.1 to 35	91	[94]
39	$[C_3m_{(3)}py][NTf_2]$	416.37	293.15 to 393.15	0.1 to 35	91	[94]
40	$[C_4mim][NTf_2]$	419.36	298.15 to 348.15	0.1 to 50	30	[139]
41	$[C_4mpyrro][NTf_2]$	422.41	293.49 to 414.94	0.1 to 40	46	[31]

42	$[C_3mpip][NTf_2]$	422.41	293.15 to 393.15	0.1 to 35	91	[94]
43	$[C_1OC_2mpyrro][NTf_2]$	424.38	278.15 to 398.15	0.1 to 120	126	[140]
44	$[C_5mim][NTf_2]$	433.39	298.15 to 333.15	0.1 to 60	165	[138]
45	$[C_2m_{(2)}py][NTf_2]$	402.33	283.15 to 333.15	0.1 to 65	143	[141]
46	$[C_6mim][NTf_2]$	447.42	293.15 to 452.3	0.1 to 200	177	[142]
47	$[C_7mim][NTf_2]$	461.45	293.15 to 393.15	0.1 to 30	96	[127]
48	$[C_8mim][NTf_2]$	475.48	293.15 to 393.15	0.1 to 30	96	[127]
49	$[C_{10}mim][NTf_2]$	503.52	293.15 to 393.15	0.1 to 35	80	[93]
50	$[P_{66614}]Cl$	519.31	273.15 to 318.15	0.1 to 25	72	[143]
51	$[P_{66614}][OAc]$	542.90	298.15 to 334.11	0.21 to 65.01	144	[29]
52	$[P_{66614}][DCA]$	549.90	273.15 to 318.15	0.1 to 35	173	[143]
53	$[C_2mim][FAP]$	556.17	293.13 to 343.18	0.1 to 25	54	[144]
54	$[P_{66614}]Br$	563.76	283.15 to 333.15	0.1 to 45	84	[145]
55	$[P_{66614}][C_1SO_3]$	578.95	283.15 to 333.15	0.1 to 45	84	[145]
56	$[C_4mim][FAP]$	584.23	293.15 to 353.05	0.1 to 25	63	[144]
57	$[C_4mpyrro][FAP]$	587.27	278.15 to 398.15	0.1 to 120	63	[146]
58	$[C_1OC_2mpyrro][FAP]$	589.24	278.15 to 398.15	0.1 to 120	63	[147]
59	$[C_6mim][FAP]$	612.28	293.16 to 343.19	0.1 to 25	60	[144]
60	$[P_{66614}][NTf_2]$	764.00	283.15 to 333.15	0.1 to 45	84	[145]
61	$[P_{66614}][FAP]$	928.87	293.2 to 353.25	0.1 to 25	63	[148]
62	$[C_6mim]Cl$	202.72	303.15 to 451.2	0.1 to 200	169	[142]
63	$[C_6mim][OTf]$	316.34	303.14 to 351.77	0.1 to 60.67	48	[149]
64	$[C_4mmim][FAP]$	598.25	278.15 to 398.15	0.1 to 120	126	[150]
65	$[C_4mmim][NTf_2]$	433.39	278.15 to 398.15	0.1 to 120	126	[150]

66	$[C_2OHC_1NH_2][C_2COO]$	149.19	298.15 to 358.15	0.1 to 25	104	[151]
67	$[C_2OHC_1NH_2][C_3COO]$	163.22	298.15 to 358.15	0.1 to 25	42	[151]
68	$[C_2OHC_1NH_2][C_4COO]$	177.24	298.15 to 358.15	0.1 to 25	42	[151]
69	$[C_1mim][DMP]$	222.18	278.15 to 398.15	0.1 to 120	63	[146]
70	$[C_2mim][C_6SO_4]$	292.4	278.15 to 398.15	0.1 to 120	63	[146]
71	$[C_4mpyrro][B(CN)_4]$	257.15	298.15 to 398.15	0.1 to 60	75	[146]
72	$[C_4mpyrro][OTf]$	291.34	278.15 to 398.15	0.1 to 120	63	[146]
73	$[C_3py][BF_4]$	208.99	283.15 to 333.15	0.1 to 65	154	[125]
74	$[C_4py][OTf]$	285.28	303.15 to 333.15	0.1 to 65	98	[125]
75	$[C_4m_{(3)}py][DCA]$	216.28	293.15 to 333.15	0.1 to 65	126	[125]
76	$[C_8m_{(3)}py][BF_4]$	293.15	283.15 to 333.15	0.1 to 65	154	[125]
77	[amim]Cl	158.63	293.15 to 373.15	0.1 to 200	89	[152]
78	$[C_2mim][MP]$	222.17	293.15 to 411.1	0.1 to 200	129	[153]
79	$[C_2mim][DEP]$	264.26	293.15 to 411.1	0.1 to 200	129	[153]
80	$[C_2eim][NTf_2]$	405.34	293.15 to 393.15	0.1 to 35	80	[93]
81	$[C_3m_{(2)}py][NTf_2]$	416.36	283.15 to 333.15	0.1 to 65	143	[141]

3.2 Development of the Group Contribution Model

An extension of the group contribution method based on the previously developed model by Jacquemin *et al.*[9,31] has been developed.

Due to the thermal and chemical stability of $[NTf_2]^-$, the effective molar volumes of $[NTf_2]^-$ as a function of temperature and pressure were used to calculate the effective molar volumes of the corresponding cations, which constitute the ionic liquids, following this algorithm ($V^*_{cation} = V_{m_{IL}} - V^*_{[NTf_2]^-}$). The volumetric parameters (D_i, G, and H_i) of $[NTf_2]^-$ have been calculated by Jacquemin *et al.*[31] The experimental data of 19 $[NTf_2]^-$-based ionic liquids at high pressure have been reported. These 19 $[NTf_2]^-$-based ILs are: $[C_2mim][NTf_2]$, $[N_{1114}][NTf_2]$, $[C_3mim][NTf_2]$, $[C_3mpyrro][NTf_2]$, $[C_3m_{(3)}py][NTf_2]$, $[C_4mim][NTf_2]$, $[C_4mpyrro][NTf_2]$, $[C_3mpip][NTf_2]$, $[C_1OC_2mpyrro][NTf_2]$, $[C_5mim][NTf_2]$, $[C_6mim][NTf_2]$, $[C_7mim][NTf_2]$, $[C_8mim][NTf_2]$, $[C_{10}mim][NTf_2]$, $[P_{66614}][NTf_2]$, $[C_4mmim][NTf_2]$, $[C_2m_{(2)}py][NTf_2]$, $[C_3m_{(2)}py][NTf_2]$, and $[C_2eim][NTf_2]$. Thus, volumetric parameters of the counterpart cations were determined. Next step, experimental data of other ILs, which consist of these 19 cations, were used to calculate the molar volumes of the corresponding anions. For example, the effective molar volumes of Br^- were calculated using this algorithm ($V^*_{Br^-} = V_{m_{[P_{66614}]Br}} - V^*_{[P_{666\,14}]^+}$). Then the volumetric parameters of Br^- were obtained by correlating its effective molar volumes as a function of temperature and pressure. Following this methodology, the coefficients (D_i, G, and H_i) of 51 ions were calculated.

The experimental data at high pressures of another three ILs ($[C_2OHC_1NH_2][C_2COO]$, $[C_2OHC_1NH_2][C_3COO]$, and $[C_2OHC_1NH_2][C_4COO]$) have been collected from literature.[151] These three ILs consist of the same cation and three different anions. However, the knowledge of the volumetric properties of these four ions had not been reported in the literature. Herein, we proposed a method fitting the experimental data of these three ILs altogether to obtain the volumetric parameters of $[C_2OHC_1NH_2]^+$, $[C_2COO]^-$, $[C_3COO]^-$ and $[C_4COO]^-$, simultaneously.

3.3 Results and Discussion

3.3.1 Performance of the Proposed GCM

The volumetric parameters (D_i, G, and H_i) of 31 cations and 24 anions are presented in table 3-7. Then the molar volumes of ILs, random cation-anion combinations, can be evaluated as a function of temperature and pressure. The experimental data of other 27 ILs, which had not been correlated, were used to compare with the pure evaluated values. The number of data used to correlate and evaluate, and the Relative Average Absolute Deviations (RAAD) of pure evaluation and global estimation, for each ion were reported in Table 3-8.

Table 3-7. The Volumetric Parameters Used to Calculate the Effective Molar Volume of Cation/Anion

cation	D_0	D_1	D_2	H_0	H_1	H_2	G
	$cm^3 \cdot mol^{-1}$	$cm^3 \cdot mol^{-1} \cdot K^{-1}$	$cm^3 \cdot mol^{-1} \cdot K^{-2}$	MPa	$MPa \cdot K^{-1}$	$MPa \cdot K^{-2}$	
$[C_2mim]^+$	100.25	0.0656	4.57E-05	217.92	2.048	6.164E-03	-0.0925
$[N_{1114}]^+$	127.14	0.0772	6.94E-05	16135	2878.6	-5.808E+01	-0.6541
$[C_3mim]^+$	117.14	0.0445	1.18E-03	206.05	1.828	-4.042E-02	-0.1487
$[C_3mpyrro]^+$	127.28	0.0961	-3.72E-05	152.21	0.120	-2.948E-04	-0.1119
$[C_2m_{(2)}py]^+$	109.62	0.0684	-7.17E-06	61.31	0.046	7.048E-04	-0.0427
$[C_3m_{(2)}py]^+$	126.76	0.0797	9.73E-06	69.60	0.017	-1.029E-04	-0.0492
$[C_3m_{(3)}py]^+$	129.64	0.1032	-8.74E-06	118.93	0.158	-1.828E-03	-0.0948
$[C_4mim]^+$	134.11	0.0927	-2.99E-05	144.63	-0.476	1.169E-02	-0.1009
$[C_4mpyrro]^+$	145.43	0.0820	7.17E-05	299.79	0.990	-7.970E-03	-0.1645
$[C_3mpip]^+$	141.53	0.1106	-6.04E-05	134.55	0.103	-1.929E-03	-0.0939
$[C_1OC_2mpyrro]^+$	134.23	0.0921	-7.52E-05	161.45	0.150	-6.371E-04	-0.1046
$[C_5mim]^+$	151.00	0.0887	5.02E-04	171.05	0.736	-1.732E-02	-0.1254
$[C_6mim]^+$	168.60	0.1131	4.93E-05	147.63	0.298	-4.620E-03	-0.1120
$[C_7mim]^+$	184.82	0.1548	-1.98E-04	50642	6132.9	-3.078E+02	-8.5993
$[C_8mim]^+$	202.14	0.1852	-3.53E-04	874.86	40.89	-8.544E-01	-0.5610
$[C_{10}mim]^+$	236.36	0.1748	1.76E-04	59.77	0.102	-2.717E-03	-0.0557
$[P_{66614}]^+$	558.87	0.3891	2.21E-04	129.57	-0.660	2.849E-03	-0.0846
$[C_8py]^+$	198.22	0.1295	2.70E-05	145.98	0.362	-1.634E-02	-0.0799
$[C_6py]^+$	163.89	0.1014	9.90E-05	136.06	0.726	-2.217E-02	-0.0704
$[C_4py]^+$	129.98	0.0799	2.60E-05	149.82	0.800	-1.901E-02	-0.0673
$[C_4m_{(2)}py]^+$	143.46	0.0850	9.12E-05	163.34	2.076	-5.741E-02	-0.0699
$[C_4m_{(3)}py]^+$	146.72	0.0900	8.61E-05	240.30	-0.382	-5.114E-03	-0.1166
$[C_4m_{(4)}py]^+$	145.73	0.0907	3.82E-05	240.97	-0.404	-4.081E-03	-0.1164
$[N_{1112OH}]^+$	95.06	0.0552	-1.01E-05	778.60	-14.45	3.847E-01	-0.1414
$[C_1mim]^+$	84.61	0.0367	7.72E-05	-549.24	35.86	-7.761E-01	0.0224
$[C_4mmim]^+$	147.30	0.0974	6.75E-05	166.44	0.055	-2.028E-03	-0.1085
$[C_3py]^+$	113.05	0.0713	1.09E-05	149.33	1.029	-2.029E-02	-0.0627
$[C_8m_{(3)}py]^+$	213.92	0.1362	6.11E-05	148.56	0.110	-1.088E-02	-0.0792
$[amim]^+$	111.53	0.0726	4.22E-06	423.16	-1.080	8.108E-03	-0.1446
$[C_2OHC_1NH_2]^+$	59.02	0.0471	-2.62E-04	1343.9	332.7	-1.586E+00	0.0106
$[C_2eim]^+$	119.38	0.1047	-1.69E-05	71.22	-0.040	-1.484E-06	-0.0648
anion	D_0	D_1	D_2	H_0	H_1	H_2	G
	$cm^3 \cdot mol^{-1}$	$cm^3 \cdot mol^{-1} \cdot K^{-1}$	$cm^3 \cdot mol^{-1} \cdot K^{-2}$	MPa	$MPa \cdot K^{-1}$	$MPa \cdot K^{-2}$	
$[SCN]^-$	51.31	0.0194	-9.57E-05	32201	14982	-5.159E+02	-4.1231
$[OAc]^-$	54.44	0.0237	-7.98E-05	367069	27415	-1.864E+04	-2.5040
$[DCA]^-$	59.59	0.0237	4.49E-05	21.20	2.015	1.800E-01	0.0064
$[BF_4]^-$	53.75	0.0258	-3.40E-05	1442.6	-60.568	1.207E+00	-0.2816
$[Lactate]^-$	74.46	0.0419	-6.12E-05	911.77	-8.626	2.963E-02	-0.2774
$[C_1SO_4]^-$	72.32	0.0429	-8.86E-05	355.00	-5.886	3.436E-02	-0.0815

$[C_2SO_4]^-$	90.72	0.0394	-1.66E-05	524.17	-11.328	1.210E-01	-0.1280
$[OTf]^-$	89.02	0.0628	-3.66E-05	561.03	-6.307	3.259E-02	-0.2552
$[Tos]^-$	130.89	0.0582	-1.21E-04	189.85	100.13	-1.006E+00	-0.0772
$[C_6SO_4]^-$	158.64	0.0899	-2.38E-05	334.89	-3.122	1.289E-02	-0.1376
$[MP]^-$	85.66	0.0363	-4.07E-05	1046.5	-10.970	4.347E-02	-0.2664
$[DEP]^-$	130.61	0.0716	-1.19E-05	335.58	-2.806	9.293E-03	-0.1476
$[FAP]^-$	225.74	0.1651	-2.71E-06	1005.0	118.98	-4.050E+00	-0.1531
$[C(CN_3)]^-$	84.73	0.0669	-1.53E-04	2135.8	-137.11	1.756E+00	0.0251
$[PF_6]^-$	73.26	0.0275	2.00E-04	-5560.5	3158	-8.477E+02	-3.7218
$[C_8SO_4]^-$	192.36	0.0741	3.15E-04	531.29	-4.303	1.089E-02	-0.1587
$[B(CN)_4]^-$	117.92	0.0979	-7.63E-07	181.40	-1.502	5.064E-03	-0.0932
Cl^-	26.83	0.0007	-4.25E-05	-4524.5	58.582	-2.000E-01	0.1529
Br^-	32.45	-0.0038	2.25E-05	0.37	-0.076	2.994E-03	0.0003
$[DMP]^-$	91.51	0.0646	-6.12E-05	2127.0	-29.335	-6.208E+00	-0.1397
$[C_1SO_3]^-$	64.49	0.0233	-1.80E-05	166366	-352.92	-1.855E+01	-54.535
$[C_2COO]^-$	80.97	0.0356	3.67E-04	943.26	-4.690	1.742E-02	-0.6372
$[C_3COO]^-$	98.64	0.0552	3.15E-04	644.47	-2.767	3.621E-03	-0.4469
$[C_4COO]^-$	116.58	0.0677	1.12E-03	630.89	-2.264	-5.409E-03	-0.4560

Table 3-8. The Number of Data Points Used for the Correlation and Evaluation, Along with the RAADs of Evaluation, and Estimation for Each Ion

Ion	N_{Corre}	ILs used for correlation	N_{Eva}	ILs used for pure evaluation	$RAAD_{Eva}$(%)	$RAAD_{Est}$(%)
$[C_2mim]^+$	46	$[C_2mim][NTf_2]$	322	$[C_2mim][DCA]$, $[C_2mim][PF_6]$, and $[C_2mim][FAP]$	2.925	0.610
$[N_{1114}]^+$	46	$[N_{1114}][NTf_2]$	0	-	-	0
$[C_3mim]^+$	165	$[C_3mim][NTf_2]$	0	-	-	0
$[C_3mpyrro]^+$	91	$[C_3mpyrro][NTf_2]$	0	-	-	0
$[C_3m_{(3)}py]^+$	91	$[C_3m_{(3)}py][NTf_2]$	0	-	-	0
$[C_4mim]^+$	30	$[C_4mim][NTf_2]$	649	$[C_4mim][SCN]$, $[C_4mim][OAc]$, $[C_4mim][BF_4]$, $[C_4mim][C_1SO_4]$, $[C_4mim][PF_6]$, and $[C_4mim][OTf]$,	0.497	0.259
$[C_4mpyrro]^+$	46	$[C_4mpyrro][NTf_2]$	126	$[C_4mpyrro][FAP]$, and $[C_4mpyrro][OTf]$	1.001	0.510
$[C_3mpip]^+$	91	$[C_3mpip][NTf_2]$	0	-	-	0
$[C_1OC_2mpyrro]^+$	126	$[C_1OC_2mpyrro][NTf_2]$	63	$[C_1OC_2mpyrro][FAP]$	1.198	0.399
$[C_5mim]^+$	165	$[C_5mim][NTf_2]$	0	-	-	0
$[C_6mim]^+$	177	$[C_6mim][NTf_2]$	394	$[C_6mim][BF_4]$, $[C_6mim][FAP]$, $[C_6mim]Cl$, and $[C_6mim][OTf]$	0.780	0.530
$[C_7mim]^+$	96	$[C_7mim][NTf_2]$	0	-	-	0
$[C_8mim]^+$	96	$[C_8mim][NTf_2]$	29	$[C_8mim][BF_4]$ and $[C_8mim][PF_6]$	0.419	0.001
$[C_{10}mim]^+$	80	$[C_{10}mim][NTf_2]$	0	-	-	0
$[P_{66614}]^+$	84	$[P_{66614}][NTf_2]$	452	$[P_{66614}]Cl$, $[P_{66614}][OAc]$, $[P_{66614}][DCA]$ and $[P_{66614}][FAP]$	0.723	0.464
$[C_8py]^+$	35	$[C_8py][BF_4]$	0	-	-	0
$[C_6py]^+$	35	$[C_6py][BF_4]$	0	-	-	0
$[C_4py]^+$	154	$[C_4py][BF_4]$	98	$[C_4py][OTf]$	0.982	0.382

$[C_4m_{(2)}py]^+$	120	$[C_4m_{(2)}py][BF_4]$	0	-	-	0
$[C_4m_{(3)}py]^+$	105	$[C_4m_{(3)}py][BF_4]$	126	$[C_4m_{(3)}py][DCA]$	0.256	0.140
$[C_4m_{(4)}py]^+$	103	$[C_4m_{(4)}py][BF_4]$	65	$[C_4m_{(4)}py][SCN]$	0.353	0.137
$[C_2m_{(2)}py]^+$	143	$[C_2m_{(2)}py][NTf_2]$	0	-	-	0
$[C_3m_{(2)}py]^+$	143	$[C_3m_{(2)}py][NTf_2]$	0	-	-	0
$[N_{1112OH}]^+$	114	$[N_{1112OH}]$[Lactate]	0	-	-	0
$[C_1mim]^+$	168	$[C_1mim][C_1SO_4]$	0	-	-	0
$[C_4mmim]^+$	126	$[C_4mmim][NTf_2]$	198	$[C_4mmim][PF_6]$ and $[C_4mmim]$[FAP]	0.824	0.503
$[C_3py]^+$	154	$[C_3py][BF_4]$	0	-	-	0
$[C_8m_{(3)}py]^+$	154	$[C_8m_{(3)}py][BF_4]$	0	-	-	0
$[amim]^+$	89	[amim]Cl	0	-	-	0
$[C_2OHC_1NH_2]^+$	188	$[C_2OHC_1NH_2][C_2COO]$, $[C_2OHC_1NH_2][C_3COO]$, and $[C_2OHC_1NH_2][C_4COO]$	0	-	-	0.138
$[C_2eim]^+$	80	$[C_2eim][NTf_2]$	0	-	-	0
$[SCN]^-$	65	$[C_2mim][SCN]$	130	$[C_4mim][SCN]$ and $[C_4m_{(4)}py][SCN]$	0.469	0.312
$[OAc]^-$	63	$[C_2mim][OAc]$	314	$[C_4mim][OAc]$ and $[P_{66614}][OAc]$	0.469	0.391
$[DCA]^-$	104	$[C_4mim][DCA]$	384	$[C_2mim][DCA]$, $[P_{66614}][DCA]$ and $[C_4m_{(3)}py][DCA]$	0.651	0.335
$[BF_4]^-$	117	$[C_2mim][BF_4]$	204	$[C_4mim][BF_4]$, $[C_6mim][BF_4]$, and $[C_8mim][BF_4]$	0.268	0
$[Lactate]^-$	153	$[C_2mim]$[Lactate]	0	-	-	0
$[C_1SO_4]^-$	80	$[C_2mim][C_1SO_4]$	261	$[C_4mim][C_1SO_4]$	0.563	0.289
$[C_2SO_4]^-$	117	$[C_2mim][C_2SO_4]$	0	-	-	0
$[OTf]^-$	91	$[C_2mim][OTf]$	286	$[C_4mim][OTf]$, $[C_4mpyrro][OTf]$, $[C_4py][OTf]$ and	0.764	0.579

				$[C_6mim][OTf]$		
$[Tos]^-$	168	$[C_2mim][Tos]$	0	-	-	0
$[C_6SO_4]^-$	63	$[C_2mim][C_6SO_4]$	0	-	-	0
$[MP]^-$	129	$[C_2mim][MP]$	0	-	-	0
$[DEP]^-$	129	$[C_2mim][DEP]$	0	-	-	0
$[FAP]^-$	63	$[C_4mim][FAP]$	429	$[C_2mim][FAP]$, $[C_4mpyrro][FAP]$, $[C_1OC_2mpyrro][FAP]$, $[C_6mim][FAP]$, $[P_{66614}][FAP]$, and $[C_4mmim][FAP]$	0.813	0.709
$[C(CN_3)]^-$	96	$[C_4mim][C(CN)_3]$	0	-	-	0
$[PF_6]^-$	9	$[C_6mim][PF_6]$	273	$[C_2mim][PF_6]$, $[C_4mim][PF_6]$, $[C_4mmim][PF_6]$, and $[C_8mim][PF_6]$	3.363	3.256
$[C_8SO_4]^-$	178	$[C_4mim][C_8SO_4]$	0	-	-	0
$[B(CN)_4]^-$	75	$[C_4mpyrro][B(CN)_4]$	0	-	-	0
Cl^-	127	$[C_4mim]Cl$	241	$[P_{66614}]Cl$ and $[C_6mim]Cl$	1.129	0.595
Br^-	84	$[P_{66614}]Br$	0	-	-	0
$[DMP]^-$	63	$[C_1mim][DMP]$	0	-	-	0
$[C_1SO_3]^-$	84	$[P_{66614}][C_1SO_3]$	0	-	-	0
$[C_2COO]^-$	104	$[C_2OHC_1NH_2][C_2COO]$	0	-	-	0.003
$[C_3COO]^-$	42	$[C_2OHC_1NH_2][C_3COO]$	0	-	-	0.004
$[C_4COO]^-$	42	$[C_2OHC_1NH_2][C_4COO]$	0	-	-	0.604

With the exception of $[PF_6]^-$ (RAAD=3.26%), the RAAD determined for all the other ions are less than 0.8%. Herein, we further discuss the possible reasons that result to higher deviations for $[PF_6]^-$. We used this algorithm ($V^*_{[PF_6]^-} = V_{m_{[C_6mim][PF_6]}} - V^*_{[C_6mim]^+}$) to calculate the effective molar volume of $[PF_6]^-$, and then fitted $[C_6mim][PF_6]$ experimental data to obtain the volumetric parameters of $[PF_6]^-$ as the function of the temperature and pressure. Since the volumetric parameters of the $[C_2mim]^+$, $[C_4mim]^+$, $[C_6mim]^+$, $[C_8mim]^+$, and $[C_4mmim]^+$ have been obtained using data for other ILs, the volumetric properties of the corresponding ILs containing the $[PF_6]^-$ are purely evaluated as a function of temperature and pressure based on the sum of the effective molar volumes of two ions. Table 3-9 shows the estimation result and estimation method for each IL containing the $[PF_6]^-$ anion. In Table 3-9, the evaluated data for the $[C_4mim][PF_6]$, $[C_8mim][PF_6]$ and $[C_4mmim][PF_6]$ are in excellent agreements (RAAD are both lower than 0.4%) with the experimental data collected from the literature. However, in the case of the $[C_2mim][PF_6]$, larger deviations, close to 4.9%, are observed. This could be related to the fact that the $[C_2mim][PF_6]$ is solid at ambient temperature and 0.1 MPa. Furthermore, the impurity, water, has a significant effect on the molar volume of $[PF_6]^-$ based ILs by formation of hydrogen bonding between water and the anion ($[PF_6]^-$). In addition, Taguchi *et al.*[134] measured the experimental density data of $[C_2mim][PF_6]$ as a function of temperature (312.8 – 472.4) K and over a pressure range from 0.1 to 200 MPa, where the wide temperature range and broad pressure range both increase the data fitting difficulties and thus the accurate evaluation of the effective molar volume of these ions.

Table 3-9. Estimation method and result for each investigated IL containing the $[PF_6]^-$ anion.

Ionic Liquid	Estimation method	RAAD (%)	Ref.
$[C_6mim][PF_6]$	Correlation	0	Tomida *et al.*[135]
$[C_2mim][PF_6]$	Evaluation	4.91%	Taguchi *et al.*[134]
$[C_4mim][PF_6]$	Evaluation	0.36%	Tomida *et al.*[135]
$[C_8mim][PF_6]$	Evaluation	0.37%	Tomida *et al.*[135]
$[C_4mmim][PF_6]$	Evaluation	0.17%	Gardas *et al.*[114]

Figure 3-3 shows the parity plot between the calculated and experimental densities and molar volumes of 81 ILs. The correlated and evaluated data are differentiated by filled circles and empty circles, respectively. 5,399 data points of 54 ILs are used for correlation with an excellent accuracy of 0.005%, and 2,522 data points of other 27 ILs are used for comparison with the pure evaluated values within 0.96%. A good agreement is proved using this developed model, with a global RAAD lower than 0.31%.

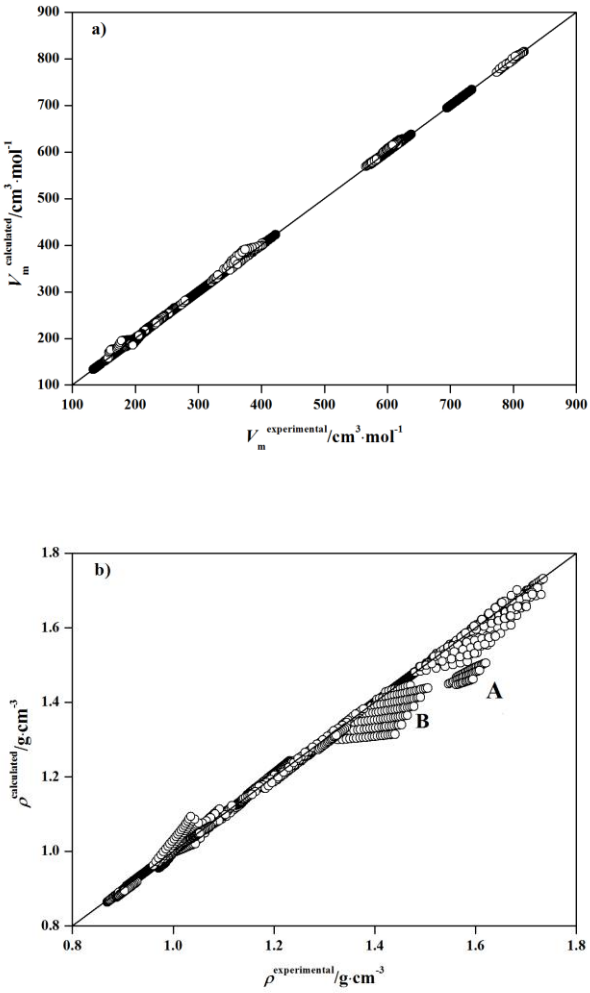

Figure 3-3. Experimental versus calculated molar volumes (a) and calculated densities (b) for 81 ionic liquids where data used for developing correlation (●) and evaluated data (○) are shown.

In figure 3-3(b), the data points marked by (A) and (B) are from $[C_2mim][PF_6]$. The density data of $[C_2mim][PF_6]$ at high pressures and high temperatures locate in area (B). Area (A) corresponds to the data at high pressures and low temperatures. The reason has been explained before.

This work mainly focuses on the evaluation of high-pressure density (volume)

properties by only collecting the references reporting the high-pressure experimental data. Therefore, the method proposed in my study was compared with other literature models in terms of the density calculation at high pressures. Figure 3-4(a) and 3-4(b) summarize the calculations at high pressures for the 33 common ILs and 80 ILs, respectively. It can be seen in Figure 3-4 that our method developed in this work shows the lowest global RAAD% in both cases. Our method is responsible for the estimation of densities (volumes) of ILs, especially at high pressures. However, the GCMs proposed by Taherifard-Raeissi[154], and Paduszyński-Domańska[32] divide the IL into smaller functional groups, which enlarge the range of applicability and increase the complexity of calculations, in turn.

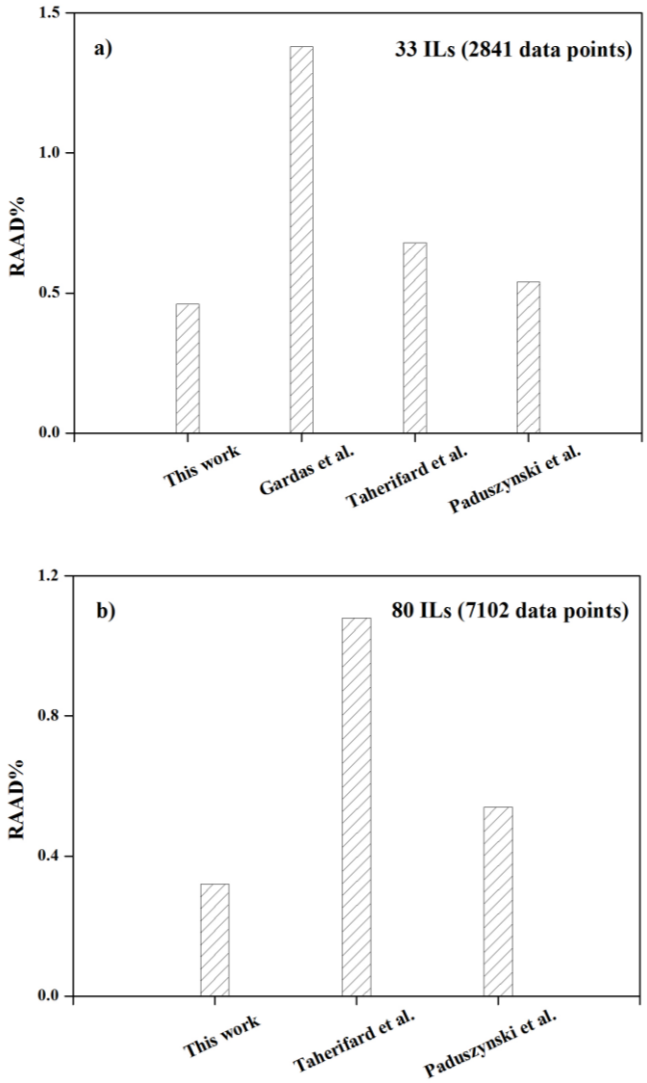

Figure 3-4. Comparison between the recommended experimental density data and the calculated values only at high pressures (P > 0.1 MPa), by using our method, and the methods proposed by Gardas-Coutinho[28], Taherifard-Raeissi[154], and Paduszyński-Domańska[32], for (a) 33 ILs and (b) 80 ILs, respectively.

Figure 3-5 shows the calculated effective molar volumes of cations with different core function groups based on the volumetric parameters obtained. Piperidinium and pyridinium cations are both six-membered ring, while imidazolium and pyrrolidinium are both five-membered ring. The six-membered ring has a larger molecular volume

than the five-membered ring. Moreover, imidazolium and pyridinium contain C-C double bonds and C-N double bonds, which pack tighter than the corresponding ring without double bonds. Therefore, we can conclude that, for the equivalent alkyl chain on the cation, the effective molar volumes follow this order: $[C_nmpip]^+ > [C_nm_{(3)}py]^+ > [C_nmpyrro]^+ > [C_nmim]^+$.

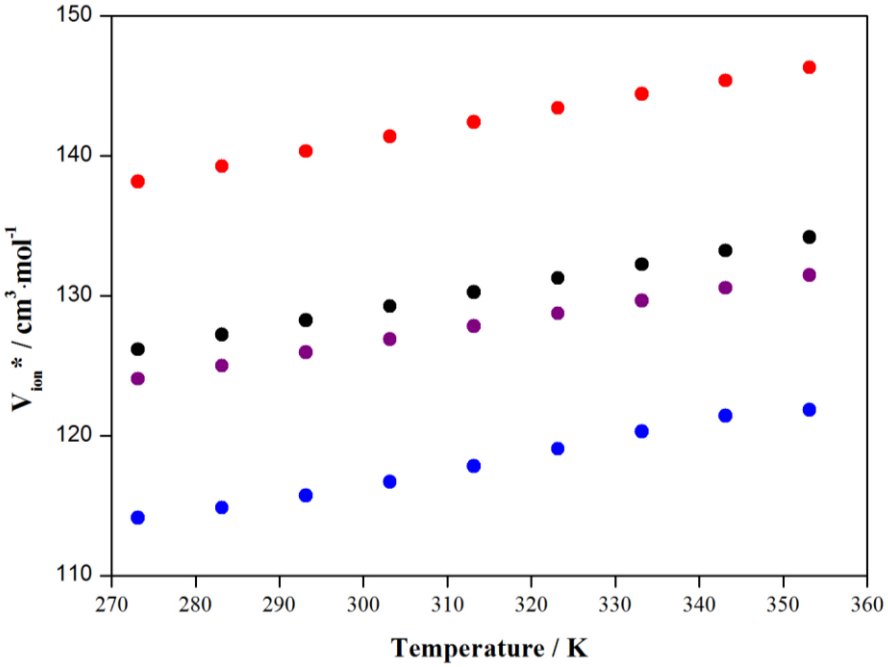

Figure 3-5. Effective molar volumes of cations at 40 MPa with different core function groups: red, $[C_3mpip]^+$; black, $[C_3m_{(3)}py]^+$; purple, $[C_3mpyrro]^+$; blue, $[C_3mim]^+$.

3.3.2 Comparison with Other GCMs in the Case of Binary IL Mixtures

Comparison between different GCMs in the evaluation ability of pure ILs has been reported in the literature.[9,28,31,32,34] Herein, various GCMs are compared in the case of evaluation of density of binary IL mixtures. 1,756 experimental density points for 29 binary systems were collected from the literature over a temperature range (283.15 K to 358.15 K) at 0.1 MPa. Since the binary densities having been reported in the literature

are only at atmosphere pressure, the comparison between different GCMs, made in this work, can only contrast their performance at atmosphere pressure. Table 3-10 shows all the selected types of the binary ILs systems, the number of data points for each system, the temperature range for each data set, as well as the evaluation result using four GCMs. The 29 binary systems contain three-component systems with the same cation or anion (such as $[C_4mim][OAc]+[C_4mim][NTf_2]$), and also contain four-component systems (for example $[C_4m_{(4)}py][NTf_2]+[C_2mim][C_2SO_4]$). As in the case of pure ILs, the molar volume data of the binary systems were also calculated using the 'ideal volume' principle. In Table 3-10, the first 20 binary mixtures were evaluated using four methods and the last 9 binary mixtures were evaluated using three methods, due to a limited number of the effective molar volumes of ions having been reported in Gardas' method.[28] The evaluation results, for 1230 data points of 20 binary mixtures, are 0.21 (this work), 0.71 (Gardas-Coutinho[28]), 0.28 (Taherifard-Raeissi[154]), and 0.18 (Paduszyński-Domańska[32]), respectively. The evaluation accuracy, using the 1,756 data points for 29 different binary mixtures, is 0.243 (this work), 0.371 (Taherifard-Raeissi[154]), and 0.236 (Paduszyński-Domańska[32]), respectively. Generally, the method proposed by Paduszyński and Domańska[32] shows the best performance and the evaluation accuracy by our method is very close to that of Paduszyński and Domańska.[32]

Table 3-10. Comparison of GCMs for estimation of density of binary mixtures

Binary system	Ref.	Points	Temp. range	%RAAD (this work)	%RAAD (Gardas-Coutinho[28])	%RAAD (Taherifard-Raeissi[154])	%RAAD (Paduszyński-Domańska[32])
$[C_4mim][OAc]+[C_4mim][NTf_2]$	[155]	32	283.15-333.15	0.24	1.4	0.48	0.67
$[C_2mim][NTf_2]+[C_4mim][NTf_2]$	[156,157]	21	293.15-358.15	0.23	0.32	0.39	0.34
$[C_4py][BF_4]+[C_4py][NTf_2]$	[158]	72	303.15-353.15	0.12	0.38	0.72	0.52
$[C_4py][BF_4]+[C_4m_{(4)}py][NTf_2]$	[159]	84	293.15-353.15	0.39	0.48	0.64	0.48
$[C_6mim][BF_4]+[C_2mim][BF_4]$	[160,161]	256	293.15-343.15	0.17	0.6	0.16	0.08
$[C_4mim][BF_4]+[C_6mim][BF_4]$	[160]	108	298.15-308.15	0.13	0.52	0.03	0.04
$[C_4mim][PF_6]+[C_4mim][BF_4]$	[160]	126	298.15-308.15	0.26	0.35	0.09	0.12
$[C_8mim][BF_4]+[C_8mim]Cl$	[162]	42	303.15-333.15	0.51	2.12	0.06	0.15
$[C_6mim][BF_4]+[C_6mim]Cl$	[162]	42	303.15-333.15	0.26	2.41	0.14	0.1
$[C_6mim][P_{F6}]+[C_6mim]Cl$	[162]	35	303.15-333.15	0.08	1.87	0.17	0.08
$[C_3mpyrro][NTf_2]+[C_4mim][NTf_2]$	[163]	7	298.15	0.04	0.11	0.13	0.27
$[C_3m_{(3)}py][NTf_2]+[C_4mim][NTf_2]$	[163]	7	298.15	0.03	0.14	0.13	0.19
$[C_1mim][NTf_2]+ [C_4mim][NTf_2]$	[156]	7	298.15	0.42	0.4	0.16	0.48
$[C_5mim][NTf_2]+ [C_4mim][NTf_2]$	[156]	7	298.15	0.24	0.27	0.24	0.3
$[C_6mim][NTf_2]+ [C_4mim][NTf_2]$	[156]	7	298.15	0.09	0.11	0.05	0.15
$[C_8mim][NTf_2]+ [C_4mim][NTf_2]$	[156]	7	298.15	0.04	0.08	0.05	0.1
$[C_{10}mim][N_{Tf2}]+ [C_4mim][NTf_2]$	[156]	7	298.15	0.06	0.07	0.1	0.11
$[C_2mim][BF_4]+[C_3mim][BF_4]$	[161]	121	293.15-343.15	0.38	0.71	0.31	0.11
$[C_3mim][BF_4]+[C_6mim][BF_4]$	[161]	121	293.15-343.15	0.15	0.58	0.18	0.07
$[C_4mim][BF_4]+[C_4py][BF_4]$	[164]	121	293.15-343.15	0.1	0.62	0.62	0.28

20 binary mixtures		1230		0.21	0.71	0.28	0.18
$[C_2mim][SCN]+[C_2mim][DCA]$	[165]	60	298.15-353.15	0.41	-	0.43	0.42
$[C_2mim][SCN]+[C_2mim][C_2SO_4]$	[165]	96	298.15-353.15	0.43	-	0.67	0.5
$[C_2mim][C(CN)_3]+[C_2mim][DCA]$	[165]	42	293.15-353.15	0.63	-	0.59	0.4
$[C_4m_{(4)}py][NTf_2]+[C_2mim][C_2SO_4]$	[166]	84	293.15-353.15	0.36	-	0.52	0.21
$[C_4mim][BF_4]+[C_4mim][C_1SO_4]$	[160]	144	298.15-308.15	0.2	-	0.45	0.24
$[C_4mmim][NTf_2]+ [C_4mim][NTf_2]$	[163]	7	298.15	0.02	-	0.04	0.27
$[C_3mpip][NTf_2]+ [C_4mim][NTf_2]$	[163]	7	298.15	0.34	-	0.3	0.39
$[C_2mim][OAc]+[C_2mim][C_2SO_4]$	[167]	77	298.15-358.15	0.09	-	1.06	0.51
$[C_2mim][BF4]+[C_2mim][DCA]$	[168]	9	298.15	0.57	-	0.5	0.33
29 binary mixtures		1756		0.243		0.371	0.236

3.4 Mechanical Coefficients

A limited number of experimental data of isobaric thermal expansion (α_p) for ionic liquids have been reported in the literature to date. However, no experimental data of isothermal compressibility (κ_T) for ionic liquids has been published, to date, as this property is mainly derived from density measurements as a function of temperature and pressure. Table 3-11summarizes the number of experimental data, temperature range, pressure range, references and the variation with temperature and pressure for α_p of ILs.

Table 3-11. All the experimental data of α_p for ILs collected from the literature

ILs	T_{range}(K)	P_{range}(MPa)	N_{data}	Variation (T)	Variation (P)	Ref.
$[C_4mim][BF_4]$	278.15-348.15	5-50	80	↓	↓	[169]
$[C_4mim][OTf]$	278.15-348.15	5-50	80	↓	↓	[169]
$[C_4mim][SbF_6]$	278.15-348.15	5-50	80	↓	↓	[169]
$[C_4mim][NTf_2]$	278.15-348.15	5-50	80	↓	↓	[169]
$[C_4mim][C_1SO_4]$	278.15-348.15	5-50	80	↓	↓	[169]
$[C_4m_{(3)}py][BF_4]$	278.15-348.15	5-50	80	↓	↓	[170]
$[C_2mim][BF_4]$	278.15-348.15	5-50	80	↓	↓	[170]
$[C_6mim][BF_4]$	278.15-348.15	5-50	80	↓	↓	[170]
$[C_8mim][BF_4]$	278.15-348.15	5-50	80	↓	↓	[170]
$[C_2mim][NTf_2]$	278.15-348.15	5-50	80	↓	↓	[170]
$[C_6mim][NTf_2]$	278.15-348.15	5-50	80	↓	↓	[170]

The experimental data of α_p reported by Navia *et al*.[169,170] are not affected by any a priori assumption because α_p is directly measured, unlike the values of α_p reported

by other groups[31,93,94,125,137,150,171–176] were derived from fitting equations, which predetermine the dependence of α_p against temperature. It is observed from the experimental data measured by Navia *et al.*[169,170] that α_p of the investigated ILs decreases with temperature (indicated by using the downward arrow symbols in Table 3-11), due to their ionic character, which is an anomalous behaviour from traditional solvents. However, very limited directly measured data of α_p for ILs have been published in literature, hence, further studies are required to prove whether the anomalous behaviour is suitable for all ILs. A negative dependence of α_p against pressure for the investigated ILs (shown by using the downward arrow symbols in Table 3-11) is similar with traditional solvents.

The densities as a function of temperature and pressure can be used to derive the mechanical coefficients, the isothermal compressibility (κ_T) and the isobaric thermal expansion coefficient (α_p). The calculation of these mechanical coefficients provides useful information on the temperature and pressure dependences on the ILs volumetric properties.

The following expressions, described in chapter 2 are used to calculate the values of α_p and κ_T.

$$\alpha_p = -\left\{\frac{\left[\frac{d\rho(T,P=0.1\ MPa)}{dT}\right]}{\rho(T,P=0.1\ MPa)}\right\} + C\left\{\frac{\frac{dB}{dT}(P-0.1)}{\left[1-C\cdot\ln\left(\frac{B+P}{B+0.1}\right)\right](B+0.1)(B+P)}\right\} \tag{2-11}$$

$$\kappa_T = \left(\frac{C}{B+P}\right)\left(\frac{\rho}{\rho(T,P=0.1\ MPa)}\right) \tag{2-9}$$

where two different forms of $B(T)$ are commonly used for derivation of κ_T and α_p,

as shown in equations 2-3 and 3-3.

$$B(T) = \sum_{i=0}^{2}(B_i \cdot T^i) \quad (2\text{-}3)$$

$$B(T) = b_0 + \frac{b_1}{T} \quad (3\text{-}3)$$

The differentiation of different fitting equations could lead to different results of κ_T and α_p. Herein, two different forms of $B(T)$ were both used to calculate the values of α_p for ten ILs, of which the directly measured values of α_p have been reported by Navia.[169,170] Then the deviation from the directly measured α_p was calculated, presented in Table 3-12. The comparison of the results calculated by two fitting equations clearly shows that the hyperbolic form of $B(T)$ provides more accurate values of α_p for each IL, except in the case of [C_6mim][NTf_2]. The average deviation for these ten ILs was 3.46% (calculated by the hyperbolic equation) and 18.7% (calculated by the quadratic equation), respectively, which proves that it is reliable to use the hyperbolic form of $B(T)$ to calculate the values of α_p for other ILs.

Table 3-12. The relative deviation between the experimental data of α_p and the calculated values by using different forms of $B(T)$

IL	RAAD% ($B(T) = b_0 + \frac{b_1}{T}$)	RAAD% ($B(T) = b_0 + b_1 \cdot T + b_2 \cdot T^2$)
[C_4mim][NTf_2]	2.19	22.62
[C_4mim][OTf]	14.8	37.54
[C_4mim][BF_4]	1.52	15.11
[C_4mim][C_1SO_4]	3.24	19.95
[C_2mim][BF_4]	1.33	13.88
[$C_4m_{(3)}$py][BF_4]	2.91	14.71
[C_6mim][BF_4]	1.03	16.85
[C_8mim][BF_4]	2.48	23.94
[C_2mim][NTf_2]	3.47	21.2
[C_6mim][NTf_2]	1.60	1.21
Average	3.46	18.4

Therefore, the Tait equation (eq. 2-1) and the eq. 3-3 were selected to calculate the values of α_p and κ_T for 81 ILs investigated in this work. Herein, the recommended experimental density data and the estimated density values by using the GCM developed in this work are used to correlate the Tait equation, respectively. Figure 3-6 shows the comparison of different results of α_p and κ_T from different sources of density data.

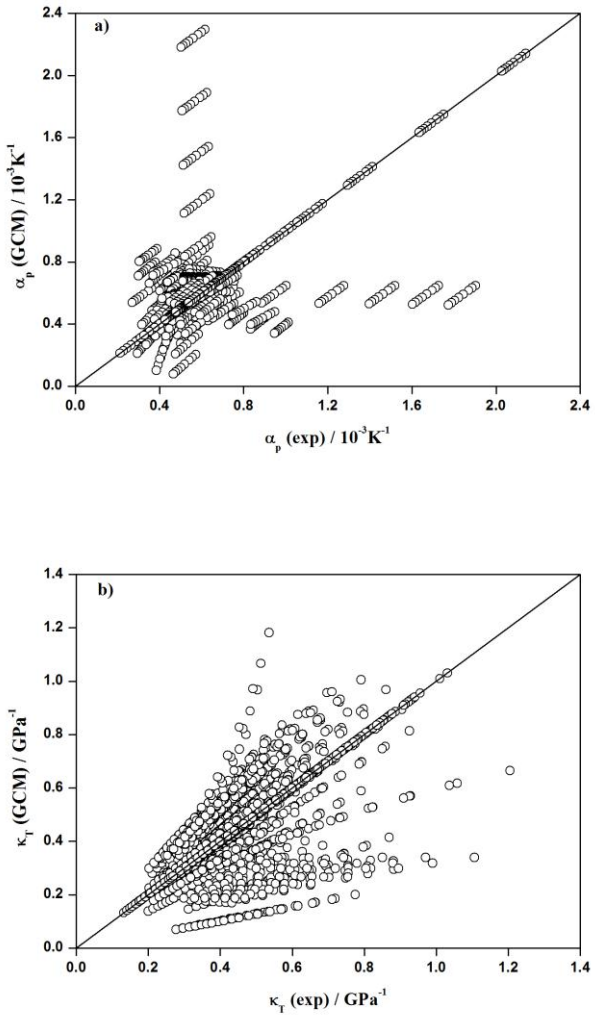

Figure 3-6. The results of (a) α_p and (b) κ_T correlated from the recommended experimental density and the GCM estimated density data.

The global deviation between the α_p values correlated from the experimental data and the GCM estimated density data is 7.5%. 9.8% is calculated for the κ_T values from two different sets of density data. As shown in figure 3-6(a), some data points deviate far away from the diagonal line are from the two ILs: $[C_2OHC_1NH_2][C_4COO]$ corresponding to the data points above the diagonal line, and $[C_2mim][PF_6]$ of which the data points are below the diagonal line. The observed fact maybe ascribed to the

less accurate evaluation result for these two ILs.

Chapter 4
Viscosity

4.1 Data Treatment

4.1.1 Data Collection

The experimental viscosity data of pure ionic liquids as a function of temperature from (253 to 573) K at atmospheric pressure were collected from the literature, comprising over 2,765 data points for more than 70 ionic liquids. Table 8-4 in the appendix presents an overview of all the experimental data, summarizing the references reporting the measurement viscosities for each ILs, the number of data points, and temperature range.

Another database for the viscosity of binary ionic liquids mixtures was also created by collecting 966 data points of eleven binary systems from the literature, as a function of temperature (293.15 to 358.15) K and composition range from (0.0495 to 0.9552) mole fraction. The compositions of the mixtures, temperature range, the number of data points, and references are shown in table 4-9.

4.1.2 Data Analysis

The impurities (like halides, water, and metals) in ionic liquids and the different measurement techniques have a significant effect on the accuracy of measurement,[89] as we discussed in the introduction. In the present work, mathematical gnostics[111,177] was also used to analyse the experimental viscosity data and recommend dataset for each IL. Due to a limited number of data for the binary mixtures of ionic liquids having been reported to date, the given data were regarded as the recommended data.

Nonlinear regression along with an influence function in mathematical gnostics is

utilized to analyse the viscosity data of pure ionic liquids. Mathematical gnostics stems from the methodology of robust statistics[178] where the data errors are assumed to have a normal distribution with zero mean, but the sample is contaminated by a few values having a gross error. Knowing a distribution function of these gross errors an influence function is derived. During regression, the influence function is used for iterative reweighting of the residuals. The procedure is stopped when the values of residuals do not change. The influence function derived from mathematical gnostics does not require any assumption on the distribution function of measurement errors, both the precise data and outliers can be described by the same distribution function estimated during regression. In addition, these posterior weights obtained by application of the influence function are directly related to the distribution density where the weight equal to one coincides with the location of its maximum, i.e. the most probable value. Owing to these properties the values of the posterior weights together with results of marginal analysis of residuals can successfully be applied to the critical evaluation of scattered data. The gnostic weight is calculated as follows:

$$\omega = \frac{2}{(w_i)^2+(1/w_i)^2} \tag{4-1}$$

$$w_i = (\frac{\mu_i}{Z_O})^{Sc} \tag{4-2}$$

where, ω is the gnostic weight of the *i*-th datum; μ_i is the *i*-th datum; S_C is the scale parameter, and Z_O is the estimated most probable value, which has been described in Chapter 3.

For example, several authors[179–187] have reported viscosity values of [C_2mim][OTf].

The number of data points, temperature range, purity, and measurement techniques in each reference are summarized in table 4-1.

Table 4-1. Summary of related information for experimental viscosities of 1-ethyl-3-methylimidazolium triflate [C_2mim][OTf] collected in literature

Ref.	N_{data}	T_{range}	Source	Purity	Water (ppm)	Chloride (ppm)	Experimental technique
[180]	1	293	Synthesized	NA	NA	NA	NA
[181]	1	298.15	Fluka	98%	NA	NA	$HP^{3D}CE$
[184]	8	278.15-348.15	Synthesized	NA	96	NA	Cone-plate rheometer
[182]	18	278.15-363.15	Iolitec	99%	20	NA	Stabinger viscometer
[185]	5	303.15-363.15	Sigma Aldrich	98%	NA	NA	Concentric cylinders
[179]	9	283.15-363.15	NA	NA	237	1300	Cone-plate viscometer
[183]	1	303.15	EMD Chemicals	NA	NA	<2000	Cone-plate viscometer
[186]	5	298.15-343.15	Solvionic	99.5%	50-100	NA	Anton Paar viscosimeter
[187]	4	288.15-318.15	Iolitec	99%	130	NA	Stabinger viscometer
Total	52	278.15-363.15					

[a]N_{data}, the number of data points; T_{range}, temperature range.

Figure 4-1 shows the data weight of experimental viscosities for [C_2mim][OTf]. Only two data points[182,184] were measured at 278.15 K. The weight of one point is close to zero, and the other is close to one. However, one can not say that the viscosity measured by Freire *et al.*[182] at 278.15 K causes a very large difference from the estimated location. Only the qualitative judgment can be made by comparison between the data weights at the same temperature. It can be seen from figure 4-1 that the viscosity data reported by Freire *et al.*[182] manifest better performances than other data at each reported temperature, except at 278.15 K.

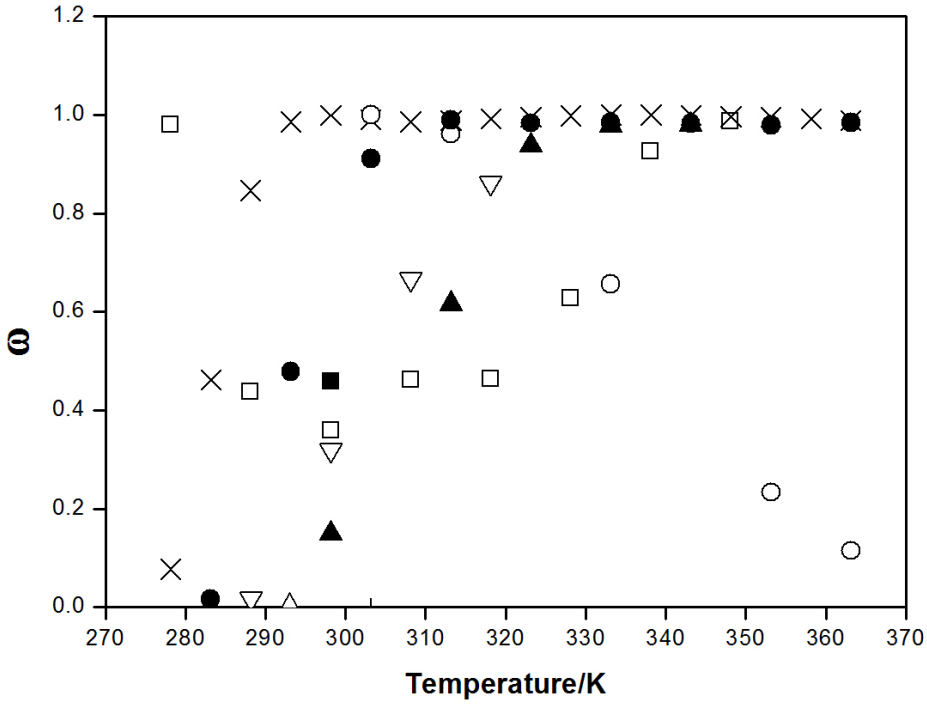

Figure 4-1. The data weight of the literature values for [C_2mim][OTf]: △, Abbott *et al.*;[180] ■, François *et al.*;[181] □, Rodríguez *et al.*;[184] ×, Freire *et al.*;[182] ○, Yusoff *et al.*;[185] ●, Seddon *et al.*;[179] +, Morgan *et al.*;[183] ▲, Tsamba *et al.*;[186] ▽, Vuksanovic *et al.*[187]

The comparison between the estimated locations and the experimental values is demonstrated in figure 4-2. Considerable differences are observed in figure 4-2,

especially with the temperature increasing. At 363.15 K, Yusoff *et al.*[185] measured a viscosity value of 11.14 mPa·s. A difference of 30% was found from 7.75 mPa·s reported by Seddon *et al.*[179] and 26.7% deviation from 8.169 mPa·s reported by Freire *et al.*[182] The fact, this can be attributed to different measurement techniques, purity of samples or poor temperature control. Generally speaking, the performance of the data set measured by Freire *et al.*[182] is better than the other three data sets[179,184,185] in visual, ignoring three individual data points reported by three different references.[180,181,183] The data reported by Seddon *et al.*[179] show a good agreement at the temperature range from 303.15 K to 343.15 K, while deviations increase at the higher temperature and lower temperature. The average relative deviation of the data set reported by Freire *et al.*[182] is -0.7% compared with the estimated locations, lower than -4.1% of deviation from Seddon *et al.*[179] and -4.5% of deviation from Rodríguez *et al.*[184] While the average deviation is up to 9.7% for the data set measured by Yusoff *et al.*[185] in a comparison from the estimated locations. Therefore, we recommend the data set from Freire *et al.*[182] used for the optimization of the binary interaction parameters.

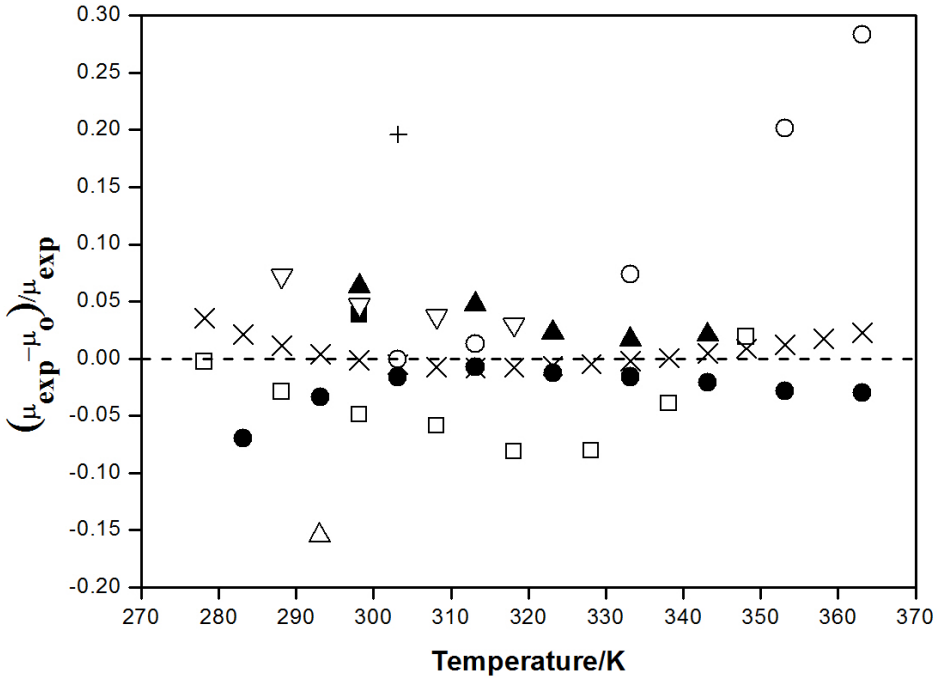

Figure 4-2. Deviations of the literature values from the estimated locations for [C_2mim][OTf]: △, Abbott *et al.*;[180] ■, François *et al.*;[181] □, Rodríguez *et al.*;[184] ×, Freire *et al.*;[182] ○, Yusoff *et al.*;[185] ●, Seddon *et al.*;[179] +, Morgan *et al.*;[183] ▲, Tsamba *et al.*;[186] ▽, Vuksanovic *et al.*[187]

Viscosity (μ) decreases approximately exponentially with temperature, consequently the change in viscosity ($\Delta\mu$) reduced significantly with increasing temperature. Another possible analysis method is to treat $\ln(\mu)$ instead of μ by using gnostic weights. Thus, the large variability in data weight (Figure 4-1) at temperature lower than 290 K maybe reduce and more significant differences at temperature higher than 350 K would be observed. However, the deviation, which is used to evaluate the result and quality of our proposed method is the difference between the experimental viscosity and calculated viscosity (i.e. RAAD, eq. 3-1), rather than the difference between the logarithm of experimental viscosity and calculated viscosity (eq. 4-3).

Hence, it is more direct and accurate to analyse viscosity data than logarithm of viscosity by using the gnostic method.

$$RAAD = \frac{1}{M}\sum_{i=0}^{M}\left|\frac{x_{exp}-x_{cal}}{x_{exp}}\right| \quad (3\text{-}1)$$

$$lnRAAD = \frac{1}{M}\sum_{i=0}^{M}\left|\frac{\ln(x_{exp})-\ln(x_{cal})}{\ln(x_{exp})}\right| \quad (4\text{-}3)$$

where M is the number of data points, x_{exp} and x_{cal} are the experimental and calculated values of properties, respectively.

Herein, the statistical analysis and the gnostic analysis were also compared. If the distribution function of a data sample is unimodal, which is a frequent case in classical (non-robust) statistical analysis, the same data set is thus recommended by using the statistical analysis and the gnostic analysis. However, if the distribution function is multimodal, it is difficult to obtain an obvious result from the statistical analysis. For example of the experimental data of $[C_4mmim][NTf_2]$[188–190], figure 4-3 and figure 4-4 show the gnostic weight and deviations by gnostic analysis, respectively. Figure 4-5 shows the fitting deviations by statistical analysis. It is obviously observed from figure 4-3 and 4-4 that the data set reported by Gaciño *et al.*[190] shows better performance and is recommended. But the statistical analysis result (as shown in figure 4-5) presents the large deviations for both data sets reported by Okoturo *et al.*[188] (at lower temperature) and by Gaciño *et al.*[190] (at higher temperature). Hence, it is difficult to recommend one data set through the statistical analysis result (i.e. figure 4-5). In view of this reason, the gnostic analysis is preferable to statistical analysis.

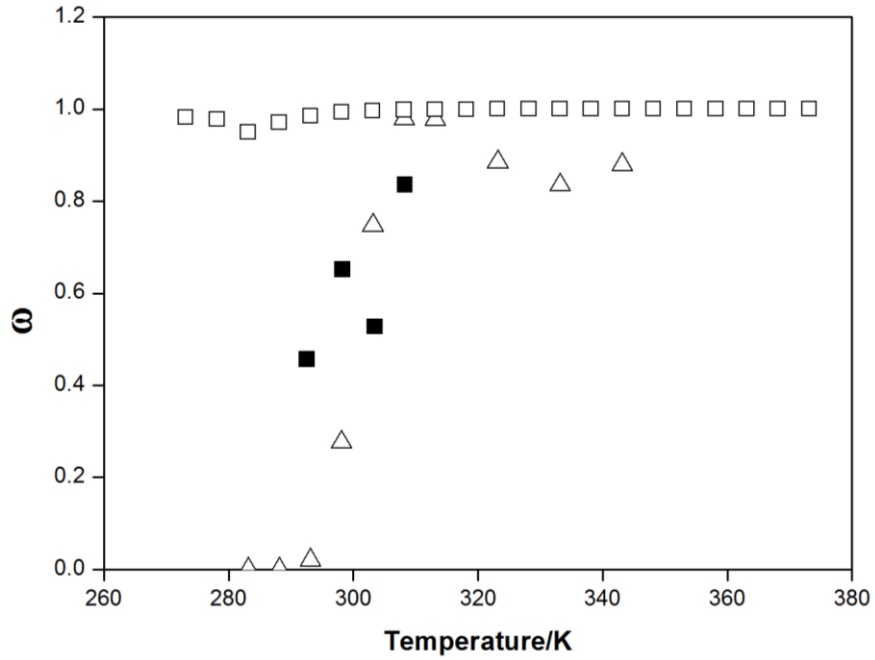

Figure 4-3. The gnostic weight of the literature values for $[C_4mmim][NTf_2]$: △, Okoturo *et al.*;[188] ■, Katsuta *et al.*;[189] □, Gaciño *et al.*;[190]

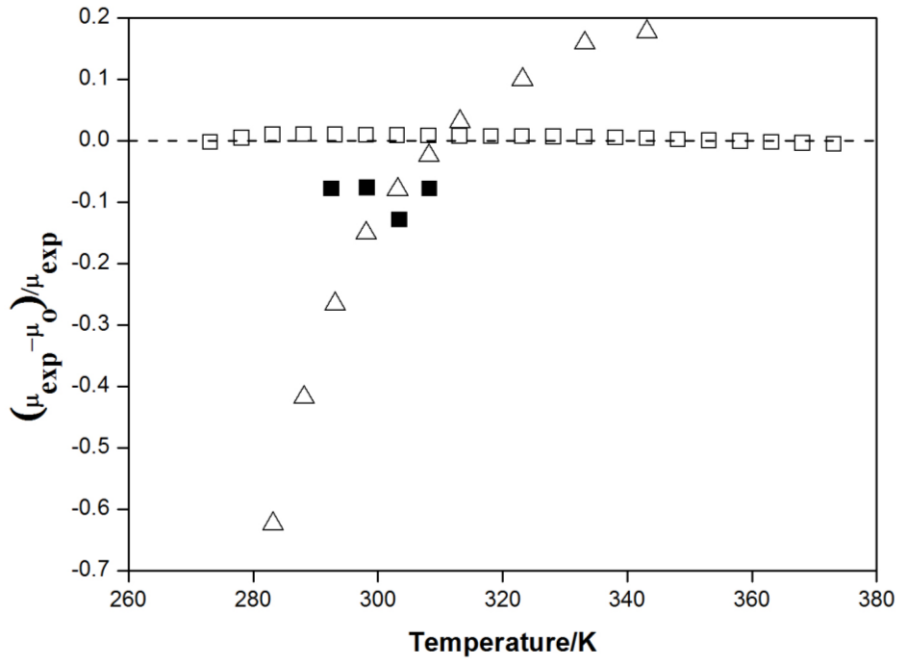

Figure 4-4. Deviations of the literature values from the gnostic analysis for $[C_4mmim][NTf_2]$: △,Okoturo *et al.*;[188] ■, Katsuta *et al.*;[189] □, Gaciño *et al.*;[190]

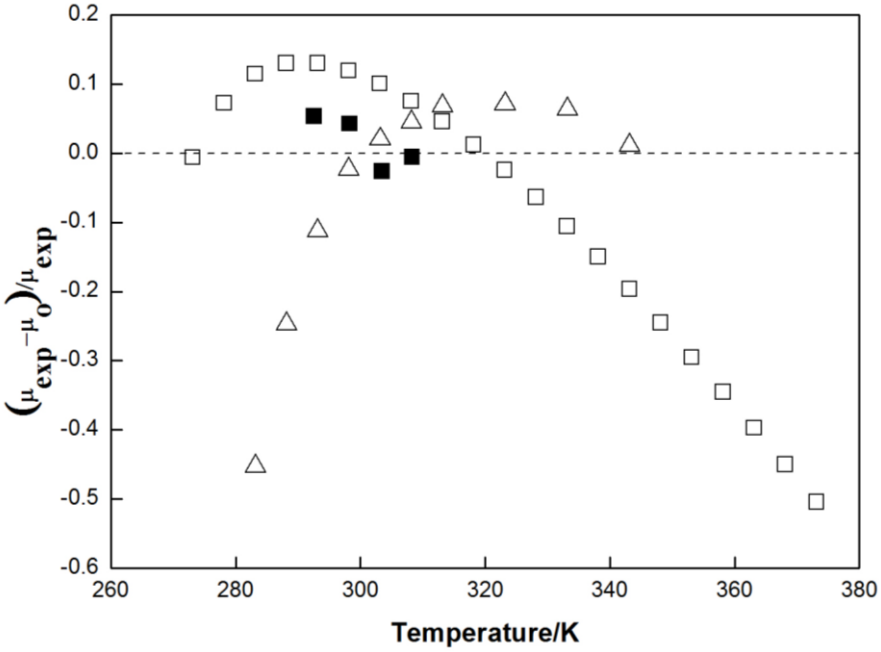

Figure 4-5. Deviations of the literature values from the statistical analysis for $[C_4mmim][NTf_2]$: △,Okoturo *et al.*;[188] ■, Katsuta *et al.*;[189] □, Gaciño *et al.*;[190]

Following the gnostic methodology, we recommended one dataset for each selected ionic liquid. The cations and anions used are among the most commonly studied structures. The cations used include imidazolium, ammonium, phosphonium, pyridinium, and pyrrolidinium series. 15 different inorganic anions are used, for example, tetrafluoroborate ($[BF_4]^-$), methyl sulfate ($[C_1SO_4]^-$), and thiocyanate ($[SCN]^-$). Selected cations and anions are listed in table 4-2 along with the number of data points for the ionic liquid consisting of this ion, temperature range and the references from which the experimental viscosity data were taken. The selected 70 different ILs, the number of the recommended data points, and the temperature range are shown in table 4-3. Only one data set has been published, or several data sets have been published, of which only one data set contains sufficient data for the regression, for example, $[C_6mim][Br]$ and $[C_{10}mim][BF_4]$. Recommended data could thus not be

obtained by the described method, and the given data set was then considered as recommendation dataset.

Table 4-2. Selected Ions, Counterparts Constituting the Selected ILs, and References from Which Experimental Data Were Collected[a]

Code	Cation	Counterparts	N_{data}	T_{range} (K)	Ref.
1	$[C_2mim]^+$	$[BF_4]^-$, $[C_1SO_4]^-$, $[NTf_2]^-$, $[SCN]^-$, $[OAc]^-$, $[OTf]^-$, $[FAP]^-$, $[DCA]^-$, $[C_2SO_4]^-$, $[C_8SO_4]^-$, $[C_1SO_3]^-$, $[Tos]^-$, $[Cl]^-$	172	263.15-373.15	112,182,191–196
2	$[C_4mim]^+$	$[BF_4]^-$, $[C_1SO_4]^-$, $[NTf_2]^-$, $[PF_6]^-$, $[SCN]^-$, $[OAc]^-$, $[OTf]^-$, $[FAP]^-$, $[DCA]^-$, $[C_8SO_4]^-$	112	273.15-373.15	116,179,194,197–203
3	$[C_3mim]^+$	$[NTf_2]^-$, $[PF_6]^-$	20	298.15-363.15	204,205
4	$[C_4m_{(3)}py]^+$	$[BF_4]^-$, $[NTf_2]^-$, $[DCA]^-$	36	278.15-363.15	8,206,207
5	$[P_{66614}]^+$	$[FAP]^-$, $[DCA]^-$, $[NTf_2]^-$, $[C_1SO_3]^-$, $[Br]^-$	86	268.15-373.15	190,208,209
6	$[C_4mmim]^+$	$[BF_4]^-$, $[NTf_2]^-$, $[FAP]^-$	50	273.15-373.15	188,190
7	$[C_4py]^+$	$[BF_4]^-$, $[NTf_2]^-$	22	278.15-363.15	207,210
8	$[C_6mim]^+$	$[BF_4]^-$, $[PF_6]^-$, $[FAP]^-$, $[NTf_2]^-$, $[Br]^-$, $[Cl]^-$	54	283.15-363.15	179,197,211–213
9	$[C_{10}mim]^+$	$[BF_4]^-$, $[PF_6]^-$, $[NTf_2]^-$, $[OTf]^-$	28	283.15-363.15	179,214
10	$[C_1mim]^+$	$[NTf_2]^-$, $[C_1SO_4]^-$	15	283.15-353.15	215,216
11	$[C_4mpyrro]^+$	$[C_1SO_4]^-$, $[NTf_2]^-$, $[SCN]^-$, $[OAc]^-$, $[OTf]^-$, $[FAP]^-$, $[DCA]^-$	90	283.15-373.15	190,208,217–220
12	$[C_4m_{(4)}py]^+$	$[BF_4]^-$, $[NTf_2]^-$, $[SCN]^-$	32	278.15-363.15	207,218,221
13	$[C_8mim]^+$	$[BF_4]^-$, $[PF_6]^-$, $[NTf_2]^-$, $[OTf]^-$, $[Cl]^-$	40	273.15-363.15	179,222–225

14	$[C_8py]^+$	$[BF_4]^-$, $[NTf_2]^-$	33	278.15-363.15	207,226
15	$[N_{1114}]^+$	$[NTf_2]^-$	15	283.15-353.15	227
16	$[N_{8881}]^+$	$[NTf_2]^-$	8	273.15-333.15	228
17	$[C_6py]^+$	$[NTf_2]^-$	9	298.15-338.15	229

Code	**Anion**	**Counterparts**	**N_{data}**	**T_{range} (K)**	**Ref.**
1	$[BF_4]^-$	$[C_2mim]^+$, $[C_4mim]^+$, $[C_4mmim]^+$, $[C_4py]^+$, $[C_6mim]^+$, $[C_{10}mim]^+$, $[C_4m_{(4)}py]^+$, $[C_8mim]^+$, $[C_8py]^+$, $[C_4m_{(3)}py]^+$	87	273.15-363.15	8,112,179,188,197,210,221,223,226
2	$[C_1SO_4]^-$	$[C_2mim]^+$, $[C_4mim]^+$, $[C_4mpyrro]^+$, $[C_1mim]^+$	45	283.15-373.15	191,198,216,217
3	$[NTf_2]^-$	$[C_4mim]^+$, $[C_3mim]^+$, $[P_{66614}]^+$, $[C_4py]^+$, $[C_4m_{(3)}py]^+$, $[C_4mmim]^+$, $[C_1mim]^+$, $[C_2mim]^+$, $[C_4mpyrro]^+$, $[C_4m_{(4)}py]^+$, $[C_8mim]^+$, $[C_8py]^+$, $[C_6mim]^+$, $[N_{1114}]^+$, $[N_{8881}]^+$, $[C_6py]^+$	223	263.15-373.15	116,190,192,204,207–209,213–215,222,227–229
4	$[PF_6]^-$	$[C_4mim]^+$, $[C_3mim]^+$, $[C_8mim]^+$, $[C_6mim]^+$, $[C_{10}mim]^+$	38	293.15-363.15	179,199,205,211,224
5	$[DCA]^-$	$[P_{66614}]^+$, $[C_4m_{(3)}py]^+$, $[C_2mim]^+$, $[C_4mpyrro]^+$, $[C_4mim]^+$	68	278.15-363.15	182,202,206,208,220
6	$[SCN]^-$	$[C_2mim]^+$, $[C_4mim]^+$, $[C_4m_{(4)}py]^+$, $[C_4mpyrro]^+$	48	278.15-368.15	182,200,218
7	$[OAc]^-$	$[C_2mim]^+$, $[C_4mim]^+$, $[C_4mpyrro]^+$	29	298.15-363.15	193,201,219
8	$[OTf]^-$	$[C_2mim]^+$, $[C_4mim]^+$, $[C_4mpyrro]^+$, $[C_8mim]^+$, $[C_{10}mim]^+$	64	278.15-373.15	179,182,190

9	$[FAP]^-$	$[C_2mim]^+$, $[C_4mim]^+$, $[C_4mpyrro]^+$, $[C_6mim]^+$, $[P_{66614}]^+$, $[C_4mmim]^+$	89	268.15-373.15	[190,194,211]
10	$[C_2SO_4]^-$	$[C_2mim]^+$	10	298.15-343.15	[195]
11	$[Br]^-$	$[C_6mim]^+$, $[P_{66614}]^+$	27	278.15-363.15	[209,212]
12	$[C_8SO_4]^-$	$[C_2mim]^+$, $[C_4mim]^+$	28	283.15-373.15	[191,203]
13	$[C_1SO_3]^-$	$[C_2mim]^+$, $[P_{66614}]^+$	36	278.15-363.15	[182,209]
14	$[Tos]^-$	$[C_2mim]^+$	13	303.15-363.15	[182]
15	$[Cl]^-$	$[C_2mim]^+$, $[C_8mim]^+$, $[C_6mim]^+$	17	283.15-363.15	[179,196,225]

[a] N_{data}, no. of data points; T_{range}, temperature range.

Table 4-3. Ionic Liquids, Number of Recommended Data Points and Temperature Ranges in Each Corresponding Reference

Code	Ionic Liquid	N_{data}	T_{range} (K)	Ref.
1	$[C_2mim][BF_4]$	4	282.55-323.65	[112]
2	$[C_4mim][BF_4]$	7	293.15-323.15	[197]
3	$[C_4mim][C_1SO_4]$	9	293.15-343.15	[198]
4	$[C_2mim][C_1SO_4]$	19	283.15-373.15	[191]
5	$[C_4mim][NTf_2]$	21	273.15-353.15	[116]
6	$[C_3mim][NTf_2]$	10	298.15-343.15	[204]
7	$[C_3mim][PF_6]$	10	318.15-363.15	[205]
8	$[C_4mim][PF_6]$	7	293.15-323.15	[199]
9	$[C_4m_{(3)}py][DCA]$	10	283.15-328.15	[206]
10	$[P_{66614}][DCA]$	11	298.15-343.15	[208]
11	$[P_{66614}][NTf_2]$	17	278.15-358.15	[209]
12	$[C_4m_{(3)}py][NTf_2]$	18	278.15-363.15	[207]
13	$[C_4mmim][BF_4]$	7	313.15-373.15	[188]
14	$[C_4py][BF_4]$	4	293.15-323.15	[210]
15	$[C_4py][NTf_2]$	18	278.15-363.15	[207]
16	$[C_4mmim][NTf_2]$	21	273.15-373.15	[190]
17	$[C_6mim][BF_4]$	8	288.15-323.15	[197]
18	$[C_{10}mim][BF_4]$	9	283.15-363.15	[179]
19	$[C_{10}mim][PF_6]$	6	313.15-363.15	[179]
20	$[C_6mim][PF_6]$	11	293.15-343.15	[211]
21	$[C_1mim][NTf_2]$	8	283.15-353.15	[215]
22	$[C_4mpyrro][NTf_2]$	11	293.15-343.15	[208]
23	$[C_4mpyrro][C_1SO_4]$	10	298.15-343.15	[217]
24	$[C_1mim][C_1SO_4]$	7	293.15-343.15	[216]
25	$[C_2mim][NTf_2]$	12	263.15-353.15	[192]
26	$[C_4m_{(4)}py][BF_4]$	8	298.15-348.15	[221]

27	$[C_4m_{(4)}py][NTf_2]$	18	278.15-363.15	[207]
28	$[C_2mim][SCN]$	18	278.15-363.15	[182]
29	$[C_4mim][SCN]$	18	283.15-368.15	[200]
30	$[C_4m_{(4)}py][SCN]$	6	298.15-348.15	[218]
31	$[C_4mpyrro][SCN]$	6	298.15-348.15	[218]
32	$[C_2mim][OAc]$	10	298.15-343.15	[193]
33	$[C_4mim][OAc]$	5	303.15-343.15	[201]
34	$[C_4mpyrro][OAc]$	14	298.15-363.15	[219]
35	$[C_2mim][OTf]$	18	278.15-363.15	[182]
36	$[C_4mim][OTf]$	9	283.15-363.15	[179]
37	$[C_8mim][OTf]$	9	283.15-363.15	[179]
38	$[C_4mpyrro][OTf]$	19	283.15-373.15	[190]
39	$[C_{10}mim][OTf]$	9	283.15-363.15	[179]
40	$[C_8mim][NTf_2]$	9	283.15-353.15	[222]
41	$[C_8mim][BF_4]$	14	273.15-353.15	[223]
42	$[C_8mim][PF_6]$	4	293.15-353.15	[224]
43	$[C_2mim][FAP]$	9	293.15-373.15	[194]
44	$[C_4mim][FAP]$	9	293.15-373.15	[194]
45	$[C_6mim][FAP]$	11	293.15-343.15	[211]
46	$[C_4mpyrro][FAP]$	19	283.15-373.15	[190]
47	$[C_4mmim][FAP]$	19	283.15-373.15	[190]
48	$[P_{66614}][FAP]$	22	268.15-373.15	[190]
49	$[C_2mim][DCA]$	18	278.15-363.15	[182]
50	$[C_2mim][C_2SO_4]$	10	298.15-343.15	[195]
51	$[C_6mim][Br]$	9	293.15-333.15	[212]
52	$[P_{66614}][Br]$	18	278.15-363.15	[209]
53	$[C_4mim][DCA]$	18	278.15-363.15	[202]
54	$[C_4mpyrro][DCA]$	11	293.15-343.15	[220]
55	$[C_8py][BF_4]$	15	283.15-353.15	[226]
56	$[C_8py][NTf_2]$	18	278.15-363.15	[207]

57	$[C_4m_{(3)}py][BF_4]$	8	283-343	[8]
58	$[C_2mim][C_8SO_4]$	19	283.15-373.15	[191]
59	$[C_4mim][C_8SO_4]$	9	293.15-373.15	[203]
60	$[C_2mim][C_1SO_3]$	18	278.15-363.15	[182]
61	$[P_{66614}][C_1SO_3]$	18	278.15-363.15	[209]
62	$[C_2mim][Tos]$	13	303.15-363.15	[182]
63	$[C_6mim][NTf_2]$	6	298.15-343.15	[213]
64	$[C_{10}mim][NTf_2]$	4	293.15-323.15	[214]
65	$[N_{1114}][NTf_2]$	15	283.15-353.15	[227]
66	$[N_{8881}][NTf_2]$	8	273.15-333.15	[228]
67	$[C_6py][NTf_2]$	9	298.15-338.15	[229]
68	$[C_2mim][Cl]$	4	298.15-313.15	[196]
69	$[C_6mim][Cl]$	9	283.15-363.15	[179]
70	$[C_8mim][Cl]$	4	298.15-343.15	[225]
Total		**819**	**263.15-373.15**	

4.2 Development of Predictive Models

The UNIFAC-VISCO model is utilized to predict the viscosity of organic liquid mixtures originally. In this work, the UNIFAC-VISCO method was modified and developed to estimate the viscosity of pure and binary mixtures of ionic liquids. The UNIFAC-VISCO model is a group contribution model, in which the contribution value of each functional group has to be calculated. Therefore, defining the functional groups in the ionic liquids is necessary. Herein, the cation and anion, constituting the ionic liquid, are regarded as individual groups. In the calculation of pure ionic liquid, the ionic liquid is taken as a ‘mixture’ of two components (the cation and anion) with mole fractions both equal to 0.5. Each component (the cation or anion) is composed of a single group. In the calculation of binary mixtures of ionic liquids, either ionic liquid

is a component, each consisting of two groups (the cation and anion).

The first set of parameters required for the calculation of IL viscosity using the modified UNIFAC-VISCO method is the molar volume (V_i) of pure components and the molar volume (V_m) of their mixture (see eq. 2-16). For a single ionic liquid, these correspond to the effective molar volume of the cation and anion (i.e., components) and the molar volume of pure ionic liquid, respectively. In chapter three, we have introduced our work to calculate the volumetric parameters of ions and evaluate the volumetric properties of ionic liquids using a group contribution model. Herein, the effective molar volumes of ions and the molar volumes of ionic liquids as a function of temperature were calculated using the obtained volumetric parameters following the eq. 2-5.

The second set of parameters required for the calculation of IL viscosity using the UNIFAC-VISCO method is the van der Waals volume (*R*) and surface area (*Q*) of ions. The *R* and *Q* values of cations and anions were simulated using TURBOMOLE and COSMO*therm*X, which have been described in chapter 2.4.

Another set of parameters required for the UNIFAC-VISCO method is the viscosities of components, that is, the effective viscosities of ions (see eq. 2-16). In this work, the effective viscosity of cations and anions as a function of temperature is represented by the Vogel-Fulcher-Tamman (VFT) equation (see eq. 2-15).

The last set of parameters is the binary interaction parameters (α_{mn}) between functional groups, such as $\alpha_{cation/anion}$ and $\alpha_{anion/cation}$.

In order to estimate the unknown binary interaction parameters and ions VFT parameters, the recommended viscosity data were used for regression analysis by minimizing the objective function in the Marquardt optimization technique (eq. 2-32). For each ionic liquid, eight parameters are unknown. For example of [C_2mim][NTf_2], $\alpha_{[C_2mim]^+/[NTf_2]^-}$, $\alpha_{[NTf_2]^-/[C_2mim]^+}$, $VFT_{[C_2mim]^+}(A, B, T_0)$, and $VFT_{[NTf_2]^-}(A, B, T_0)$ are unknown and need to be optimized. However, the more unknown parameters involved, the more experimental data are requested. Herein a method of combining four ionic liquids with common ions was adopted to reduce the number of unknown parameters. For example, the following four ionic liquids; [C_2mim][BF_4], [C_4mim][BF_4], [C_2mim][NTf_2], and [C_4mim][NTf_2] consist of two different cations ([C_2mim]$^+$ and [C_4mim]$^+$) and two different anions ([BF_4]$^-$ and [NTf_2]$^-$), as shown in figure 4-6. Originally 32 parameters were unknown for four ionic liquids. While, in figure 4-6, the first and the second ILs have the same anion; the second and the third ones have the same cation; *etc.* It means that the VFT parameters of only four different ions need to be determined in the regression of four different ILs. Thus, the number of parameters for four ILs is significantly reduced to 20.

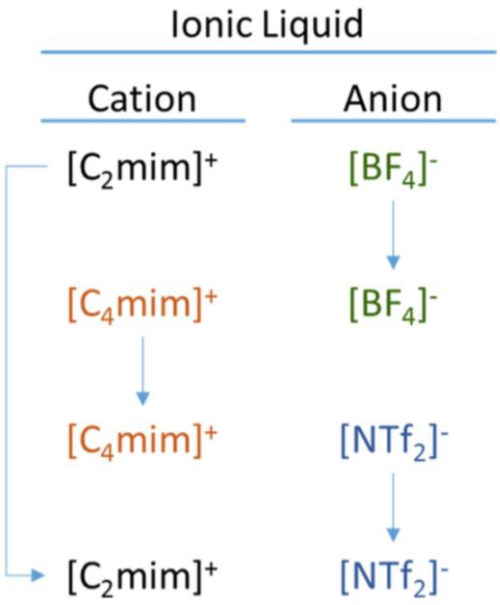

Figure 4-6. Example of the approach proposed for the regression analysis[89]

In the first stage, the recommended data of the selected 25 most common ionic liquids were used to estimate the interaction parameter and ions VFT parameters. Two steps to complete the regression: 1) the 'solver' add-on in Excel was used to minimize the objective function and get the initial values of parameters; 2) initial values of parameters were implemented into the MATLAB files for the further regression analysis to obtain the final values of the binary interaction parameters and ions VFT parameters using non-linear fitting method. Based on the parameters of these 25 ionic liquids, proceeding to the next stage, binary parameters and VFT parameters for other 45 ionic liquids were optimized by correlating the recommended data of these 45 ionic liquids.

Following the same methodology, the parameters of binary ionic liquids mixtures were estimated by correlating one data set of each binary system, totally including 128 data points. Other 838 data points of these eleven binary

mixtures were tested and compared with pure evaluated values. The regression processes were completed using MATLAB software.

4.3 Results and Discussion

The binary interaction parameters (Table 4-4) and ions VFT parameters (Table 4-5) for 70 ionic liquids, comprising 17 cations and 15 anions, were estimated by correlating 819 experimental data points.

Table 4-4. Estimated Binary Interaction Parameters between ions

m	n	α_{mn}	α_{nm}
$[BF_4]^-$	$[DCA]^-$	331.97	-562.66
$[BF_4]^-$	$[C_1SO_4]^-$	-111.50	41.59
$[BF_4]^-$	$[PF_6]^-$	-20.70	-59.91
$[C_{10}mim]^+$	$[BF_4]^-$	77.85	-410.46
$[C_{10}mim]^+$	$[PF_6]^-$	1004.9	-452.60
$[C_{10}mim]^+$	$[OTf]^-$	394.03	-402.07
$[C_{10}mim]^+$	$[NTf_2]^-$	128.91	97.59
$[C_1mim]^+$	$[NTf_2]^-$	-391.35	931.41
$[C_1mim]^+$	$[C_1SO_4]^-$	-158.30	-54.69
$[C_2mim]^+$	$[BF_4]^-$	-222.19	-130.81
$[C_2mim]^+$	$[C_1SO_4]^-$	566.37	-354.46
$[C_2mim]^+$	$[NTf_2]^-$	-322.07	1978.2
$[C_2mim]^+$	$[SCN]^-$	5717.4	376.59
$[C_2mim]^+$	$[OAc]^-$	-611.17	6394.8
$[C_2mim]^+$	$[OTf]^-$	1717.39	-465.92
$[C_2mim]^+$	$[FAP]^-$	-376.69	807.02
$[C_2mim]^+$	$[DCA]^-$	9765.3	-260.54
$[C_2mim]^+$	$[C_2SO_4]^-$	355.51	423.56

$[C_2mim]^+$	$[C_8SO_4]^-$	-423.54	2156.2
$[C_2mim]^+$	$[C_1SO_3]^-$	1210.8	1163.3
$[C_2mim]^+$	$[Tos]^-$	35.38	-13.35
$[C_2mim]^+$	Cl^-	-2855.0	-0.56
$[C_2mim]^+$	$[C_6mim]^+$	-215.62	199.37
$[C_3mim]^+$	$[NTf_2]^-$	67.96	-111.31
$[C_3mim]^+$	$[PF_6]^-$	2723.3	-599.61
$[C_4m_{(4)}py]^+$	$[BF_4]^-$	-678.30	1116.6
$[C_4m_{(4)}py]^+$	$[NTf_2]^-$	65.77	-9.79
$[C_4m_{(4)}py]^+$	$[SCN]^-$	917.22	-113.69
$[C_4m_{(4)}py]^+$	$[C_2mim]^+$	154.59	21.49
$[C_4m_{(4)}py]^+$	$[C_2SO_4]^-$	130.48	30.82
$[C_4m_{(4)}py]^+$	$[C_4py]^+$	-109.87	41.82
$[C_4m_{(3)}py]^+$	$[DCA]^-$	4174.7	-336.84
$[C_4m_{(3)}py]^+$	$[NTf_2]^-$	702.97	-262.88
$[C_4m_{(3)}py]^+$	$[BF_4]^-$	-660.43	1990.6
$[C_4mim]^+$	$[BF_4]^-$	-0.06	-464.73
$[C_4mim]^+$	$[C_1SO_4]^-$	112.45	-365.32
$[C_4mim]^+$	$[NTf_2]^-$	322.36	-228.33
$[C_4mim]^+$	$[PF_6]^-$	1248.42	-544.06
$[C_4mim]^+$	$[SCN]^-$	57.26	346530
$[C_4mim]^+$	$[OAc]^-$	4669.6	-712.86
$[C_4mim]^+$	$[OTf]^-$	-280.50	-14.04
$[C_4mim]^+$	$[FAP]^-$	-256.62	270.83
$[C_4mim]^+$	$[DCA]^-$	361.00	-291.30
$[C_4mim]^+$	$[C_8SO_4]^-$	-179.20	124.94
$[C_4mim]^+$	$[C_4py]^+$	272.88	-294.87
$[C_4mim]^+$	$[C_6mim]^+$	-79.43	62.39
$[C_4mmim]^+$	$[FAP]^-$	-264.20	74.33
$[C_4mmim]^+$	$[BF_4]^-$	-105.01	-768.66

$[C_4mmim]^+$	$[NTf_2]^-$	-193.25	-8.28
$[C_4mpyrro]^+$	$[NTf_2]^-$	-127.47	-29.34
$[C_4mpyrro]^+$	$[C_1SO_4]^-$	405.62	-609.91
$[C_4mpyrro]^+$	$[SCN]^-$	-42.61	-18.69
$[C_4mpyrro]^+$	$[OAc]^-$	-365.86	-53.83
$[C_4mpyrro]^+$	$[OTf]^-$	121.62	-486.62
$[C_4mpyrro]^+$	$[FAP]^-$	-416.08	356.83
$[C_4mpyrro]^+$	$[DCA]^-$	-208.95	-53.51
$[C_4py]^+$	$[BF_4]^-$	-404.47	7644.6
$[C_4py]^+$	$[NTf_2]^-$	86.82	417.64
$[C_6mim]^+$	$[BF_4]^-$	-155.98	-414.47
$[C_6mim]^+$	$[PF_6]^-$	2912.7	-584.72
$[C_6mim]^+$	$[FAP]^-$	439.06	-274.24
$[C_6mim]^+$	Br^-	649.67	-652.40
$[C_6mim]^+$	$[NTf_2]^-$	-251.08	415.53
$[C_6mim]^+$	Cl^-	905.23	-1620.8
$[C_6py]^+$	$[NTf_2]^-$	10.57	-8.10
$[C_8mim]^+$	$[OTf]^-$	304.75	-419.22
$[C_8mim]^+$	$[NTf_2]^-$	80.21	36.46
$[C_8mim]^+$	$[BF_4]^-$	-443.32	29.73
$[C_8mim]^+$	$[PF_6]^-$	-506.07	1351.0
$[C_8mim]^+$	Cl^-	35183	-1499.7
$[C_8py]^+$	$[BF_4]^-$	-504.65	909.79
$[C_8py]^+$	$[NTf_2]^-$	-232.89	73830
$[N_{1114}]^+$	$[NTf_2]^-$	-3.97	-9.63
$[N_{8881}]^+$	$[NTf_2]^-$	17.24	27.69
$[NTf_2]^-$	$[C_2SO_4]^-$	132.29	-123.01
$[NTf_2]^-$	$[BF_4]^-$	-314.98	113.81
$[OAc]^-$	$[C_2SO_4]^-$	-136.52	2380.7
$[P_{66614}]^+$	$[DCA]^-$	2040.7	-577.60

$[P_{66614}]^+$	$[NTf_2]^-$	1463.7	-403.99
$[P_{66614}]^+$	$[FAP]^-$	1001.6	-359.16
$[P_{66614}]^+$	Br^-	-873.04	29571
$[P_{66614}]^+$	$[C_1SO_3]^-$	29517	-276.78
$[SCN]^-$	$[C_2SO_4]^-$	-324.50	287.34
$[SCN]^-$	$[DCA]^-$	-22.96	252.44

Table 4-5. VFT fitting parameters of ions

Cation/Anion	***A* (mPa•s)**	***B* (K)**	T_o **(K)**	**Cation/Anion**	***A* (mPa•s)**	***B* (K)**	T_o **(K)**
$[C_1mim]^+$	0.521	385.2	182.9	$[C_6py]^+$	0.034	1066.3	171.6
$[C_2mim]^+$	0.436	792.8	110.1	$[BF_4]^-$	0.403	532.9	182.7
$[C_3mim]^+$	0.091	664.4	180.4	$[C_1SO_4]^-$	0.517	756.9	186.0
$[C_4mim]^+$	0.062	926.9	155.8	$[NTf_2]^-$	2.007	581.0	170.7
$[C_6mim]^+$	0.032	1192.9	145.7	$[PF_6]^-$	6.206	378.1	215.4
$[C_{10}mim]^+$	0.013	1965.2	142.1	$[DCA]^-$	4.760	282.5	197.9
$[C_4mmim]^+$	0.010	1075.2	161.1	$[SCN]^-$	8.425	690.3	177.9
$[C_4py]^+$	0.587	1031.8	171.6	$[OAc]^-$	3.497	254.1	244.2
$[C_4m_{(3)}py]^+$	0.250	766.9	174.8	$[OTf]^-$	1.492	412.2	188.0
$[C_4mpyrro]^+$	0.022	966.9	160.7	$[FAP]^-$	1.371	587.6	183.6
$[P_{66614}]^+$	2.520	1029.4	130.0	$[C_2SO_4]^-$	1.049	1285.1	174.4
$[C_4m_{(4)}py]^+$	0.063	944.8	171.2	Br^-	0.036	1958.5	161.8
$[C_8mim]^+$	0.021	1577.3	143.6	$[C_8SO_4]^-$	0.611	1159.5	184.4
$[C_8py]^+$	1.781	772.0	182.7	$[C_1SO_3]^-$	2.190	1344.0	183.1
$[N_{1114}]^+$	0.060	989.1	176.8	$[Tos]^-$	0.226	1006.4	232.7
$[N_{8881}]^+$	0.022	1828.4	161.8	Cl^-	0.006	71.7	258.6

RAAD values for the regression of each pure IL are presented in table 4-6. The model results show a global relative average absolute deviation of 1.4% from the 819 experimental data, which demonstrate an excellent correlation ability of this model,

except in the case of the [C_6mim]Br (RAAD = 12.3 %) and [C_{10}mim][NTf_2] (RAAD = 14.7%).

Table 4-6. Relative Absolute Average Deviation (RAAD) of the Calculated Viscosity from the Experimental Viscosity Data for Selected ILs

IL	RAAD (%)	IL	RAAD (%)
[C_2mim][BF_4]	1.71	[C_4mim][OTf]	1.09
[C_4mim][BF_4]	0.25	[C_8mim][OTf]	1.00
[C_4mim][C_1SO_4]	0.17	[C_4mpyrro][OTf]	0.72
[C_2mim][C_1SO_4]	0.16	[C_{10}mim][OTf]	0.99
[C_4mim][NTf_2]	0.38	[C_8mim][NTf_2]	0.88
[C_3mim][NTf_2]	0.13	[C_8mim][BF_4]	0.53
[C_3mim][PF_6]	0.11	[C_8mim][PF_6]	0.88
[C_4mim][PF_6]	0.29	[C_2mim][FAP]	0.39
[$C_4m_{(3)}$py][DCA]	0.23	[C_4mim][FAP]	1.45
[P_{66614}][DCA]	0.42	[C_6mim][FAP]	0.48
[P_{66614}][NTf_2]	0.22	[C_4mpyrro][FAP]	1.60
[$C_4m_{(3)}$py][NTf_2]	0.12	[C_4mmim][FAP]	2.16
[C_4mmim][BF_4]	1.63	[P_{66614}][FAP]	1.23
[C_4py][BF_4]	3.46	[C_2mim][DCA]	2.31
[C_4py][NTf_2]	0.83	[C_2mim][C_2SO_4]	0.14
[C_4mmim][NTf_2]	1.84	[C_6mim]Br	12.33
[C_6mim][BF_4]	0.45	[P_{66614}]Br	1.44
[C_{10}mim][BF_4]	1.73	[C_4mim][DCA]	0.40
[C_{10}mim][PF_6]	0.57	[C_4mpyrro][DCA]	7.19
[C_6mim][PF_6]	0.54	[C_8py][BF_4]	1.12
[C_1mim][NTf_2]	0.73	[C_8py][NTf_2]	0.24
[C_4mpyrro][NTf_2]	0.32	[$C_4m_{(3)}$py][BF_4]	1.48
[C_4mpyrro][C_1SO_4]	0.66	[C_2mim][C_8SO_4]	0.80
[C_1mim][C_1SO_4]	0.45	[C_4mim][C_8SO_4]	3.37

$[C_2mim][NTf_2]$	1.78	$[C_2mim][C_1SO_3]$	2.71
$[C_4m_{(4)}py][BF_4]$	3.32	$[P_{66614}][C_1SO_3]$	2.60
$[C_4m_{(4)}py][NTf_2]$	0.20	$[C_2mim][Tos]$	0.25
$[C_2mim][SCN]$	0.15	$[C_6mim][NTf_2]$	0.23
$[C_4mim][SCN]$	0.68	$[C_{10}mim][NTf_2]$	14.72
$[C_4m_{(4)}py][SCN]$	0.57	$[N_{1114}][NTf_2]$	0.04
$[C_4mpyrro][SCN]$	2.20	$[N_{8881}][NTf_2]$	0.75
$[C_2mim][OAc]$	7.72	$[C_6py][NTf_2]$	0.34
$[C_4mim][OAc]$	0.62	$[C_2mim]Cl$	9.84
$[C_4mpyrro][OAc]$	4.31	$[C_6mim]Cl$	3.46
$[C_2mim][OTf]$	0.09	$[C_8mim]Cl$	3.99

The estimated viscosities in comparison with the experimental values are presented in figure 4-7. In addition, the relative deviation of the model in comparison with the experimental data is shown in figure 4-8. The distribution of absolute relative deviations from experimental data is illustrated in figure 4-9. Approximately 94.9% of the viscosities are calculated within 0 – 5%, 2.7% within 5 – 10%, 2% within 10 -20%, and the deviations of only four data points beyond 20%. The four points with a larger difference are from $[C_6mim]Br$ and $[C_{10}mim][NTf_2]$. Due to an extensive range of viscosity values from bromide and chloride based ILs, it is difficult to regress and obtain the optimal parameters of all ILs combined all together.

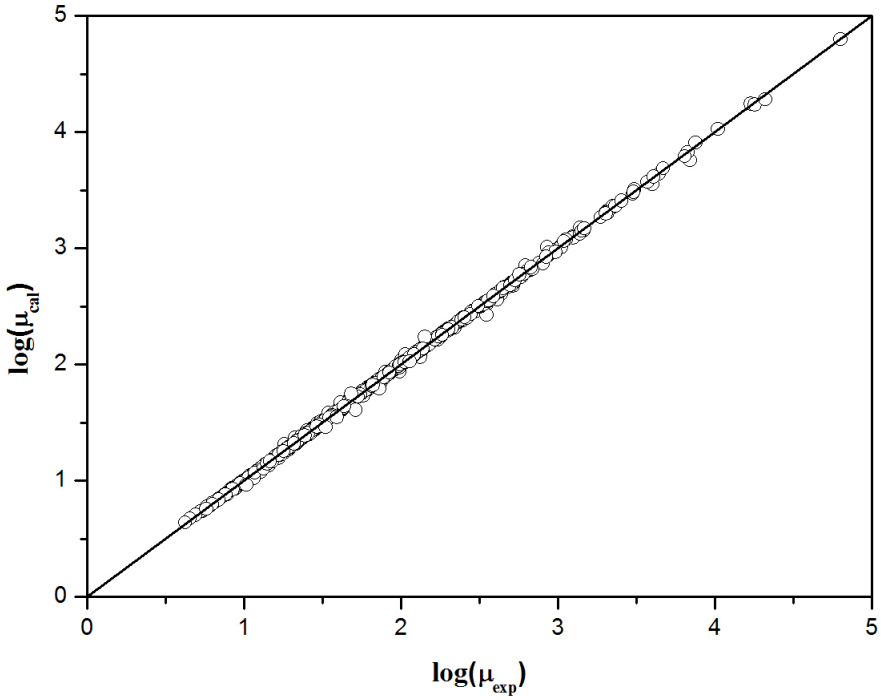

Figure 4-7. Comparison between the experimental viscosities and the estimated values for pure ionic liquids.

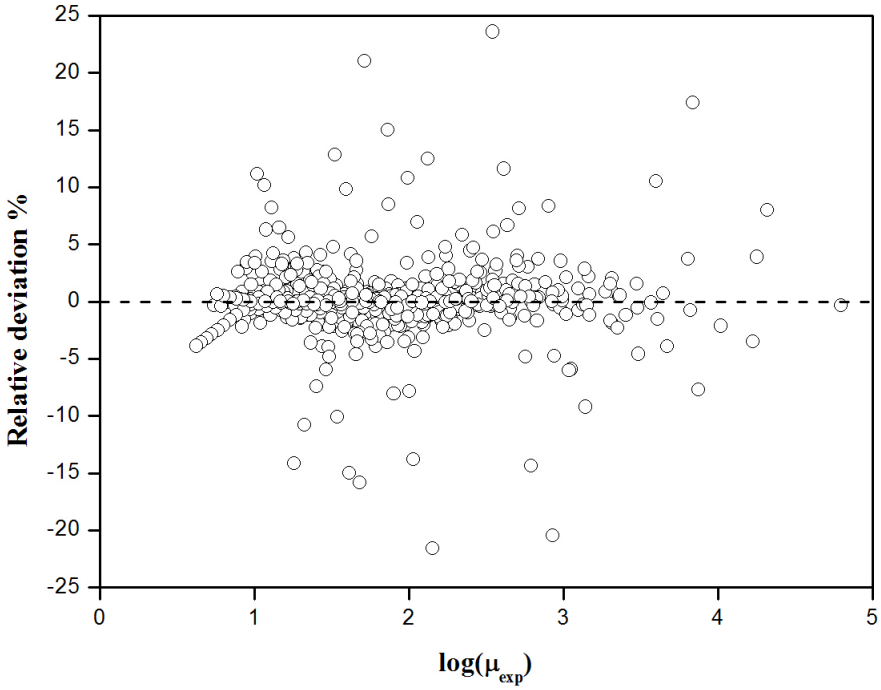

Figure 4-8. Relative deviation of calculated viscosity values versus experimental data.

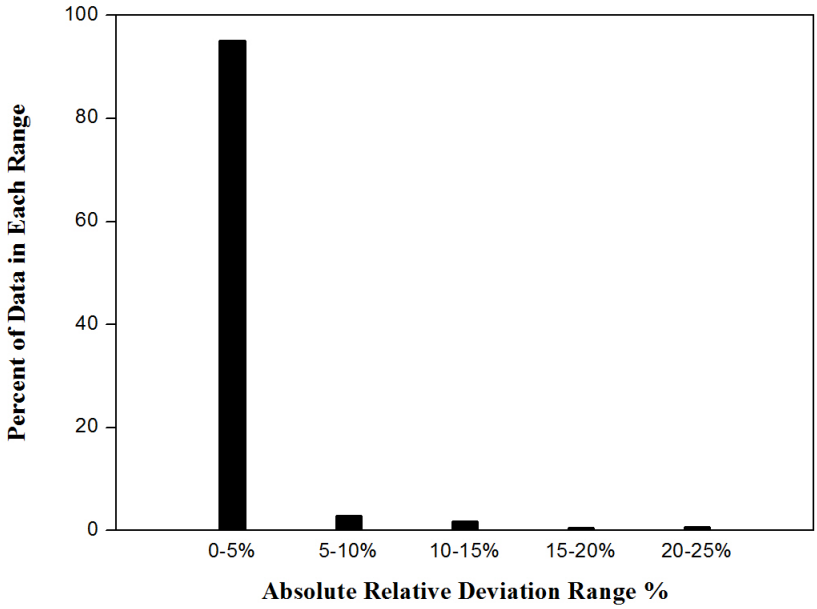

Figure 4-9. Distribution of relative deviations of the estimated viscosities from experimental ones.

Tables 4-7 and 4-8 show the results for different cation series of ILs and different anion types of ILs, respectively. This deviation for the estimation follows the orders, 1) cations: Ammonium < Pyridinium < Phosphonium < Imidazolium < Pyrrolidinium; 2) anions: $[C_2SO_4]^-$ < $[Tos]^-$ < $[C_1SO_4]^-$ < $[PF_6]^-$ < $[SCN]^-$ < $[OTf]^-$ < $[NTf_2]^-$ < $[FAP]^-$ < $[BF_4]^-$ < $[C_8SO_4]^-$ < $[DCA]^-$ < $[C_1SO_3]^-$ < $[OAc]^-$ < Br^- < Cl^-. As explained previously, it is more difficult to obtain the optimal parameters for bromide and chloride based ILs because their viscosity range is larger than three orders of magnitude.

Table 4-7. RAAD for Different Cation Types of ILs

Cation Type	No. of Structures	No. of Data	Range of Temperature (K)	Range of Experimental Viscosity (mP.s)	RAAD (%)
Pyridinium	11	132	278.15 - 363.15	7.673 - 640.14	0.78
Pyrrolidinium	7	90	283.15 - 373.15	8.98 - 593.7	2.30
Phosphonium	5	86	268.15 - 373.15	17.567 - 16955	1.26
Imidazolium	45	488	263.15 - 373.15	4.229 - 63100	1.53
Ammonium	2	23	273.15 - 353.15	14.7 - 3729.6	0.29

Table 4-8. RAAD for Different Anion Types of ILs

Anion Type	No. of Structures	No. of Data	Range of Temperature (K)	Range of Experimental Viscosity (mP.s)	RAAD (%)
$[PF_6]^-$	5	38	293.15 - 363.15	17.77 - 1052	0.42
$[C_1SO_4]^-$	4	45	283.15 - 373.15	9 - 467.5	0.32
Cl^-	3	17	283.15 - 363.15	33.2 - 63100	5.09
$[C_1SO_3]^-$	2	36	278.15 - 363.15	13.33 - 7526.5	2.65
$[NTf_2]^-$	17	223	263.15 - 373.15	7.673 - 3729.6	0.83
$[BF_4]^-$	10	84	273.15 - 373.15	18.4 - 2291	1.38

$[DCA]^-$	5	68	278.15 - 363.15	4.229 - 562.45	1.99
$[SCN]^-$	4	48	278.15 - 368.15	5.485 – 112.41	0.66
$[FAP]^-$	6	89	268.15 - 373.15	7.45 – 3067.3	1.35
$[OAc]^-$	3	29	298.15 – 363.15	8.98 – 288.8	4.85
$[C_2SO_4]^-$	1	10	298.15 – 343.15	18.72 – 97.6	0.14
$[C_8SO_4]^-$	2	28	283.15 - 373.15	23.3 - 1879	1.62
Br^-	2	27	278.15 – 363.15	85.436 - 16955	5.07
$[Tos]^-$	1	13	303.15 – 363.15	33.22 - 1417	0.25
$[OTf]^-$	5	64	278.15 – 373.15	8.169 - 2059	0.67

Based on the group interaction potential energy and VFT parameters obtained by the regression of the pure ILs and by following the same methodology, the viscosity of binary mixtures of ILs was then correlated using the UNIFAC-VISCO model. The compositions of the mixtures, temperature range, the number of data points, and references are shown in table 4-9. Herein, one set of data for each binary system was correlated to estimate the group interaction potential energy parameters. Other data of each binary system were used to compare with the predicted viscosities. The prediction result is highlighted by the RAAD values, presented in table 4-10, which is 3.8% for all collected binary data. Also, the parity plot given in figure 4-10 shows a good agreement between the experimental viscosities and calculated values for binary mixtures by using the UNIFAC-VISCO model.

Table 4-9. Binary Viscosity Data Collected in Literature

Binary system	Mole fraction range (x)	Temp range (K)	No. of data	Ref.
x[C_2mim][DCA]+(1-x)[C_2mim][BF_4]	0.05527-0.9552	298.15	7	[168]
x[C_6mim][BF_4]+(1-x)[C_2mim][BF_4]	0.0978-0.9455	293.15-343.15	216	[230, 161]
x[C_2mim][OAc]+(1-x)[C_2mim][C_2SO_4]	0.0993-0.9007	298.15-358.15	63	[167]
x[C_2mim][C_2SO_4]+(1-x)[C_2mim][SCN]	0.0495-0.801	298.15-353.15	72	[165]
x[C_2mim][DCA]+(1-x)[C_2mim][SCN]	0.2397-0.7415	298.15-353.15	36	[165]
x[$C_4m_{(4)}$py][NTf_2]+(1-x)[C_2mim][C_2SO_4]	0.0513-0.9525	293.15-353.15	70	[166]
x[C_4py][BF_4]+(1-x)[$C_4m_{(4)}$py][NTf_2]	0.0575-0.9535	293.15-353.15	70	[159]
x[C_4mim][BF_4]+(1-x)[C_4mim][C_1SO_4]	0.1209-0.9447	298.15-308.15	117	[230]
x[C_4mim][PF_6]+(1-x)[C_4mim][BF_4]	0.0568-0.945	298.15-308.15	117	[230]
x[C_4mim][BF_4]+(1-x)[C_4py][BF_4]	0.1009-0.8998	293.15-343.15	99	[164]
x[C_6mim][BF_4]+(1-x)[C_4mim][BF_4]	0.1083-0.946	298.15-308.15	99	[230]

Table 4-10. RAADs of Training Data, Test Data, and All Experimental Data for Each Binary Mixture of ILs

Binary system	No. of Training Data	RAAD for Training	No. of Test Data	RAAD for Test	RAAD for each system
x[C_2mim][DCA]+(1-x)[C_2mim][BF_4]	7	2.25	0	-	2.25
x[C_6mim][BF_4]+(1-x)[C_2mim][BF_4]	20	7.88	196	5.58	5.79
x[C_2mim][OAc]+(1-x)[C_2mim][C_2SO_4]	7	5.05	56	4.77	4.80
x[C_2mim][C_2SO_4]+(1-x)[C_2mim][SCN]	12	4.32	60	8.27	7.61
x[C_2mim][DCA]+(1-x)[C_2mim][SCN]	12	1.35	24	2.60	2.18
x[$C_4m_{(4)}$py][NTf_2]+(1-x)[C_2mim][C_2SO_4]	7	2.19	63	4.54	4.31
x[C_4py][BF_4]+(1-x)[$C_4m_{(4)}$py][NTf_2]	14	2.39	56	2.57	2.54
x[C_4mim][BF_4]+(1-x)[C_4mim][C_1SO_4]	9	0.56	108	1.46	1.39
x[C_4mim][PF_6]+(1-x)[C_4mim][BF_4]	9	0.37	108	2.74	2.56
x[C_4mim][BF_4]+(1-x)[C_4py][BF_4]	22	1.48	77	1.76	1.70
x[C_6mim][BF_4]+(1-x)[C_4mim][BF_4]	9	0.76	90	3.86	3.57
All mixtures	128	2.92	838	3.92	3.79

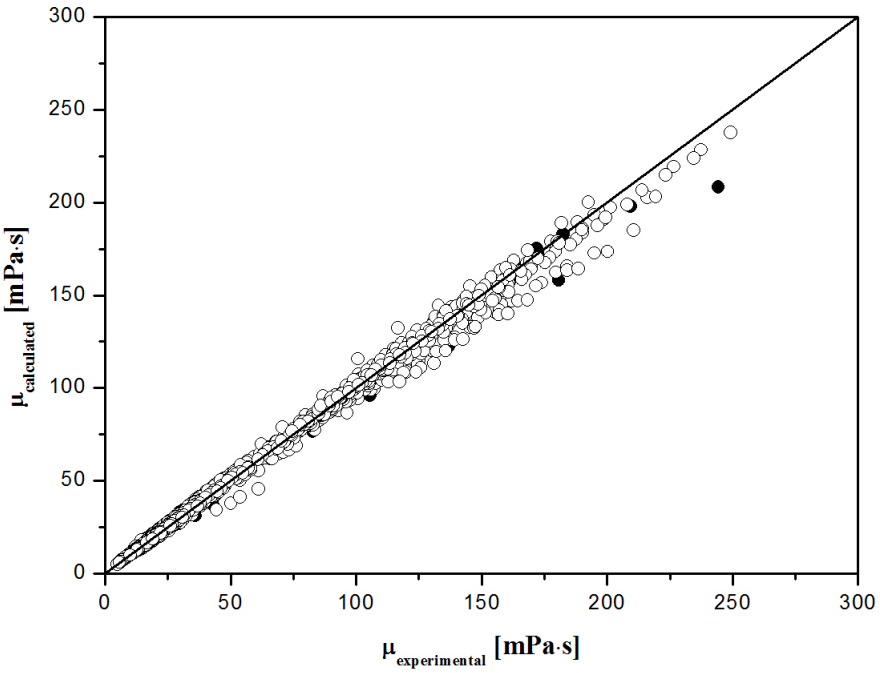

Figure 4-10. Comparison of experimental viscosity and evaluated viscosity for binary ionic liquids where data used for developing correlation (●) and evaluation data (○) are shown.

Moreover, the sensitivity analysis of binary interaction parameters has been made. Binary interaction parameters for each ionic liquid consist of two values, $\alpha_{cation/anion}$ and $\alpha_{anion/cation}$. Small difference in the values of the binary interaction parameters maybe lead to a strong impact on the evaluated viscosity values. While the influence of values of other interaction parameters is very little and can be ignored. Table 4-11 shows the effect of the binary parameter values on the calculated results of four $[C_1SO_4]^-$ based ionic liquids.

Table 4-11. Sensitivity analysis of binary interaction parameters for four $[C_1SO_4]^-$ based ILs

Ionic Liquid	$\alpha_{cation/anion}$	$\alpha_{anion/cation}$	RAAD (%)
$[C_1mim][C_1SO_4]$	-158.30	-54.69	0.445
	-159.30	-54.69	0.588
	-163.30	-54.69	1.475
	-158.30	-55.69	0.573
	-158.30	-59.69	1.370
$[C_2mim][C_1SO_4]$	566.37	-354.46	0.158
	566.37	-359.46	2.081
	566.37	-364.46	4.232
	571.37	-354.46	0.444
	576.37	-354.46	0.858
$[C_4mim][C_1SO_4]$	112.45	-365.32	0.171
	112.45	-370.32	2.618
	112.45	-375.32	5.314
	117.45	-365.32	1.219
	122.45	-365.32	2.419
$[C_4mpyrro][C_1SO_4]$	405.62	-609.91	0.659.
	405.62	-614.91	3.351
	405.62	-619.91	6.847
	410.62	-609.91	1.026
	415.62	-609.91	1.542

Herein, the control-variable method was applied to test the sensitivity of each parameter. As shown in table 4-11, the values with blue colour are the optimized values and the values with red colour are used for the sensitivity analysis. For $[C_1mim][C_1SO_4]$, the calculated deviations with decreasing $\alpha_{cation/anion}$ and $\alpha_{anion/cation}$ by one, respectively, are of nearly the same quantity, 0.58%. Decreasing $\alpha_{cation/anion}$ from -158.30 to -163.30, the estimated accuracy changes to 1.47%. Also decreasing $\alpha_{anion/cation}$ by 5, the estimated accuracy decreases to 1.37%. This means that $\alpha_{cation/anion}$ and $\alpha_{anion/cation}$ have nearly the same influence weight for the

determination of viscosity of $[C_1mim][C_1SO_4]$. However, for other three $[C_1SO_4]^-$ based ILs, $[C_2mim][C_1SO_4]$, $[C_4mim][C_1SO_4]$, and $[C_4mpyrro][C_1SO_4]$, the effect of $\alpha_{anion/cation}$ on the determination of viscosity is at least more than two times stronger than that of $\alpha_{cation/anion}$. For example of $[C_2mim][C_1SO_4]$, increasing $\alpha_{cation/anion}$ and $\alpha_{anion/cation}$ by 5, the estimated accuracy is 0.44% and 2.08%, respectively. Furthermore, increasing $\alpha_{cation/anion}$ and $\alpha_{anion/cation}$ by 10, the deviation is 0.86% and 4.23%, respectively. It means that $\alpha_{anion/cation}$ is more sensitive to the value changes for $[C_2mim][C_1SO_4]$. Larger difference changed on $\alpha_{anion/cation}$ value, more dominant the effect on the viscosity is.

Therefore, the value of $\alpha_{anion/cation}$ represents the degree of binary interaction between cation and anion. For $[C_2mim][C_1SO_4]$, $[C_4mim][C_1SO_4]$, and $[C_4mpyrro][C_1SO_4]$, its value is -354.46, -365.32, and -609.91, respectively. One can conclude that the binary interaction between cation and anion follows this order qualitatively: $[C_2mim][C_1SO_4] < [C_4mim][C_1SO_4] < [C_4mpyrro][C_1SO_4]$. This maybe attribute to the large hydrophobicity and stronger H-bond interaction between ions with the carbon number on the cation increasing.

Chapter 5
Ionic Liquid Solubility in Molecular Solvent

5.1 Data Treatment

5.1.1 Data Collection

A database on ionic liquids solubility in molecular solvents was compiled by collecting 6,948 solubility data points for 670 different binary mixtures (IL + solvent) over a broad range of temperature (211 to 459) K from 131 articles. The 670 different binary mixtures involve 142 ionic liquids (such as imidazolium, pyridinium, pyrrolidinium, ammonium, and phosphonium-based ILs) and 128 solvents (like water, alcohols, and aliphatic and aromatic hydrocarbons). The purity, impurity content and the impurity analysis methods were also recorded for the samples of ionic liquids and molecular solvents. The experimental method and uncertainties of each measurement were collected from the literature as well. 718 tie-line data for 224 binary mixtures are included in the 6,948 experimental solubility data points.

According to the database, some general trends are observed. The solubility of the equivalent cation based ILs with alcohols follows the order: $[DCA]^-$ > $[OTf]^-$ > $[NTf_2]^-$ > $[BF_4]^-$ > $[PF_6]^-$. For example, $[C_4mim][DCA]$ is completely miscible with alcohols (1-$C_nH_{2n+1}OH$, n=2, 4, 6, 8, and 10), while $[C_4mim][OTf]$ is only miscible with alcohols (1-$C_nH_{2n+1}OH$, n=2, 4, 6, and 8). Generally, the mutual solubility between ILs and alcohols decreases by increasing the alkyl chain length on the alcohol structure. However, the mutual solubility of ILs and alcohols increases by increasing the alkyl chain length on the cation. In contrary, the mutual solubility of ILs and water decreases

with the alkyl chain length on the cation. Furthermore, polar liquids are more soluble than the non-polar liquids in ILs, since ILs are extremely polar compounds.

5.1.2 Data Upload

A user-friendly web based interface was established (as fig. 5-1). The website address is illias.icpf.cas.cz. Up to now, all the functionalities on the website have been verified and this web based interface has been open to the public. All the mutual solubility data were uploaded to the user-friendly web based interface, including 718 tie-line (*x*-*x*-*T*) data points and 5,512 *T*-*x* data points. This online database will be open to the public and allow end users to get reference data with ease. Before uploading the data of each system, the components (IL and solvent) need to be defined. Four different ways can be used to define the component, such as by CAS, by name, by formula, and from Chemblink. Then the reference from which the solubility data were collected is only characterized by DOI. After the determination of both components and the reference, mutual solubility data can be uploaded along with impurity contents, analysis methods, experimental methods, and measurement uncertainties.

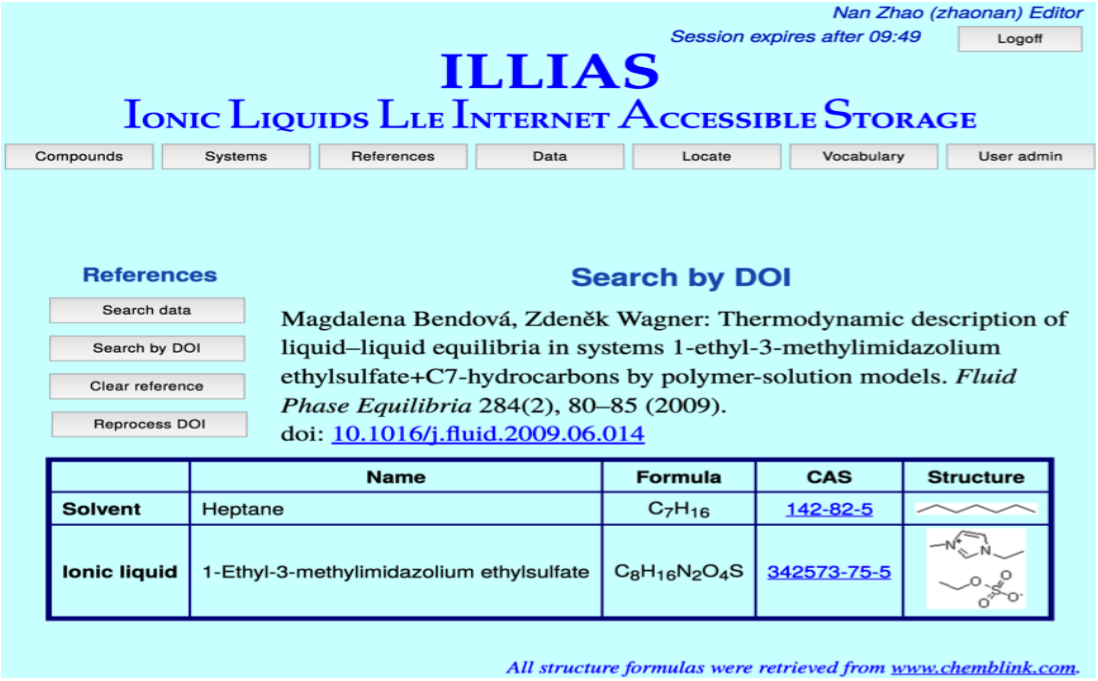

Figure 5-1. The user-friendly web based interface

5.1.3 Data Analysis

In this work, mathematical gnostics[177] was used to estimate the distribution function of residuals. Herein, the residual is the difference between experimental data (mole fraction of the IL) and the correlated values (the calculated mole fraction of IL by UNIFAC). The set of residuals are treated as an unordered set of experimental values and the same procedure is applied as for any experimental data. The estimating local distribution function (ELDF) derived by mathematical gnostics was used to calculate and describe the density distribution of residuals for each phase. The data point, with the maximum of the distribution density is the most probable value.

Herein, we give an example of the liquid-liquid equilibrium (LLE) data analysis for the mixture ($[C_4mim][PF_6]$ + water). First, the experimental data were correlated by using

the UNIFAC model. Figure 5-2 shows the LLE experimental data collected from the literature[10,231–234] and the fitting values by UNIFAC. In figure 5-2 the experimental data in IL phase reported by different groups have a good agreement with the fitting result. But large discrepancies in water phase were observed, and thus influence the fitting by UNIFAC.

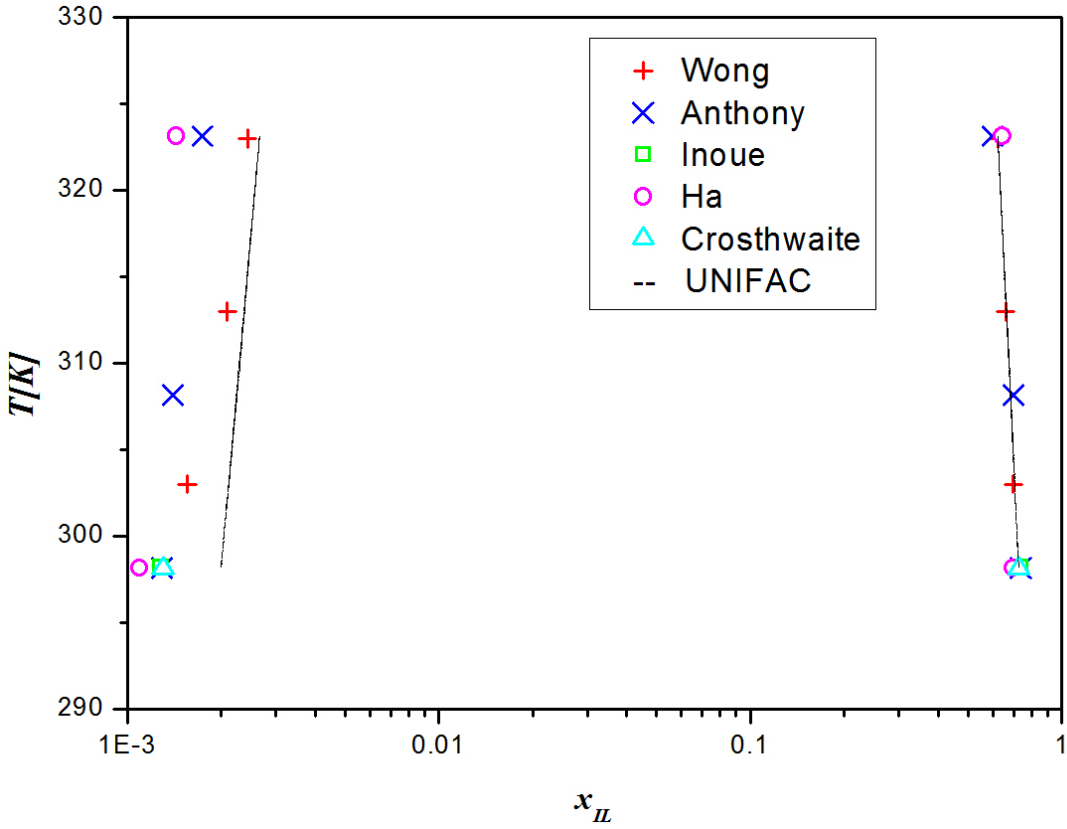

Figure 5-2. The LLE experimental data and the UNIFAC fitting values for the mixture of [C_4mim][PF_6] and water.[10,231–234]

Figures 5-3 and 5-4 show the distribution density of residuals in the IL phase and water phase, respectively.

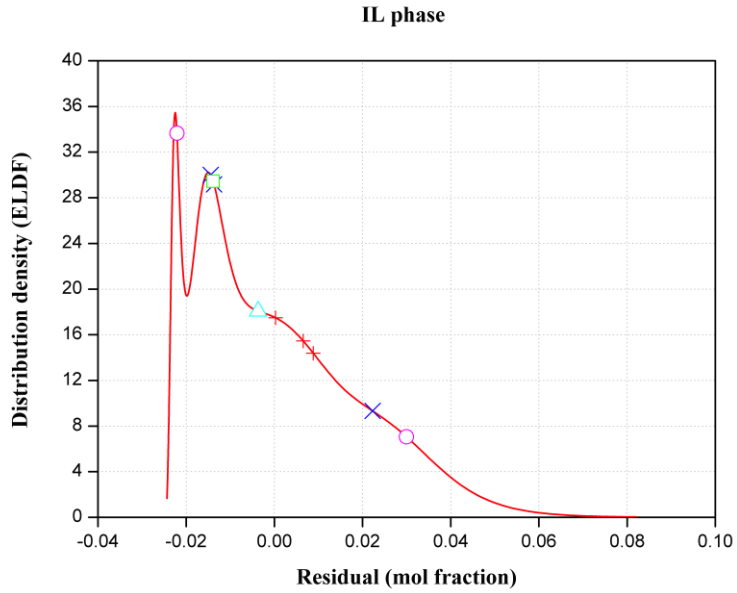

Figure 5-3. Distribution function of residuals (mole fraction) in $[C_4mim][PF_6]$ phase

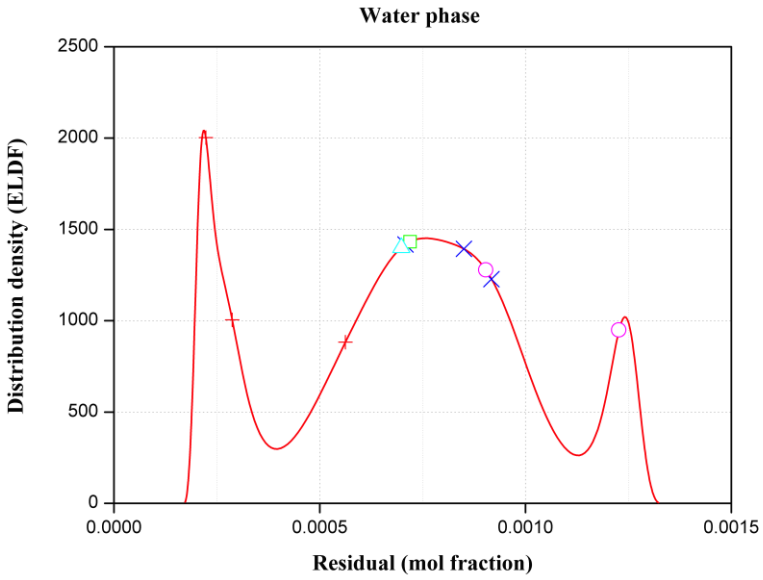

Figure 5-4. Distribution function of residuals (mole fraction) in water phase

As shown in figure 5-3, the distribution density of the three data points in the IL phase reported by Wong *et al.*[231] is 14.38 (303 K), 14.45 (313 K), and 17.48 (323 K), respectively. The same trend is observed in figure 5-4 that the distribution density of the

three data points increases with the temperature increasing, which means the data point at higher temperature reported by Wong *et al*.[231] is more precise than the data point at low temperature. However, as shown in figure 5-4, the distribution density of the data in the water phase measured by Anthony *et al*.[232] is 1418 (298.15 K), 1394 (308.15 K), and 1228 (323.15 K), respectively. Thus Anthony *et al*.[232] provided more accurate experimental data at lower temperature. Therefore, the experimental data at low temperature reported by Anthony *et al*.[232] and the data at high temperature reported by Wong *et al*.[231] are recommended.

5.2 Development of Predictive Models

In this work, all the tie-line data for binary mixtures (IL + solvent) collected from the literature have been modelled using the UNIQUAC and UNIFAC methods, respectively. The original UNIQUAC and UNIFAC equations have been given in chapter two. Both UNIQUAC and UNIFAC models are used to describe the phase equilibrium and calculate the activity coefficients of components in the mixture. In the UNIQUAC model, the activity coefficient of components is the sum of a combinatorial and a residual terms. But the UNIFAC method is based on the UNIQUAC model and further considers the contributions of functional groups in the pure components. In this case, the combinatorial term is changed. Therefore, it is necessary and also important to define the UNIFAC functional groups in the pure component, ionic liquid.

5.2.1 Choice of the UNIFAC Functional Groups

For the choice of the UNIFAC functional groups, three methods were reported to split the ionic liquid. Kim *et al.*[235] and Lei *et al.*[236,237] proposed one approach by treating the most of cation and anion as a whole and splitting the rest of groups. This approach is mainly used for methylimidazolium-based ionic liquids. For example, the ionic liquid $[C_2mim][NTf_2]$ can be divided into one CH_3 group, one CH_2 group, and one $[mim][NTf_2]$ group. Lei *et al.*[236,237] pointed out that ion pair often had strong electrostatic interactions so it is better to treat the centre of the cation and anion as a whole. However, Kim's method[235] was only applied into the $[mim]^+$ and $[py]^+$ based ionic liquids. Further work is required to test the availability of this method for other types of ILs.

Alevizou *et al.*[238] and Nebig *et al.*[239,240] divided the IL into three parts: the centre structure of the cation, the functional groups on the alkyl chain of the cation, and the anion. This approach produces more interaction parameters, which shows a higher flexibility, compared from Lei and Kim's method. This scheme is mainly applied in the modified UNIFAC (Dortmund) method.[239–241]

Santiago *et al.*[79,80] proposed a new cleavage method by simply splitting the ionic liquid into the cation and anion, thus neglecting the structure of cation. However, the deviation of correlation is lower than expected.

The number of functional groups determined by using the method proposed by

Santiago *et al*.[79,80] is the least, compared with the other two method for splitting. The number of functional groups within the system is reduced, thus the number of binary interaction parameters between different groups is reduced, less experimental data are required for parameters optimization and thus the calculation complexity for the activity coefficients based on the UNIFAC model is more simple. Herein, the method proposed by Santiago *et al*.[79,80] was selected for the determination of the functional groups in the pure component, ionic liquids.

5.2.2 Parameter Estimation

The UNIFAC and UNIQUAC models provide the calculation of the activity coefficients. Due to lack of the values of the interaction parameters for ionic liquids, the initial guess values were assigned to the interaction parameters. Then an iterative mathematical calculation (as shown in fig. 5-5), the modified Rachford-Rice flash calculation method,[242] was used to estimate the optimized interaction parameters. In each loop iteration, the phase equilibrium constant K is calculated and the phase distribution factor $\boldsymbol{\Psi}$ is determined as well. The estimated composition of each phase is also calculated based on the phase distribution factor $\boldsymbol{\Psi}$ and the phase equilibrium constant K.

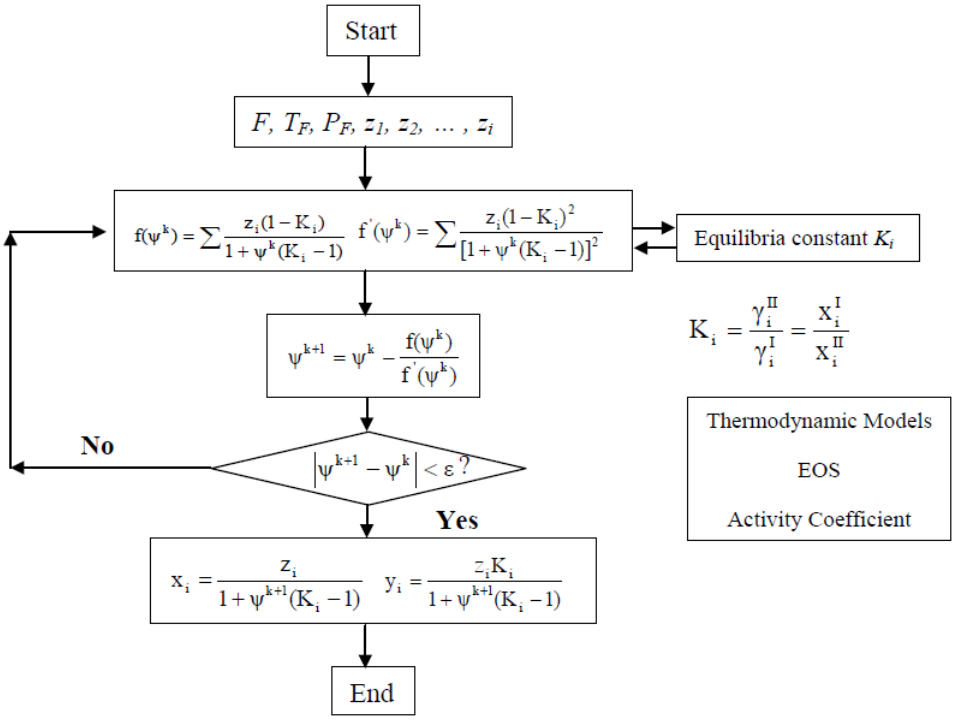

Figure 5-5. Modified Rachford-Rice algorithm for equilibrium flash calculation

Firstly, based on the initial guess values of the binary interaction parameters α_{mn}, the first set of activity coefficients is calculated. According to the calculated activity coefficients, the equilibrium constant, typically known as the K-value, is determined as:

$$K_i = \frac{(\gamma_i)^{organic-rich\ phase}}{(\gamma_i)^{ionic-rich\ phase}} \tag{5-1}$$

where subscript *i* refers to the component.

The initial value of ψ^k is chosen to be 0.9. $f(\psi^k)$ and $f'(\psi^k)$ are defined as equations 5-2 and 5-3.

$$f(\psi^k) = \sum \frac{z_i \times (1-K_i)}{1+\psi^k \times (K_i-1)} \tag{5-2}$$

$$f'(\psi^k) = \sum \frac{z_i \times (1-K_i)^2}{\left[1+\psi^k \times (K_i-1)\right]^2} \quad (5\text{-}3)$$

ψ^{k+1} is be calculated based on ψ^k, $f(\psi^k)$ and $f'(\psi^k)$:

$$\psi^{k+1} = \psi^k - \frac{f(\psi^k)}{f'(\psi^k)} \quad (5\text{-}4)$$

If the value of $|\psi^{k+1} - \psi^k|$ is less than the criterion value ε, the K-value and the distribution factor can be output to calculate the composition of both phases. Otherwise, $f(\psi^k)$ and $f'(\psi^k)$ are recalculated iteratively, until the judgment condition is satisfied.

The 'Solver' add-on in Excel was used to perform the minimization of a concentration-based objective function, *S* defined by[243]:

$$S = \sum_k^D \sum_j^M \sum_i^{N-1} \{ \left(x_{ijk}^{I,exp} - x_{ijk}^{I,cal}\right)^2 + \left(x_{ijk}^{II,exp} - x_{ijk}^{II,cal}\right)^2 \} \quad (5\text{-}5)$$

where, *D* is the number of data sets, *N* and *M* are the number of components and tie-lines in each data set, respectively; the superscripts *I* and *II* refer to the two liquid phases in equilibrium, while the superscripts '*exp*' and '*cal*' refer to the experimental and calculated values of the liquid phase concentration.

5.3 COSMO-RS Method

In this work, the liquid-liquid equilibrium for binary systems with ionic liquids was also simulated by using the (COnductor like Screening MOdel for Real Solvents) method. The COSMO*therm* software achieved this simulation.

The COSMO-RS method is an priori predictive method. Based on the quantum

mechanical and chemical calculation of each molecule of pure components and complexes involved, surface charge distributions of each molecule/cluster is calculated as profiles of charge density called ‘sigma profiles’. Each molecule/cluster has the unique sigma profile to describe the properties of the molecule in a solvent via conductor-like solvent.

In this work, all cosmo files have been generated using the Turbomole software within the BP-DFT method and the Ahlrichs-TZVP basis set as already recommended by COSMOLogic[244] and reported by Manan *et al*.[245]

In comparison, the UNIFAC method takes into account the interactions between functional groups and it requires experimental data to regress interaction parameters between the groups, which the COSMO-RS method calculates the activity coefficient by considering interactions between the charge of each segment in the molecule. This allows the COSMO-RS method to calculate the real mixture behaviour based on the sigma profiles of the components only, leading to the fact that it does not require any experimental data to predict the activity coefficients. However, it does not always give satisfactory results, because the COSMO-RS method is so universal that it has to rely on the assumption that the complex behaviour of liquid mixtures can be calculated from only a few simple and universal equations and empirical constants. Thus, the UNIFAC method normally gives mores satisfactory results than the COSMO-RS method.

5.4 Results and Discussion

The composition of each component in two phases is calculated based on the optimized interaction parameters. The result is highlighted by root mean square (*rms*) deviation, defined as follows:

$$\delta(x) = 100\sqrt{\frac{\sum_i^M \sum_j^N \left(x_{ij}^{I,exp} - x_{ij}^{I,cal}\right)^2 + \left(x_{ij}^{II,exp} - x_{ij}^{II,cal}\right)^2}{2MN}} \quad (5\text{-}6)$$

Table 8-5 shows the UNIFAC and UNIQUAC correlation results for the LLE experimental data of binary mixtures (IL + solvent) collected from the literature.

Figure 5-6 shows the modelling result for the selected system, $[C_2mim][C_2SO_4]$ + heptane. It can be observed that the simulation result from COSMO-RS shows the poorest accuracy, as the reason is explained above. At low temperatures, the fitting result by UNIQUAC is better than UNIFAC. As the temperature increases, the correlated values by UNIFAC are closer to the experimental data than the correlated values by UNIQUAC. No significant differences appear in the quality of the UNIFAC/UNIQUAC fitting for the $[C_2mim][C_2SO_4]$ + heptane binary system, due to a small number of experimental data points used for correlation. As the number of the correlated experimental data increases, the difference between the fitting results by using the two models UNIFAC/UNIQUAC will be more and more obvious.

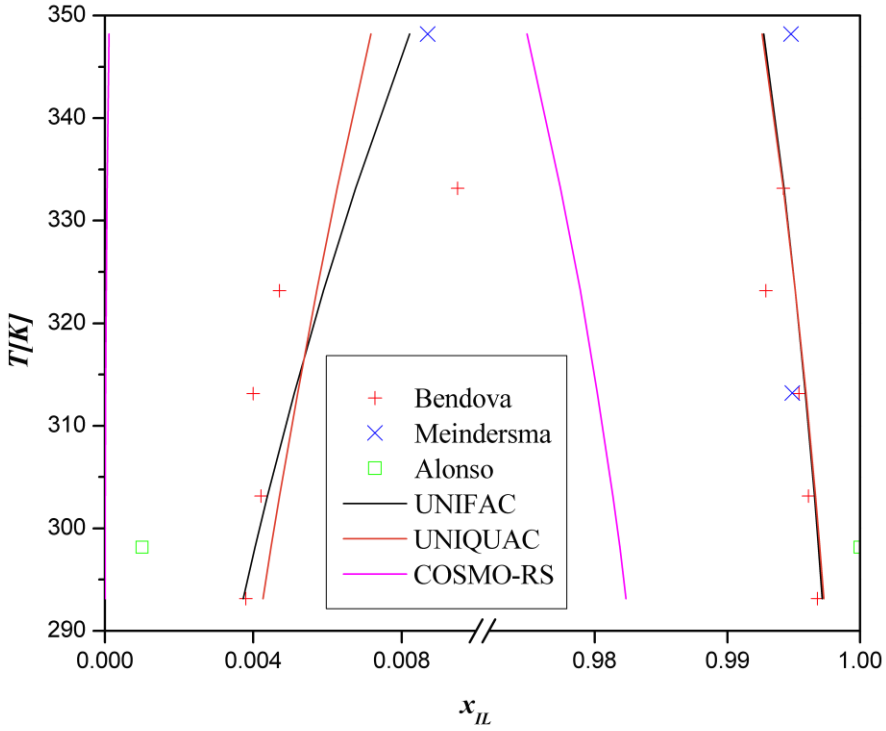

Figure 5-6. Liquid-liquid equilibrium for the heptane + $[C_2mim][C_2SO_4]$ system

The global deviation for all investigated tie-line data is 1.58% and 3.70% by the UNIFAC and UNIQUAC methods, respectively. For all the mixtures, 119 mixture types show that the result correlated by UNIFAC is more accurate than that correlated by UNIQUAC. However, Santiago *et al.*[77,79,80] simulated 35 ternary systems using both UNIFAC and UNIQUAC methods. A better accuracy was observed by UNIQUAC (1.37%) than by UNIFAC (2.86%) except in three ternary systems, according to the correlation results reported by Santiago *et al.*[77,79,80] This fact attributes to the different optimization procedures used for the parameter estimation. The UNIFAC/UNIQUAC fitting investigated in my work is performed by using the 'Solver' in Excel, which is based on the general roughness gradient (GRG) method. The calculation procedure

reported by Santiago *et al*[77,79,80] is based on the Simplex method. In terms of COSMO-RS method, the prediction is based on the assumption that the complex behaviour of liquid mixtures can be calculated from only a few simple and universal equations and empirical constants. Therefore, the COSMO-RS method gives less accurate result than the UNIFAC and UNQUAC models.

Chapter 6
Conclusions and Future Work

6.1 Conclusions

Comprehensive databases for ionic liquids properties, such as volumetric properties, viscosity, and mutual solubility with other liquids, have been created. The density database contains 16,092 experimental density data for 81 ionic liquids as a function of temperature (217 – 473) K and pressure (0.1 – 207) MPa. Two viscosity databases were created, one for pure ionic liquid and the other for binary mixtures of ionic liquids. The viscosity database for pure ionic liquid consists of more than 2,765 data points for 70 ionic liquids over a broad temperature range (253 – 573) K at 0.1 MPa. Another viscosity database for binary mixtures collected 966 data points of 11 binary mixtures as a function of temperature from 293 to 358 K. The composition of the binary mixture ranges from 0.0495 to 0.9552 mole fraction. The database on ionic liquids solubility in molecular solvents is composed of 6,948 data points for 670 types of binary mixtures (IL + Solvent), which contains 142 ILs and 128 solvents.

For the density and viscosity of the same IL and the mutual solubility of the same system reported by more than one reference, mathematical gnostics was used to analyse the experimental data from different resources and recommend one dataset. Mathematical gnostics is an efficient way to mine the information of uncertainty of the data sample.

The recommended density data were used to establish a group contribution model. Among these recommended data, 5,399 data points of 54 ionic liquids were trained to

estimate the volumetric parameters of ions and thus the contributions of each ion to the molar volumes of ionic liquids. 2,522 data points of other 27 ionic liquids, not included in the training set, were compared with the evaluated values. The estimation accuracy of 0.31% shows that this method is able to evaluate the volumetric properties of ionic liquids satisfactorily. Four group contribution methods (Gardas-Coutinho's method[28], Taherifard-Raeissi's method[154], Paduszyński-Domańska's method[32], and our method) were compared in terms of the prediction of high-pressure density for pure ILs and the method proposed in my work shows the best performance. In case of the prediction of density of binary ILs mixtures, while the Paduszyński-Domańska's method[32] gives the best accuracy (0.236%), the result obtained by our method is 0.241%, which is very close to that of Paduszyński-Domańska[32]. In addition, the better thermodynamic formalism was determined for the calculation of mechanical coefficients with more accuracy during my work.

The recommended viscosity data for pure ionic liquids were correlated using the modified UNIFAC-VISCO method. The binary interaction parameters and ions VFT parameters were estimated by means of the Marquardt optimization technique. The optimized values of binary interaction parameters were implemented into the correlation of the training viscosity data for binary mixtures. The other binary viscosity data, used as the test set, were compared with the pure evaluated values. The method shows good correlation ability for the pure ionic liquid with a relative average absolute deviation of 1.4% and shows a good evaluation agreement for the binary mixtures

within 3.8%. The work for the evaluation of viscosity of pure ILs is indeed mainly correlation. However, the UNIFAC-VISCO based method has the potential, thanks to the optimized binary interaction parameters by correlation of this work, for the pure prediction of the viscosity of mixtures (ILs + molecular solvents) and even the conductivity of mixtures containing ILs, which was the next step of our work and has been proved practicable up to now.

All the tie-line (*x*-*x*-*T*) data in the solubility database were correlated using the UNIQUAC and UNIFAC methods, respectively. The UNIFAC method originates from the UNIQUAC method. The UNIQUAC method requires the binary interaction parameters between components (i.e. the ionic liquid and the solvent). The UNIFAC method further considered the contributions of functional groups and involved the binary interaction parameters between groups. In this work, the parameters estimation, no matter in the UNIQUAC and UNIFAC methods, were carried out based on the flash calculation method. Finally, 718 tie-lines were correlated with a global deviation of 1.37% (UNIFAC) and 2.86% (UNIQUAC). The fitting results by using the UNIFAC and UNIQUAC methods were analysed. Because the UNIFAC model divides the components into smaller functional groups, the number of the binary interaction parameters between groups in the UNIFAC model is more than that in the UNIQUAC model. UNIFAC shows more accuracy than UNIQUAC in case of fitting to the systems with limited number of different functional groups. As the number of functional groups involved in the mixtures increases, the number of the interaction parameters in the

UNIFAC model significantly increases, which increases the difficulties in the regression to obtain the optimal values for all the interactions parameters. Thus, the UNIQUAC model gives better results in terms of fitting to the mixtures containing many different groups.

6.2 Future Work

During my Ph.D. study, a modified UNIFAC-VISCO method was developed to evaluate the viscosity of pure ionic liquids and binary ionic liquids mixtures. We are now working on this model in the case of the evaluation of viscosity for binary mixtures (ionic liquids + molecular solvents). Furthermore, this extension of the UNIFAC-VISCO model could be then applied for the evaluation of the viscosity of any electrolytes including those based on classical molten salts used in supercapacitors and/or batteries applications. Due to a similarity of another important property – conductivity, to the viscosity, a new method based on the UNIFAC-CONDUCT model will be proposed by our group very soon to evaluate the conductivity of pure ionic liquids and more generally electrolytes as a function of temperature at atmospheric pressure. More generally, these original and new UNIFAC methods could be then applied for multiple components mixtures, as well as, under high-pressure to verify their applicability under more drastic and realistic conditions. In addition, a review, on the mutual solubility between ionic liquids and molecular solvents will be prepared soon which will be submitted to the Journal of Physical and Chemical Reference Data

thanks to the IUPAC project done in collaboration with M. Bendová's research group.

Chapter 7
Publications and Participated Conferences

7.1 Publication List

1. **Zhao N.**, Jacquemin J., Oozeerally R., Degirmenci V. New method for the estimation of viscosity of pure and mixtures of ionic liquids based on the UNIFAC-VISCO model. *J. Chem. Eng. Data* 2016, 61, 2160-2169.

2. **Zhao N.**, Oozeerally R., Degirmenci V., Wagner Z., Bendová M., Jacquemin J. New method based on the UNIFAC-VISCO model for the estimation of ionic liquids viscosity using the experimental data recommended by mathematical gnostics. *J. Chem. Eng. Data* 2016, 61, 3908-3921.

3. **Zhao N.**, Menegolla H. B., Degirmenci V., Wagner Z., Bendová M., Jacquemin J. A group contribution method for the evaluation of the volumetric properties of ionic liquids using the experimental data recommended by mathematical gnostics. *Ind. Eng. Chem. Res.* DOI: 10.1021/acs.iecr.7b00753.

4. **Zhao N.**, Jacquemin J. New method based on the UNIFAC-VISCO model for the estimation of viscosity of (ionic liquid + molecular solvent) binary mixtures. (Submitted to *Fluid Phase Equilibria* on 23 Feb. 2017)

5. **Zhao N.**, Jacquemin J. New method for the estimation of conductivity of pure ionic liquids based on the UNIFAC-CONDUCT model. (Submitted to *Fluid Phase Equilibria* on 23 Feb. 2017)

7.2 Participated Conferences

1. Bi-annual QUILL Meeting – April 2015, October 2015, April 2016, and October 2016, poster presentation.

2. The 14th PPEPPD Conference in Porto, Portugal – May 2016, post presentation.

3. The EU COST Action Workshop in Prague, Czech Republic – April 2015, participation.

4. The Joliot Curie Conference in York, UK – September 2016, poster presentation.

5. A visit to Dr. Bendová's research group, E. Hála Laboratory of Separation Processes, Institute of Chemical Process Fundamentals of the Czech Academy of Sciences, three weeks' training course.

Chapter 8
Appendices

Table 8.1 Tait Parameters Used to Fit Each Dataset From Different References

IL	Ref.	a_0 / g·cm^{-3}	a_1 / g·cm^{-3}·K^{-1}	a_2 / g·cm^{-3}·K^{-2}	RAAD (%)	b_0 / MPa	b_1 / MPa·K^{-1}	b_2 / MPa·K^{-2}	10^2·C	RAAD (%)
[C_2mim][SCN]	119	1.364	-1.03E-03	6.79E-07	0.017	100.00	4.992	0.098	3.783	0.023
[C_2mim][OAc]	120	1.340	-9.74E-04	5.69E-07	0.008	99.71	5.013	0.112	3.794	0.049
[C_4mim]Cl	121	1.331	-1.04E-03	7.14E-07	0.002	98.83	4.999	0.060	3.777	0.473
[C_2mim][DCA]	122	1.202	1.56E-05	-1.03E-06	0.558	70.44	5.258	0.212	3.107	0.236
[N_{1112OH}][Lactate]	121	1.391	-1.04E-03	6.57E-07	0.003	98.77	5.001	0.109	3.781	0.500
[C_4mim][SCN]	119	1.325	-1.10E-03	8.14E-07	0.008	100.00	4.986	0.085	3.778	0.015
[C_2mim][BF_4]	127	1.659	-1.54E-03	1.14E-06	0.009	99.51	4.998	0.083	3.784	0.086
	134	1.544	-9.94E-04	3.75E-07	0.002	696.4	-1.761	0.002	0.102	0.025
	112	1.544	-9.73E-04	3.52E-07	0.001	99.56	4.996	0.112	3.782	0.072
	149	1.488	-6.81E-04	5.51E-08	-	81.46	5.193	0.222	3.145	0.326
[C_4mim][OAc]	120	1.230	-5.89E-04	-5.08E-09	0.006	99.88	4.994	0.073	3.784	0.060
	153	1.256	-7.65E-04	2.59E-07	0.009	99.51	4.996	0.084	3.783	0.620
[C_2mim][Lactate]	121	1.402	-1.01E-03	5.09E-07	0.003	99.77	4.996	0.078	3.782	0.921
[C_4mim][DCA]	122	1.176	-1.47E-04	-7.28E-07	-	20.17	5.988	0.338	3.767	0.348
	173	1.283	-8.57E-04	3.66E-07	0.007	99.49	4.996	0.075	3.782	0.205
	124	1.276	-8.13E-04	2.95E-07	0.003	99.54	4.992	0.088	3.779	0.473
[C_1mim][C_1SO_4]	117	2.621	-7.34E-03	1.02E-05	0.006	100.00	4.992	0.107	3.783	0.052
	118	1.561	-9.00E-04	3.86E-07	0.019	99.46	4.999	0.098	3.782	0.176
[$C_4m_{(4)}$py][SCN]	119	1.108	2.36E-04	-1.31E-06	0.025	99.50	4.996	0.089	3.782	0.027
[C_2mim][C_1SO_4]	93	1.594	-1.25E-03	7.35E-07	0.022	99.46	4.996	0.092	3.782	0.178

	[113]	1.314	-6.60E-05	-9.01E-07	0.008	99.21	4.999	0.131	3.782	0.399
$[C_4py][BF_4]$	[133]	1.430	-7.63E-04	1.19E-07	0.007	99.79	4.994	0.076	3.783	0.072
	[125]	1.462	-9.65E-04	4.48E-07	0.005	99.47	4.996	0.101	3.782	0.159
	[112]	1.457	-9.94E-04	4.63E-07	0.001	99.46	4.996	0.098	3.783	0.081
	[246]	1.496	-1.24E-03	8.89E-07	0.017	99.47	4.996	0.090	3.783	0.102
	[126]	1.476	-1.10E-03	6.43E-07	0.006	98.84	5.000	0.090	3.782	0.098
	[247]	1.485	-1.12E-03	6.25E-07	0.008	99.49	4.997	0.081	3.784	0.131
	[114]	1.556	-1.55E-03	1.23E-06	0.005	99.45	4.992	0.062	3.780	0.042
	[248]	1.433	-8.02E-04	2.11E-07	-	70.49	5.280	0.082	3.145	0.209
	[137]	1.418	-7.36E-04	2.40E-08	0.019	99.77	4.995	0.067	3.783	0.213
$[C_4mim][BF_4]$	[249]	1.441	-8.52E-04	2.99E-07	-	70.49	5.294	0.116	3.150	0.259
	[136]	1.407	-7.00E-04	3.15E-08	0.029	551.00	-1.261	0.001	0.094	0.031
	[250]	1.456	-1.03E-03	5.51E-07	-	103.44	6.611	2.008	2.014	0.035
	[251]	10.902	-6.19E-02	9.85E-05	0.412	96.71	5.836	-2.176	-28.363	0.207
	[252]	1.470	-1.07E-03	5.71E-07	0.001	99.56	4.996	0.088	3.783	0.106
	[253]	1.495	-1.31E-03	1.17E-06	0.706	101.65	5.421	0.564	3.246	0.465
	[132]	1.422	-7.60E-04	6.33E-08	0.009	99.46	4.996	0.079	3.783	0.116
	[254]	1.447	-9.35E-04	3.65E-07	0.008	100.46	4.991	0.087	3.784	0.834
$[C_4mim][C(CN)_3]$	[127]	1.384	-1.50E-03	1.24E-06	0.018	99.45	4.998	0.064	3.784	0.108
	[173]	1.450	-7.50E-04	1.25E-07	0.007	99.48	4.997	0.080	3.783	0.297
	[93]	1.489	-9.04E-04	2.80E-07	0.023	99.52	4.996	0.084	3.783	0.139
$[C_2mim][C_2SO_4]$	[137]	1.417	-5.97E-04	-3.32E-09	0.013	98.75	4.996	0.025	3.780	0.382
	[132]	1.447	-7.32E-04	7.94E-08	0.006	99.46	4.996	0.096	3.782	0.099
	[174]	1.486	-9.75E-04	4.63E-07	0.004	99.53	4.996	0.107	3.782	0.073

	[128]	1.457	-7.91E-04	1.86E-07	0.002	99.47	4.996	0.100	3.782	0.087
	[140]	1.504	-1.07E-03	5.86E-07	0.019	99.29	4.998	0.103	3.782	0.481
	[255]	1.452	-7.58E-04	-1.34E-07	0.008	99.49	4.997	0.103	3.782	0.688
	[256]	Dataset was measured at the same temperature								
	[257]	1.509	-1.10E-03	6.27E-07	0.016	99.49	4.997	0.103	3.782	0.481
$[C_4m_{(2)}py][BF_4]$	[129]	1.407	-6.99E-04	3.90E-08	0.002	99.46	4.996	0.096	3.782	0.111
$[C_4m_{(3)}py][BF_4]$	[129]	1.422	-9.14E-04	3.78E-07	0.003	99.46	4.996	0.096	3.782	0.164
	[130]	1.367	-5.58E-04	-2.00E-07	-	571.61	-1.897	0.002	0.076	0.008
$[C_4m_{(4)}py][BF_4]$	[129]	1.416	-8.75E-04	3.12E-07	0.005	99.46	4.996	0.098	3.782	0.162
	[131]	1.347	-4.04E-04	-3.20E-07	-	-49.48	5.588	0.136	2.848	0.531
$[C_4mim][C_1SO_4]$	[132]	1.420	-7.49E-04	1.19E-07	0.009	99.46	4.996	0.092	3.782	0.102
	[258]	1.399	-6.36E-04	-1.68E-08	0.006	99.47	4.996	0.100	3.782	0.076
$[C_6py][BF_4]$	[133]	1.360	-7.10E-04	5.95E-08	0.006	99.77	4.994	0.067	3.783	0.078
$[C_6mim][BF_4]$	[134]	1.374	-8.44E-04	2.50E-07	0.002	543.00	-1.288	0.001	0.102	0.030
	[112]	1.386	-9.20E-04	3.77E-07	0.001	99.56	4.995	0.088	3.783	0.092
	[149]	1.324	-4.81E-04	-2.78E-07	0.876	30.39	5.619	0.257	3.096	0.396
	[259]	1.425	-1.19E-03	9.07E-07	-	1498.22	-1.693	-1.125	-31.202	0.373
$[C_2mim][PF_6]$	[134]	3.219	-7.87E-03	8.23E-06	2.521	1153.9	-4.470	0.005	0.080	0.985
$[C_2mim][OTf]$	[149]	1.575	-4.36E-04	-6.04E-07	-	-55.23	2.900	-0.007	0.066	0.175
	[94]	1.699	-1.24E-03	5.25E-07	0.004	99.45	4.996	0.065	3.783	0.116
$[C_8py][BF_4]$	[133]	1.349	-9.38E-04	4.29E-07	0.004	99.45	4.994	0.060	3.782	0.089
$[C_8mim][BF_4]$	[112]	1.333	-8.53E-04	2.88E-07	0.001	99.48	4.996	0.081	3.783	0.102
	[113]	1.234	-3.16E-04	-5.42E-07	0.028	100.00	4.991	0.103	3.784	0.599
	[114]	1.466	-1.62E-03	1.38E-06	0.007	99.53	4.994	0.051	3.782	0.056

	[223]	1.332	-8.44E-04	2.61E-07	0.002	100.51	4.990	0.082	3.783	0.762
	[260]	1.338	-8.83E-04	3.20E-07	0.000	99.56	4.995	0.089	3.783	0.800
$[C_2mim][Tos]$	[118]	1.470	-1.02E-03	6.29E-07	0.006	99.50	4.998	0.082	3.783	0.193
$[C_4mim][PF_6]$	[113]	1.582	-6.86E-04	-1.95E-07	0.014	100.17	4.993	0.115	3.784	0.493
	[126]	1.575	-4.74E-04	-7.09E-07	0.008	99.45	4.996	0.061	3.784	0.146
	[247]	1.610	-8.20E-04	-4.30E-19	0.015	101.00	4.989	0.079	3.782	0.110
	[248]	1.517	-2.71E-04	-7.48E-07	-	88.49	5.675	0.290	3.350	0.458
	[137]	1.627	-9.14E-04	1.30E-07	0.009	99.90	4.994	0.076	3.783	0.194
	[136]	1.602	-8.36E-04	1.17E-07	0.076	527.00	-1.211	0.001	0.095	0.042
	[135]	1.733	-1.60E-03	1.24E-06	0.000	99.50	5.060	0.091	3.819	0.090
$[C_4mim][OTf]$	[149]	1.617	-1.32E-03	9.86E-07	-	108.46	5.210	1.258	2.549	0.638
	[114]	1.702	-1.76E-03	1.39E-06	0.012	99.53	4.993	0.050	3.781	0.056
$[C_4C_1mim][PF_6]$	[114]	1.778	-1.88E-03	1.55E-06	0.013	99.53	4.993	0.055	3.781	0.038
$[C_6mim][PF_6]$	[134]	1.592	-1.19E-03	6.25E-07	0.003	748.00	-2.190	0.002	0.118	0.074
	[114]	1.703	-1.80E-03	1.45E-06	0.006	99.53	4.994	0.053	3.782	0.054
	[224]	1.524	-7.80E-04	-3.58E-19	0.016	80.00	5.147	0.171	3.798	0.588
	[116]	1.569	-1.05E-03	4.24E-07	0.005	100.48	4.905	0.088	3.705	0.347
	[135]	1.441	-2.56E-04	-8.30E-07	0.000	99.50	4.997	0.066	3.784	0.065
$[C_8mim][PF_6]$	[134]	1.528	-1.16E-03	6.25E-07	0.005	774.00	-2.238	0.002	0.126	0.087
	[113]	1.360	-2.30E-04	-7.53E-07	0.010	100.54	4.990	0.101	3.783	0.563
	[114]	1.662	-1.94E-03	1.71E-06	0.260	97.67	4.825	0.020	3.663	0.163
	[223]	1.492	-9.46E-04	3.00E-07	0.003	99.77	4.995	0.067	3.783	0.204
	[260]	1.503	-1.01E-03	4.00E-07	0.000	99.49	4.995	0.075	3.781	0.557
	[224]	1.452	-7.30E-04	-4.91E-19	0.016	101.00	4.588	0.053	3.506	0.070

	[135]	1.335	4.07E-06	-1.15E-06	0.000	99.50	4.995	0.059	3.784	0.043
$[C_4mim][C_8SO_4]$	[136]	1.201	-3.24E-04	-4.07E-07	0.061	99.53	4.997	0.044	3.783	1.533
	[261]	1.327	-1.13E-03	8.23E-07	0.069	98.91	4.984	0.040	3.773	0.376
	[262]	1.300	-8.91E-04	4.53E-07	-	104.95	6.382	0.296	4.202	0.421
$[C_2mim][NTf_2]$	[127]	1.963	-1.84E-03	1.19E-06	0.004	98.91	5.001	0.052	3.784	0.123
	[137]	1.829	-1.09E-03	1.42E-07	0.008	99.45	4.997	0.062	3.783	0.226
	[263]	1.765	-7.83E-04	-5.89E-08	-	5501.18	-104.264	-0.322	-17.168	0.428
$[N_{1114}][NTf_2]$	[31]	1.661	-9.14E-04	4.09E-08	0.005	98.91	5.000	0.055	3.783	0.277
$[C_3mim][NTf_2]$	[138]	1.202	2.64E-03	-5.77E-06	0.005	98.83	5.000	0.065	3.784	0.140
$[C_3mpyrro][NTf_2]$	[94]	1.787	-1.36E-03	5.93E-07	0.002	98.91	4.998	0.052	3.782	0.144
$[C_3m_{(3)}py][NTf_2]$	[94]	1.808	-1.36E-03	5.17E-07	0.004	99.53	4.995	0.050	3.784	0.153
$[C_4mim][NTf_2]$	[173]	1.714	-9.31E-04	-4.26E-09	0.021	98.91	4.998	0.039	3.782	0.560
	[137]	1.731	-1.02E-03	1.11E-07	0.002	99.53	4.996	0.042	3.783	0.322
	[116]	1.746	-1.12E-03	2.78E-07	0.001	99.71	4.996	0.066	3.784	0.839
	[139]	1.774	-1.29E-03	5.33E-07	0.000	98.91	4.993	0.059	3.777	0.234
	[264]	1.597	-1.60E-04	-1.27E-06	0.008	98.83	5.000	0.064	3.784	0.112
	[265]	1.747	-1.13E-03	2.84E-07	0.001	99.50	4.996	0.086	3.783	0.739
	[153]	1.747	-1.13E-03	3.01E-07	0.005	472.45	-1.321	0.001	0.089	0.012
$[C_4mpyrro][NTf_2]$	[94]	1.747	-1.31E-03	5.44E-07	0.002	98.91	4.998	0.051	3.782	0.152
	[31]	1.652	-8.72E-04	2.18E-08	0.002	99.53	4.996	0.050	3.783	0.274
	[266]	1.684	-1.06E-03	2.95E-07	0.005	99.43	4.995	0.081	3.783	0.398
	[147]	1.702	-1.15E-03	3.96E-07	0.038	99.77	4.995	0.068	3.784	0.731
$[C_3mpip][NTf_2]$	[94]	1.776	-1.43E-03	6.99E-07	0.018	98.91	4.998	0.053	3.782	0.152
	[267]	1.621	-5.93E-04	-4.00E-07	0.000	99.45	4.996	0.066	3.783	0.207

$[C_1OC_2mpyrro][NTf_2]$	140	1.811	-1.41E-03	7.26E-07	0.027	99.73	4.995	0.070	3.784	0.709
$[C_5mim][NTf_2]$	138	1.507	1.91E-04	-1.80E-06	0.010	99.45	4.996	0.061	3.784	0.147
$[N_{8881}][DCA]$	173	1.059	-5.54E-04	-1.32E-08	0.025	99.53	4.997	0.048	3.784	0.381
$[C_6mim][NTf_2]$	264	1.575	-4.74E-04	-7.09E-07	0.008	98.91	4.998	0.060	3.783	0.152
	268	1.643	-9.12E-04	1.95E-19	0.030	98.18	4.997	0.034	3.779	0.554
	172	1.682	-1.16E-03	4.20E-07	0.013	98.91	4.997	0.059	3.782	0.222
	142	1.664	-1.05E-03	2.19E-07	0.015	449.48	-1.287	0.001	0.086	0.012
	269	1.621	-7.71E-04	-2.14E-07	0.004	409.85	-1.327	0.001	0.070	0.013
	265	1.670	-1.08E-03	2.67E-07	0.007	99.80	4.986	0.097	3.784	0.337
$[C_7mim][NTf_2]$	127	1.755	-1.72E-03	1.18E-06	0.009	99.84	4.995	0.045	3.785	0.141
$[C_8mim][NTf_2]$	127	1.788	-2.07E-03	1.70E-06	0.038	99.53	4.998	0.044	3.784	0.167
	270	1.649	-1.31E-03	6.78E-07	0.005	99.53	4.995	0.050	3.783	0.071
$[C_{10}mim][NTf_2]$	93	1.546	-8.92E-04	-2.49E-08	0.029	99.53	4.995	0.040	3.783	0.277
$[P_{66614}]Cl$	29	2.177	-7.62E-03	1.12E-05	-	107.76	5.136	0.282	3.110	0.779
	143	1.135	-1.01E-03	6.35E-07	0.010	99.88	4.994	0.071	3.785	0.064
	145	1.080	-6.88E-04	1.61E-07	0.002	98.91	4.997	0.059	3.782	0.151
$[P_{66614}][OAc]$	29	2.129	-7.28E-03	1.06E-05	-	109.50	4.919	1.313	2.506	0.977
$[P_{66614}][DCA]$	143	1.111	-8.31E-04	4.04E-07	0.013	99.89	4.994	0.076	3.785	0.097
	145	1.073	-5.89E-04	1.79E-08	0.003	99.45	4.996	0.063	3.784	0.141
$[C_2mim][FAP]$	144	2.098	-1.42E-03	3.61E-07	0.013	98.91	4.996	0.052	3.781	0.097
$[P_{66614}]Br$	145	1.140	-6.32E-04	1.79E-08	0.003	98.91	4.997	0.056	3.782	0.157
$[P_{66614}][C_1SO_3]$	145	1.121	-6.78E-04	1.07E-07	0.003	98.91	4.997	0.055	3.782	0.161
$[C_4mim][FAP]$	144	2.051	-1.70E-03	9.10E-07	0.003	99.53	4.994	0.046	3.783	0.109
$[C_4mpyrro][FAP]$	148	1.983	-1.47E-03	6.24E-07	0.003	98.91	5.011	0.057	3.790	0.093

	[146]	1.915	-1.13E-03	9.53E-08	0.008	98.83	4.999	0.063	3.782	0.820
[C_1OC_2mpyrro][FAP]	[147]	2.003	-1.38E-03	4.29E-07	0.013	98.83	4.999	0.063	3.782	0.808
[C_6mim][FAP]	[144]	1.949	-1.56E-03	7.53E-07	0.004	99.53	4.995	0.047	3.783	0.078
[P_{66614}][TNf_2]	[29]	0.132	6.57E-03	-1.14E-05	-	105.10	5.367	-4.922	9.047	1.094
	[145]	1.295	-7.98E-04	1.07E-07	0.003	98.91	4.996	0.058	3.781	0.163
[P_{66614}][FAP]	[148]	1.476	-1.13E-03	4.73E-07	0.005	99.53	5.000	0.046	3.787	0.112
	[271]	1.385	-5.91E-04	-3.03E-07	0.001	99.53	4.994	0.042	3.783	0.101
	[146]	1.445	-9.14E-04	1.18E-07	0.010	98.91	4.998	0.053	3.782	0.967
[C_6mim]Cl	[142]	1.218	-6.45E-04	1.41E-07	0.020	536.89	-1.300	0.001	0.088	0.012
[C_6mim][OTf]	[149]	1.116	1.35E-03	-3.04E-06	-	102.05	5.179	0.173	2.965	0.505
[C_4C_1mim][FAP]	[150]	1.955	-1.24E-03	1.76E-07	0.021	484.97	-1.500	0.001	0.085	0.024
[C_4C_1mim][NTf_2]	[150]	1.711	-1.00E-03	1.07E-07	0.018	483.08	-1.345	0.001	0.088	0.021
[$C_2OHC_1NH_2$][C_2COO]	[151]	1.220	-4.05E-04	-3.79E-07	0.000	99.77	4.995	0.067	3.783	0.081
[$C_2OHC_1NH_2$][C_3COO]	[151]	1.247	-7.45E-04	1.20E-07	0.000	98.91	4.998	0.059	3.782	0.127
[$C_2OHC_1NH_2$][C_4COO]	[151]	1.233	-8.41E-04	3.06E-07	0.000	99.53	4.995	0.052	3.783	0.140
[C_1mim][DMP]	[146]	1.504	-9.01E-04	2.94E-07	0.014	99.53	4.997	0.108	3.782	0.489
[C_2mim][C_6SO_4]	[146]	1.358	-8.55E-04	2.97E-07	0.014	99.48	4.997	0.081	3.783	0.629
[C_4mpyrro][$B(CN)_4$]	[146]	1.193	-7.84E-04	1.96E-07	0.010	99.53	4.996	0.043	3.783	0.352
[C_4mpyrro][OTf]	[146]	1.491	-8.46E-04	1.75E-07	0.015	99.49	4.997	0.081	3.783	0.627
[C_3py][BF_4]	[125]	1.523	-1.08E-03	5.87E-07	0.005	99.54	4.995	0.109	3.782	0.151
[C_4py][OTf]	[125]	1.525	-6.49E-04	-1.90E-07	0.004	99.51	4.996	0.077	3.783	0.123
[$C_4m_{(3)}$py][DCA]	[125]	1.191	-3.52E-04	-4.16E-07	0.010	99.46	4.996	0.094	3.783	0.135
[$C_8m_{(3)}$py][BF_4]	[125]	1.318	-8.32E-04	2.84E-07	0.004	99.47	4.995	0.080	3.783	0.199
[amim]Cl	[152]	1.380	-9.57E-04	5.89E-07	0.006	98.76	5.000	0.115	3.780	0.416

[C_2mim][MP]	[153]	1.418	-8.40E-04	3.11E-07	0.003	98.84	5.000	0.089	3.781	0.762
[C_2mim][DEP]	[153]	1.368	-8.20E-04	2.35E-07	0.006	474.33	-1.211	0.001	0.083	0.013
[C_2eim][NTf_2]	[93]	1.846	-0.001	6.08E-07	0.006	99.53	4.995	0.047	3.783	0.013

Table 8.2 COSMO Area (*A*) and Volume (*V*), UNIFAC Volume (*R*) and Surface Area (*Q*) Parameters For Cations and Anions

Cation/Anion	*A* (Å^2)	*V*(Å^3)	*R*	*Q*
$[C_1mim]^+$	143.6002	133.8301	4.1183	3.4946
$[C_2mim]^+$	161.1985	154.7108	4.7608	4.0087
$[C_3mim]^+$	179.0980	176.5918	5.4342	4.5473
$[C_4mim]^+$	200.8316	198.3601	6.1040	5.0832
$[C_5mim]^+$	221.0143	220.6703	6.7906	5.6325
$[C_6mim]^+$	240.8024	242.4989	7.4623	6.1698
$[C_7mim]^+$	260.7208	264.6426	8.1437	6.7150
$[C_8mim]^+$	280.5705	286.4357	8.8143	7.2515
$[C_{10}mim]^+$	320.5828	330.3650	10.1662	8.3329
$[C_{12}mim]^+$	360.4221	374.4861	11.5239	9.4191
$[C_{14}mim]^+$	400.3099	418.4717	12.8774	10.5019
$[benmim]^+$	220.8244	229.6997	7.0684	5.8548
$[C_2OHmim]^+$	171.1799	165.8417	5.1034	4.2827
$[C_2mmim]^+$	175.3365	175.9131	5.4133	4.5306
$[C_3mmim]^+$	195.0583	198.0304	6.0939	5.0751
$[C_4mmim]^+$	214.6826	219.6602	6.7595	5.6076
$[C_6mmim]^+$	254.8100	263.9526	8.1225	6.6980
$[C_2py]^+$	155.5940	150.2216	4.6227	3.8982
$[C_4py]^+$	195.2272	194.1242	5.9737	4.9790
$[C_6py]^+$	235.1054	238.2544	7.3317	6.0654
$[C_8py]^+$	274.9784	282.3957	8.6900	7.1520
$[C_2m_{(3)}py]^+$	174.8855	172.7745	5.3819	4.5055
$[C_3m_{(1)}py]^+$	195.3973	195.2348	6.0081	5.0065
$[C_3m_{(3)}py]^+$	195.1102	195.2630	6.0090	5.0072
$[C_4C_2py]^+$	232.2243	238.1235	7.3277	6.0621
$[C_4m_{(2)}py]^+$	206.8813	214.2285	6.5924	5.4739
$[C_4m_{(3)}py]^+$	213.8947	215.1593	6.6210	5.4968
$[C_4m_{(4)}py]^+$	213.8053	215.4843	6.6310	5.5048
$[C_4m_{(3)}m_{(4)}py]^+$	230.0961	236.0786	7.2647	6.0118
$[C_4m_{(3)}m_{(5)}py]^+$	232.9659	237.4357	7.3065	6.0452
$[C_6m_{(3)}py]^+$	253.7834	259.3342	7.9804	6.5843
$[C_6m_{(4)}py]^+$	244.5804	249.0927	7.6652	6.3322
$[C_6m_{(3)}m_{(5)}py]^+$	270.0042	284.2257	8.7467	7.1974
$[C_6m_{(2)}m_{(4)}py]^+$	258.5318	285.2467	8.7781	7.2225
$[C_6C_2mmpy]^+$	297.5112	322.9212	9.9375	8.1500

$[C_6DMApy]^+$	275.7962	294.7824	9.0656	7.4525
$[C_6mDMApy]^+$	288.9952	316.9315	9.7531	8.0025
$[C_8m_{(3)}py]^+$	293.4556	303.1504	9.3287	7.6630
$[C_8m_{(4)}py]^+$	293.9197	303.8951	9.3516	7.6813
$[C_1mpyrro]^+$	148.6857	150.9291	4.6445	3.9156
$[C_4mpyrro]^+$	202.7789	214.6760	6.6061	5.4849
$[C_4C_2pyrro]^+$	217.6567	236.2094	7.2688	6.0150
$[C_6mpyrro]^+$	242.6089	258.7624	7.9628	6.5702
$[C_8mpyrro]^+$	282.3652	302.68365	9.3143	7.6515
$[COC_2mpyrro]^+$	192.7529	205.0862	6.3112	5.2490
$[COC_2mmor]^+$	202.1930	214.3062	6.5950	5.4760
$[COC_2mpip]^+$	206.4940	220.7122	6.7921	5.6337
$[P_{i(444)1}]^+$	284.4425	338.8644	10.4277	8.5422
$[P_{66614}]^+$	668.0665	748.1136	23.0213	18.6171
$[N_{1114}]^+$	179.8881	185.0516	5.6947	4.7558
$[N_{11120H}]^+$	151.8923	153.5328	4.7246	3.9797
$[N_{8881}]^+$	528.8326	580.1772	17.8542	14.4834
$[BF_4]^-$	90.5957	72.8610	2.2421	1.9937
$[C_1SO_4]^-$	118.0414	103.9738	3.1995	2.7596
$[NTf_2]^-$	203.7327	220.7723	6.7937	5.6350
$[PF_6]^-$	114.4755	103.6641	3.1900	2.7520
$[DCA]^-$	101.6045	82.3670	2.5346	2.2277
$[SCN]^-$	86.4618	69.5757	2.1410	1.9128
$[OAc]^-$	90.1298	72.1171	2.2192	1.9754
$[OTf]^-$	137.4601	128.7666	3.9625	3.3700
$[FAP]^-$	260.5544	321.3697	9.890	8.112
$[C_2SO_4]^-$	138.5912	125.1324	3.8506	3.2805
Br^-	58.6297	42.2134	1.2990	1.2392
$[C_8SO_4]^-$	257.5625	257.0302	7.9095	6.5276
$[C_1SO_3]^-$	107.2061	89.1805	2.7443	2.3954
$[Tos]^-$	186.3163	186.8862	5.7510	4.8008
Cl^-	52.8102	36.0874	1.1105	1.0884
$[I_3]^-$	152.5258	143.1761	4.4061	3.7248
$[HSO_4]^-$	97.8337	80.3428	2.4724	2.1779
$[C_4SO_4]^-$	178.4577	169.1366	5.2048	4.3638
$[C_8SO_4]^-$	257.5625	257.0302	7.9095	6.5276
$[DEP]^-$	180.6050	173.0418	5.3249	4.4599
$[DMP]^-$	139.5354	130.5071	4.0160	3.4128
$[B(CN)_4]^-$	160.6364	147.8143	4.5486	3.8389
$[TOS]^-$	186.3163	186.8862	5.7510	4.8008
$[Meesu]^-$	218.6692	216.4830	6.6620	5.5296
$[C(CN)_3]^-$	131.3405	113.8444	3.5034	3.0027
$[Tf_3C]^-$	255.0483	314.6554	9.6831	7.9465

Table 8.3 Density Data As a Function of Temperature and Pressure Reported in the Literature

IL	Ref.	$N_{0.1MPa}$	$T_{0.1MPa}$	$N_{>0.1MPa}$	$T_{>0.1MPa}$	P (MPa)
$[C_2mim][SCN]$	119	5	298-338	60	298-338	0.1-10
$[C_2mim][OAc]$	120	7	293-353	56	293-353	0.1-25
$[C_4mim]Cl$	121	6	348-373	120	352-452	0.1-200
$[C_2mim][DCA]$	122	1	298	84	256-346	0.6-60
$[N_{11120H}][Lactate]$	121	13	293-353	100	312-392	0.1-200
$[C_4mim][SCN]$	119	5	298-338	60	298-338	0.1-10
$[C_2mim][BF_4]$	127	8	293-393	88	293-393	0.1-30
	134	4	293-353	180	312-472	0.1-200
	112	9	283-323	108	283-323	0.1-60
	149	0	0	76	284-356	1-61
$[C_4mim][OAc]$	120	7	298-353	56	298-353	0.1-25
	153	9	293-373	80	311-371	0.1-200
$[C_2mim][Lactate]$	121	13	293-353	140	312-432	0.1-200
$[C_4mim][DCA]$	122	0	0	58	237-349	0.6-60
	173	81	293-393	160	293-393	0.1-60
	124	8	283-343	96	283-393	0.1-100
$[C_1mim][C_1SO_4]$	117	4	318-333	30	313-333	0.1-25
	118	12	318-428	156	318-428	0.1-60
$[C_4m_{(4)}py][SCN]$	119	5	298-338	60	298-338	0.1-10
$[C_2mim][C_1SO_4]$	93	8	293-393	72	293-393	0.1-35
$[C_4py][BF_4]$	113	10	298-343	12	298-323	0.1-204
	133	7	293-353	28	293-353	0.1-20
	125	11	283-333	143	283-333	0.1-65
$[C_4mim][BF_4]$	112	9	283-323	108	283-323	0.1-60
	246	11	278-333	15	298-333	0.1-60
	126	5	298-332	62	298-332	0.1-60
	247	4	293-353	16	293-353	0.1-20
	114	11	293-393	66	293-393	0.1-10
	248	0	0	45	298-398	0.2-40
	137	10	292-415	36	293-415	0.1-40
	254	36	273-363	40	283-348	0.1-300
	249	0	0	45	298-398	0.2-40
	136	9	313-472	180	313-472	0.1-200
	250	0	0	20	313-433	0.2-2

	[251]	2	298-323	12	298-323	0.1-30
	[252]	6	283-333	54	283-333	0.1-40
	[253]	1	298	60	239-354	0.1-61
	[132]	29	283-353	232	283-353	0.1-35
$[C_4mim][C(CN)_3]$	[127]	8	293-393	88	293-393	0.1-30
$[C_2mim][C_2SO_4]$	[173]	83	293-433	156	293-433	0.1-60
	[93]	8	293-393	72	293-393	0.1-35
	[137]	10	292-415	36	293-415	0.1-40
	[132]	29	283-353	232	283-353	0.1-35
	[174]	7	283-333	56	283-333	0.1-35
	[128]	13	283-343	104	283-343	0.1-35
	[140]	14	278-398	112	278-398	0.1-120
	[255]	7	283-363	136	283-413	0.1-140
	[256]	0	0	5	302.88	5-40
	[257]	7	278-398	56	278-398	0.1-120
$[C_4m_{(2)}py][BF_4]$	[129]	9	293-333	111	293-333	0.1-65
$[C_4m_{(3)}py][BF_4]$	[129]	11	283-333	143	283-333	0.1-65
	[130]	0	0	96	283-393	1-100
$[C_4m_{(4)}py][BF_4]$	[129]	11	283-333	143	283-333	0.1-65
	[131]	0	0	96	283-393	1-100
$[C_4mim][C_1SO_4]$	[132]	29	283-353	232	283-353	0.1-35
	[258]	11	283-333	88	283-333	0.1-35
$[C_6py][BF_4]$	[133]	7	293-353	28	293-353	0.1-20
$[C_6mim][BF_4]$	[134]	4	293-353	180	313-472	0.1-200
	[112]	9	283-323	108	283-323	0.1-60
	[149]	1	298	66	219-357	0.1-61
	[259]	0	0	84	283-373	0.5-100
$[C_2mim][PF_6]$	[134]	2	353-373	180	312-472	10-200
$[C_2mim][OTf]$	[149]	0	0	61	264-347	0.1-61
	[94]	7	293-393	84	293-393	0.1-35
$[C_8py][BF_4]$	[133]	7	293-353	28	293-353	0.1-20
$[C_8mim][BF_4]$	[112]	9	283-323	108	283-323	0.1-60
	[113]	6	298-343	13	298-323	0.1-207
	[114]	11	293-393	66	293-393	0.1-10
	[223]	40	273-363	54	298-348	0.1-224
	[260]	3	298-348	24	298-348	0.1-196
$[C_2mim][Tos]$	[118]	12	318-428	156	318-428	0.1-60
$[C_4mim][PF_6]$	[113]	10	298-343	12	298-323	0.1-202
	[126]	15	298-333	141	298-333	0.1-60
	[247]	4	293-353	16	293-353	0.1-20

	[248]	0	0	45	298-398	0.7-40
	[137]	10	293-415	36	293-415	0.1-40
	[136]	9	312-472	180	312-472	0.1-200
	[135]	3	294-335	6	294-335	0.1-20
$[C_4mim][OTf]$	[149]	0	0	61	290-350	0.2-60
	[114]	11	293-393	66	293-393	0.1-10
$[C_4C_1mim][PF_6]$	[114]	18	313-393	54	313-393	0.1-10
$[C_6mim][PF_6]$	[134]	4	293-353	180	312-472	0.1-200
	[114]	11	293-393	66	293-393	0.1-10
	[224]	4	293-353	20	293-353	0.1-20
	[116]	39	273-363	32	298-348	0.1-238
	[135]	3	294-335	6	294-335	0.1-20
$[C_8mim][PF_6]$	[134]	4	293-353	180	312-472	0.1-200
	[113]	10	298-343	12	298-323	0.1-204
	[114]	21	293-393	66	293-393	0.1-10
	[223]	27	273-363	28	298-343	0.1-176
	[260]	3	298-348	22	298-348	0.1-196
	[224]	4	293-353	16	293-353	0.1-20
	[135]	3	295-335	6	295-335	0.1-20
$[C_4mim][C_8SO_4]$	[136]	9	312-472	169	312-472	0.1-200
	[261]	58	278-428	252	278-428	0.1-60
	[262]	0	0	45	298-398	0.11-40
$[C_2mim][NTf_2]$	[127]	8	293-393	88	293-393	0.1-30
	[137]	10	293-415	36	293-415	0.1-40
	[263]	0	0	84	283-373	0.7-1007
$[N_{1114}][NTf_2]$	[31]	10	293-415	36	293-415	0.1-40
$[C_3mim][NTf_2]$	[138]	15	298-333	150	298-333	0.1-60
$[C_3mpyrro][NTf_2]$	[94]	7	293-393	84	293-393	0.1-35
$[C_3m_{(3)}py][NTf_2]$	[94]	7	293-393	84	293-393	0.1-35
$[C_4mim][NTf_2]$	[173]	85	293-473	224	293-473	0.1-60
	[137]	10	293-415	36	293-415	0.1-40
	[116]	45	273-363	36	283-348	0.1-299
	[139]	3	298-348	27	298-348	0.1-50
	[264]	7	298-328	154	298-328	0.1-59
	[265]	16	273-363	77	288-348	0.1-251
	[153]	9	293-373	120	311-412	0.1-200
$[C_4mpyrro][NTf_2]$	[94]	7	293-393	84	293-393	0.1-35
	[31]	10	293-415	36	293-415	1-40
	[266]	48	273-363	54	273-348	0.1-103
	[147]	7	278-398	56	278-398	0.1-120

$[C_3mpip][NTf_2]$	94	7	293-393	84	293-393	0.1-35
	267	3	298-348	27	298-348	0.1-50
$[C_1OC_2mpyrro][NTf_2]$	140	14	278-398	112	278-398	0.1-120
$[C_5mim][NTf_2]$	138	15	298-333	150	298-333	0.1-60
$[N_{8881}][DCA]$	173	82	293-413	176	293-413	0.1-60
$[C_6mim][NTf_2]$	264	15	298-333	148	298-333	0.1-60
	268	8	298-373	48	298-423	0.1-40
	172	18	293-338	145	293-338	0.1-65
	142	17	293-452	160	312-452	0.1-200
	269	10	273-413	256	273-413	0.1-140
	265	39	273-363	11	288	0.1-175
$[C_7mim][NTf_2]$	127	8	293-393	88	293-393	0.1-30
$[C_8mim][NTf_2]$	127	8	293-393	88	293-393	0.1-30
	270	6	293-343	54	293-343	0.1-25
$[C_{10}mim][NTf_2]$	93	8	293-393	72	293-393	0.1-35
$[P_{66614}]Cl$	29	0	0	134	298-333	0.2-65
	143	8	273-318	64	273-318	0.1-25
	145	6	283-333	78	283-333	0.1-45
$[P_{66614}][OAc]$	29	0	0	144	298-334	0.2-65
$[P_{66614}][DCA]$	143	19	273-318	154	273-318	0.1-35
	145	6	283-333	78	283-333	0.1-45
$[C_2mim][FAP]$	144	6	293-343	48	293-343	0.1-25
$[P_{66614}]Br$	145	6	283-333	78	283-333	0.1-45
$[P_{66614}][C_1SO_3]$	145	6	283-333	78	283-333	0.1-45
$[C_4mim][FAP]$	144	6	303-353	57	293-353	0.1-25
$[C_4mpyrro][FAP]$	148	7	293-353	56	293-353	0.1-25
	146	7	278-398	56	278-398	0.1-120
$[C_1OC_2mpyrro][FAP]$	147	7	278-398	56	278-398	0.1-120
$[C_6mim][FAP]$	144	6	293-343	54	293-343	0.1-25
$[P_{66614}][TNf_2]$	29	0	0	126	298-333	0.2-65
	145	6	283-333	78	283-333	0.1-45
$[P_{66614}][FAP]$	148	7	293-353	56	293-353	0.2-25
	271	11	293-343	77	293-343	0.1-25
	146	7	278-398	56	278-398	0.1-120
$[C_6mim]Cl$	142	16	303-451	160	311-451	0.1-200
$[C_6mim][OTf]$	149	0	0	48	303-352	0.1-61
$[C_4C_1mim][FAP]$	150	14	278-398	112	278-398	0.1-120
$[C_4C_1mim][NTf_2]$	150	14	278-398	112	278-398	0.1-120
$[C_2OHC_1NH_2][C_2COO]$	151	13	298-358	91	298-358	0.1-25
$[C_2OHC_1NH_2][C_3COO]$	151	7	298-358	35	298-358	0.1-25

$[C_2OHC_1NH_2][C_4COO]$	[151]	7	298-358	35	298-358	0.1-25
$[C_1mim][DMP]$	[146]	7	278-398	56	278-398	0.1-120
$[C_2mim][C_6SO_4]$	[146]	7	278-398	56	278-398	0.1-120
$[C_4mpyrro][B(CN)_4]$	[146]	6	298-398	69	298-398	0.1-60
$[C_4mpyrro][OTf]$	[146]	7	278-398	56	278-398	0.1-120
$[C_3py][BF_4]$	[125]	11	283-333	143	283-333	0.1-65
$[C_4py][OTf]$	[125]	7	303-333	91	303-333	0.1-65
$[C_4m_{(3)}py][DCA]$	[125]	9	293-333	117	293-333	0.1-65
$[C_8m_{(3)}py][BF_4]$	[125]	11	283-333	143	283-333	0.1-65
[amim]Cl	[152]	9	293-373	80	313-373	0.1-200
$[C_2mim][MP]$	[153]	9	293-373	120	311-411	0.1-200
$[C_2mim][DEP]$	[153]	9	293-373	120	311-412	0.1-200
$[C_2eim][NTf_2]$	[93]	8	293-393	72	293-393	0.1-35

Table 8.4 Viscosity Data As a Function of Temperature Reported in the Literature

IL	No.	T	Ref.
$[C_2mim][BF_4]$	1	299	272
	1	293	17
	2	293-303	274
	1	298	276
	1	298	278
	1	298	280
	1	298	281
	1	298	180
	1	298	283
	16	290-365	285
	4	283-324	112
	12	269-353	192
	9	283-363	286
	4	288-318	288
	4	283-313	179
$[C_4mim][C_1SO_4]$	9	293-343	198
	1	298	291
	2	298-323	43
	11	283-368	292
	6	303-353	294
	4	298-328	296
$[C_2mim][C_1SO_4]$	19	283-373	191
$[C_4mim][NTf_2]$	1	293	299
	1	298	275
	1	298	277
	1	293	279
	1	293	302
	10	283-343	188
	1	298	180
	1	298	181
	1	293	305
	1	298	289
	1	298	290
	21	273-353	116
	1	298	291
	1	298	297
	1	293	54
	2	298-323	43
	1	298	283
	1	303	308
	4	293-308	189
$[C_4mim][BF_4]$	1	303	273
	1	293	17
	1	298	275
	1	298	277
	1	303	279
	3	283-303	274
	1	298	276
	1	298	282
	1	298	284
	10	283-343	188
	1	298	280
	1	298	180
	1	298	287
	4	293-353	247
	1	298	289
	1	298	290
	21	273-348	254
	7	293-323	197
	1	293	293
	1	298	295
	1	298	297
	1	298	298
	1	298	283
	1	303	300
	8	293-353	192
	5	303-343	301
	4	298-318	288
	18	283-368	200
	9	278-358	303
	5	298-318	304
	3	313-353	185
	11	293-388	23
	1	298	306
	8	303-353	307
$[C_3mim][NTf_2]$	1	293	54
	10	298-343	204
$[C_3mim][PF_6]$	10	318-363	205
$[C_4mim][PF_6]$	1	303	273
	1	298	275
	1	298	277
	10	293-338	309

	1	298	310
	1	298	311
	12	298-353	312
	8	283-353	215
	9	283-353	222
	11	293-388	23
	1	303	183
	4	295-353	317
$[C_4m_{(3)}py][DCA]$	10	283-328	206
	8	298-348	221
$[P_{66614}][DCA]$	1	298	318
	1	293	319
	1	313	321
	1	303	160
	11	298-343	208
	18	278-363	209
	6	293-318	323
$[P_{66614}][NTf_2]$	2	293-353	325
	1	298	318
	1	293	319
	1	313	321
	1	303	160
	1	298	329
	1	298	291
	17	278-358	209
$[C_4m_{(3)}py][NTf_2]$	8	283-343	8
	2	298-323	43
	18	278-363	207
	12	298-353	331
$[C_4mmim][BF_4]$	7	298-353	333
	1	298	306
	7	313-373	334
$[C_4py][BF_4]$	10	298-343	335
	15	283-353	226
	4	293-323	210
	7	293-353	159
$[C_4py][NTf_2]$	1	353	325
	1	293	54
	18	278-363	207
	9	298-338	339
	6	303-353	158
	9	283-353	222
$[C_4mpyrro][NTf_2]$	1	298	342
	1	298	343
	1	298	344
	10	283-343	188
	1	296	345
	1	298	346
	1	303	279
	3	283-303	274
	1	343	313
	10	283-343	188
	1	293	314
	22	273-343	315
	1	298	316
	1	298	180
	4	293-353	247
	1	298	289
	1	298	290
	1	298	320
	10	288-313	322
	7	293-323	199
	1	298	297
	2	298-323	43
	8	293-343	324
	1	303	308
	13	283-353	326
	1	297	327
	1	303	300
	6	313-413	328
	9	283-353	222
	9	283-363	179
	1	298	330
	11	293-388	23
	1	303	183
	1	298	317
	1	293	332
$[C_4mmim][NTf_2]$	10	283-343	188
	4	292-308	189
	21	273-373	190
$[C_6mim][BF_4]$	6	288-338	336
	1	293	337
	8	288-323	197
	4	298-318	288
	1	298	338
	4	293-353	115
	18	283-368	200
	10	293-338	340
	5	293-333	341
	11	283-368	292
	9	283-363	179
	3	298-343	330
$[C_{10}mim][BF_4]$	3	283-303	274
	9	283-363	179
$[C_{10}mim][PF_6]$	6	313-363	179
$[C_6mim][PF_6]$	1	298	275

	1	301	347
	1	298	291
	1	298	297
	2	298-343	43
	1	293	348
	1	298	283
	1	303	349
	1	297	350
	11	293-343	208
	1	298	352
	9	283-363	286
	4	292-308	189
	50	273-363	266
	20	278-373	190
	6	293-343	355
	12	298-353	312
	9	283-353	222
	1	298	356
$[C_4mpyrro][C_1SO_4]$	10	298-343	217
	7	293-343	216
$[C_1mim][C_1SO_4]$	4	298-328	359
	3	298-328	360
	1	293	299
	1	299	272
	1	293	279
	1	293	343
	1	293	302
	8	283-343	8
	1	293	180
	1	298	365
	1	298	366
	1	298	181
	5	303-343	368
$[C_2mim][NTf_2]$	1	298	291
	8	273-333	228
	1	298	370
	1	298	283
	12	263-353	192
	7	293-323	373
	11	283-368	292
	8	283-353	215
	9	283-353	222
	3	298-343	330
	11	293-388	23
	1	303	183
	1	293	299
$[C_4mim][OTf]$	1	303	279
	10	288-343	188
	7	288-348	336
	14	273-353	116
	7	293-323	199
	4	293-353	224
	11	293-343	211
	18	283-368	200
	9	283-363	179
	4	298-343	330
	1	293	351
	8	298-333	353
	7	303-333	162
	15	293-363	354
	1	293	299
$[C_1mim][NTf_2]$	8	283-353	215
	7	298-353	222
	6	298-323	335
	4	293-323	210
$[C_4m_{(4)}py][BF_4]$	4	298-373	357
	8	298-348	221
	3	298-323	358
	18	278-363	207
$[C_4m_{(4)}py][NTf_2]$	13	298-358	361
	7	293-353	159
	1	298	362
	1	298	291
$[C_2mim][SCN]$	6	298-348	363
	18	278-363	182
	6	298-348	364
$[C_4mim][SCN]$	18	283-368	200
$[C_4m_{(4)}py][SCN]$	6	298-348	218
	1	298	367
$[C_4mpyrro][SCN]$	6	298-348	218
	1	293	299
	1	294	369
	18	278-363	182
$[C_2mim][OAc]$	4	298-393	371
	10	298-343	193
	13	283-343	372
	8	283-343	8
	1	298	291
	2	298-323	43
	2	298-353	374
$[C_4mim][Oac]$	4	298-393	371
	17	283-363	219
	5	303-343	201
	13	283-343	372
$[C_4mpyrro][Oac]$	14	298-363	219
$[C_2mim][OTf]$	1	293	180

	1	298	181
	1	298	291
	2	298-323	43
	9	283-363	286
	9	283-353	222
	9	283-363	179
	7	303-343	375
$[C_8mim][OTf]$	1	293	376
	9	283-363	179
$[C_4mpyrro][OTf]$	1	293	348
	19	283-373	190
$[C_{10}mim][OTf]$	1	293	376
	9	283-363	179
$[C_8mim][NTf_2]$	1	293	302
	1	298	377
	1	293	376
	1	298	291
	1	298	378
	8	283-353	215
	9	283-353	222
	1	293	351
	1	298	379
	1	298	380
$[C_8mim][BF_4]$	3	283-303	274
	14	273-353	223
	8	288-323	197
	1	303	300
	4	288-318	381
	4	293-353	115
	9	283-363	179
	5	293-328	382
	17	283-363	384
	9	283-363	221
	1	298	386
$[C_2mim][C_2SO_4]$	1	298	388
	1	298	389
	1	313	390
	1	333	287
	1	353	247
	8	278-348	184
	1	298	291
	8	273-333	228
	25	253-373	190
	7	293-333	394
	12	278-373	255
	1	298	193
	8	293-318	323
	11	296-388	23
	1	298	181
	8	278-348	184
	18	278-363	182
	5	303-363	185
	9	283-363	179
	1	303	183
$[C_8mim][PF_6]$	1	298	275
	3	283-298	274
	1	298	313
	1	303	180
	23	273-353	223
	7	293-323	199
	4	293-353	224
	1	303	308
	1	303	300
	9	283-363	179
	1	293	351
$[C_2mim][FAP]$	9	293-373	144
$[C_4mim][FAP]$	9	293-373	144
$[C_6mim][FAP]$	1	293	337
	9	293-373	144
	11	293-343	211
$[C_4mpyrro][FAP]$	1	298	291
	16	290-365	285
	19	283-373	190
	9	293-373	148
$[C_4mmim][FAP]$	19	283-373	190
$[P_{66614}][FAP]$	22	268-373	190
	159	283-363	271
	9	293-373	148
$[C_2mim][DCA]$	1	298	383
	1	298	279
	1	295	385
	1	295	387
	1	298	180
	1	298	362
	1	298	391
	5	273-313	228
	1	297	392
	1	301	393
	16	290-365	285
	14	258-353	192
	18	278-363	182
	10	298-343	193
$[C_4mim][DCA]$	1	298	284
	1	298	391
	1	298	395
	1	298	291

	10	298-343	195
	7	293-353	294
$[C_6mim][NTf_2]$	2	293-353	325
	5	288-328	336
	8	283-343	387
	19	258-373	396
	17	288-433	268
	1	298	291
	1	303	308
	8	293-363	397
	6	298-343	213
	5	303-343	301
	3	283-323	398
	8	283-353	215
	9	283-353	222
	4	298-343	330
	1	293	351
	1	323	400
	8	298-368	379
$[N_{1114}][NTf_2]$	2	293-323	401
	1	303	403
	1	298	405
	6	293-343	355
	11	293-388	23
	9	283-353	222
	7	298-573	406
	15	283-353	227
$[N_{8881}][NTf_2]$	8	273-333	228
	1	303	403
	4	293-323	214
	1	293	376
	1	293	305
$[C_4m_{(3)}py][BF_4]$	8	283-343	8
	2	298-323	43
	6	298-323	335
	4	293-323	210
$[C_8py][NTf_2]$	2	293-353	325
	1	293	305
	18	278-363	207
$[C_2mim]Cl$	3	353-393	371
	5	323-363	179
	4	298-313	196
$[P_{66614}]Br$	1	298	318
	18	278-363	209
$[P_{66614}][C_1SO_3]$	18	278-363	209
$[C_2mim][Tos]$	13	303-363	182
	1	301	393
	18	278-363	202
	4	298-393	371
	4	298-373	357
	5	303-363	185
	8	293-363	221
$[C_6mim]Cl$	1	298	275
	1	298	274
	1	293	337
	4	298-343	225
	1	298	290
	3	353-393	371
	9	283-363	179
	6	323-373	142
	3	323-333	162
	2	308-318	399
$[C_8mim]Cl$	4	298-343	225
	3	353-393	371
	9	283-363	179
	1	298	402
	3	298-328	404
	8	298-333	353
	3	323-333	162
$[C_{10}mim][NTf_2]$	1	293	302
	1	293	305
	4	293-323	214
	1	298	291
	3	298-343	330
	1	293	351
$[C_4mpyrro][DCA]$	1	298	383
	1	298	291
	1	301	393
	11	293-343	220
$[C_6py][NTf_2]$	8	293-343	8
	2	293-353	325
	9	298-338	229
	18	278-363	207
$[C_4mim][C_8SO_4]$	9	293-373	203
	1	298	291
	9	314-395	407
$[C_2mim][C_1SO_3]$	18	278-363	182
	1	298	408
$[C_6mim]Br$	9	293-333	212
$[C_8py][BF_4]$	15	283-353	226
$[C_2mim][C_8SO_4]$	19	283-373	191

Table 8.5 UNIFAC and UNIQUAC Correlations For LLE of Binary Mixtures (IL + Solvent)

Systems	Tie-lines	T (*K*)	Ref.	δx (%)	
				UNIFAC	UNIQUAC
$[C_2mmim][C_2SO_4]$+hexene	1	313	[409]	1.18E-05	1.78E-03
$[C_2mim][C_2SO_4]$+hexane	1	313	[409]	2.71E-06	0.03
$[C_8mim]$Cl+1-octanol	11	289-315	[410]	6.59	11.13
$[C_2mim][C_2SO_4]$+2,2,4-trimethylpentane	1	298	[411]	0.05	0.01
$[C_4m_{(4)}py][BF_4]$+heptane	2	313-348	[71]	0.04	0.25
$[C_4mim][C_1SO_4]$+heptane	2	313-348	[71]	0.04	0.05
$[C_4mim][C_1SO_4]$+toluene	2	313-348	[71]	5.00E-03	4.67E-03
$[C_1mim][C_1SO_4]$+heptane	2	313-348	[71]	0.06	0.22
$[C_1mim][C_1SO_4]$+toluene	2	313-348	[71]	0.02	0.02
$[C_8mim][NTf_2]$+hexane	1	298	[412]	0.01	0.01
$[C_8mim][NTf_2]$+heptane	1	298	[412]	0.01	0.02
$[C_8mim][NTf_2]$+thiophene	2	298	[412,413]	0.36	0.53
$[C_8mim][NTf_2]$+n-hexadecane	1	298	[412]	0.01	1.74E-04
$[C_2mim][C_2SO_4]$+n-hexadecane	1	298	[414]	0.07	0.05
$[C_2mim][C_2SO_4]$+n-dodecane	1	298	[414]	0.07	0.05
$[C_2mim][C_2SO_4]$+hexane	1	298	[414]	0.01	4.73E-03
$[C_2mim][C_2SO_4]$+thiophene	2	298	[411,414]	0.05	3.58E-03
$[C_2mim][C_2SO_4]$+heptane	8	293-348	[71,414,415]	0.16	0.18
$[C_2mim][C_2SO_4]$+toluene	7	293-348	[71,411,415]	1.90	2.20

$[C_2mim][C_2SO_4]$+methylcyclohexane	5	293-333	[415]	0.33	0.30
$[C_2mim][NTf_2]$+octane	1	298	[416]	0.01	0.04
$[C_8mim][BF_4]$+water	18	278-340	[66,232,234]	2.36	4.58
$[C_6mim][BF_4]$+water	15	278-333	[66,234]	1.32	3.44
$[C_2mim][NTf_2]$+heptane	2	298	[417,418]	0.07	0.05
$[C_2mim][C_2SO_4]$+di-isopropyl ether	6	293-313	[419]	0.18	0.24
$[C_4mim][BF_4]$+di-isopropyl ether	5	293-313	[419]	0.21	0.28
$[C_4m_{(3)}py][B(CN)_4]$+ethylbenzene	3	313-353	[420]	0.07	0.08
$[C_4m_{(3)}py][B(CN)_4]$+styrene	3	313-353	[420]	4.22E-03	0.39
$[C_3mim][NTf_2]$+hexane	1	298	[421]	0.01	0.04
$[C_6mim][DCA]$+hexane	1	298	[421]	0.01	3.91E-03
$[C_6mim][NTf_2]$+hexane	1	298	[421]	0.01	4.55E-03
$[C_6mim][OTf]$+hexane	1	298	[421]	0.01	0.01
$[C_2mim][Oac]$+thiophene	1	298	[422]	0.05	4.36E-03
$[C_2mim][DEP]$+toluene	1	298	[422]	0.04	3.55E-03
$[C_2mim][DEP]$+hexane	2	298	[422]	0.07	0.07
$[C_2mim][DEP]$+thiophene	2	298	[422]	0.64	0.64
$[C_2mim][Oac]$+hexane	1	298	[422]	0.01	0.28
$[C_3mim][NTf_2]$+cyclohexane	1	298	[423]	0.05	0.04
$[C_3mim][NTf_2]$+toluene	1	298	[423]	4.99E-03	0.04
$[C_3mim][NTf_2]$+cyclooctane	1	298	[423]	0.05	0.04
$[C_4mim][NTf_2]$+cyclohexane	1	298	[423]	0.05	0.01
$[C_4mim][NTf_2]$+ethylbenzene	1	293	[423]	0.04	3.85E-03
$[C_4mim][NTf_2]$+toluene	2	298-313	[418,423]	0.04	0.12

[C_3mim][NTf_2]+benzene	2	298	[423,424]	0.04	0.04
[C_8mim][NTf_2]+n-dodecane	1	298	[413]	0.01	0.02
[C_8mim][NTf_2]+cyclohexane	1	298	[413]	0.21	2.85E-04
[C_8mim][BF_4]+thiophene	1	298	[425]	0.05	0.04
[C_8mim][BF_4]+heptane	1	298	[425]	4.42E-03	0.05
[C_8mim][BF_4]+n-hexadecane	1	298	[425]	0.01	0.05
[C_8mim][BF_4]+n-dodecane	1	298	[425]	0.01	0.04
[$C_4m_{(3)}$py][DCA]+hexane	4	303-328	[426]	0.12	0.12
[$C_4m_{(3)}$py][DCA]+benzene	2	303-328	[426]	0.03	0.10
[$C_4m_{(3)}$py][DCA]+p-xylene	2	303-328	[426]	0.04	0.07
[$C_4m_{(3)}$py][DCA]+n-nonane	2	303-328	[426]	0.07	0.07
[$C_4m_{(3)}$py][DCA]+cumene	2	303-328	[426]	0.03	1.11
[C_4C_1mim][BF_4]+1-pentanol	15	303-352	[427]	3.09	9.49
[C_4C_1mim][BF_4]+1-hexanol	14	326-376	[427]	3.79	9.73
[C_4C_1mim][BF_4]+1-butanol	13	310-337	[427]	3.38	7.83
[C_4C_1mim][BF_4]+1-propanol	12	292-323	[427]	0.40	8.05
[C_4C_1mim][BF_4]+2-propanol	12	298-326	[427]	0.43	6.66
[$C_4m_{(3)}$py] [$B(CN)_4$]+benzene	2	303-328	[428]	0.11	0.21
[$C_4m_{(3)}$py] [$B(CN)_4$]+hexane	2	303-328	[428]	0.07	0.10
[$C_4m_{(3)}$py] [$B(CN)_4$]+heptane	1	303	[428]	0.08	2.82E-05
[$C_4m_{(3)}$py] [$B(CN)_4$]+n-octane	2	303-328	[428]	0.06	0.13
[$C_4m_{(3)}$py] [$B(CN)_4$]+p-xylene	1	328	[428]	5.59E-05	2.02E-04
[C_2mim][SCN]+ethylbenzene	3	313-353	[429]	0.05	0.01
[C_2mim][SCN]+styrene	3	313-353	[429]	0.04	0.03

$[C_4mim][OTf]$+heptane	1	298	[430]	0.04	0.01
$[C_4mim][OTf]$+toluene	1	313	[430]	4.98E-03	3.58E-03
$[C_4mim][OTf]$+cyclohexane	1	298	[430]	0.05	3.56E-03
$[C_6mim][NTf_2]$+cyclohexane	1	298	[430]	0.05	3.03E-03
$[C_6mim][OTf]$+heptane	1	298	[430]	0.01	4.27E-03
$[C_6mim][OTf]$+toluene	1	313	[430]	4.96E-03	3.55E-03
$[C_6mim][OTf]$+cyclohexane	1	298	[430]	0.05	5.36E-03
$[C_6mim][NTf_2]$+heptane	2	298-313	[418,430]	0.02	4.60E-03
$[C_6mim][NTf_2]$+toluene	2	298-313	[418,430]	3.53E-03	3.96E-03
$[C_6mim][B(CN)_4]$+water	1	308	[431]	0.04	0.02
$[C_{10}mim][B(CN)_4]$+water	1	308	[431]	0.05	0.01
$[P_{66614}][B(CN)_4]$+water	1	308	[431]	0.21	0.21
$[C_2mim][NTf_2]$+ethanol	1	298	[432]	0.05	0.05
$[C_3mim][NTf_2]$+ethanol	1	298	[432]	0.05	0.04
$[C_4mim][NTf_2]$+ethanol	1	298	[432]	0.05	4.99E-03
$[C_2mim][NTf_2]$+hexane	1	298	[433]	3.61E-03	0.04
$[C_2mim][NTf_2]$+thiophene	2	298	[417,433]	0.39	0.39
$[C_4mpyrro][B(CN)_4]$+heptane	1	298	[434]	3.54E-03	3.58E-03
$[C_4mpyrro][B(CN)_4]$+thiophene	1	298	[434]	0.04	0.05
$[C_4mpyrro][FAP]$+heptane	1	298	[434]	3.95E-03	4.49E-03
$[C_4mpyrro][FAP]$+thiophene	1	298	[434]	0.05	3.86E-03
$[C_4mim][NTf_2]$+water	3	293-323	[10,234]	1.09	1.38
$[C_6mim][NTf_2]$+water	3	296-323	[14,234]	1.63	1.77
$[C_8mim][NTf_2]$+water	3	296-323	[14,234]	1.27	1.27

[C_6mim][OTf]+water	2	298-323	[234]	0.01	0.07
[C_6mim][PF_6]+water	2	298-323	[234]	0.04	0.42
[C_8mim][OTf]+water	2	298-323	[234]	3.45E-03	0.05
[$P_{i(444)1}$][Tos]+toluene	20	320-361	[435]	0.29	1.62
[$P_{i(444)1}$][Tos]+n-propylbenzene	13	304-362	[435]	0.95	0.90
[$P_{i(444)1}$][Tos]+ethylbenzene	12	309-361	[435]	1.42	1.45
[$P_{i(444)1}$][Tos]+heptane	11	315-353	[435]	3.34	4.69
[$P_{i(444)1}$][Tos]+n-octane	10	317-360	[435]	0.79	4.89
[$P_{i(444)1}$][Tos]+n-nonane	9	320-361	[435]	0.99	4.82
[$P_{i(444)1}$][Tos]+n-butylbenzene	8	303-364	[435]	0.89	0.87
[$P_{i(444)1}$][Tos]+hexane	7	308-338	[435]	3.38	3.73
[$P_{i(444)1}$][Tos]+n-decane	7	330-363	[435]	4.33	4.34
[C_4mim][PF_6]+water	10	298-323	[10,231–234]	1.14	2.02
[C_2mim][PF_6]+water	5	318-323	[231]	0.11	0.48
[C_2mim][OAc]+heptane	1	298	[436]	0.01	3.54E-03
[C_2mim][OAc]+cyclohexane	1	298	[436]	0.04	4.49E-03
[C_2mim][OAc]+toluene	2	298	[422,436]	0.22	0.89
[C_4mim][PF_6]+ethanol	12	288-328	[437]	0.73	7.27
[C_4mim][PF_6]+1-propanol	6	333-352	[437]	0.40	2.38
[C_4mim][PF_6]+1-butanol	7	288-361	[437,438]	0.17	4.98
[C_4mim][PF_6]+2-propanol	14	278-343	[439]	0.32	4.83
[C_6mim][PF_6]+2-propanol	11	278-328	[439]	0.85	5.58
[C_6mim]Cl+butylacetate	6	356-380	[440]	0.19	0.19
[C_1mim][NTf_2]+heptane	1	313	[418]	3.67E-03	0.04

$[C_1mim][NTf_2]$+toluene	1	313	[418]	0.04	0.04
$[C_{10}mim][NTf_2]$+limonene	1	298	[441]	0.04	0.04
$[C_2mim][NTf_2]$+limonene	1	298	[441]	0.05	0.05
$[C_2mim][NTf_2]$+linalool	1	298	[441]	0.04	0.04
$[C_6mim][NTf_2]$+limonene	1	298	[441]	0.05	0.05
$[C_{10}mim][NTf_2]$+linalool	1	298	[441]	9.22	3.11E-05
$[C_6mim][NTf_2]$+linalool	1	298	[441]	4.12E-08	7.33E-04
$[C_3mim][NTf_2]$+methylcyclohexane	1	298	[424]	0.04	0.04
$[C_4mim][NTf_2]$+benzene	1	298	[424]	0.04	0.01
$[C_4mim][NTf_2]$+octane	1	298	[424]	0.05	4.56E-03
$[C_4mim][NTf_2]$+cyclooctane	1	298	[424]	0.05	4.97E-03
$[C_4mim][NTf_2]$+methylcyclohexane	1	298	[424]	0.04	3.56E-03
$[C_4mim][NTf_2]$+heptane	2	298-313	[418,424]	0.05	0.26
$[C_4m_{(3)}py][NTf_2]$+water	8	296-318	[14,442]	0.11	0.99
$[C_6py][NTf_2]$+water	8	296-318	[14,442]	0.30	1.11
$[C_2mim][B(CN)_4]$+water	1	296	[14]	5.71E-04	9.67E-04
$[C_2mim][B(CN)_4]$+1-octanol	1	296	[14]	1.28E-05	3.91E-05
$[C_4m_{(3)}py][NTf_2]$+1-octanol	1	296	[14]	2.77E-05	5.22E-04
$[C_6C_1mim][NTf_2]$+water	1	298	[14]	3.81E-05	2.87E-03
$[C_6m_{(3)}py][NTf_2]$+water	1	298	[14]	3.36E-03	4.73E-03
$[C_6m_{(3)}py][NTf_2]$+1-octanol	1	296	[14]	5.57E-04	1.69E-05
$[C_6py][NTf_2]$+1-octanol	1	296	[14]	9.76E-05	1.02E-03
$[C_8m_{(3)}py][NTf_2]$+water	1	296	[14]	2.54E-04	3.91E-03
$[C_8m_{(3)}py][NTf_2]$+1-octanol	1	296	[14]	5.69E-05	1.09E-03

$[C_2OHmim][NTf_2]$+water	1	296	[14]	0.01	0.04
$[C_2mim][OTf]$+chloroform	6	293-333	[443,444]	0.06	0.14
$[C_2mim][NTf_2]$+fluorobenzene	6	282-373	[445]	0.03	0.46
$[C_2mim][NTf_2]$+1,3-difluorobenzene	6	283-373	[445]	0.05	0.31
$[C_2mim][NTf_2]$+1,4-difluorobenzene	6	283-373	[445]	0.08	0.26
$[C_2mim][NTf_2]$+1,3,5-trifluorobenzene	6	283-373	[445]	0.20	0.21
$[C_2mim][NTf_2]$+1,2,3,5-tetrafluorobenzene	6	283-373	[445]	0.07	0.27
$[C_2mim][NTf_2]$+1,2,4,5-tetrafluorobenzene	6	283-373	[445]	0.06	0.28
$[C_2mim][NTf_2]$+pentafluorobenzene	6	283-373	[445]	0.17	0.31
$[C_2mim][NTf_2]$+1,2,4-trifluorobenzene	3	362-372	[445]	0.07	0.25
$[C_2mim][NTf_2]$+toluene	7	297-372	[418,433,446]	0.49	0.61
$[C_2mim][NTf_2]$+ethylbenzene	5	293-373	[446]	0.11	0.12
$[C_2mim][NTf_2]$+propylbenzene	5	293-373	[446]	0.07	0.11
$[C_2mim][NTf_2]$+o-xylene	6	297-372	[416,446]	0.68	0.81
$[C_2mim][NTf_2]$+m-xylene	6	297-372	[416,446]	0.47	0.59
$[C_2mim][NTf_2]$+p-xylene	6	297-372	[416,446]	0.45	0.52
$[C_2mim][NTf_2]$+1,2,3-trimethylbenzene	5	292-373	[446]	0.17	0.17
$[C_2mim][NTf_2]$+1,2,4-trimethylbenzene	5	293-373	[446]	0.14	0.12
$[C_2mim][NTf_2]$+1,3,5-trimethylbenzene	5	292-373	[446]	0.13	0.16
$[C_6mim][NTf_2]$+1-octene	4	283-348	[447]	0.85	1.08
$[C_4m_{(4)}py][BF_4]$+toluene	5	298-348	[71,448]	1.72	1.72
$[C_4m_{(2)}py][BF_4]$+toluene	3	298-338	[448]	0.09	0.12
$[C_4py][BF_4]$+toluene	3	298-338	[448]	0.07	0.10
$[C_6py][BF_4]$+toluene	3	298-338	[448]	0.01	0.05

$[C_8mim][PF_6]$+water	3	295-323	[232,234]	1.35	1.39
$[C_2mmim][NTf_2]$+water	1	298	[10]	0.04	0.04
$[C_2mim][NTf_2]$+water	1	298	[10]	5.25	3.86
$[C_3mmim][NTf_2]$+water	1	298	[10]	0.01	0.02
$[C_4m_{(4)}py][NTf_2]$+water	7	288-318	[442]	0.35	1.29
$[C_4py][NTf_2]$+water	7	288-318	[442]	0.10	1.42
$[C_8py][NTf_2]$+water	7	288-318	[442]	0.12	1.14
$[C_6m_{(3)}m_{(5)}py][NTf_2]$+hexane	2	298	[449]	0.29	0.21
$[C_6m_{(3)}m_{(5)}py][NTf_2]$+thiophene	1	298	[449]	3.76E-03	0.04
$[C_6m_{(3)}m_{(5)}py][NTf_2]$+dodecane	1	298	[449]	0.05	0.04
$[C_6m_{(3)}m_{(5)}py][NTf_2]$+hexadecane	1	298	[449]	0.05	0.04
$[C_2mim][Meesu]$+limonene	3	298-318	[450]	0.07	0.08
$[C_4m_{(3)}py][C(CN)_3]$+benzene	2	303-328	[44]	0.05	0.05
$[C_4m_{(3)}py][C(CN)_3]$+hexane	2	303-328	[44]	0.08	0.08
$[C_4m_{(3)}py][C(CN)_3]$+heptane	2	303-328	[44]	0.11	0.11
$[C_4m_{(3)}py][C(CN)_3]$+toluene	2	303-328	[44]	0.03	0.03
$[C_4m_{(3)}py][C(CN)_3]$+n-octane	2	303-328	[44]	3.42E-05	1.33E-04
$[C_4m_{(3)}py][C(CN)_3]$+p-xylene	2	303-328	[44]	0.06	0.06
$[C_6m_{(2)}m_{(4)}py][NTf_2]$+thiophene	1	298	[451]	0.01	1.07E-03
$[C_6m_{(2)}m_{(4)}py][NTf_2]$+hexane	1	298	[451]	0.005	0.02
$[C_6m_{(2)}m_{(4)}py][NTf_2]$+toluene	1	298	[451]	3.92E-03	0.04
$[COC_2mmor][NTf_2]$+thiophene	1	298	[452]	0.04	0.04
$[COC_2mmor][NTf_2]$+heptane	1	298	[452]	0.05	0.05
$[COC_2mpip][NTf_2]$+thiophene	1	298	[452]	0.04	0.04

[COC_2mpip][NTf_2]+heptane	1	298	[452]	0.05	0.04
[COC_2mpyrro][NTf_2]+thiophene	1	298	[452]	0.04	0.04
[COC_2mpyrro][NTf_2]+heptane	1	298	[452]	0.05	0.04
[$C_6m_{(3)}m_{(5)}$py][NTf_2]+toluene	1	298	[453]	3.54E-03	0.04
[$C_6m_{(3)}m_{(5)}$py][NTf_2]+heptane	1	298	[453]	0.05	0.04
[COC_2mmor][FAP]+thiophene	1	298	[454]	0.04	0.04
[COC_2mmor][FAP]+heptane	2	298	[454,455]	0.64	0.64
[COC_2mpip][FAP]+thiophene	1	298	[454]	0.04	0.04
[COC_2mpip][FAP]+heptane	1	298	[454]	0.05	0.04
[COC_2mpyrro][FAP]+thiophene	1	298	[454]	0.04	0.04
[COC_2mpyrro][FAP]+heptane	1	298	[454]	0.05	0.03
[$C_3m_{(1)}$py][NTf_2]+heptane	1	298	[456]	5.00E-03	4.99E-03
[$C_3m_{(1)}$py][NTf_2]+hexane	1	298	[456]	5.00E-03	4.99E-03
[$C_2m_{(3)}$py][NTf_2]+heptane	1	298	[456]	5.00E-03	5.00E-03
[$C_2m_{(3)}$py][NTf_2]+hexane	1	298	[456]	5.00E-03	5.00E-03
[C_4mpyrro][$C(CN)_3$]+heptane	1	298	[434]	3.64E-03	4.52E-03
[C_4mpyrro][$C(CN)_3$]+thiophene	1	298	[434]	0.04	4.74E-03
[C_4mim][Tf_3C]+water	1	296	[14]	3.53E-03	2.55E-03
[$C_6m_{(3)}m_{(5)}$py][NTf_2]+water	1	296	[14]	3.32E-06	4.85E-03
[$C_6m_{(3)}m_{(5)}$py][NTf_2]+1-octanol	1	296	[14]	2.53E-04	1.46E-04
[C_6C_2mmpy][NTf_2]+water	1	296	[14]	1.88E-03	4.08E-03
[C_6C_2mmpy][NTf_2]+1-octanol	1	296	[14]	1.78E-04	3.28E-04
[choline][NTf_2]+1-octanol	1	296	[14]	3.54E-05	1.36E-05
[C_6DMApy][NTf_2]+water	1	296	[14]	2.62E-03	2.09E-03

$[C_6DMApy][NTf_2]$+1-octanol	1	296	[14]	1.79E-04	1.25E-03
$[C_6DMAmpy][NTf_2]$+water	1	296	[14]	1.59E-03	1.27E-03
$[C_6DMAmpy][NTf_2]$+1-octanol	1	296	[14]	7.77E-05	4.35E-05
$[C_4mim][I_3]$+toluene	1	308	[457]	8.18E-09	3.54E-03
$[C_2mim][I_3]$+toluene	1	318	[457]	1.06E-03	5.27E-03
$[C_3m_{(3)}py][NTf_2]$+water	7	288-318	[442]	0.19	1.34

Chapter 9
References

(1) Plechkova, N. V; Seddon, K. R. Applications of Ionic Liquids in the Chemical Industry. *Chem. Soc. Rev.* **2008**, *37*, 123–150.

(2) Sirdeshmukh, D. B.; Sirdeshmukh, L.; Subhadra, K. G. *Alkali Halides : A Handbook of Physical Properties ; with 202 Tables*; Springer, 2001.

(3) Johnson, K. E. What's an Ionic Liquid ? *Electrochem. Soc. Interface* **2007**, 38–41.

(4) Mantz, R. A.; Trulove, P. C. Physicochemical Properties. In *Ionic Liquids in Synthesis*; Wasserscheid, P.; Welton, T., Eds.; Wiley-VCH Verlag GmbH & Co. KGaA, 2008; pp. 57–174.

(5) *Structures and Interactions of Ionic Liquids*; Zhang, S.; Wang, J.; Lu, X.; Zhou, Q., Eds.; Structure and Bonding; Springer: Berlin, Heidelberg, 2014; Vol. 151.

(6) Rooney, D.; Jacquemin, J.; Gardas, R. Thermophysical Properties of Ionic Liquid. In *Topics in Current Chemistry*; Kirchner, B., Ed.; Springer-Verlag Berlin Heidelberg, 2009; pp. 185–212.

(7) Seoane, R. G.; Corderí, S.; Gómez, E.; Calvar, N.; González, E. J.; Macedo, E. A.; Domínguez, Á. Temperature Dependence and Structural Influence on the Thermophysical Properties of Eleven Commercial Ionic Liquids. *Ind. Eng. Chem. Res.* **2012**, *51*, 2492–2504.

(8) Crosthwaite, J. M.; Muldoon, M. J.; Dixon, J. K.; Anderson, J. L.; Brennecke, J.

F. Phase Transition and Decomposition Temperatures, Heat Capacities and Viscosities of Pyridinium Ionic Liquids. *J. Chem. Thermodyn.* **2005**, *37*, 559–568.

(9) Jacquemin, J.; Ge, R.; Nancarrow, P.; Rooney, D. W.; Costa Gomes, M. F.; Pádua, A. A. H.; Hardacre, C. Prediction of Ionic Liquid Properties. I. Volumetric Properties as a Function of Temperature at 0.1 MPa. *J. Chem. Eng. Data* **2008**, *53*, 716–726.

(10) Crosthwaite, J. M.; Aki, S. N. V. K.; Maginn, E. J.; Brennecke, J. F. Liquid Phase Behavior of Imidazolium-Based Ionic Liquids with Alcohols. *J. Phys. Chem. B* **2004**, *108*, 5113–5119.

(11) Heintz, A.; Lehmann, J. K.; Wertz, C. Thermodynamic Properties of Mixtures Containing Ionic Liquids. 3. Liquid−Liquid Equilibria of Binary Mixtures of 1-Ethyl-3-Methylimidazolium Bis(trifluoromethylsulfonyl)amide with Propan-1-ol, Butan-1-ol, and Pentan-1-ol. *J. Chem. Eng. Data* **2003**, *48*, 472–474.

(12) Heintz, A.; Kulikov, D. V.; Verevkin, S. P. Thermodynamic Properties of Mixtures Containing Ionic Liquids. 2. Activity Coefficients at Infinite Dilution of Hydrocarbons and Polar Solutes in 1-Methyl-3-Ethyl-Imidazolium Bis(trifluoromethyl-Sulfonyl) Amide and in 1,2-Dimethyl-3-Ethyl-Imidazolium Bis(trifluoromethyl-Sulfonyl) Amide. *J. Chem. Eng. Data* **2002**, *47*, 894–899.

(13) Heintz, A.; Kulikov, D. V; Verevkin, S. P. Thermodynamic Properties of Mixtures Containing Ionic Liquids. Activity Coefficients at Infinite Dilution of Polar Solutes in 4-Methyl-N-Butyl-Pyridinium Tetrafluoroborate Using Gas--Liquid Chromatography. *J. Chem. Thermodyn.* **2002**, *34*, 1341–1347.

(14) Chapeaux, A.; Simoni, L. D.; Stadtherr, M. A.; Brennecke, J. F. Liquid Phase Behavior of Ionic Liquids with Water and 1-Octanol and Modeling of 1-Octanol/Water Partition Coefficients. *J. Chem. Eng. Data* **2007**, *52*, 2462–2467.

(15) Crosthwaite, J. M.; Muldoon, M. J.; Aki, S. N. V. K.; Maginn, E. J.; Brennecke, J. F. Liquid Phase Behavior of Ionic Liquids with Alcohols: Experimental Studies and Modeling. *J. Phys. Chem. B* **2006**, *110*, 9354–9361.

(16) Freire, M. G.; Neves, C. M. S. S.; Carvalho, P. J.; Gardas, R. L.; Fernandes, A. M.; Marrucho, I. M.; Santos, L. M. N. B. F.; Coutinho, J. A. P. Mutual Solubilities of Water and Hydrophobic Ionic Liquids. *J. Phys. Chem. B* **2007**, *111*, 13082–13089.

(17) Seddon, K. R.; Stark, A.; Torres, M.-J. Influence of Chloride, Water, and Organic Solvents on the Physical Properties of Ionic Liquids. *Pure Appl. Chem.* **2000**, *72*, 2275–2287.

(18) Chauvin, Y.; Bourbigou, H. O. Nonaqueous Ionic Liquids as Reaction Solvents. *Chemtech* **1995**, *25*, 26–30.

(19) Baker, S. N.; Baker, G. A.; Bright, F. V. Temperature-Dependent Microscopic Solvent Properties of ‘dry’ and ‘wet’ 1-Butyl-3-Methylimidazolium Hexafluorophosphate: Correlation with ET(30) and Kamlet–Taft Polarity Scales. *Green Chem.* **2002**, *4*, 165–169.

(20) Widegren, J. A.; Laesecke, A.; Magee, J. W. The Effect of Dissolved Water on the Viscosities of Hydrophobic Room-Temperature Ionic Liquids. *Chem. Commun.* **2005**, 1610.

(21) Silvester, D. S.; Compton, R. G. Electrochemistry in Room Temperature Ionic Liquids: A Review and Some Possible Applications. *Zeitschrift für Phys. Chemie* **2006**, *220*, 1247–1274.

(22) Saha, S.; Hamaguchi, H. Effect of Water on the Molecular Structure and Arrangement of Nitrile-Functionalized Ionic Liquids. *J. Phys. Chem. B* **2006**, *110*, 2777–2781.

(23) Jacquemin, J.; Husson, P.; Padua, A. A. H.; Majer, V. Density and Viscosity of Several Pure and Water-Saturated Ionic Liquids. *Green Chem.* **2006**, *8*, 172–180.

(24) Breitbach, Z. S.; Armstrong, D. W. Characterization of Phosphonium Ionic Liquids through a Linear Solvation Energy Relationship and Their Use as GLC Stationary Phases. *Anal. Bioanal. Chem.* **2008**, *390*, 1605–1617.

(25) Zhao, Q.; Anderson, J. L. Highly Selective GC Stationary Phases Consisting of

Binary Mixtures of Polymeric Ionic Liquids. *J. Sep. Sci.* **2010**, *33*, 79–87.

(26) *Ionic Liquids*; Kirchner, B., Ed.; Topics in Current Chemistry; Springer: Berlin, Heidelberg, 2010; Vol. 290.

(27) Ye, C.; Shreeve, J. M. Rapid and Accurate Estimation of Densities of Room-Temperature Ionic Liquids and Salts. *J. Phys. Chem. A* **2007**, *111*, 1456–1461.

(28) Gardas, R. L.; Coutinho, J. A. P. Extension of the Ye and Shreeve Group Contribution Method for Density Estimation of Ionic Liquids in a Wide Range of Temperatures and Pressures. *Fluid Phase Equilib.* **2008**, *263*, 26–32.

(29) Esperança, J. M. S. S.; Guedes, H. J. R.; Blesic, M.; Rebelo, L. P. N. Densities and Derived Thermodynamic Properties of Ionic Liquids. 3. Phosphonium-Based Ionic Liquids over an Extended Pressure Range. *J. Chem. Eng. Data* **2006**, *51*, 237–242.

(30) Slattery, J. M.; Daguenet, C.; Dyson, P. J.; Schubert, T. J. S.; Krossing, I. How to Predict the Physical Properties of Ionic Liquids: A Volume-Based Approach. *Angew. Chem. Int. Ed.* **2007**, *46*, 5384–5388.

(31) Jacquemin, J.; Nancarrow, P.; Rooney, D. W.; Costa Gomes, M. F.; Husson, P.; Majer, V.; Pádua, A. A. H.; Hardacre, C. Prediction of Ionic Liquid Properties. II. Volumetric Properties as a Function of Temperature and Pressure. *J. Chem. Eng. Data* **2008**, *53*, 2133–2143.

(32) Paduszyński, K.; Domańska, U. A New Group Contribution Method For Prediction of Density of Pure Ionic Liquids over a Wide Range of Temperature and Pressure. *Ind. Eng. Chem. Res.* **2012**, *51*, 591–604.

(33) Qiao, Y.; Ma, Y.; Huo, Y.; Ma, P.; Xia, S. A Group Contribution Method to Estimate the Densities of Ionic Liquids. *J. Chem. Thermodyn.* **2010**, *42*, 852–855.

(34) Lazzús, J. A. A Group Contribution Method to Predict ρ-T-P of Ionic Liquids. *Chem. Eng. Commun.* **2010**, *197*, 974–1015.

(35) Bandrés, I.; Giner, B.; Artigas, H.; Royo, F. M.; Lafuente, C. Thermophysic Comparative Study of Two Isomeric Pyridinium-Based Ionic Liquids. *J. Phys. Chem. B* **2008**, *112*, 3077–3084.

(36) Ji, X.; Adidharma, H. Thermodynamic Modeling of Ionic Liquid Density with Heterosegmented Statistical Associating Fluid Theory. *Chem. Eng. Sci.* **2009**, *64*, 1985–1992.

(37) Alavianmehr, M. M.; Hosseini, S. M.; Moghadasi, J. Densities of Ionic Liquids from Ion Contribution-Based Equation of State: Electrolyte Perturbation Approach. *J. Mol. Liq.* **2014**, *197*, 287–294.

(38) Shen, C.; Li, C.; Li, X.; Lu, Y.; Muhammad, Y. Estimation of Densities of Ionic Liquids Using Patel–Teja Equation of State and Critical Properties Determined from Group Contribution Method. *Chem. Eng. Sci.* **2011**, *66*, 2690–2698.

(39) Lazzús, J. A. ρ–T–P Prediction for Ionic Liquids Using Neural Networks. *J. Taiwan Inst. Chem. Eng.* **2009**, *40*, 213–232.

(40) Lazzús, J. A. ρ (T , P) Model for Ionic Liquids Based on Quantitative Structure-Property Relationship Calculations. *J. Phys. Org. Chem.* **2009**, *22*, 1193–1197.

(41) Trohalaki, S.; Pachter, R.; Drake, G. W.; Hawkins, T. Quantitative Structure−Property Relationships for Melting Points and Densities of Ionic Liquids. *Energy Fuels* **2005**, *19*, 279–284.

(42) Palomar, J.; Ferro, V. R.; Torrecilla, J. S.; Rodríguez, F. Density and Molar Volume Predictions Using COSMO-RS for Ionic Liquids. An Approach to Solvent Design. *Ind. Eng. Chem. Res.* **2007**, *46*, 6041–6048.

(43) Gardas, R. L.; Coutinho, J. A. P. A Group Contribution Method for Viscosity Estimation of Ionic Liquids. *Fluid Phase Equilib.* **2008**, *266*, 195–201.

(44) Meindersma, W. G. W.; van Acker, T.; de Haan, A. B. Physical Properties of 3-Methyl-N-Butylpyridinium Tricyanomethanide and Ternary LLE Data with an Aromatic and an Aliphatic Hydrocarbon at T=(303.2 and 328.2)K and p=0.1MPa. *Fluid Phase Equilib.* **2011**, *307*, 30–38.

(45) Galán Sánchez, L. M.; Meindersma, G. W.; de Haan, A. B. Solvent Properties of Functionalized Ionic Liquids for CO_2 Absorption. *Chem. Eng. Res. Des.* **2007**, *85*, 31–39.

(46) Ghatee, M. H.; Bahrami, M.; Khanjari, N. Measurement and Study of Density, Surface Tension, and Viscosity of Quaternary Ammonium-Based Ionic Liquids ($[N_{222(n)}]Tf_2N$). *J. Chem. Thermodyn.* **2013**, *65*, 42–52.

(47) Gaciño, F. M.; Paredes, X.; Comuñas, M. J. P.; Fernández, J. Pressure Dependence on the Viscosities of 1-Butyl-2,3-Dimethylimidazolium Bis(trifluoromethylsulfonyl)amide and Two Tris(pentafluoroethyl)trifluorophosphate Based Ionic Liquids: New Measurements and Modelling. *J. Chem. Thermodyn.* **2013**, *62*, 162–169.

(48) Haghbakhsh, R.; Raeissi, S. Two Simple Correlations to Predict Viscosities of Pure and Aqueous Solutions of Ionic Liquids. *J. Mol. Liq.* **2015**, *211*, 948–956.

(49) Ghatee, M. H.; Zare, M. Power-Law Behavior in the Viscosity of Ionic Liquids: Existing a Similarity in the Power Law and a New Proposed Viscosity Equation. *Fluid Phase Equilib.* **2011**, *311*, 76–82.

(50) Lazzús, J. A.; Pulgar-Villarroel, G. A Group Contribution Method to Estimate the Viscosity of Ionic Liquids at Different Temperatures. *J. Mol. Liq.* **2015**, *209*, 161–168.

(51) Daniel, C. I.; Albo, J.; Santos, E.; Portugal, C. A. M.; Crespo, J. G.; Irabien, A. A Group Contribution Method for the Influence of the Temperature in the Viscosity of Magnetic Ionic Liquids. *Fluid Phase Equilib.* **2013**, *360*, 29–35.

(52) Gharagheizi, F.; Ilani-Kashkouli, P.; Mohammadi, A. H.; Ramjugernath, D.;

Richon, D. Development of a Group Contribution Method for Determination of Viscosity of Ionic Liquids at Atmospheric Pressure. *Chem. Eng. Sci.* **2012**, *80*, 326–333.

(53) Gardas, R. L.; Coutinho, J. A. P. Group Contribution Methods for the Prediction of Thermophysical and Transport Properties of Ionic Liquids. *AIChE J.* **2009**, *55*, 1274–1290.

(54) Bini, R.; Malvaldi, M.; Pitner, W. R.; Chiappe, C. QSPR Correlation for Conductivities and Viscosities of Low-Temperature Melting Ionic Liquids. *J. Phys. Org. Chem.* **2008**, *21*, 622–629.

(55) Yu, G.; Wen, L.; Zhao, D.; Asumana, C.; Chen, X. QSPR Study on the Viscosity of Bis(trifluoromethylsulfonyl)amide-Based Ionic Liquids. *J. Mol. Liq.* **2013**, *184*, 51–59.

(56) Chen, B.-K.; Liang, M.-J.; Wu, T.-Y.; Wang, H. P. A High Correlate and Simplified QSPR for Viscosity of Imidazolium-Based Ionic Liquids. *Fluid Phase Equilib.* **2013**, *350*, 37–42.

(57) Han, C.; Yu, G.; Wen, L.; Zhao, D.; Asumana, C.; Chen, X. Data and QSPR Study for Viscosity of Imidazolium-Based Ionic Liquids. *Fluid Phase Equilib.* **2011**, *300*, 95–104.

(58) Matsuda, H.; Yamamoto, H.; Kurihara, K.; Tochigi, K. Computer-Aided Reverse Design for Ionic Liquids by QSPR Using Descriptors of Group

Contribution Type for Ionic Conductivities and Viscosities. *Fluid Phase Equilib.* **2007**, *261*, 434–443.

(59) Matsuda, H.; Yamamoto, H.; Kurihara, K.; Tochigi, K. Prediction of The Ionic Conductivity and Viscosity of Ionic Liquids by QSPR Using Descriptors of Group Contribution Type. *J. Comput. Aided Chem.* **2007**, *8*, 114–127.

(60) Tochigi, K.; Yamamoto, H. Estimation of Ionic Conductivity and Viscosity of Ionic Liquids Using a QSPR Model. *J. Phys. Chem. C* **2007**, *111*, 15989–15994.

(61) Mirkhani, S. A.; Gharagheizi, F. Predictive Quantitative Structure–Property Relationship Model for the Estimation of Ionic Liquid Viscosity. *Ind. Eng. Chem. Res.* **2012**, *51*, 2470–2477.

(62) Polishuk, I. Modeling of Viscosities in Extended Pressure Range Using SAFT + Cubic EoS and Modified Yarranton-Satyro Correlation. *Ind. Eng. Chem. Res.* **2012**, *51*, 13527–13537.

(63) Abolala, M.; Peyvandi, K.; Varaminian, F. Modeling the Viscosity of Pure Imidazolium-Based Ionic Liquids Using SAFT-VR-Mie EoS. *Fluid Phase Equilib.* **2015**, *394*, 61–70.

(64) Ikeda, M.; Aniya, M. Bond Strength-Coordination Number Fluctuation Model of Viscosity: An Alternative Model for the Vogel-Fulcher-Tammann Equation and an Application to Bulk Metallic Glass Forming Liquids. *Materials (Basel).* **2010**, *3*, 5246–5262.

(65) Reid, R. *The Properties of Gases and Liquids*; McGraw-Hill: New York, 1987.

(66) Maia, F. M.; Rodríguez, O. LLE for (Water+ionic Liquid) Binary Systems Using [$C_x$mim][BF_4] (*x*=6, 8) Ionic Liquids. *Fluid Phase Equilib.* **2010**, *296*, 184–191.

(67) Arce, A.; Rodríguez, O.; Soto, A. *Tert* -Amyl Ethyl Ether Separation from Its Mixtures with Ethanol Using the 1-Butyl-3-Methylimidazolium Trifluoromethanesulfonate Ionic Liquid: Liquid−Liquid Equilibrium. *Ind. Eng. Chem. Res.* **2004**, *43*, 8323–8327.

(68) Aznar, M. Correlation of (Liquid + Liquid) Equilibrium of Systems Including Ionic Liquids. *Braz. J. Chem. Eng.* **2007**, *24*, 143–149.

(69) Renon, H.; Prausnitz, J. M. Local Compositions in Thermodynamic Excess Functions for Liquid Mixtures. *AIChE J.* **1968**, *14*, 135–144.

(70) Hu, X.; Yu, J.; Liu, H. Liquid−Liquid Equilibria of the System 1-(2-Hydroxyethyl)-3-Methylimidozolium Tetrafluoroborate or 1-(2-Hydroxyethyl)-2,3-Dimethylimidozolium Tetrafluoroborate + Water + 1-Butanol at 293.15 K. *J. Chem. Eng. Data* **2006**, *51*, 691–695.

(71) Meindersma, G. W.; Podt, A. J. G.; de Haan, A. B. Ternary Liquid–liquid Equilibria for Mixtures of Toluene+n-Heptane+an Ionic Liquid. *Fluid Phase Equilib.* **2006**, *247*, 158–168.

(72) Arce, A.; Rodríguez, O.; Soto, A. A Comparative Study on Solvents for

Separation of Tert-Amyl Ethyl Ether and Ethanol Mixtures. New Experimental Data for 1-Ethyl-3-Methyl Imidazolium Ethyl Sulfate Ionic Liquid. *Chem. Eng. Sci.* **2006**, *61*, 6929–6935.

(73) Domańska, U.; Marciniak, A. Liquid Phase Behaviour of 1-Butyl-3-Methylimidazolium 2-(2-Methoxyethoxy)-Ethylsulfate with Organic Solvents and Water. *Green Chem.* **2007**, *9*, 262–266.

(74) Banerjee, T.; Singh, M. K.; Sahoo, R. K.; Khanna, A. Volume, Surface and UNIQUAC Interaction Parameters for Imidazolium Based Ionic Liquids via Polarizable Continuum Model. *Fluid Phase Equilib.* **2005**, *234*, 64–76.

(75) Simoni, L. D.; Lin, Y.; Brennecke, J. F.; Stadtherr, M. A. Modeling Liquid−Liquid Equilibrium of Ionic Liquid Systems with NRTL, Electrolyte-NRTL, and UNIQUAC. *Ind. Eng. Chem. Res.* **2008**, *47*, 256–272.

(76) Haghtalab, A.; Paraj, A. Computation of Liquid–liquid Equilibrium of Organic-Ionic Liquid Systems Using NRTL, UNIQUAC and NRTL-NRF Models. *J. Mol. Liq.* **2012**, *171*, 43–49.

(77) Santiago, R. S.; Santos, G. R.; Aznar, M. UNIQUAC Correlation of Liquid–liquid Equilibrium in Systems Involving Ionic Liquids: The DFT–PCM Approach. *Fluid Phase Equilib.* **2009**, *278*, 54–61.

(78) Santiago, R. S.; Santos, G. R.; Aznar, M. UNIQUAC Correlation of Liquid–liquid Equilibrium in Systems Involving Ionic Liquids: The DFT–PCM

Approach. Part II. *Fluid Phase Equilib.* **2010**, *293*, 66–72.

(79) Santiago, R. S.; Aznar, M. Liquid-Liquid Equilibrium in Ternary Ionic Liquid Systems by UNIFAC: New Volume, Surface Area and Interaction Parameters. Part I. *Fluid Phase Equilib.* **2010**, *295*, 93–97.

(80) Santiago, R. S.; Aznar, M. Liquid-Liquid Equilibrium in Ternary Ionic Liquid Systems by UNIFAC: New Volume, Surface Area and Interaction Parameters. Part II. *Fluid Phase Equilib.* **2011**, *303*, 111–114.

(81) Tsioptsias, C.; Tsivintzelis, I.; Panayiotou, C. Equation-of-State Modeling of Mixtures with Ionic Liquids. *Phys. Chem. Chem. Phys.* **2010**, *12*, 4843–4851.

(82) Paduszyński, K.; Chiyen, J.; Ramjugernath, D.; Letcher, T. M.; Domańska, U. Liquid–liquid Phase Equilibrium of (Piperidinium-Based Ionic Liquid+an Alcohol) Binary Systems and Modelling with NRHB and PCP-SAFT. *Fluid Phase Equilib.* **2011**, *305*, 43–52.

(83) Paduszyński, K.; Domańska, U. Solubility of Aliphatic Hydrocarbons in Piperidinium Ionic Liquids: Measurements and Modeling in Terms of Perturbed-Chain Statistical Associating Fluid Theory and Nonrandom Hydrogen-Bonding Theory. *J. Phys. Chem. B* **2011**, *115*, 12537–12548.

(84) Álvarez, V. H.; Serrão, D.; da Silva, J. L.; Barbosa, M. R.; Aznar, M. Vapor–liquid and Liquid–liquid Equilibrium for Binary Systems Ester + a New Protic Ionic Liquid. *Ionics (Kiel).* **2013**, *19*, 1263–1269.

(85) Maia, F. M.; Tsivintzelis, I.; Rodriguez, O.; Macedo, E. A.; Kontogeorgis, G. M. Equation of State Modelling of Systems with Ionic Liquids: Literature Review and Application with the Cubic Plus Association (CPA) Model. *Fluid Phase Equilib.* **2012**, *332*, 128–143.

(86) Ferreira, A. R.; Freire, M. G.; Ribeiro, J. C.; Lopes, F. M.; Crespo, J. G.; Coutinho, J. A. P. Overview of the Liquid–Liquid Equilibria of Ternary Systems Composed of Ionic Liquid and Aromatic and Aliphatic Hydrocarbons, and Their Modeling by COSMO-RS. *Ind. Eng. Chem. Res.* **2012**, *51*, 3483–3507.

(87) Mullins, E.; Oldland, R.; Liu, Y. A.; Wang, S.; Sandler, S. I.; Chen, C.-C.; Zwolak, M.; Seavey, K. C. Sigma-Profile Database for Using COSMO-Based Thermodynamic Methods. *Ind. Eng. Chem. Res.* **2006**, *45*, 4389–4415.

(88) Shah, M. R.; Yadav, G. D. Prediction of Liquid−liquid Equilibria of (Aromatic+aliphatic+ionic Liquid) Systems Using the Cosmo-SAC Model. *J. Chem. Thermodyn.* **2012**, *49*, 62–69.

(89) Zhao, N.; Jacquemin, J.; Oozeerally, R.; Degirmenci, V. New Method for the Estimation of Viscosity of Pure and Mixtures of Ionic Liquids Based on the UNIFAC–VISCO Model. *J. Chem. Eng. Data* **2016**, *61*, 2160–2169.

(90) Dymond, J. H.; Malhotra, R. The Tait Equation: 100 Years on. *Int. J. Thermophys.* **1988**, *9*, 941–951.

(91) Rebelo, L. P. N.; Najdanovic-Visak, V.; Gomes de Azevedo, R.; Esperança, J. M.

S. S.; Nunes da Ponte, M.; Guedes, H. J. R.; Visak, Z. P.; de Sousa, H. C.; Szydlowski, J.; Canongia Lopes, J. N.; Cordeiro, T. C. *Phase Behavior and Thermodynamic Properties of Ionic Liquids, Ionic Liquid Mixtures and Ionic Liquid Solutions. In Ionic Liquids IIIA: Fundamentals, Progress, Challenges, and Opportunities, Properties and Structure-ACS Symposium Series;* Rogers, R. D.; Seddon, K. R., Eds.; American Chemical Society: Washington, D.C., 2005; Vol. 901.

(92) Rebelo, L. P. N.; Lopes, J. N. C.; Esperança, J. M. S. S.; Guedes, H. J. R.; Łachwa, J.; Najdanovic-Visak, V.; Visak, Z. P. Accounting for the Unique, Doubly Dual Nature of Ionic Liquids from a Molecular Thermodynamic and Modeling Standpoint. *Acc. Chem. Res.* **2007**, *40*, 1114–1121.

(93) Tomé, L. I. N.; Carvalho, P. J.; Freire, M. G.; Marrucho, I. M.; Fonseca, I. M. A.; Ferreira, A. G. M.; Coutinho, J. A. P.; Gardas, R. L. Measurements and Correlation of High-Pressure Densities of Imidazolium-Based Ionic Liquids. *J. Chem. Eng. Data* **2008**, *53*, 1914–1921.

(94) Gardas, R. L.; Costa, H. F.; Freire, M. G.; Carvalho, P. J.; Marrucho, I. M.; Fonseca, I. M. A.; Ferreira, A. G. M.; Coutinho, J. A. P. Densities and Derived Thermodynamic Properties of Imidazolium-, Pyridinium-, Pyrrolidinium-, and Piperidinium-Based Ionic Liquids. *J. Chem. Eng. Data* **2008**, *53*, 805–811.

(95) Bondi, A. Van Der Waals Volumes and Radii. *J. Phys. Chem.* **1964**, *68*, 441–

451.

(96) Magnussen, T.; Rasmussen, P.; Fredenslund, A. UNIFAC Parameter Table for Prediction of Liquid-Liquid Equilibriums. *Ind. Eng. Chem. Process Des. Dev.* **1981**, *20*, 331–339.

(97) Chakrabarty, A.; Mannan, S.; Cagin, T.; Chakrabarty, A.; Mannan, S.; Cagin, T. Chapter 3 – Molecular-Level Modeling and Simulation in Process Safety. In *Multiscale Modeling for Process Safety Applications*; 2016; pp. 111–210.

(98) Wang, Y.; Hao, W.; Jacquemin, J.; Goodrich, P.; Atilhan, M.; Khraisheh, M.; Rooney, D.; Thompson, J. Enhancing Liquid-Phase Olefin-Paraffin Separations Using Novel Silver-Based Ionic Liquids. *J. Chem. Eng. Data* **2015**, *60*, 28–36.

(99) Zhou, J. Development of Property Prediction Methods for Ionic Liquids, Queen's University Belfast.

(100) Anderson, T. F.; Prausnitz, J. M. Application of the UNIQUAC Equation to Calculation of Multicomponent Phase Equilibria. 2. Liquid-Liquid Equilibria. *Ind. Eng. Chem. Process Des. Dev.* **1978**, *17*, 561–567.

(101) Anderson, T. F.; Prausnitz, J. M. Application of the UNIQUAC Equation to Calculation of Multicomponent Phase Equilibria. 1. Vapor-Liquid Equilibria. *Ind. Eng. Chem. Process Des. Dev.* **1978**, *17*, 552–561.

(102) Fredenslund, A.; Jones, R. L.; Prausnitz, J. M. Group-Contribution Estimation of

Activity Coefficients in Nonideal Liquid Mixtures. *AIChE J.* **1975**, *21*, 1086–1099.

(103) Vogel, H. The Law of the Relation between the Viscosity of Liquids and the Temperature. *Phys. Zeitschrift* **1921**, *22*, 645–646.

(104) Tammann, G.; Hesse, W. Die Abhängigkeit Der Viscosität von Der Temperatur Bie Unterkühlten Flüssigkeiten. *Zeitschrift für Anorg. und Allg. Chemie* **1926**, *156*, 245–257.

(105) Fulcher, G. S. Analysis of Recent Measurements of the Viscosity of Glasses. *J. Am. Ceram. Soc.* **1925**, *8*, 339–355.

(106) Chevalier, J. L.; Petrino, P.; Gaston-Bonhomme, Y. Estimation Method for the Kinematic Viscosity of a Liquid-Phase Mixture. *Chem. Eng. Sci.* **1988**, *43*, 1303–1309.

(107) Gaston-Bonhomme, Y.; Petrino, P.; Chevalier, J. L. UNIFAC—VISCO Group Contribution Method for Predicting Kinematic Viscosity: Extension and Temperature Dependence. *Chem. Eng. Sci.* **1994**, *49*, 1799–1806.

(108) Poling, B. E.; Thomson, G. H.; Friend, D. G.; Rowley, R. L.; Wilding, W. V. *Perrys Chemical Engineers Handbook, 02 Physical and Chemical Data;* 8th ed.; McGraw-Hill: New York, 2008.

(109) Marquardt, D. W. An Algorithm for Least-Squares Estimation of Nonlinear

Parameters. *J. Soc. Indust. Appl. Math.* **1963**, *11*, 431–441.

(110) Dong, Q.; Muzny, C. D.; Kazakov, A.; Diky, V.; Magee, J. W.; Widegren, J. A.; Chirico, R. D.; Marsh, K. N.; Frenkel, M. ILThermo: A Free-Access Web Database for Thermodynamic Properties of Ionic Liquids. *J. Chem. Eng. Data* **2007**, *52*, 1151–1159.

(111) Kovanic, P.; Humber, M. B. The Economics of Information-Mathematical Gnostics for Data Analysis (available only online); http://www.math-gnostics.eu (accessed Jan 5, 2016).

(112) Sanmamed, Y. A.; González-Salgado, D.; Troncoso, J.; Romani, L.; Baylaucq, A.; Boned, C. Experimental Methodology for Precise Determination of Density of RTILs as a Function of Temperature and Pressure Using Vibrating Tube Densimeters. *J. Chem. Thermodyn.* **2010**, *42*, 553–563.

(113) Gu, Z.; Brennecke, J. F. Volume Expansivities and Isothermal Compressibilities of Imidazolium and Pyridinium-Based Ionic Liquids. *J. Chem. Eng. Data* **2002**, *47*, 339–345.

(114) Gardas, R. L.; Freire, M. G.; Carvalho, P. J.; Marrucho, I. M.; Fonseca, I. M. A.; Ferreira, A. G. M.; Coutinho, J. A. P. High-Pressure Densities and Derived Thermodynamic Properties of Imidazolium-Based Ionic Liquids. *J. Chem. Eng. Data* **2007**, *52*, 80–88.

(115) Tomida, D.; Kenmochi, S.; Tsukada, T.; Qiao, K.; Bao, Q.; Yokoyama, C.

Viscosity and Thermal Conductivity of 1-Hexyl-3-Methylimidazolium Tetrafluoroborate and 1-Octyl-3-Methylimidazolium Tetrafluoroborate at Pressures up to 20 MPa. *Int. J. Thermophys.* **2012**, *33*, 959–969.

(116) Harris, K. R.; Kanakubo, M.; Woolf, L. A. Temperature and Pressure Dependence of the Viscosity of the Ionic Liquids 1-Hexyl-3-Methylimidazolium Hexafluorophosphate and 1-Butyl-3-Methylimidazolium Bis(trifluoromethylsulfonyl)amide. *J. Chem. Eng. Data* **2007**, *52*, 1080–1085.

(117) Gołdon, A.; Dąbrowska, K.; Hofman, T. Densities and Excess Volumes of the 1,3-Dimethylimidazolium Methylsulfate + Methanol System at Temperatures from (313.15 to 333.15) K and Pressures from (0.1 to 25) MPa. *J. Chem. Eng. Data* **2007**, *52*, 1830–1837.

(118) Aparicio, S.; Alcalde, R.; García, B.; Leal, J. M. High-Pressure Study of the Methylsulfate and Tosylate Imidazolium Ionic Liquids. *J. Phys. Chem. B* **2009**, *113*, 5593–5606.

(119) Królikowska, M.; Hofman, T. Densities, Isobaric Expansivities and Isothermal Compressibilities of the Thiocyanate-Based Ionic Liquids at Temperatures (298.15-338.15 K) and Pressures up to 10 MPa. *Thermochim. Acta* **2012**, *530*, 1–6.

(120) Stevanovic, S.; Podgoršek, A.; Pádua, A. A. H.; Costa Gomes, M. F. Effect of

Water on the Carbon Dioxide Absorption by 1-Alkyl-3-Methylimidazolium Acetate Ionic Liquids. *J. Phys. Chem. B* **2012**, *116*, 14416–14425.

(121) Machida, H.; Taguchi, R.; Sato, Y.; Smith, R. L. Measurement and Correlation of High Pressure Densities of Ionic Liquids, 1-Ethyl-3-Methylimidazolium L-Lactate ([emim][Lactate]), 2-Hydroxyethyl-Trimethylammonium $_{L}$-Lactate ($[(C_2H_4OH)(CH_3)_3N]$[Lactate]), and 1-Butyl-3-Methylimidazolium Chloride ([bmim][Cl]. *J. Chem. Eng. Data* **2011**, *56*, 923–928.

(122) Klomfar, J.; Součková, M.; Pátek, J. *P* –ρ– *T* Measurements for 1-Ethyl and 1-Butyl-3-Methylimidazolium Dicyanamides from Their Melting Temperature to 353 K and up to 60 MPa in Pressure. *J. Chem. Eng. Data* **2012**, *57*, 1213–1221.

(123) Safarov, J.; Geppert-Rybczyńska, M.; Kul, I.; Hassel, E. Thermophysical Properties of 1-Butyl-3-Methylimidazolium Acetate over a Wide Range of Temperatures and Pressures. *Fluid Phase Equilib.* **2014**, *383*, 144–155.

(124) Engelmann, M.; Schmidt, H.; Safarov, J.; Nocke, J.; Hassel, E. Thermal Properties of 1-Butyl-3-Methylimidazolium Dicyanamide at High Pressures and Temperatures. *Acta Chim. Slovaca* **2012**, *5*, 86–94.

(125) Guerrero, H.; Martín, S.; Pérez-Gregorio, V.; Lafuente, C.; Bandrés, I. Volumetric Characterization of Pyridinium-Based Ionic Liquids. *Fluid Phase Equilib.* **2012**, *317*, 102–109.

(126) Gomes de Azevedo, R.; Esperança, J. M. S. S.; Najdanovic-Visak, V.; Visak, Z. P.; Guedes, H. J. R.; Nunes da Ponte, M.; Rebelo, L. P. N. Thermophysical and Thermodynamic Properties of 1-Butyl-3-Methylimidazolium Tetrafluoroborate and 1-Butyl-3-Methylimidazolium Hexafluorophosphate over an Extended Pressure Range. *J. Chem. Eng. Data* **2005**, *50*, 997–1008.

(127) Gardas, R. L.; Freire, M. G.; Carvalho, P. J.; Marrucho, I. M.; Fonseca, I. M. A.; Ferreira, A. G. M.; Coutinho, J. A. P. PρT Measurements of Imidazolium-Based Ionic Liquids. *J. Chem. Eng. Data* **2007**, *52*, 1881–1888.

(128) Matkowska, D.; Gołdon, A.; Hofman, T. Densities, Excess Volumes, Isobaric Expansivities, and Isothermal Compressibilities of the 1-Ethyl-3-Methylimidazolium Ethylsulfate + Ethanol System at Temperatures (283.15 to 343.15) K and Pressures from (0.1 to 35) MPa. *J. Chem. Eng. Data* **2010**, *55*, 685–693.

(129) Guerrero, H.; García-Mardones, M.; Cea, P.; Lafuente, C.; Bandrés, I. Correlation of the Volumetric Behaviour of Pyridinium-Based Ionic Liquids with Two Different Equations. *Thermochim. Acta* **2012**, *531*, 21–27.

(130) Safarov, J.; Kul, I.; El-Awady, W. A.; Shahverdiyev, A.; Hassel, E. Thermodynamic Properties of 1-Butyl-3-Methylpyridinium Tetrafluoroborate. *J. Chem. Thermodyn.* **2011**, *43*, 1315–1322.

(131) Safarov, J.; Kul, I.; El-Awady, W. A.; Nocke, J.; Shahverdiyev, A.; Hassel, E.

Thermophysical Properties of 1-Butyl-4-Methylpyridinium Tetrafluoroborate. *J. Chem. Thermodyn.* **2012**, *51*, 82–87.

(132) Matkowska, D.; Hofman, T. High-Pressure Volumetric Properties of Ionic Liquids: 1-Butyl-3-Methylimidazolium Tetrafluoroborate, $[C_4mim][BF_4]$, 1-Butyl-3-Methylimidazolium Methylsulfate $[C_4mim][MeSO_4]$ and 1-Ethyl-3-Methylimidazolium Ethylsulfate, $[C_2mim][EtSO_4]$. *J. Mol. Liq.* **2012**, *165*, 161–167.

(133) Tomida, D.; Kenmochi, S.; Qiao, K.; Tsukada, T.; Yokoyama, C. Densities and Thermal Conductivities of N-Alkylpyridinium Tetrafluoroborates at High Pressure. *Fluid Phase Equilib.* **2013**, *340*, 31–36.

(134) Taguchi, R.; Machida, H.; Sato, Y.; Smith, R. L. High-Pressure Densities of 1-Alkyl-3-Methylimidazolium Hexafluorophosphates and 1-Alkyl-3-Methylimidazolium Tetrafluoroborates at Temperatures from (313 to 473) K and at Pressures up to 200 MPa. *J. Chem. Eng. Data* **2009**, *54*, 22–27.

(135) Tomida, D.; Kenmochi, S.; Tsukada, T.; Qiao, K.; Yokoyama, C. Thermal Conductivities of $[bmim][PF_6]$, $[hmim][PF_6]$, and $[omim][PF_6]$ from 294 to 335 K at Pressures up to 20 MPa. *Int. J. Thermophys.* **2007**, *28*, 1147–1160.

(136) Machida, H.; Sato, Y.; Smith, R. L. Pressure-Volume-Temperature (PVT) Measurements of Ionic Liquids ($[bmim^+][PF_6^-]$, $[bmim^+][BF_4^-]$, $[bmim^+][OcSO_4^-]$) and Analysis with the Sanchez-Lacombe Equation of State.

Fluid Phase Equilib. **2008**, *264*, 147–155.

(137) Jacquemin, J.; Husson, P.; Mayer, V.; Cibulka, I. High-Pressure Volumetric Properties of Imidazolium-Based Ionic Liquids: Effect of the Anion. *J. Chem. Eng. Data* **2007**, *52*, 2204–2211.

(138) Esperança, J. M. S. S.; Visak, Z. P.; Plechkova, N. V.; Seddon, K. R.; Guedes, H. J. R.; Rebelo, L. P. N. Density, Speed of Sound, and Derived Thermodynamic Properties of Ionic Liquids over an Extended Pressure Range. 4. $[C_3mim][NTf_2]$ and $[C_5mim][NTf_2]$. *J. Chem. Eng. Data* **2006**, *51*, 2009–2015.

(139) Widowati, E.; Lee, M.-J. P–V–T Properties of Binary Mixtures of the Ionic Liquid 1-Butyl-3-Methylimidazolium Bis(trifluoromethylsulfonyl)amide with Anisole or Acetophenone at Elevated Pressures. *J. Chem. Thermodyn.* **2013**, *63*, 95–101.

(140) Regueira, T.; Lugo, L.; Fernández, J. High Pressure Volumetric Properties of 1-Ethyl-3-Methylimidazolium Ethylsulfate and 1-(2-Methoxyethyl)-1-Methyl-Pyrrolidinium Bis(trifluoromethylsulfonyl)amide. *J. Chem. Thermodyn.* **2012**, *48*, 213–220.

(141) Antón, V.; García-Mardones, M.; Lafuente, C.; Guerrero, H. Volumetric Behavior of Two Pyridinium-Based Ionic Liquids. *Fluid Phase Equilib.* **2014**, *382*, 59–64.

(142) Iguchi, M.; Hiraga, Y.; Sato, Y.; Aida, T. M.; Watanabe, M.; Smith, R. L.

Measurement of High-Pressure Densities and Atmospheric Viscosities of Ionic Liquids: 1-Hexyl-3-Methylimidazolium Bis(trifluoromethylsulfonyl)amide and 1-Hexyl-3-Methylimidazolium Chloride. *J. Chem. Eng. Data* **2014**, *59*, 709–717.

(143) Gonçalves, F. A. M. M.; Costa, C. S. M. F.; Ferreira, C. E.; Bernardo, J. C. S.; Johnson, I.; Fonseca, I. M. A.; Ferreira, A. G. M. Pressure-Volume-Temperature Measurements of Phosphonium-Based Ionic Liquids and Analysis with Simple Equations of State. *J. Chem. Thermodyn.* **2011**, *43*, 914–929.

(144) Almantariotis, D.; Stevanovic, S.; Fandiño, O.; Pensado, A. S.; Padua, A. A. H.; Coxam, J.-Y.; Costa Gomes, M. F. Absorption of Carbon Dioxide, Nitrous Oxide, Ethane and Nitrogen by 1-Alkyl-3-Methylimidazolium ($C_n$mim, *n* = 2,4,6) Tris(pentafluoroethyl)trifluorophosphate Ionic Liquids (FAP). *J. Phys. Chem. B* **2012**, *116*, 7728–7738.

(145) Tomé, L. I. N.; Gardas, R. L.; Carvalho, P. J.; Pastoriza-Gallego, M. J.; Piñeiro, M. M.; Coutinho, J. A. P. Measurements and Correlation of High-Pressure Densities of Phosphonium Based Ionic Liquids. *J. Chem. Eng. Data* **2011**, *56*, 2205–2217.

(146) Gaciño, F. M.; Regueira, T.; Bolotov, A. V.; Sharipov, A.; Lugo, L.; Comuñas, M. J. P.; Fernández, J. Volumetric Behaviour of Six Ionic Liquids from T = (278 to 398) K and up to 120 MPa. *J. Chem. Thermodyn.* **2016**, *93*, 24–33.

(147) Regueira, T.; Lugo, L.; Fernández, J. Influence of the Pressure, Temperature, Cation and Anion on the Volumetric Properties of Ionic Liquids: New Experimental Values for Two Salts. *J. Chem. Thermodyn.* **2013**, *58*, 440–448.

(148) Stevanovic, S.; Costa Gomes, M. F. Solubility of Carbon Dioxide, Nitrous Oxide, Ethane, and Nitrogen in 1-Butyl-1-Methylpyrrolidinium and Trihexyl(tetradecyl)phosphonium Tris(pentafluoroethyl)trifluorophosphate (FAP) Ionic Liquids. *J. Chem. Thermodyn.* **2013**, *59*, 65–71.

(149) Klomfar, J.; Součková, M.; Pátek, J. *P* –ρ– *T* Measurements for 1-Alkyl-3-Methylimidazolium-Based Ionic Liquids with Tetrafluoroborate and a Trifluoromethanesulfonate Anion. *J. Chem. Eng. Data* **2012**, *57*, 708–720.

(150) Gaciño, F. M.; Regueira, T.; Comuñas, M. J. P.; Lugo, L.; Fernández, J. Density and Isothermal Compressibility for Two Trialkylimidazolium-Based Ionic Liquids at Temperatures from (278 to 398) K and up to 120 MPa. *J. Chem. Thermodyn.* **2015**, *81*, 124–130.

(151) Talavera-Prieto, N. M. C.; Ferreira, A. G. M.; Simões, P. N.; Carvalho, P. J.; Mattedi, S.; Coutinho, J. A. P. Thermophysical Characterization of N-Methyl-2-Hydroxyethylammonium Carboxilate Ionic Liquids. *J. Chem. Thermodyn.* **2014**, *68*, 221–234.

(152) Hiraga, Y.; Kato, A.; Sato, Y.; Aida, T. M.; Watanabe, M.; Smith, R. L. Separation Factors for [amim]Cl–CO_2 Biphasic Systems from High Pressure

Density and Partition Coefficient Measurements. *Sep. Purif. Technol.* **2015**, *155*, 139–148.

(153) Hiraga, Y.; Kato, A.; Sato, Y.; Smith, R. L. Densities at Pressures up to 200 MPa and Atmospheric Pressure Viscosities of Ionic Liquids 1-Ethyl-3-Methylimidazolium Methylphosphate, 1-Ethyl-3-Methylimidazolium Diethylphosphate, 1-Butyl-3-Methylimidazolium Acetate, and 1-Butyl-3-Methylimidazolium Bis(trifluoromethylsulfonyl)amide. *J. Chem. Eng. Data* **2015**, *60*, 876–885.

(154) Taherifard, H.; Raeissi, S. Estimation of the Densities of Ionic Liquids Using a Group Contribution Method. *J. Chem. Eng. Data* **2016**, *61*, 4031–4038.

(155) Kanakubo, M.; Makino, T.; Umecky, T. CO_2 Solubility in and Physical Properties for Ionic Liquid Mixtures of 1-Butyl-3-Methylimidazolium Acetate and 1-Butyl-3-Methylimidazolium Bis(trifluoromethanesulfonyl)amide. *J. Mol. Liq.* **2016**, *217*, 112–119.

(156) Oliveira, M. B.; Domínguez-Pérez, M.; Freire, M. G.; Llovell, F.; Cabeza, O.; Lopes-da-Silva, J. A.; Vega, L. F.; Coutinho, J. A. P. Surface Tension of Binary Mixtures of 1-Alkyl-3-Methylimidazolium Bis(trifluoromethylsulfonyl)amide Ionic Liquids: Experimental Measurements and Soft-SAFT Modeling. *J. Phys. Chem. B* **2012**, *116*, 12133–12141.

(157) Kato, R.; Gmehling, J. Systems with Ionic Liquids: Measurement of VLE and Γ^{∞}

Data and Prediction of Their Thermodynamic Behavior Using Original UNIFAC, Mod. UNIFAC(Do) and COSMO-RS(Ol). *J. Chem. Thermodyn.* **2005**, *37*, 603–619.

(158) Larriba, M.; García, S.; Navarro, P.; García, J.; Rodríguez, F. Physical Properties of N-Butylpyridinium Tetrafluoroborate and N-Butylpyridinium Bis(trifluoromethylsulfonyl)amide Binary Ionic Liquid Mixtures. *J. Chem. Eng. Data* **2012**, *57*, 1318–1325.

(159) Larriba, M.; García, S.; Navarro, P.; García, J.; Rodríguez, F. Physical Characterization of an Aromatic Extraction Solvent Formed by [bpy][BF_4] and [4bmpy][Tf_2N] Mixed Ionic Liquids. *J. Chem. Eng. Data* **2013**, *58*, 1496–1504.

(160) Ferguson, L.; Scovazzo, P. Solubility, Diffusivity, and Permeability of Gases in Phosphonium-Based Room Temperature Ionic Liquids: Data and Correlations. *Ind. Eng. Chem. Res.* **2007**, *46*, 1369–1374.

(161) Song, D.; Chen, J. Density and Viscosity Data for Mixtures of Ionic Liquids with a Common Anion. *J. Chem. Eng. Data* **2014**, *59*, 257–262.

(162) Ning, H.; Hou, M.; Mei, Q.; Liu, Y.; Yang, D.; Han, B. The Physicochemical Properties of Some Imidazolium-Based Ionic Liquids and Their Binary Mixtures. *Sci. China Chem.* **2012**, *55*, 1509–1518.

(163) Oliveira, M. B.; Domínguez-Pérez, M.; Cabeza, O.; Lopes-da-Silva, J. A.; Freire, M. G.; Coutinho, J. A. P. Surface Tensions of Binary Mixtures of Ionic Liquids

with Bis(trifluoromethylsulfonyl)amide as the Common Anion. *J. Chem. Thermodyn.* **2013**, *64*, 22–27.

(164) Song, D.; Chen, J. Densities and Viscosities for Ionic Liquids Mixtures Containing [eOHmim][BF_4], [bmim][BF_4] and [bpy][BF_4]. *J. Chem. Thermodyn.* **2014**, *77*, 137–143.

(165) Bastos, P. D. A.; Oliveira, F. S.; Rebelo, L. P. N.; Pereiro, A. B.; Marrucho, I. M. Separation of Azeotropic Mixtures Using High Ionicity Ionic Liquids Based on 1-Ethyl-3-Methylimidazolium Thiocyanate. *Fluid Phase Equilib.* **2015**, *389*, 48–54.

(166) Larriba, M.; Navarro, P.; Beigbeder, J.-B.; García, J.; Rodríguez, F. Mixing and Decomposition Behavior of {[4bmpy][Tf_2N]+[emim][$EtSO_4$]} and {[4bmpy][Tf_2N]+[emim][TFES]} Ionic Liquid Mixtures. *J. Chem. Thermodyn.* **2015**, *82*, 58–75.

(167) Pinto, A. M.; Rodríguez, H.; Arce, A.; Soto, A. Combined Physical and Chemical Absorption of Carbon Dioxide in a Mixture of Ionic Liquids. *J. Chem. Thermodyn.* **2014**, *77*, 197–205.

(168) Stoppa, A.; Buchner, R.; Hefter, G. How Ideal Are Binary Mixtures of Room-Temperature Ionic Liquids? *J. Mol. Liq.* **2010**, *153*, 46–51.

(169) Navia, P.; Troncoso, J.; Romaní, L. Isobaric Thermal Expansivity for Ionic Liquids with a Common Cation as a Function of Temperature and Pressure. *J.*

Chem. Eng. Data **2010**, *55*, 590–594.

(170) Navia, P.; Troncoso, J.; Romaní, L. Dependence against Temperature and Pressure of the Isobaric Thermal Expansivity of Room Temperature Ionic Liquids. *J. Chem. Eng. Data* **2010**, *55*, 595–599.

(171) Troncoso, J.; Cerdeiriña, C. A.; Navia, P.; Sanmamed, Y. A.; González-Salgado, D.; Romaní, L. Unusual Behavior of the Thermodynamic Response Functions of Ionic Liquids. *J. Phys. Chem. Lett.* **2010**, *1*, 211–214.

(172) Esperança, J. M. S. S.; Guedes, H. J. R.; Lopes, J. N. C.; Rebelo, L. P. N. Pressure−Density−Temperature (p−ρ−T) Surface of [C_6mim][NTf_2]. *J. Chem. Eng. Data* **2008**, *53*, 867–870.

(173) Nieto de Castro, C. A.; Langa, E.; Morais, A. L.; Lopes, M. L. M.; Lourenço, M. J. V.; Santos, F. J. V.; Santos, M. S. C. S.; Lopes, J. N. C.; Veiga, H. I. M.; Macatrão, M.; Esperança, J. M. S. S.; Marques, C. S.; Rebelo, L. P. N.; Afonso, C. A. M. Studies on the Density, Heat Capacity, Surface Tension and Infinite Dilution Diffusion with the Ionic Liquids [C_4mim][NTf_2], [C_4mim][dca], [C_2mim][$EtOSO_3$] and [Aliquat][dca]. *Fluid Phase Equilib.* **2010**, *294*, 157–179.

(174) Hofman, T.; Gołdon, A.; Nevines, A.; Letcher, T. M. Densities, Excess Volumes, Isobaric Expansivity, and Isothermal Compressibility of the (1-Ethyl-3-Methylimidazolium Ethylsulfate + Methanol) System at

Temperatures (283.15 to 333.15) K and Pressures from (0.1 to 35) MPa. *J. Chem. Thermodyn.* **2008**, *40*, 580–591.

(175) Gonfa, G.; Bustam, M. A.; Muhammad, N.; Khan, A. S. Evaluation of Thermophysical Properties of Functionalized Imidazolium Thiocyanate Based Ionic Liquids. *Ind. Eng. Chem. Res.* **2015**, *54*, 12428–12437.

(176) Troncoso, J.; Navia, P.; Romaní, L.; Bessieres, D.; Lafitte, T. On the Isobaric Thermal Expansivity of Liquids. *J. Chem. Phys.* **2011**, *134*, 94502.

(177) Kovanic, P. Guide to Gnostic Analysis of Uncertain Data (available only online); http://www.math-gnostics.eu/books/ (accessed May 1, 2016).

(178) Heiberger, R. M.; Becker, R. A. Design of an *S* Function for Robust Regression Using Iteratively Reweighted Least Squares. *J. Comput. Graph. Stat.* **1992**, *1*, 181–196.

(179) Seddon, K. R.; Stark, A.; Torres, M. J. Viscosity and Density of 1-Alkyl-3-Methylimidazolium Ionic Liquids. In *Clean Solvents: Alternative Media for Chemical Reactions and Processiong*; Abraham, M. A.; Moens, L., Eds.; ACS Symposium Series; American Chemical Society: Washington, USA, 2002; Vol. 819, pp. 34–49.

(180) Abbott, A. P.; McKenzie, K. J. Application of Ionic Liquids to the Electrodeposition of Metals. *Phys. Chem. Chem. Phys.* **2006**, *8*, 4265–4279.

(181) François, Y.; Zhang, K.; Varenne, A.; Gareil, P. New Integrated Measurement Protocol Using Capillary Electrophoresis Instrumentation for the Determination of Viscosity, Conductivity and Absorbance of Ionic Liquid-Molecular Solvent Mixtures. *Anal. Chim. Acta* **2006**, *562*, 164–170.

(182) Freire, M. G.; Teles, A. R. R.; Rocha, M. A. A.; Schröder, B.; Neves, C. M. S. S.; Carvalho, P. J.; Evtuguin, D. V.; Santos, L. M. N. B. F.; Coutinho, J. A. P. Thermophysical Characterization of Ionic Liquids Able to Dissolve Biomass. *J. Chem. Eng. Data* **2011**, *56*, 4813–4822.

(183) Morgan, D.; Ferguson, L.; Scovazzo, P. Diffusivities of Gases in Room-Temperature Ionic Liquids: Data and Correlations Obtained Using a Lag-Time Technique. *Ind. Eng. Chem. Res.* **2005**, *44*, 4815–4823.

(184) Rodríguez, H.; Brennecke, J. Temperature and Composition Dependence of the Density and Viscosity of Binary Mixtures of Water + Ionic Liquid. *J. Chem. Eng. Data* **2006**, *51*, 2145–2155.

(185) Yusoff, R.; Aroua, M. K.; Shamiri, A.; Ahmady, A.; Jusoh, N. S.; Asmuni, N. F.; Bong, L. C.; Thee, S. H. Density and Viscosity of Aqueous Mixtures of N -Methyldiethanolamines (MDEA) and Ionic Liquids. *J. Chem. Eng. Data* **2013**, *58*, 240–247.

(186) Mbondo Tsamba, B. E.; Sarraute, S.; Traïkia, M.; Husson, P. Transport Properties and Ionic Association in Pure Imidazolium-Based Ionic Liquids as a

Function of Temperature. *J. Chem. Eng. Data* **2014**, *59*, 1747–1754.

(187) Vuksanovic, J. M.; Calado, M. S.; Ivanis, G. R.; Kijevcanin, M. L.; Serbanovic, S. P.; Visak, Z. P. Environmentally Friendly Solutions of Liquid Poly(ethylene Glycol) and Imidazolium Based Ionic Liquids with Bistriflamide and Triflate Anions: Volumetric and Viscosity Studies. *Fluid Phase Equilib.* **2013**, *352*, 100–109.

(188) Okoturo, O. O.; VanderNoot, T. J. Temperature Dependence of Viscosity for Room Temperature Ionic Liquids. *J. Electroanal. Chem.* **2004**, *568*, 167–181.

(189) Katsuta, S.; Shiozawa, Y.; Imai, K.; Kudo, Y.; Takeda, Y. Stability of Ion Pairs of Bis(trifluoromethanesulfonyl)amide-Based Ionic Liquids in Dichloromethane. *J. Chem. Eng. Data* **2010**, *55*, 1588–1593.

(190) Gaciño, F. M.; Regueira, T.; Lugo, L.; Comuñas, M. J. P.; Fernández, J. Influence of Molecular Structure on Densities and Viscosities of Several Ionic Liquids. *J. Chem. Eng. Data* **2011**, *56*, 4984–4999.

(191) Costa, A. J. L.; Esperança, J. M. S. S.; Marrucho, I. M.; Rebelo, L. P. N. Densities and Viscosities of 1-Ethyl-3-Methylimidazolium N-Alkyl Sulfates. *J. Chem. Eng. Data* **2011**, *56*, 3433–3441.

(192) Schreiner, C.; Zugmann, S.; Hartl, R.; Gores, H. J. Fractional Walden Rule for Ionic Liquids: Examples from Recent Measurements and a Critique of the so-Called Ideal KCl Line for the Walden Plot. *J. Chem. Eng. Data* **2010**, *55*,

1784–1788.

(193) Quijada-Maldonado, E.; van der Boogaart, S.; Lijbers, J. H.; Meindersma, G. W.; de Haan, A. B. Experimental Densities, Dynamic Viscosities and Surface Tensions of the Ionic Liquids Series 1-Ethyl-3-Methylimidazolium Acetate and Dicyanamide and Their Binary and Ternary Mixtures with Water and Ethanol at T = (298.15 to 343.15 K). *J. Chem. Thermodyn.* **2012**, *51*, 51–58.

(194) Almantariotis, D.; Stevanovic, S.; Fandiño, O.; Pensado, A. S.; Padua, A. A. H.; Coxam, J.-Y.; Costa Gomes, M. F. Absorption of Carbon Dioxide, Nitrous Oxide, Ethane and Nitrogen by 1-Alkyl-3-Methylimidazolium ($C_{(n)}$mim, *n* = 2,4,6) Tris(pentafluoroethyl)trifluorophosphate Ionic Liquids (FAP). *J. Phys. Chem. B* **2012**, *116*, 7728–7738.

(195) Gómez, E.; González, B.; Calvar, N.; Tojo, E.; Domínguez, Á. Physical Properties of Pure 1-Ethyl-3-Methylimidazolium Ethylsulfate and Its Binary Mixtures with Ethanol and Water at Several Temperatures. *J. Chem. Eng. Data* **2006**, *51*, 2096–2102.

(196) Kavitha, T.; Vasantha, T.; Venkatesu, P.; Rama Devi, R. S.; Hofman, T. Thermophysical Properties for the Mixed Solvents of N-Methyl-2-Pyrrolidone with Some of the Imidazolium-Based Ionic Liquids. *J. Mol. Liq.* **2014**, *198*, 11–20.

(197) Sanmamed, Y. A.; González-Salgado, D.; Troncoso, J.; Cerdeiriña, C. A.;

Romaní, L. Viscosity-Induced Errors in the Density Determination of Room Temperature Ionic Liquids Using Vibrating Tube Densitometry. *Fluid Phase Equilib.* **2007**, *252*, 96–102.

(198) Pereiro, A. B.; Verdía, P.; Tojo, E.; Rodríguez, A. Physical Properties of 1-Butyl-3-Methylimidazolium Methyl Sulfate as a Function of Temperature. *J. Chem. Eng. Data* **2007**, *52*, 377–380.

(199) Pereiro, A. B.; Legido, J. L.; Rodrı´guez, A. Physical Properties of Ionic Liquids Based on 1-Alkyl-3-Methylimidazolium Cation and Hexafluorophosphate as Anion and Temperature Dependence. *J. Chem. Thermodyn.* **2007**, *39*, 1168–1175.

(200) Vakili-Nezhaad, G.; Vatani, M.; Asghari, M.; Ashour, I. Effect of Temperature on the Physical Properties of 1-Butyl-3-Methylimidazolium Based Ionic Liquids with Thiocyanate and Tetrafluoroborate Anions, and 1-Hexyl-3-Methylimidazolium with Tetrafluoroborate and Hexafluorophosphate Anions. *J. Chem. Thermodyn.* **2012**, *54*, 148–154.

(201) Xu, A.; Zhang, Y.; Li, Z.; Wang, J. Viscosities and Conductivities of 1-Butyl-3-Methylimidazolium Carboxylates Ionic Liquids at Different Temperatures. *J. Chem. Eng. Data* **2012**, *57*, 3102–3108.

(202) Carvalho, P. J.; Regueira, T.; Santos, L. M. N. B. F.; Fernandez, J.; Coutinho, J. A. P. Effect of Water on the Viscosities and Densities of

1-Butyl-3-Methylimidazolium Dicyanamide and 1-Butyl-3-Methylimidazolium Tricyanomethane at Atmospheric Pressure. *J. Chem. Eng. Data* **2010**, *55*, 645–652.

(203) Wasserscheid, P.; Hal, R.; Bösmann, A. 1-N-Butyl-3-Methylimidazolium ([Bmim]) Octylsulfate-an Even 'Greener' Ionic Liquid. *Green Chem.* **2002**, *4*, 400–404.

(204) Gómez, E.; Calvar, N.; Macedo, E. A.; Domínguez, Á. Effect of the Temperature on the Physical Properties of Pure 1-Propyl 3-Methylimidazolium Bis(trifluoromethylsulfonyl)amide and Characterization of Its Binary Mixtures with Alcohols. *J. Chem. Thermodyn.* **2012**, *45*, 9–15.

(205) Neves, C. M. S. S.; Batista, M. L. S.; Cláudio, A. F. M.; Santos, L. M. N. B. F.; Marrucho, I. M.; Freire, M. G.; Coutinho, J. A. P. Thermophysical Properties and Water Saturation of $[PF_6]^-$Based Ionic Liquids. *J. Chem. Eng. Data* **2010**, *55*, 5065–5073.

(206) Bandrés, I.; Giner, B.; Gascón, I.; Castro, M.; Lafuente, C. Physicochemical Characterization of N-Butyl-3-Methylpyridinium Dicyanamide Ionic Liquid. *J. Phys. Chem. B* **2008**, *112*, 12461–12467.

(207) Oliveira, F. S.; Freire, M. G.; Carvalho, P. J.; Coutinho, J. A. P.; Lopes, J. N. C.; Rebelo, L. P. N.; Marrucho, I. M. Structural and Positional Isomerism Influence in the Physical Properties of Pyridinium NTf_2-Based Ionic Liquids: Pure and

Water-Saturated Mixtures. *J. Chem. Eng. Data* **2010**, *55*, 4514–4520.

(208) Pereiro, A. B.; Veiga, H. I. M.; Esperança, J. M. S. S.; Rodríguez, A. Effect of Temperature on the Physical Properties of Two Ionic Liquids. *J. Chem. Thermodyn.* **2009**, *41*, 1419–1423.

(209) Neves, C. M. S. S.; Carvalho, P. J.; Freire, M. G.; Coutinho, J. A. P. Thermophysical Properties of Pure and Water-Saturated Tetradecyltrihexylphosphonium-Based Ionic Liquids. *J. Chem. Thermodyn.* **2011**, *43*, 948–957.

(210) García-Mardones, M.; Gascón, I.; López, M. C.; Royo, F. M.; Lafuente, C. Viscosimetric Study of Binary Mixtures Containing Pyridinium-Based Ionic Liquids and Alkanols. *J. Chem. Eng. Data* **2012**, *57*, 3549–3556.

(211) Li, J.-G.; Hu, Y.-F.; Ling, S.; Zhang, J.-Z. Physicochemical Properties of $[C_6mim][PF_6]$ and $[C_6mim][(C_2F_5)_3PF_3]$ Ionic Liquids. *J. Chem. Eng. Data* **2011**, *56*, 3068–3072.

(212) Li, J.-G.; Hu, Y.-F.; Sun, S.-F.; Liu, Y.-S.; Liu, Z.-C. Densities and Dynamic Viscosities of the Binary System (water+1-Hexyl-3-Methylimidazolium Bromide) at Different Temperatures. *J. Chem. Thermodyn.* **2010**, *42*, 904–908.

(213) Santos, F. J. V.; Nieto de Castro, C. A.; Mota, P. J. F.; Ribeiro, A. P. C. Electrical Conductivity and Viscosity of 1-Hexyl-3-Methylimidazolium Bis(trifluorosulfonyl)imide, $[C_6mim]$ $[(CF_3SO_2)_2N]$. *Int. J. Thermophys.* **2010**,

31, 1869–1879.

(214) Gan, Q.; Xue, M.; Rooney, D. A Study of Fluid Properties and Microfiltration Characteristics of Room Temperature Ionic Liquids [C_{10}-min][NTf_2] and [N_{8881}][NTf_2] and Their Polar Solvent Mixtures. *Sep. Purif. Technol.* **2006**, *51*, 185–192.

(215) Tokuda, H.; Hayamizu, K.; Ishii, K.; Susan, M. A. B. H.; Watanabe, M. Physicochemical Properties and Structures of Room Temperature Ionic Liquids. 2. Variation of Alkyl Chain Length in Imidazolium Cation. *J. Phys. Chem. B* **2005**, *109*, 6103–6110.

(216) Pereiro, A. B.; Santamarta, F.; Tojo, E.; Rodríguez, A.; Tojo, J. Temperature Dependence of Physical Properties of Ionic Liquid 1,3-Dimethylimidazolium Methyl Sulfate. *J. Chem. Eng. Data* **2006**, *51*, 952–954.

(217) González, B.; Gómez, E.; Domínguez, A.; Vilas, M.; Tojo, E. Physicochemical Characterization of New Sulfate Ionic Liquids. *J. Chem. Eng. Data* **2011**, *56*, 14–20.

(218) Domańska, U.; Królikowska, M. Density and Viscosity of Binary Mixtures of Thiocyanate Ionic Liquids + Water as a Function of Temperature. *J. Solution Chem.* **2012**, *41*, 1422–1445.

(219) Almeida, H. F. D.; Passos, H.; Lopes-da-Silva, J. A.; Fernandes, A. M.; Freire, M. G.; Coutinho, J. A. P. Thermophysical Properties of Five Acetate-Based

Ionic Liquids. *J. Chem. Eng. Data* **2012**, *57*, 3005–3013.

(220) González, E. J.; González, B.; Macedo, E. A. Thermophysical Properties of the Pure Ionic Liquid 1-Butyl-1-Methylpyrrolidinium Dicyanamide and Its Binary Mixtures with Alcohols. *J. Chem. Eng. Data* **2013**, *58*, 1440–1448.

(221) Sánchez, L. G.; Espel, J. R.; Onink, F.; Meindersma, G. W.; Haan, A. B. de. Density, Viscosity, and Surface Tension of Synthesis Grade Imidazolium, Pyridinium, and Pyrrolidinium Based Room Temperature Ionic Liquids. *J. Chem. Eng. Data* **2009**, *54*, 2803–2812.

(222) Tokuda, H.; Tsuzuki, S.; Susan, M. A. B. H.; Hayamizu, K.; Watanabe, M. How Ionic Are Room-Temperature Ionic Liquids? An Indicator of the Physicochemical Properties. *J. Phys. Chem. B* **2006**, *110*, 19593–19600.

(223) Harris, K. R.; Kanakubo, M.; Woolf, L. A. Temperature and Pressure Dependence of the Viscosity of the Ionic Liquids 1-Methyl-3-Octylimidazolium Hexafluorophosphate and 1-Methyl-3-Octylimidazolium Tetrafluoroborate. *J. Chem. Eng. Data* **2006**, *51*, 1161–1167.

(224) Tomida, D.; Kumagai, A.; Kenmochi, S.; Qiao, K.; Yokoyama, C. Viscosity of 1-Hexyl-3-Methylimidazolium Hexafluorophosphate and 1-Octyl-3-Methylimidazolium Hexafluorophosphate at High Pressure. *J. Chem. Eng. Data* **2007**, *52*, 577–579.

(225) Gómez, E.; González, B.; Domínguez, Á.; Tojo, E.; Tojo, J. Dynamic

Viscosities of a Series of 1-Alkyl-3-Methylimidazolium Chloride Ionic Liquids and Their Binary Mixtures with Water at Several Temperatures. *J. Chem. Eng. Data* **2006**, *51*, 696–701.

(226) Mokhtarani, B.; Sharifi, A.; Mortaheb, H. R.; Mirzaei, M.; Mafi, M.; Sadeghian, F. Density and Viscosity of Pyridinium-Based Ionic Liquids and Their Binary Mixtures with Water at Several Temperatures. *J. Chem. Thermodyn.* **2009**, *41*, 323–329.

(227) Bhattacharjee, A.; Luís, A.; Lopes-da-Silva, J. A.; Freire, M. G.; Carvalho, P. J.; Coutinho, J. A. P. Thermophysical Properties of Sulfonium- and Ammonium-Based Ionic Liquids. *Fluid Phase Equilib.* **2014**, *381*, 36–45.

(228) Fröba, A. P.; Kremer, H.; Leipertz, A. Density, Refractive Index, Interfacial Tension, and Viscosity of Ionic Liquids [EMIM][$EtSO_4$], [EMIM][NTf_2], [EMIM][$N(CN)_2$], and [OMA][NTf_2] in Dependence on Temperature at Atmospheric Pressure. *J. Phys. Chem. B* **2008**, *112*, 12420–12430.

(229) Liu, Q.-S.; Yang, M.; Li, P.-P.; Sun, S.-S.; Welz-Biermann, U.; Tan, Z.-C.; Zhang, Q.-G. Physicochemical Properties of Ionic Liquids [C_3py][NTf_2] and [C_6py][NTf_2]. *J. Chem. Eng. Data* **2011**, *56*, 4094–4101.

(230) Navia, P.; Troncoso, J.; Romaní, L. Viscosities for Ionic Liquid Binary Mixtures with a Common Ion. *J. Solution Chem.* **2008**, *37*, 677–688.

(231) Wong, D. S. H.; Chen, J. P.; Chang, J. M.; Chou, C. H. Phase Equilibria of Water

and Ionic Liquids [emim][PF_6] and [bmim][PF_6]. *Fluid Phase Equilib.* **2002**, *194*, 1089–1095.

(232) Anthony, J. L.; Maginn, E. J.; Brennecke, J. F. Solution Thermodynamics of Imidazolium-Based Ionic Liquids and Water. *J. Phys. Chem. B* **2001**, *105*, 10942–10949.

(233) Inoue, G.; Shimoyama, Y.; Su, F.; Takada, S.; Iwai, Y.; Arai, Y. Measurement and Correlation of Partition Coefficients for Phenolic Compounds in the 1-Butyl-3-Methylimidazolium Hexafluorophosphate/Water Two-Phase System. *J. Chem. Eng. Data* **2007**, *52*, 98–101.

(234) Ha, S. H.; Mai, N. L.; Koo, Y.-M. Butanol Recovery from Aqueous Solution into Ionic Liquids by Liquid–liquid Extraction. *Process Biochem.* **2010**, *45*, 1899–1903.

(235) Kim, J. E.; Lim, J. S.; Kang, J. W. Measurement and Correlation of Solubility of Carbon Dioxide in 1-Alkyl-3-Methylimidazolium Hexafluorophosphate Ionic Liquids. *Fluid Phase Equilib.* **2011**, *306*, 251–255.

(236) Lei, Z.; Dai, C.; Liu, X.; Xiao, L.; Chen, B. Extension of the UNIFAC Model for Ionic Liquids. *Ind. Eng. Chem. Res.* **2012**, *51*, 12135–12144.

(237) Lei, Z.; Chen, B.; Li, C.; Liu, H. Predictive Molecular Thermodynamic Models for Liquid Solvents, Solid Salts, Polymers, and Ionic Liquids. *Chem. Rev.* **2008**, *108*, 1419–1455.

(238) Alevizou, E. I.; Pappa, G. D.; Voutsas, E. C. Prediction of Phase Equilibrium in Mixtures Containing Ionic Liquids Using UNIFAC. *Fluid Phase Equilib.* **2009**, *284*, 99–105.

(239) Nebig, S.; Bölts, R.; Gmehling, J. Measurement of Vapor–liquid Equilibria (VLE) and Excess Enthalpies (HE) of Binary Systems with 1-Alkyl-3-Methylimidazolium Bis(trifluoromethylsulfonyl)amide and Prediction of These Properties and Γ^{∞} Using Modified UNIFAC (Dortmund). *Fluid Phase Equilib.* **2007**, *258*, 168–178.

(240) Nebig, S.; Gmehling, J. Measurements of Different Thermodynamic Properties of Systems Containing Ionic Liquids and Correlation of These Properties Using Modified UNIFAC (Dortmund). *Fluid Phase Equilib.* **2010**, *294*, 206–212.

(241) Paduszyński, K.; Domańska, U. *Extension of Modified UNIFAC (Dortmund) Matrix to Piperidinium Ionic Liquids*. Fluid Phase Equilib. **2013**, *353*, 115-120.

(242) Rachford, H. H.; Rice, J. D. Procedure for Use of Electronic Digital Computers in Calculating Flash Vaporization Hydrocarbon Equilibrium. *J. Pet. Technol.* **1952**, *4*, 19–3.

(243) Sørensen, J. M.; Magnussen, T.; Rasmussen, P.; Fredenslund, A. Liquid—liquid Equilibrium Data: Their Retrieval, Correlation and Prediction Part II: Correlation. *Fluid Phase Equilib.* **1979**, *3*, 47–82.

(244) Eckert, F. *COSMOtherm Reference Manual*; COSMOlogic GmbH & Co KG:

Leverkusen, Germany.

(245) Manan, N. A.; Hardacre, C.; Jacquemin, J.; Rooney, D. W.; Youngs, T. G. A. Evaluation of Gas Solubility Prediction in Ionic Liquids Using COSMOthermX. *J. Chem. Eng. Data* **2009**, *54*, 2005–2022.

(246) Rebelo, L. P. N.; Najdanovic-Visak, V.; Visak, Z. P.; Nunes da Ponte, M.; Szydlowski, J.; Cerdeiriña, C. A.; Troncoso, J.; Romaní, L.; Esperanza, J. M. S. S.; Guedes, H. J. R.; de Sousa, H. C. A Detailed Thermodynamic Analysis of [C_4mim][BF_4] + Water as a Case Study to Model Ionic Liquid Aqueous Solutions. *Green Chem.* **2004**, *6*, 369–381.

(247) Tomida, D.; Kumagai, A.; Qiao, K.; Yokoyama, C. Viscosity of [bmim][PF_6] and [bmim][BF_4] at High Pressure. *Int. J. Thermophys.* **2006**, *27*, 39–47.

(248) Tekin, A.; Safarov, J.; Shahverdiyev, A.; Hassel, E. (P, V, T) Properties of 1-Butyl-3-Methylimidazolium Tetrafluoroborate and 1-Butyl-3-Methylimidazolium Hexafluorophosphate at T=(298.15 to 398.15) K and Pressures up to P = 40 MPa. *J. Mol. Liq.* **2007**, *136*, 177–182.

(249) Abdulagatov, I. M.; Tekin, A.; Safarov, J.; Shahverdiyev, A.; Hassel, E. Densities and Excess, Apparent, and Partial Molar Volumes of Binary Mixtures of BMIMBF_4 + Ethanol as a Function of Temperature, Pressure, and Concentration. *Int. J. Thermophys.* **2008**, *29*, 505–533.

(250) Han, C.; Xia, S.; Ma, P.; Zeng, F. Densities of Ionic Liquid [BMIM][BF_4] +

Ethanol, + Benzene, and + Acetonitrile at Different Temperature and Pressure. *J. Chem. Eng. Data* **2009**, *54*, 2971–2977.

(251) Rilo, E.; Ferreira, A. G. M.; Fonseca, I. M. A.; Cabeza, O. Densities and Derived Thermodynamic Properties of Ternary Mixtures 1-Butyl-3-Methyl-Imidazolium Tetrafluoroborate + Ethanol + Water at Seven Pressures and Two Temperatures. *Fluid Phase Equilib.* **2010**, *296*, 53–59.

(252) Currás, M. R.; Vijande, J.; Piñeiro, M. M.; Lugo, L.; Salgado, J.; García, J. Behavior of the Environmentally Compatible Absorbent 1-Butyl-3-Methylimidazolium Tetrafluoroborate with 2,2,2-Trifluoroethanol: Experimental Densities at High Pressures and Modeling of *PVT* and Phase Equilibria Behavior with PC-SAFT EoS. *Ind. Eng. Chem. Res.* **2011**, *50*, 4065–4076.

(253) Klomfar, J.; Součková, M.; Pátek, J. Experimental p−ρ−T Data for 1-Butyl-3-Methylimidazolium Tetrafluoroborate at Temperatures from (240 to 353) K and at Pressures up to 60 MPa. *J. Chem. Eng. Data* **2011**, *56*, 426–436.

(254) Harris, K. R.; Kanakubo, M.; Woolf, L. A. Temperature and Pressure Dependence of the Viscosity of the Ionic Liquid 1-Butyl-3-Methylimidazolium Tetrafluoroborate: Viscosity and Density Relationships in Ionic Liquids. *J. Chem. Eng. Data* **2007**, *52*, 2425–2430.

(255) Schmidt, H.; Stephan, M.; Safarov, J.; Kul, I.; Nocke, J.; Abdulagatov, I. M.;

Hassel, E. Experimental Study of the Density and Viscosity of 1-Ethyl-3-Methylimidazolium Ethyl Sulfate. *J. Chem. Thermodyn.* **2012**, *47*, 68–75.

(256) Jacquemin, J.; Husson, P. Comments and Additional Work on 'High-Pressure Volumetric Properties of Imidazolium-Based Ionic Liquids: Effect of the Anion'. *J. Chem. Eng. Data* **2012**, *57*, 2409–2414.

(257) Carvalho, P. J.; Regueira, T.; Fernández, J.; Lugo, L.; Safarov, J.; Hassel, E.; Coutinho, J. A. P. High Pressure Density and Solubility for the CO_2 + 1-Ethyl-3-Methylimidazolium Ethylsulfate System. *J. Supercrit. Fluids* **2014**, *88*, 46–55.

(258) Matkowska, D.; Hofman, T. Volumetric Properties of the {x_1[C_4mim][$MeSO_4$] + (1 - x_1)MeOH} System at Temperatures from (283.15 to 333.15) K and Pressures from (0.1 to 35) MPa. *J. Solution Chem.* **2013**, *42*, 979–990.

(259) Safarov, J.; Hassel, E. Thermodynamic Properties of 1-Hexyl-3-Methylimidazolium Tetrafluoroborate. *J. Mol. Liq.* **2010**, *153*, 153–158.

(260) Kanakubo, M.; Harris, K. R.; Tsuchihashi, N.; Ibuki, K.; Ueno, M. Temperature and Pressure Dependence of the Electrical Conductivity of the Ionic Liquids 1-Methyl-3-Octylimidazolium Hexafluorophosphate and 1-Methyl-3-Octylimidazolium Tetrafluoroborate. *Fluid Phase Equilib.* **2007**,

261, 414–420.

(261) Dávila, M. J.; Aparicio, S.; Alcalde, R.; García, B.; Leal, J. M. On the Properties of 1-Butyl-3-Methylimidazolium Octylsulfate Ionic Liquid. *Green Chem.* **2007**, *9*, 221–232.

(262) Abdulagatov, I. M.; Safarov, J.; Guliyev, T.; Shahverdiyev, A.; Hassel, E. High Temperature and High Pressure Volumetric Properties of (Methanol + [$BMIM^+$][$OcSO^-_4$]) Mixtures. *Phys. Chem. Liq.* **2009**, *47*, 9–34.

(263) Safarov, J.; El-Awady, W. A.; Shahverdiyev, A.; Hassel, E. Thermodynamic Properties of 1-Ethyl-3-Methylimidazolium Bis(trifluoromethylsulfonyl)amide. *J. Chem. Eng. Data* **2011**, *56*, 106–112.

(264) Gomes de Azevedo, R.; Esperança, J. M. S. S.; Szydlowski, J.; Visak, Z. P.; Pires, P. F.; Guedes, H. J. R.; Rebelo, L. P. N. Thermophysical and Thermodynamic Properties of Ionic Liquids over an Extended Pressure Range: [bmim][NTf_2] and [hmim][NTf_2]. *J. Chem. Thermodyn.* **2005**, *37*, 888–899.

(265) Kanakubo, M.; Harris, K. R. Density of 1-Butyl-3-Methylimidazolium Bis(trifluoromethanesulfonyl)amide and 1-Hexyl-3-Methylimidazolium Bis(trifluoromethanesulfonyl)amide over an Extended Pressure Range up to 250 MPa. *J. Chem. Eng. Data* **2015**, *60*, 1408–1418.

(266) Harris, K. R.; Woolf, L. A.; Kanakubo, M.; Rüther, T. Transport Properties of N-Butyl-N-Methylpyrrolidinium Bis(trifluoromethylsulfonyl)amide. *J. Chem.*

Eng. Data **2011**, *56*, 4672–4685.

(267) Widowati, E.; Lee, M.-J. PVT Properties for Binary Ionic Liquids of 1-Methyl-1-Propylpiperidinium Bis(trifluoromethylsulfonyl)amide with Anisole or Acetophenone at Pressures up to 50 MPa. *J. Chem. Thermodyn.* **2012**, *49*, 54–61.

(268) Kandil, M. E.; Marsh, K. N.; Goodwin, A. R. H. Measurement of the Viscosity, Density, and Electrical Conductivity of 1-Hexyl-3-Methylimidazolium Bis(trifluorosulfonyl)imide at Temperatures between (288 and 433) K and Pressures below 50 MPa. *J. Chem. Eng. Data* **2007**, *52*, 2382–2387.

(269) Safarov, J.; Hamidova, R.; Zepik, S.; Schmidt, H.; Kul, I.; Shahverdiyev, A.; Hassel, E. Thermophysical Properties of 1-Hexyl-3-Methylimidazolium Bis(trifluoromethylsulfonyl)amide at High Temperatures and Pressures. *J. Mol. Liq.* **2013**, *187*, 137–156.

(270) Almantariotis, D.; Fandiño, O.; Coxam, J.-Y.; Costa Gomes, M. F. Direct Measurement of the Heat of Solution and Solubility of Carbon Dioxide in 1-Hexyl-3-Methylimidazolium Bis[trifluoromethylsulfonyl]amide and 1-Octyl-3-Methylimidazolium Bis[trifluoromethylsulfonyl]amide. *Int. J. Greenh. Gas Control* **2012**, *10*, 329–340.

(271) Ferreira, C. E.; Talavera-Prieto, N. M. C.; Fonseca, I. M. A.; Portugal, A. T. G.; Ferreira, A. G. M. Measurements of pVT, Viscosity, and Surface Tension of

Trihexyltetradecylphosphonium Tris(pentafluoroethyl)trifluorophosphate Ionic Liquid and Modelling with Equations of State. *J. Chem. Thermodyn.* **2012**, *47*, 183–196.

(272) McEwen, A. B.; Ngo, H. L.; LeCompte, K.; Goldman, J. L. Electrochemical Properties of Imidazolium Salt Electrolytes for Electrochemical Capacitor Applications. *J. Electrochem. Soc.* **1999**, *146*, 1687–1695.

(273) Suarez, P. A. Z.; Einloft, S.; Dullius, J. E. L.; de Souza, R. F.; Dupont, J. Synthesis and Physical-Chemical Properties of Ionic Liquids Based on 1-N-Butyl-3-Methylimidazolium Cation. *J. Chim. Phys. Physico-Chimie Biol.* **1998**, *95*, 1626–1639.

(274) Branco, L. C.; Rosa, J. N.; Moura Ramos, J. J.; Afonso, C. A. M. Preparation and Characterization of New Room Temperature Ionic Liquids. *Chem. - A Eur. J.* **2002**, *8*, 3671–3677.

(275) Huddleston, J. G.; Visser, A. E.; Reichert, W. M.; Willauer, H. D.; Broker, G. A.; Rogers, R. D. Characterization and Comparison of Hydrophilic and Hydrophobic Room Temperature Ionic Liquids Incorporating the Imidazolium Cation. *Green Chem.* **2001**, *3*, 156–164.

(276) Nishida, T.; Tashiro, Y.; Yamamoto, M. Physical and Electrochemical Properties of 1-Alkyl-3-Methylimidazolium Tetrafluoroborate for Electrolyte. *J. Fluor. Chem.* **2003**, *120*, 135–141.

(277) Wu, B.; Wu, B.; Reddy, R. G.; Rogers, R. D. Novel Ionic Liquid Thermal Storage for Solar Thermal Electric Power Systems. *In Proceedings of Solar Forum* 2001; pp. 445–451.

(278) Sato, T.; Masuda, G.; Takagi, K. Electrochemical Properties of Novel Ionic Liquids for Electric Double Layer Capacitor Applications. *Electrochim. Acta* **2004**, *49*, 3603–3611.

(279) Olivier-Bourbigou, H.; Magna, L. Ionic Liquids: Perspectives for Organic and Catalytic Reactions. *J. Mol. Catal. A Chem.* **2002**, *182*, 419–437.

(280) Valkenburg, M. E. V.; Vaughn, R. L.; Williams, M.; Wilkes, J. S. Thermochemistry of Ionic Liquid Heat-Transfer Fluids. *Thermochim. Acta* **2005**, *425*, 181–188.

(281) Zhou, Z.-B.; Matsumoto, H.; Tatsumi, K. Structure and Properties of New Ionic Liquids Based on Alkyl- and Alkenyltrifluoroborates. *ChemPhysChem* **2005**, *6*, 1324–1332.

(282) Ue, M.; Takeda, M.; Toriumi, A.; Kominato, A.; Hagiwara, R.; Ito, Y. Application of Low-Viscosity Ionic Liquid to the Electrolyte of Double-Layer Capacitors. *J. Electrochem. Soc.* **2003**, *150*, A499–A502.

(283) Stępniak, I.; Andrzejewska, E. Highly Conductive Ionic Liquid Based Ternary Polymer Electrolytes Obtained by in Situ Photopolymerisation. *Electrochim. Acta* **2009**, *54*, 5660–5665.

(284) Whitehead, J. A.; Lawrance, G. A.; McCluskey, A. Analysis of Gold in Solutions Containing Ionic Liquids by Inductively Coupled Plasma Atomic Emission Spectrometry. *Aust. J. Chem.* **2004**, *57*, 151–155.

(285) Fletcher, S. I.; Sillars, F. B.; Hudson, N. E.; Hall, P. J. Physical Properties of Selected Ionic Liquids for Use as Electrolytes and Other Industrial Applications. *J. Chem. Eng. Data* **2010**, *55*, 778–782.

(286) Shamsipur, M.; Beigi, A. A. M.; Teymouri, M.; Pourmortazavi, S. M.; Irandoust, M. Physical and Electrochemical Properties of Ionic Liquids 1-Ethyl-3-Methylimidazolium Tetrafluoroborate, 1-Butyl-3-Methylimidazolium Trifluoromethanesulfonate and 1-Butyl-1-Methylpyrrolidinium Bis(trifluoromethylsulfonyl)amide. *J. Mol. Liq.* **2010**, *157*, 43–50.

(287) Liu, W.; Zhao, T.; Zhang, Y.; Wang, H.; Yu, M. The Physical Properties of Aqueous Solutions of the Ionic Liquid [BMIM][BF_4]. *J. Solution Chem.* **2006**, *35*, 1337–1346.

(288) Rilo, E.; Vila, J.; Pico, J.; García-Garabal, S.; Segade, L.; Varela, L. M.; Cabeza, O. Electrical Conductivity and Viscosity of Aqueous Binary Mixtures of 1-Alkyl-3-Methyl Imidazolium Tetrafluoroborate at Four Temperatures. *J. Chem. Eng. Data* **2010**, *55*, 639–644.

(289) Fukuda, M.; Kajimoto, O.; Terazima, M.; Kimura, Y. Application of the

Transient Grating Method to the Investigation of the Photo-Thermalization Process of Malachite Green in Room Temperature Ionic Liquids. *J. Mol. Liq.* **2007**, *134*, 49–54.

(290) Arzhantsev, S.; Jin, H.; Baker, G. A.; Maroncelli, M. Measurements of the Complete Solvation Response in Ionic Liquids. *J. Phys. Chem. B* **2007**, *111*, 4978–4989.

(291) McHale, G.; Hardacre, C.; Ge, R.; Doy, N.; Allen, R. W. K.; MacInnes, J. M.; Bown, M. R.; Newton, M. I. Density−Viscosity Product of Small-Volume Ionic Liquid Samples Using Quartz Crystal Impedance Analysis. *Anal. Chem.* **2008**, *80*, 5806–5811.

(292) Miran Beigi, A. A.; Abdouss, M.; Yousefi, M.; Pourmortazavi, S. M.; Vahid, A. Investigation on Physical and Electrochemical Properties of Three Imidazolium Based Ionic Liquids (1-Hexyl-3-Methylimidazolium Tetrafluoroborate, 1-Ethyl-3-Methylimidazolium Bis(trifluoromethylsulfonyl) Imide and 1-Butyl-3-Methylimidazolium Methylsulfate). *J. Mol. Liq.* **2013**, *177*, 361–368.

(293) Silvester, D. S.; Ward, K. R.; Aldous, L.; Hardacre, C.; Compton, R. G. The Electrochemical Oxidation of Hydrogen at Activated Platinum Electrodes in Room Temperature Ionic Liquids as Solvents. *J. Electroanal. Chem.* **2008**, *618*, 53–60.

(294) Fernández, A.; García, J.; Torrecilla, J. S.; Oliet, M.; Rodríguez, F. Volumetric,

Transport and Surface Properties of [bmim][$MeSO_4$] and [emim][$EtSO_4$] Ionic Liquids As a Function of Temperature. *J. Chem. Eng. Data* **2008**, *53*, 1518–1522.

(295) Ries, L. A. S.; do Amaral, F. A.; Matos, K.; Martini, E. M. A.; de Souza, M. O.; de Souza, R. F. Evidence of Change in the Molecular Organization of 1-N-Butyl-3-Methylimidazolium Tetrafluoroborate Ionic Liquid Solutions with the Addition of Water. *Polyhedron* **2008**, *27*, 3287–3293.

(296) González, B.; Calvar, N.; Gómez, E.; Domínguez, Á. Physical Properties of the Ternary System (Ethanol + Water + 1-Butyl-3-Methylimidazolium Methylsulphate) and Its Binary Mixtures at Several Temperatures. *J. Chem. Thermodyn.* **2008**, *40*, 1274–1281.

(297) Jin, H.; O'Hare, B.; Dong, J.; Arzhantsev, S.; Baker, G. A.; Wishart, J. F.; Benesi, A. J.; Maroncelli, M. Physical Properties of Ionic Liquids Consisting of the 1-Butyl-3-Methylimidazolium Cation with Various Anions and the Bis(trifluoromethylsulfonyl)amide Anion with Various Cations. *J. Phys. Chem. B* **2008**, *112*, 81–92.

(298) Tian, Y.; Wang, X.; Wang, J. Densities and Viscosities of 1-Butyl-3-Methylimidazolium Tetrafluoroborate + Molecular Solvent Binary Mixtures. *J. Chem. Eng. Data* **2008**, *53*, 2056–2059.

(299) Bonhôte, P.; Dias, A.-P.; Papageorgiou, N.; Kalyanasundaram, K.; Grätzel, M.

Hydrophobic, Highly Conductive Ambient-Temperature Molten Salts. *Inorg. Chem.* **1996**, *35*, 1168–1178.

(300) Meredith, M. B.; McMillen, C. H.; Goodman, J. T.; Hanusa, T. P. Ambient Temperature Imidazolium-Based Ionic Liquids with tetrachloronickelate(II) Anions. *Polyhedron* **2009**, *28*, 2355–2358.

(301) Zhao, Y.; Zhang, X.; Zeng, S.; Zhou, Q.; Dong, H.; Tian, X.; Zhang, S. Density, Viscosity, and Performances of Carbon Dioxide Capture in 16 Absorbents of Amine + Ionic Liquid + H_2O, Ionic Liquid + H_2O, and Amine + H_2O Systems. *J. Chem. Eng. Data* **2010**, *55*, 3513–3519.

(302) Evans, R. G.; Klymenko, O. V.; Hardacre, C.; Seddon, K. R.; Compton, R. G. Oxidation of N,N,N′,N′-Tetraalkyl-Para-Phenylenediamines in a Series of Room Temperature Ionic Liquids Incorporating the Bis(trifluoromethylsulfonyl)amide Anion. *J. Electroanal. Chem.* **2003**, *556*, 179–188.

(303) Nikitina, V. a.; Nazet, A.; Sonnleitner, T.; Buchner, R. Properties of Sodium Tetrafluoroborate Solutions in 1-Butyl-3-Methylimidazolium Tetrafluoroborate Ionic Liquid. *J. Chem. Eng. Data* **2012**, *57*, 3019–3025.

(304) Tian, S.; Hou, Y.; Wu, W.; Ren, S.; Pang, K. Physical Properties of 1-Butyl-3-Methylimidazolium Tetrafluoroborate/N-Methyl-2-Pyrrolidone Mixtures and the Solubility of CO_2 in the System at Elevated Pressures. *J. Chem. Eng. Data* **2012**, *57*, 756–763.

(305) Gan, Q.; Rooney, D.; Xue, M.; Thompson, G.; Zou, Y. An Experimental Study of Gas Transport and Separation Properties of Ionic Liquids Supported on Nanofiltration Membranes. *J. Memb. Sci.* **2006**, *280*, 948–956.

(306) Bou Malham, I.; Turmine, M. Viscosities and Refractive Indices of Binary Mixtures of 1-Butyl-3-Methylimidazolium Tetrafluoroborate and 1-Butyl-2,3-Dimethylimidazolium Tetrafluoroborate with Water at 298K. *J. Chem. Thermodyn.* **2008**, *40*, 718–723.

(307) Zhou, Q.; Wang, L.-S.; Chen, H.-P. Densities and Viscosities of 1-Butyl-3-Methylimidazolium Tetrafluoroborate + H_2O Binary Mixtures from (303.15 to 353.15) K. *J. Chem. Eng. Data* **2006**, *51*, 905–908.

(308) Osada, R.; Hoshino, T.; Okada, K.; Ohmasa, Y.; Yao, M. Surface Tension of Room Temperature Ionic Liquids Measured by Dynamic Light Scattering. *J. Chem. Phys.* **2009**, *130*, 184705.

(309) Baker, S. N.; Baker, G. A.; Kane, M. A.; Bright, F. V. The Cybotactic Region Surrounding Fluorescent Probes Dissolved in 1-Butyl-3-Methylimidazolium Hexafluorophosphate: Effects of Temperature and Added Carbon Dioxide. *J. Phys. Chem. B* **2001**, *105*, 9663–9668.

(310) Andreatta, A. E.; Francisco, M.; Rodil, E.; Soto, A.; Arce, A. Isobaric Vapour–liquid Equilibria and Physical Properties for Isopropyl Acetate + Isopropanol + 1-Butyl-3-Methyl-Imidazolium Bis(trifluoromethylsulfonyl)amide Mixtures.

Fluid Phase Equilib. **2011**, *300*, 162–171.

(311) Andreatta, A. E.; Arce, A.; Rodil, E.; Soto, A. Physico-Chemical Properties of Binary and Ternary Mixtures of Ethyl Acetate + Ethanol + 1-Butyl-3-Methyl-Imidazolium Bis(trifluoromethylsulfonyl)amide at 298.15 K and Atmospheric Pressure. *J. Solution Chem.* **2010**, *39*, 371–383.

(312) Vranes, M.; Dozic, S.; Djeric, V.; Gadzuric, S. Physicochemical Characterization of 1-Butyl-3-Methylimidazolium and 1-Butyl-1-Methylpyrrolidinium Bis(trifluoromethylsulfonyl)amide. *J. Chem. Eng. Data* **2012**, *57*, 1072–1077.

(313) Liu, J.; Jiang, G.; Chi, Y.; Cai, Y.; Zhou, Q.; Hu, J.-T. Use of Ionic Liquids for Liquid-Phase Microextraction of Polycyclic Aromatic Hydrocarbons. *Anal. Chem.* **2003**, *75*, 5870–5876.

(314) Yung, K. K. L.; Perera, J. M.; Smith, C. D.; Stevens, G. W. The Partitioning Behavior of Tyramine and 2-Methoxyphenethylamine in a Room Temperature Ionic Liquid–Water System Compared to Traditional Organic–Water System. *Sep. Sci. Technol.* **2005**, *40*, 1555–1566.

(315) Harris, K. R.; Woolf, L. a; Kanakubo, M. Temperature and Pressure Dependence of the Viscosity of the Ionic Liquid 1-Butyl-3-Methylimidazolium Hexafluorophosphate. *J. Chem. Eng. Data* **2005**, *50*, 1777–1782.

(316) Wang, J.; Zhu, A.; Zhao, Y.; Zhuo, K. Excess Molar Volumes and Excess

Logarithm Viscosities for Binary Mixtures of the Ionic Liquid 1-Butyl-3-Methylimidazolium Hexaflurophosphate with Some Organic Compounds. *J. Solution Chem.* **2005**, *34*, 585–596.

(317) McFarlane, J.; Ridenour, W. B.; Luo, H.; Hunt, R. D.; DePaoli, D. W.; Ren, R. X. Room Temperature Ionic Liquids for Separating Organics from Produced Water. *Sep. Sci. Technol.* **2005**, *40*, 1245–1265.

(318) Ito, N.; Arzhantsev, S.; Heitz, M.; Maroncelli, M. Solvation Dynamics and Rotation of Coumarin 153 in Alkylphosphonium Ionic Liquids. *J. Phys. Chem. B* **2004**, *108*, 5771–5777.

(319) Del Sesto, R. E.; Corley, C.; Robertson, A.; Wilkes, J. S. Tetraalkylphosphonium-Based Ionic Liquids. *J. Organomet. Chem.* **2005**, *690*, 2536–2542.

(320) Zafarani-Moattar, M. T.; Majdan-Cegincara, R. Viscosity, Density, Speed of Sound, and Refractive Index of Binary Mixtures of Organic Solvent + Ionic Liquid, 1-Butyl-3-Methylimidazolium Hexafluorophosphate at 298.15 K. *J. Chem. Eng. Data* **2007**, *52*, 2359–2364.

(321) Fraser, K. J.; Izgorodina, E. I.; Forsyth, M.; Scott, J. L.; MacFarlane, D. R. Liquids Intermediate between 'molecular' and 'ionic' Liquids: Liquid Ion Pairs? *Chem. Commun.* **2007**, *0*, 3817–3819.

(322) Jiqin, Z.; Jian, C.; Chengyue, L.; Weiyang, F. Viscosities and Interfacial

Properties of 1-Methyl-3-Butylimidazolium Hexafluorophosphate and 1-Isobutenyl-3-Methylimidazolium Tetrafluoroborate Ionic Liquids. *J. Chem. Eng. Data* **2007**, *52*, 812–816.

(323) Diogo, J. C. F.; Caetano, F. J. P.; Fareleira, J. M. N. A.; Wakeham, W. A.; Afonso, C. A. M.; Marques, C. S. Viscosity Measurements of the Ionic Liquid Trihexyl(tetradecyl)phosphonium Dicyanamide [$P_{6,6,6,14}$][dca] Using the Vibrating Wire Technique. *J. Chem. Eng. Data* **2012**, *57*, 1015–1025.

(324) Mali, K. S.; Dutt, G. B.; Mukherjee, T. Photoisomerization of Cyanine Derivatives in 1-Butyl-3-Methylimidazolium Hexafluorophosphate and Aqueous Glycerol: Influence of Specific Interactions. *J. Chem. Phys.* **2008**, *128*, 124515.

(325) Hardacre, C.; Holbrey, J. D.; Katdare, S. P.; Seddon, K. R. Alternating Copolymerisation of Styrene and Carbon Monoxide in Ionic Liquids. *Green Chem.* **2002**, *4*, 143–146.

(326) Fan, W.; Zhou, Q.; Sun, J.; Zhang, S. Density, Excess Molar Volume, and Viscosity for the Methyl Methacrylate + 1-Butyl-3-Methylimidazolium Hexafluorophosphate Ionic Liquid Binary System at Atmospheric Pressure. *J. Chem. Eng. Data* **2009**, *54*, 2307–2311.

(327) Shirota, H.; Nishikawa, K.; Ishida, T. Atom Substitution Effects of $[XF_6]^-$ in Ionic Liquids. 1. Experimental Study. *J. Phys. Chem. B* **2009**, *113*, 9831–9839.

(328) Qiao, Y.; Yan, F.; Xia, S.; Yin, S.; Ma, P. Densities and Viscosities of [Bmim][PF_6] and Binary Systems [Bmim][PF_6] + Ethanol, [Bmim][PF_6] + Benzene at Several Temperatures and Pressures: Determined by the Falling-Ball Method. *J. Chem. Eng. Data* **2011**, *56*, 2379–2385.

(329) Ohno, H.; Fukumoto, K. Amino Acid Ionic Liquids. *Acc. Chem. Res.* **2007**, *40*, 1122–1129.

(330) Ahosseini, A.; Scurto, A. M. Viscosity of Imidazolium-Based Ionic Liquids at Elevated Pressures: Cation and Anion Effects. *Int. J. Thermophys.* **2008**, *29*, 1222–1243.

(331) Zhang, Q.-G.; Wei, Y.; Sun, S.-S.; Wang, C.; Yang, M.; Liu, Q.-S.; Gao, Y.-A. Study on Thermodynamic Properties of Ionic Liquid N-Butyl-3-Methylpyridinium Bis(trifluoromethylsulfonyl)amide. *J. Chem. Eng. Data* **2012**, *57*, 2185–2190.

(332) Tomida, D.; Kumagai, A.; Qiao, K.; Yokoyama, C. Viscosity of 1-Butyl-3-Methylimidazolium Hexafluorophosphate + CO_2 Mixture. *J. Chem. Eng. Data* **2007**, *52*, 1638–1640.

(333) Ciocirlan, O.; Iulian, O. Properties of Pure 1-Butyl-2,3-Dimethylimidazolium Tetrafluoroborate Ionic Liquid and Its Binary Mixtures with Dimethyl Sulfoxide and Acetonitrile. *J. Chem. Eng. Data* **2012**, *57*, 3142–3148.

(334) Andriyko, Y. O.; Reischl, W.; Nauer, G. E. Trialkyl-Substituted

Imidazolium-Based Ionic Liquids for Electrochemical Applications: Basic Physicochemical Properties. *J. Chem. Eng. Data* **2009**, *54*, 855–860.

(335) Khupse, N. D.; Kumar, A. Dramatic Change in Viscosities of Pure Ionic Liquids upon Addition of Molecular Solvents. *J. Solution Chem.* **2009**, *38*, 589–600.

(336) Muhammad, A.; Abdul Mutalib, M. I.; Wilfred, C. D.; Murugesan, T.; Shafeeq, A. Thermophysical Properties of 1-Hexyl-3-Methyl Imidazolium Based Ionic Liquids with Tetrafluoroborate, Hexafluorophosphate and Bis(trifluoromethylsulfonyl)amide Anions. *J. Chem. Thermodyn.* **2008**, *40*, 1433–1438.

(337) Ignat'ev, N. V.; Welz-Biermann, U.; Kucheryna, A.; Bissky, G.; Willner, H. New Ionic Liquids with Tris(perfluoroalkyl)trifluorophosphate (FAP) Anions. *J. Fluor. Chem.* **2005**, *126*, 1150–1159.

(338) Zhu, A.; Wang, J.; Liu, R. A Volumetric and Viscosity Study for the Binary Mixtures of 1-Hexyl-3-Methylimidazolium Tetrafluoroborate with Some Molecular Solvents. *J. Chem. Thermodyn.* **2011**, *43*, 796–799.

(339) Liu, Q.-S.; Yan, P.-F.; Yang, M.; Tan, Z.-C.; Li, C.-P.; Welz-Biermann, U. Dynamic Viscosity and Conductivity of Ionic Liquids $[C_npy][NTf_2]$ (n=2, 4, 5). *Acta Physico-Chimica Sin.* **2011**, *27*, 2762–2766.

(340) Kermanpour, F.; Niakan, H. Z. Measurement and Modeling the Excess Molar Properties of Binary Mixtures of {$[C_6mim][BF_4]$ + 3-Amino-1-Propanol} and

{[C_6mim][BF_4] + Isobutanol}: Application of Prigogine–Flory–Patterson Theory. *J. Chem. Thermodyn.* **2012**, *48*, 129–139.

(341) Kermanpour, F.; Sharifi, T. Thermodynamic Study of Binary Mixture of x_1[C_6mim][BF_4] + $x_2$1-Propanol: Measurements and Molecular Modeling. *Thermochim. Acta* **2012**, *527*, 211–218.

(342) Matsumoto, H.; Yanagida, M.; Tanimoto, K.; Nomura, M.; Kitagawa, Y.; Miyazaki, Y. Highly Conductive Room Temperature Molten Salts Based on Small Trimethylalkylammonium Cations and Bis(trifluoromethylsulfonyl)amide. *Chem. Lett.* **2000**, *29*, 922–923.

(343) Pringle, J. M.; Golding, J.; Baranyai, K.; Forsyth, C. M.; Deacon, G. B.; Scott, J. L.; MacFarlane, D. R. The Effect of Anion Fluorination in Ionic Liquids—physical Properties of a Range of Bis(methanesulfonyl)amide Salts. *New J. Chem.* **2003**, *27*, 1504–1510.

(344) Sun, J.; MacFarlane, D. R.; Forsyth, M. A New Family of Ionic Liquids Based on the 1-Alkyl-2-Methyl Pyrrolinium Cation. *Electrochim. Acta* **2003**, *48*, 1707–1711.

(345) Shirota, H.; Funston, A. M.; Wishart, J. F.; Castner, E. W. Ultrafast Dynamics of Pyrrolidinium Cation Ionic Liquids. *J. Chem. Phys.* **2005**, *122*, 184512.

(346) Zhou, Z.-B.; Matsumoto, H.; Tatsumi, K. Cyclic Quaternary Ammonium Ionic Liquids with Perfluoroalkyltrifluoroborates: Synthesis, Characterization, and

Properties. *Chem. - A Eur. J.* **2006**, *12*, 2196–2212.

(347) Deng, M.-J.; Chen, P.-Y.; Sun, I.-W. Electrochemical Study and Electrodeposition of Manganese in the Hydrophobic Butylmethylpyrrolidinium Bis((trifluoromethyl)sulfonyl)imide Room-Temperature Ionic Liquid. *Electrochim. Acta* **2007**, *53*, 1931–1938.

(348) Biso, M.; Mastragostino, M.; Montanino, M.; Passerini, S.; Soavi, F. Electropolymerization of poly(3-Methylthiophene) in Pyrrolidinium-Based Ionic Liquids for Hybrid Supercapacitors. *Electrochim. Acta* **2008**, *53*, 7967–7971.

(349) Appetecchi, G. B.; Montanino, M.; Zane, D.; Carewska, M.; Alessandrini, F.; Passerini, S. Effect of the Alkyl Group on the Synthesis and the Electrochemical Properties of N-Alkyl-N-Methyl-Pyrrolidinium Bis(trifluoromethanesulfonyl)imide Ionic Liquids. *Electrochim. Acta* **2009**, *54*, 1325–1332.

(350) Kondoh, T.; Asano, A.; Yang, J.; Norizawa, K.; Takahashi, K.; Taguchi, M.; Nagaishi, R.; Katoh, R.; Yoshida, Y. Pulse Radiolysis Study of Ion-Species Effects on the Solvated Electron in Alkylammonium Ionic Liquids. *Radiat. Phys. Chem.* **2009**, *78*, 1157–1160.

(351) Fitchett, B. D.; Knepp, T. N.; Conboy, J. C. 1-Alkyl-3-Methylimidazolium Bis(perfluoroalkylsulfonyl)imide Water-Immiscible Ionic Liquids. *J.*

Electrochem. Soc. **2004**, *151*, E219–E225.

(352) Spohr, H. V.; Patey, G. N. Structural and Dynamical Properties of Ionic Liquids: The Influence of Charge Location. *J. Chem. Phys.* **2009**, *130*, 104506.

(353) AlTuwaim, M. S.; Alkhaldi, K. H. A. E.; Al-Jimaz, A. S.; Mohammad, A. A. Temperature Dependence of Physicochemical Properties of Imidazolium-, Pyroldinium-, and Phosphonium-Based Ionic Liquids. *J. Chem. Eng. Data* **2014**, *59*, 1955–1963.

(354) Rocha, M. A. A.; Ribeiro, F. M. S.; Ferreira, A. I. M. C. L.; Coutinho, J. A. P.; Santos, L. M. N. B. F. Thermophysical Properties of $[C_N{-}1C_1im][PF_6]$ Ionic Liquids. *J. Mol. Liq.* **2013**, *188*, 196–202.

(355) Deng, Y.; Husson, P.; Delort, A.-M.; Besse-Hoggan, P.; Sancelme, M.; Costa Gomes, M. F. Influence of an Oxygen Functionalization on the Physicochemical Properties of Ionic Liquids: Density, Viscosity, and Carbon Dioxide Solubility as a Function of Temperature. *J. Chem. Eng. Data* **2011**, *56*, 4194–4202.

(356) MacFarlane, D. R.; Meakin, P.; Sun, J.; Amini, N.; Forsyth, M. Pyrrolidinium Imides: A New Family of Molten Salts and Conductive Plastic Crystal Phases. *J. Phys. Chem. B* **1999**, *103*, 4164–4170.

(357) Shiflett, M. B.; Elliott, B. A.; Yokozeki, A. Phase Behavior of Vinyl Fluoride in Room-Temperature Ionic Liquids [emim][Tf_2N], [bmim][$N(CN)_{(2)}$], [bmpy][BF_4], [bmim][HFPS] and [omim][TFES]. *Fluid Phase Equilib.* **2012**,

316, 147–155.

(358) Heintz, A.; Klasen, D.; Lehmann, J. K. Excess Molar Volumes and Viscosities of Binary Mixtures of Methanol and the Ionic Liquid 4-Methyl-N. *J. Solution Chem.* **2002**, *31*, 467–476.

(359) Shekaari, H.; Mousavi, S. S. Volumetric Properties of Ionic Liquid 1,3-Dimethylimidazolium Methyl Sulfate+molecular Solvents at T=(298.15–328.15)K. *Fluid Phase Equilib.* **2010**, *291*, 201–207.

(360) Gómez, E.; González, B.; Calvar, N.; Domínguez, Á. Excess Molar Properties of Ternary System (Ethanol + Water + 1,3-Dimethylimidazolium Methylsulphate) and Its Binary Mixtures at Several Temperatures. *J. Chem. Thermodyn.* **2008**, *40*, 1208–1216.

(361) Liu, Q.-S.; Li, P.-P.; Welz-Biermann, U.; Liu, X.-X.; Chen, J. Density, Electrical Conductivity, and Dynamic Viscosity of N-Alkyl-4-Methylpyridinium Bis(trifluoromethylsulfonyl)amide. *J. Chem. Eng. Data* **2012**, *57*, 2999–3004.

(362) Dai, Q.; Menzies, D. B.; MacFarlane, D. R.; Batten, S. R.; Forsyth, S.; Spiccia, L.; Cheng, Y.-B.; Forsyth, M. Dye-Sensitized Nanocrystalline Solar Cells Incorporating Ethylmethylimidazolium-Based Ionic Liquid Electrolytes. *Comptes Rendus Chim.* **2006**, *9*, 617–621.

(363) Domańska, U.; Królikowska, M. Density and Viscosity of Binary Mixtures of {1-Butyl-3-Methylimidazolium Thiocyanate + 1-Heptanol, 1-Octanol,

1-Nonanol, or 1-Decanol}. *J. Chem. Eng. Data* **2010**, *55*, 2994–3004.

(364) Domańska, U.; Laskowska, M. Temperature and Composition Dependence of the Density and Viscosity of Binary Mixtures of {1-Butyl-3-Methylimidazolium Thiocyanate + 1-Alcohols}. *J. Chem. Eng. Data* **2009**, *54*, 2113–2119.

(365) Matsumoto, H.; Sakaebe, H.; Tatsumi, K.; Kikuta, M.; Ishiko, E.; Kono, M. Fast Cycling of Li/$LiCoO_2$ Cell with Low-Viscosity Ionic Liquids Based on Bis(fluorosulfonyl)imide $[FSI]^-$. *J. Power Sources* **2006**, *160*, 1308–1313.

(366) Ishikawa, M.; Sugimoto, T.; Kikuta, M.; Ishiko, E.; Kono, M. Pure Ionic Liquid Electrolytes Compatible with a Graphitized Carbon Negative Electrode in Rechargeable Lithium-Ion Batteries. *J. Power Sources* **2006**, *162*, 658-662.

(367) Domańska, U.; Królikowska, M. Phase Behaviour of 1-Butyl-1-Methylpyrrolidinium Thiocyanate Ionic Liquid. *Fluid Phase Equilib.* **2011**, *308*, 55–63.

(368) Camper, D.; Becker, C.; Koval, C.; Noble, R. Diffusion and Solubility Measurements in Room Temperature Ionic Liquids. *Ind. Eng. Chem. Res.* **2006**, *45*, 445–450.

(369) Evlampieva, N. P.; Vitz, J.; Schubert, U. S.; Ryumtsev, E. I. Molecular Solutions of Cellulose in Mixtures of Ionic Liquids with Pyridine. *Russ. J. Appl. Chem.* **2009**, *82*, 666–672.

(370) Torriero, A. A. J.; Siriwardana, A. I.; Bond, A. M.; Burgar, I. M.; Dunlop, N. F.; Deacon, G. B.; MacFarlane, D. R. Physical and Electrochemical Properties of Thioether-Functionalized Ionic Liquids. *J. Phys. Chem. B* **2009**, *113*, 11222–11231.

(371) Fendt, S.; Padmanabhan, S.; Blanch, H. W.; Prausnitz, J. M. Viscosities of Acetate or Chloride-Based Ionic Liquids and Some of Their Mixtures with Water or Other Common Solvents. *J. Chem. Eng. Data* **2011**, *56*, 31–34.

(372) Araújo, J. M. M.; Pereiro, A. B.; Alves, F.; Marrucho, I. M.; Rebelo, L. P. N. Nucleic Acid Bases in 1-Alkyl-3-Methylimidazolium Acetate Ionic Liquids: A Thermophysical and Ionic Conductivity Analysis. *J. Chem. Thermodyn.* **2013**, *57*, 1–8.

(373) Yao, H.; Zhang, S.; Wang, J.; Zhou, Q.; Dong, H.; Zhang, X. Densities and Viscosities of the Binary Mixtures of 1-Ethyl-3-Methylimidazolium Bis(trifluoromethylsulfonyl)amide with N-Methyl-2-Pyrrolidone or Ethanol at T = (293.15 to 323.15) K. *J. Chem. Eng. Data* **2012**, *57*, 875–881.

(374) Bogolitsyn, K. G.; Skrebets, T. E.; Makhova, T. A. Physicochemical Properties of 1-Butyl-3-Methylimidazolium Acetate. *Russ. J. Gen. Chem.* **2009**, *79*, 125–128.

(375) Ge, M.-L.; Zhao, R.-S.; Yi, Y.-F.; Zhang, Q.; Wang, L.-S. Densities and Viscosities of 1-Butyl-3-Methylimidazolium Trifluoromethanesulfonate + H_2O

Binary Mixtures at T = (303.15 to 343.15) K. *J. Chem. Eng. Data* **2008**, *53*, 2408–2411.

(376) Kulkarni, P. S.; Branco, L. C.; Crespo, J. G.; Nunes, M. C.; Raymundo, A.; Afonso, C. A. M. Comparison of Physicochemical Properties of New Ionic Liquids Based on Imidazolium, Quaternary Ammonium, and Guanidinium Cations. *Chem. - A Eur. J.* **2007**, *13*, 8478–8488.

(377) Ogihara, W.; Yoshizawa, M.; Ohno, H. Novel Ionic Liquids Composed of Only Azole Ions. *Chem. Lett.* **2004**, *33*, 1022–1023.

(378) Andreatta, A. E.; Arce, A.; Rodil, E.; Soto, A. Physical Properties and Phase Equilibria of the System Isopropyl Acetate + Isopropanol + 1-Octyl-3-Methyl-Imidazolium Bis(trifluoromethylsulfonyl)amide. *Fluid Phase Equilib.* **2010**, *287*, 84–94.

(379) Seddon, K. R. *Densities of Ionic Liquid for IUPAC Project. Personal Communication*; 2008.

(380) Andreatta, A. E.; Arce, A.; Rodil, E.; Soto, A. Physical and Excess Properties of (Methyl Acetate + Methanol + 1-Octyl-3-Methyl-Imidazolium Bis(trifluoromethylsulfonyl)amide) and Its Binary Mixtures at T=298.15K and Atmospheric Pressure. *J. Chem. Thermodyn.* **2009**, *41*, 1317–1323.

(381) Rilo, E.; Vila, J.; García, M.; Varela, L. M.; Cabeza, O. Viscosity and Electrical Conductivity of Binary Mixtures of C_nMIM-BF_4 with Ethanol at 288 K, 298 K,

308 K, and 318 K. *J. Chem. Eng. Data* **2010**, *55*, 5156–5163.

(382) Restolho, J.; Serro, A. P.; Mata, J. L.; Saramago, B. Viscosity and Surface Tension of 1-Ethanol-3-Methylimidazolium Tetrafluoroborate and 1-Methyl-3-Octylimidazolium Tetrafluoroborate over a Wide Temperature Range. *J. Chem. Eng. Data* **2009**, *54*, 950–955.

(383) MacFarlane, D. R.; Golding, J.; Forsyth, S.; Forsyth, M.; Deacon, G. B. Low Viscosity Ionic Liquids Based on Organic Salts of the Dicyanamide Anion. *Chem. Commun.* **2001**, *68*, 1430–1431.

(384) Mokhtarani, B.; Mojtahedi, M. M.; Mortaheb, H. R.; Mafí, M.; Yazdani, F.; Sadeghian, F. Densities, Refractive Indices, and Viscosities of the Ionic Liquids 1-Methyl-3-Octylimidazolium Tetrafluoroborate and L-Methyl-3-Butylimidazolium Perchlorate and Their Binary Mixtures with Ethanol at Several Temperatures. *J. Chem. Eng. Data* **2008**, *53*, 677–682.

(385) Yoshida, Y.; Muroi, K.; Otsuka, A.; Saito, G.; Takahashi, M.; Yoko, T. 1-Ethyl-3-Methylimidazolium Based Ionic Liquids Containing Cyano Groups: Synthesis, Characterization, and Crystal Structure. *Inorg. Chem.* **2004**, *43*, 1458–1462.

(386) Arce, A.; Rodríguez, H.; Soto, A. Effect of Anion Fluorination in 1-Ethyl-3-Methylimidazolium as Solvent for the Liquid Extraction of Ethanol from Ethyl Tert-Butyl Ether. *Fluid Phase Equilib.* **2006**, *242*, 164–168.

(387) Yoshida, Y.; Fujii, J.; Muroi, K.; Otsuka, A.; Saito, G.; Takahashi, M.; Yoko, T. Highly Conducting Ionic Liquids Based on L-Ethyl-3-Methylimidazolium Cation. *Synth. Met.* **2005**, *153*, 421–424.

(388) Arce, A.; Rodil, E.; Soto, A. Volumetric and Viscosity Study for the Mixtures of 2-Ethoxy-2-Methylpropane, Ethanol, and 1-Ethyl-3-Methylimidazolium Ethyl Sulfate Ionic Liquid. *J. Chem. Eng. Data* **2006**, *51*, 1453–1457.

(389) Altin, E.; Gradl, J.; Peukert, W. First Studies on the Rheological Behavior of Suspensions in Ionic Liquids. *Chem. Eng. Technol.* **2006**, *29*, 1347–1354.

(390) Tsukada, Y.; Iwamoto, K.; Furutani, H.; Matsushita, Y.; Abe, Y.; Matsumoto, K.; Monda, K.; Hayase, S.; Kawatsura, M.; Itoh, T. Preparation of Novel Hydrophobic Fluorine-Substituted-Alkyl Sulfate Ionic Liquids and Application as an Efficient Reaction Medium for Lipase-Catalyzed Reaction. Tetrahedron Letters **2006**, *47*, 1801-1804.

(391) Yoshida, Y.; Baba, O.; Saito, G. Ionic Liquids Based on Dicyanamide Anion: Influence of Structural Variations in Cationic Structures on Ionic Conductivity. *J. Phys. Chem. B* **2007**, *111*, 4742–4749.

(392) Leong, T.-I.; Sun, I.-W.; Deng, M.-J.; Wu, C.-M.; Chen, P.-Y. Electrochemical Study of Copper in the 1-Ethyl-3-Methylimidazolium Dicyanamide Room Temperature Ionic Liquid. *J. Electrochem. Soc.* **2008**, *155*, F55–F60.

(393) Deng, M.-J.; Chen, P.-Y.; Leong, T.-I.; Sun, I.-W.; Chang, J.-K.; Tsai, W.-T.

Dicyanamide Anion Based Ionic Liquids for Electrodeposition of Metals, Electrochemistry Communications **2008**, *10*, 213-216.

(394) Larriba, M.; García, S.; García, J.; Torrecilla, J. S.; Rodríguez, F. Thermophysical Properties of 1-Ethyl-3-Methylimidazolium 1,1,2,2-Tetrafluoroethanesulfonate and 1-Ethyl-3-Methylimidazolium Ethylsulfate Ionic Liquids as a Function of Temperature. *J. Chem. Eng. Data* **2011**, *56*, 3589–3597.

(395) Yoshida, Y.; Baba, O.; Larriba, C.; Saito, G. Imidazolium-Based Ionic Liquids Formed with Dicyanamide Anion: Influence of Cationic Structure on Ionic Conductivity. *J. Phys. Chem. B* **2007**, *111*, 12204–12210.

(396) Widegren, J. A.; Magee, J. W. Density, Viscosity, Speed of Sound, and Electrolytic Conductivity for the Ionic Liquid 1-Hexyl-3-Methylimidazolium Bis(trifluoromethylsulfonyl)amide and Its Mixtures with Water †. *J. Chem. Eng. Data* **2007**, *52*, 2331–2338.

(397) Marsh, K. N.; Brennecke, J. F.; Chirico, R. D.; Frenkel, M.; Heintz, A.; Magee, J. W.; Peters, C. J.; Rebelo, L. P. N.; Seddon, K. R. Thermodynamic and Thermophysical Properties of the Reference Ionic Liquid: 1-Hexyl-3-Methylimidazolium Bis[(trifluoromethyl)sulfonyl]amide (Including Mixtures). Part 1. Experimental Methods and Results (IUPAC Technical Report). *Pure Appl. Chem.* **2009**, *81*, 781–790.

(398) Ahosseini, A.; Weatherley, L. R.; Scurto, A. M. Viscosity and Diffusivity for the Ionic Liquid 1-Hexyl-3-Methyl-Imidazolium Bis(trifluoromethylsulfonyl)amide with 1-Octene. *J. Chem. Eng. Data* **2011**, *56*, 3715–3721.

(399) Yan, X.-J.; Li, S.-N.; Zhai, Q.-G.; Jiang, Y.-C.; Hu, M.-C. Physicochemical Properties for the Binary Systems of Ionic Liquids [$C_N$mim]Cl + *N* , *N* -Dimethylformamide. *J. Chem. Eng. Data* **2014**, *59*, 1411–1422.

(400) Ahosseini, A.; Ortega, E.; Sensenich, B.; Scurto, A. M. Viscosity of N-Alkyl-3-Methyl-Imidazolium Bis(trifluoromethylsulfonyl)amide Ionic Liquids Saturated with Compressed CO_2. *Fluid Phase Equilib.* **2009**, *286*, 72–78.

(401) Le, M. L. P.; Alloin, F.; Strobel, P.; Leprêtre, J.-C.; Pérez del Valle, C.; Judeinstein, P. Structure−Properties Relationships of Lithium Electrolytes Based on Ionic Liquid. *J. Phys. Chem. B* **2010**, *114*, 894–903.

(402) Calvar, N.; Gómez, E.; González, B.; Domínguez, Á. Experimental Determination, Correlation, and Prediction of Physical Properties of the Ternary Mixtures Ethanol + Water with 1-Octyl-3-Methylimidazolium Chloride and 1-Ethyl-3-Methylimidazolium Ethylsulfate. *J. Chem. Eng. Data* **2007**, *52*, 2529–2535.

(403) Kilaru, P. K.; Scovazzo, P. Correlations of Low-Pressure Carbon Dioxide and

Hydrocarbon Solubilities in Imidazolium-, Phosphonium-, and Ammonium-Based Room-Temperature Ionic Liquids. Part 2. Using Activation Energy of Viscosity. *Ind. Eng. Chem. Res.* **2008**, *47*, 910–919.

(404) González, E. J.; Alonso, L.; Domínguez, Á. Physical Properties of Binary Mixtures of the Ionic Liquid 1-Methyl-3-Octylimidazolium Chloride with Methanol, Ethanol, and 1-Propanol at T = (298.15, 313.15, and 328.15) K and at P = 0.1 MPa. *J. Chem. Eng. Data* **2006**, *51*, 1446–1452.

(405) McFarlane, D. .; Sun, J.; Golding, J.; Meakin, P.; Forsyth, M. High Conductivity Molten Salts Based on the Imide Ion. *Electrochim. Acta* **2000**, *45*, 1271–1278.

(406) Liu, H.; Maginn, E.; Visser, A. E.; Bridges, N. J.; Fox, E. B. Thermal and Transport Properties of Six Ionic Liquids: An Experimental and Molecular Dynamics Study. *Ind. Eng. Chem. Res.* **2012**, *51*, 7242–7254.

(407) Jacquemin, J.; Husson, P.; Majer, V.; Padua, A. A. H.; Costa Gomes, M. F. Thermophysical Properties, Low Pressure Solubilities and Thermodynamics of Solvation of Carbon Dioxide and Hydrogen in Two Ionic Liquids Based on the Alkylsulfate Anion. *Green Chem.* **2008**, *10*, 944–950.

(408) Jung, Y.-H.; Jung, J.-Y.; Jin, Y.-R.; Lee, B.-C.; Baek, I.-H.; Kim, S.-H. Solubility of Carbon Dioxide in Imidazolium-Based Ionic Liquids with a Methanesulfonate Anion. *J. Chem. Eng. Data* **2012**, *57*, 3321–3329.

(409) Banerjee, T.; Verma, K. K.; Khanna, A. Liquid-Liquid Equilibrium for Ionic

Liquid Systems Using COSMO-RS: Effect of Cation and Anion Dissociation. *AIChE J.* **2008**, *54*, 1874–1885.

(410) Domańska, U.; Bogel-Łukasik, E.; Bogel-Łukasik, R. 1-Octanol/Water Partition Coefficients of 1Alkyl-3-Methylimidazolium Chloride. *Chem. - A Eur. J.* **2003**, *9*, 3033–3041.

(411) Alonso, L.; Arce, A.; Francisco, M.; Soto, A. Liquid-Liquid Equilibria of ([C_2mim][$EtSO_4$] + Thiophene + 2,2,4-Trimethylpentane) and ([C_2mim][$EtSO_4$] + Thiophene + Toluene): Experimental Data and Correlation. *J. Solution Chem.* **2008**, *37*, 1355–1363.

(412) Alonso, L.; Arce, A.; Francisco, M.; Soto, A. Phase Behaviour of 1-Methyl-3-Octylimidazolium Bis[trifluoromethylsulfonyl]imide with Thiophene and Aliphatic Hydrocarbons: The Influence of N-Alkane Chain Length. *Fluid Phase Equilib.* **2008**, *263*, 176–181.

(413) Alonso, L.; Arce, A.; Francisco, M.; Soto, A. (Liquid+liquid) Equilibria of [C_8mim][NTf_2] Ionic Liquid with a Sulfur-Component and Hydrocarbons. *J. Chem. Thermodyn.* **2008**, *40*, 265–270.

(414) Alonso, L.; Arce, A.; Francisco, M.; Soto, A. Thiophene Separation from Aliphatic Hydrocarbons Using the 1-Ethyl-3-Methylimidazolium Ethylsulfate Ionic Liquid. *Fluid Phase Equilib.* **2008**, *270*, 97–102.

(415) Bendová, M.; Wagner, Z. Thermodynamic Description of Liquid–liquid

Equilibria in Systems 1-Ethyl-3-Methylimidazolium ethylsulfate+C7-Hydrocarbons by Polymer-Solution Models. *Fluid Phase Equilib.* **2009**, *284*, 80–85.

(416) Arce, A.; Earle, M. J.; Rodríguez, H.; Seddon, K. R.; Soto, A. Isomer Effect in the Separation of Octane and Xylenes Using the Ionic Liquid 1-Ethyl-3-Methylimidazolium Bis{(trifluoromethyl)sulfonyl}amide. *Fluid Phase Equilib.* **2010**, *294*, 180–186.

(417) Rodríguez, H.; Francisco, M.; Soto, A.; Arce, A. Liquid–liquid Equilibrium and Interfacial Tension of the Ternary System heptane+thiophene+1-Ethyl-3-Methylimidazolium Bis(trifluoromethanesulfonyl)imide. *Fluid Phase Equilib.* **2010**, *298*, 240–245.

(418) García, S.; Larriba, M.; García, J.; Torrecilla, J. S.; Rodríguez, F. Liquid−Liquid Extraction of Toluene from Heptane Using 1-Alkyl-3-Methylimidazolium Bis(trifluoromethylsulfonyl)amide Ionic Liquids. *J. Chem. Eng. Data* **2011**, *56*, 113–118.

(419) Hwang, I.-C.; Kim, J.-I.; Park, S.-J. Liquid–liquid Equilibrium for Binary and Ternary Systems Containing Di-Isopropyl Ether (DIPE) and an Imidazolium-Based Ionic Liquid at Different Temperatures. *Fluid Phase Equilib.* **2010**, *299*, 294–299.

(420) Jongmans, M. T. G.; Hermens, E.; Schuur, B.; de Haan, A. B. Binary and

Ternary Vapor–liquid Equilibrium Data of the System ethylbenzene+styrene+3-Methyl-N-Butylpyridinium Tetracyanoborate at Vacuum Conditions and Liquid–liquid Equilibrium Data of Their Binary Systems. *Fluid Phase Equilib.* **2012**, *315*, 99–106.

(421) Corderí, S.; González, B.; Calvar, N.; Gómez, E. Ionic Liquids as Solvents to Separate the Azeotropic Mixture Hexane/ethanol. *Fluid Phase Equilib.* **2013**, *337*, 11–17.

(422) Rodríguez-Cabo, B.; Arce, A.; Soto, A. Desulfurization of Fuels by Liquid–liquid Extraction with 1-Ethyl-3-Methylimidazolium Ionic Liquids. *Fluid Phase Equilib.* **2013**, *356*, 126–135.

(423) Domínguez, I.; González, E. J.; Domínguez, Á. Liquid Extraction of Aromatic/cyclic Aliphatic Hydrocarbon Mixtures Using Ionic Liquids as Solvent: Literature Review and New Experimental LLE Data. *Fuel Process. Technol.* **2014**, *125*, 207–216.

(424) Domínguez, I.; González, E. J.; González, R.; Domínguez, A. Extraction of Benzene from Aliphatic Compounds Using Commercial Ionic Liquids as Solvents: Study of the Liquid–Liquid Equilibrium at T = 298.15 K. *J. Chem. Eng. Data* **2011**, *56*, 3376–3383.

(425) Alonso, L.; Arce, A.; Francisco, M.; Soto, A. Solvent Extraction of Thiophene from N-Alkanes (C7, C12, and C16) Using the Ionic Liquid [C_8mim][BF_4]. *J.*

Chem. Thermodyn. **2008**, *40*, 966–972.

(426) Hansmeier, A. R.; Jongmans, M.; Wytze Meindersma, G.; de Haan, A. B. LLE Data for the Ionic Liquid 3-Methyl-N-Butyl Pyridinium Dicyanamide with Several Aromatic and Aliphatic Hydrocarbons. *J. Chem. Thermodyn.* **2010**, *42*, 484–490.

(427) Li, X.; Tamura, K. Cloud Point Measurements of 1-Butyl-2,3-Dimethylimidazolium Tetrafluoroborate with Alcohols. *J. Chem. Thermodyn.* **2010**, *42*, 1478–1484.

(428) Meindersma, G. W.; Simons, B. T. J.; de Haan, A. B. Physical Properties of 3-Methyl-N-Butylpyridinium Tetracyanoborate and 1-Butyl-1-Methylpyrrolidinium Tetracyanoborate and Ternary LLE Data of [3-mebupy]$B(CN)_4$ with an Aromatic and an Aliphatic Hydrocarbon at T=303.2K and 328.2K and p=0.1MPa. *J. Chem. Thermodyn.* **2011**, *43*, 1628–1640.

(429) Jongmans, M. T. G.; Schuur, B.; de Haan, A. B. Binary and Ternary LLE Data of the System (ethylbenzene+styrene+1-Ethyl-3-Methylimidazolium Thiocyanate) and Binary VLE Data of the System (styrene+1-Ethyl-3-Methylimidazolium Thiocyanate). *J. Chem. Thermodyn.* **2012**, *47*, 234–240.

(430) Corderí, S.; González, E. J.; Calvar, N.; Domínguez, Á. Application of [HMim][NTf_2], [HMim][TfO] and [BMim][TfO] Ionic Liquids on the

Extraction of Toluene from Alkanes: Effect of the Anion and the Alkyl Chain Length of the Cation on the LLE. *J. Chem. Thermodyn.* **2012**, *53*, 60–66.

(431) Domańska, U.; Królikowski, M. Extraction of Butan-1-ol from Water with Ionic Liquids at T=308.15K. *J. Chem. Thermodyn.* **2012**, *53*, 108–113.

(432) Seoane, R. G.; González, E. J.; González, B. 1-Alkyl-3-Methylimidazolium Bis(trifluoromethylsulfonyl)amide Ionic Liquids as Solvents in the Separation of Azeotropic Mixtures. *J. Chem. Thermodyn.* **2012**, *53*, 152–157.

(433) Rodríguez-Cabo, B.; Soto, A.; Arce, A. Desulfurization of Fuel-Oils with [C_2mim][NTf_2]: A Comparative Study. *J. Chem. Thermodyn.* **2013**, *57*, 248–255.

(434) Domańska, U.; Lukoshko, E. V.; Królikowski, M. Separation of Thiophene from Heptane with Ionic Liquids. *J. Chem. Thermodyn.* **2013**, *61*, 126–131.

(435) Domańska, U.; Paduszyński, K. (Solid+liquid) and (Liquid+liquid) Phase Equilibria Measurements and Correlation of the Binary Systems {tri-Iso-Butyl(methyl)phosphonium Tosylate+alcohol, or +hydrocarbon}. *Fluid Phase Equilib.* **2009**, *278*, 90–96.

(436) Corderí, S.; Gómez, E.; Calvar, N.; Domínguez, Á. Measurement and Correlation of Liquid–Liquid Equilibria for Ternary and Quaternary Systems of Heptane, Cyclohexane, Toluene, and [EMim][OAc] at 298.15 K. *Ind. Eng. Chem. Res.* **2014**, *53*, 9471–9477.

(437) Sahandzhieva, K.; Tuma, D.; Breyer, S.; Pérez-Salado Kamps, Á.; Maurer, G. Liquid−Liquid Equilibrium in Mixtures of the Ionic Liquid 1- *N* -Butyl-3-Methylimidazolium Hexafluorophosphate and an Alkanol †. *J. Chem. Eng. Data* **2006**, *51*, 1516–1525.

(438) Bendova, M. Liquid - Liquid Equilibrium in Binary System [bmim][PF 6] + 1-Butanol. *J. Chem. Eng. Data* **2006**, *25*, 2126–2131.

(439) Pereiro, A. B.; Rodríguez, A. Thermodynamic Properties of Ionic Liquids in Organic Solvents from (293.15 to 303.15) K. *J. Chem. Eng. Data* **2007**, *52*, 600–608.

(440) Sahandzhieva, K.; Naydenov, D.; Pérez-Salado Kamps, A.; Bart, H.-J.; Maurer, G. Liquid−Liquid Equilibrium in Systems with an Ionic Liquid: Experimental Data for an Example of the Biphasic Acid Scavenging Utilizing Ionic Liquids Process. *J. Chem. Eng. Data* **2010**, *55*, 4903–4906.

(441) Lago, S.; Rodríguez, H.; Soto, A.; Arce, A. Deterpenation of Citrus Essential Oil by Liquid−Liquid Extraction with 1-Alkyl-3-Methylimidazolium Bis(trifluoromethylsulfonyl)amide Ionic Liquids. *J. Chem. Eng. Data* **2011**, *56*, 1273–1281.

(442) Freire, M. G.; Neves, C. M. S. S.; Shimizu, K.; Bernardes, C. E. S.; Marrucho, I. M.; Coutinho, J. A. P.; Canongia Lopes, J. N.; Rebelo, L. P. N. Mutual Solubility of Water and Structural/positional Isomers of N-Alkylpyridinium-Based Ionic

Liquids. *J. Phys. Chem. B* **2010**, *114*, 15925–15934.

(443) Orchillés, A. V.; Miguel, P. J.; Vercher, E.; Martínez-Andreu, A. Isobaric Vapor−Liquid and Liquid−Liquid Equilibria for Chloroform + Ethanol + 1-Ethyl-3-Methylimidazolium Trifluoromethanesulfonate at 100 kPa. *J. Chem. Eng. Data* **2008**, *53*, 2642–2648.

(444) Orchillés, A. V.; Miguel, P. J.; Vercher, E.; Martínez-Andreu, A. Isobaric Vapor−Liquid and Liquid−Liquid Equilibria for Chloroform + Methanol + 1-Ethyl-3-Methylimidazolium Trifluoromethanesulfonate at 100 kPa. *J. Chem. Eng. Data* **2010**, *55*, 1209–1214.

(445) Shiflett, M. B.; Yokozeki, A. Liquid−Liquid Equilibria in Binary Mixtures Containing Fluorinated Benzenes and Ionic Liquid 1-Ethyl-3-Methylimidazolium Bis(trifluoromethylsulfonyl)amide. *J. Chem. Eng. Data* **2008**, *53*, 2683–2691.

(446) Shiflett, M. B.; Niehaus, A. M. S. Liquid−Liquid Equilibria in Binary Mixtures Containing Substituted Benzenes with Ionic Liquid 1-Ethyl-3-Methylimidazolium Bis(trifluoromethylsulfonyl)amide. *J. Chem. Eng. Data* **2010**, *55*, 346–353.

(447) Ahosseini, A.; Sensenich, B.; Weatherley, L. R.; Scurto, A. M. Phase Equilibrium, Volumetric, and Interfacial Properties of the Ionic Liquid, 1-Hexyl-3-Methylimidazolium Bis(trifluoromethylsulfonyl)amide and

1-Octene. *J. Chem. Eng. Data* **2010**, *55*, 1611–1617.

(448) Dreiseitlová, J.; Řehák, K.; Vreekamp, R. Mutual Solubility of Pyridinium-Based Tetrafluoroborates and Toluene. *J. Chem. Eng. Data* **2010**, *55*, 3051–3054.

(449) Francisco, M.; Arce, A.; Soto, A. Ionic Liquids on Desulfurization of Fuel Oils. *Fluid Phase Equilib.* **2010**, *294*, 39–48.

(450) Francisco, M.; Lago, S.; Soto, A.; Arce, A. Essential Oil Deterpenation by Solvent Extraction Using 1-Ethyl-3-Methylimidazolium 2-(2-Methoxyethoxy) Ethylsulfate Ionic Liquid. *Fluid Phase Equilib.* **2010**, *296*, 149–153.

(451) Rodríguez-Cabo, B.; Francisco, M.; Soto, A.; Arce, A. Hexyl Dimethylpyridinium Ionic Liquids for Desulfurization of Fuels. Effect of the Position of the Alkyl Side Chains. *Fluid Phase Equilib.* **2012**, *314*, 107–112.

(452) Marciniak, A.; Królikowski, M. Ternary Liquid–liquid Equilibria of Bis(trifluoromethylsulfonyl)-Amide Based Ionic Liquids+thiophene+n-Heptane. The Influence of Cation Structure. *Fluid Phase Equilib.* **2012**, *321*, 59–63.

(453) Arce, A.; Francisco, M.; Soto, A. Evaluation of the Polysubstituted Pyridinium Ionic Liquid [hmmpy][Ntf_2] as a Suitable Solvent for Desulfurization: Phase Equilibria. *J. Chem. Thermodyn.* **2010**, *42*, 712–718.

(454) Marciniak, A.; Królikowski, M. Ternary (Liquid+liquid) Equilibria of

{trifluorotris(perfluoroethyl)phosphate Based Ionic Liquids+thiophene+heptane}. *J. Chem. Thermodyn.* **2012**, *49*, 154–158.

(455) Wlazło, M.; Marciniak, A. Fluid Phase Equilibria Ternary Liquid–liquid Equilibria of Trifluorotris(perfluoroethyl)phosphate Based Ionic Liquids + Methanol + Heptane. *Fluid Phase Equilib.* **2013**, *338*, 253–256.

(456) González, B.; Corderí, S.; Santamaría, A. G. Application of 1-Alkyl-3-Methylpyridinium Bis(trifluoromethylsulfonyl)amide Ionic Liquids for the Ethanol Removal from Its Mixtures with Alkanes. *J. Chem. Thermodyn.* **2013**, *60*, 9–14.

(457) Selvan, M. S.; McKinley, M. D.; Dubois, R. H.; Atwood, J. L. Liquid−Liquid Equilibria for Toluene + Heptane + 1-Ethyl-3-Methylimidazolium Triiodide and Toluene + Heptane + 1-Butyl-3-Methylimidazolium Triiodide †. *J. Chem. Eng. Data* **2000**, *45*, 841–845.